

Abdeldjalil Khelassi
Vania Vieira Estrela *Editors*

Advances in
Multidisciplinary
Medical Technologies
— Engineering,
Modeling and Findings

Proceedings of the ICHSMT 2019

Advances in Multidisciplinary Medical Technologies — Engineering, Modeling and Findings

Abdeldjalil Khelassi • Vania Vieira Estrela
Editors

Advances in Multidisciplinary Medical Technologies — Engineering, Modeling and Findings

Proceedings of the ICHSMT 2019

 Springer

Editors

Abdeljalil Khelassi 
Abou Bakr Belkaïd University of Tlemcen
Tlemcen, Algeria

Vania Vieira Estrela 
Telecommunications Department
Federal Fluminense University (UFF)
Duque de Caxias, Rio de Janeiro, Brazil

ISBN 978-3-030-57551-9 ISBN 978-3-030-57552-6 (eBook)
<https://doi.org/10.1007/978-3-030-57552-6>

© Springer Nature Switzerland AG 2021, Corrected Publication 2021

This work is subject to copyright. All rights are reserved by the Publisher, whether the whole or part of the material is concerned, specifically the rights of translation, reprinting, reuse of illustrations, recitation, broadcasting, reproduction on microfilms or in any other physical way, and transmission or information storage and retrieval, electronic adaptation, computer software, or by similar or dissimilar methodology now known or hereafter developed.

The use of general descriptive names, registered names, trademarks, service marks, etc. in this publication does not imply, even in the absence of a specific statement, that such names are exempt from the relevant protective laws and regulations and therefore free for general use.

The publisher, the authors, and the editors are safe to assume that the advice and information in this book are believed to be true and accurate at the date of publication. Neither the publisher nor the authors or the editors give a warranty, expressed or implied, with respect to the material contained herein or for any errors or omissions that may have been made. The publisher remains neutral with regard to jurisdictional claims in published maps and institutional affiliations.

This Springer imprint is published by the registered company Springer Nature Switzerland AG
The registered company address is: Gewerbestrasse 11, 6330 Cham, Switzerland

Preface

We are proud to announce this book entitled *Advances in Multidisciplinary Medical Technologies – Engineering, Modeling, and Findings*, which contains selected articles from the fourth edition of ICHSMT International Congress on Health Sciences and Medical Technologies, Tlemcen, Algeria, December 5–7, 2019. The book also contains external chapters from other researchers to enrich the content.

The International Congress on Health Science and Medical Technologies becomes a template of multidisciplinary efforts aimed towards impacting the scientific progress in several axes of health sciences and medical technologies. It was idealized by Dr. Abdeldjalil Khelassi and counted with the support of Dr. Wolfgang Seger. The fourth edition of the congress was held at Tlemcen, Algeria, between December 5 and 7, 2019.

The editors acknowledge all those who contributed to the previous congress editions and especially the reviewers, organizers, sponsors, and volunteers of this fourth one. The reviewing process was realized in two rounds: (1) pre-congress round, which was meant to select the presentations and posters of the conferences, and (2) post-congress round, through which an amalgam of chapters were chosen for publication. All submitted chapters passed by the double-blind reviewing process by one to three reputed reviewers.

This book includes 16 chapters by distinct authors organized into two main parts as follows:

Medical Technologies for the Betterment of Humankind
Medical Technologies Systems

The editors would like to thank the members of the Technical Committee who helped with the reviews and all the staff at Springer Nature.

Tlemcen, Algeria
Duque de Caxias, Rio de Janeiro, Brazil

Abdeldjalil Khelassi
Vania Vieira Estrela

Program Committees

General Chair

Dr. Abdeldjalil Khelassi, University of Tlemcen, Algeria

Program Committee Chairs

Dr. Abdeldjalil Khelassi, University of Tlemcen, Algeria

Dr. Vania Vieira Estrela, Federal Fluminense University (UFF), Brazil

Pr. Wolfgang Seger, German Federal Association for Rehabilitation, Germany

Program Committee

Dr. Abdeldjalil Khelassi, University of Tlemcen, Algeria

Pr. Kaouel Meguenni, University of Tlemcen, CHU Tlemcen, Algeria

Dr. Vania Vieira Estrela, Federal Fluminense University (UFF), Brazil

Pr. Dr. Wolfgang Seger, German Federal Association for Rehabilitation, Germany

Pr. Dr.med. H.-Peter Berlien, Director of clinic for laser medicine in Berlin, Germany

Dr. Jalalian Mehrdad, Electronic Physician Journal, Mehrafarin Scientific Publishing, Iran

Pr. Syed Tajuddin Bin Syed Hassan, Universiti Putra Malaysian, Malaysia

Pr. Habib Zaidi, Geneva University Hospital, University of Groningen, University of Southern Denmark, University of Cergy-Pontoise, Switzerland, The Netherlands, Denmark, France

Pr. Dr. Klaus-Dieter Althoff, University of Hildesheim, Germany

Pr. Noureddine Djebli, Mostaganem University, Algeria

Pr. Joseph Kajima Mulengi, University of Tlemcen, Algeria

Pr. Fethi Bereksi Reguig, University of Tlemcen, Algeria

Pr. Abdeslam Taleb, University of Tlemcen, Algeria

Pr. Abdelouahab Moussaoui, Ferhat Abbas University of Sétif, Algeria

Pr. Med Amine Chikh, University of Tlemcen, Algeria

Pr. Mohammed El Hassouni, Mohammed V University in Rabat, Morocco

Pr. Yazid Cherfa, Université Saad Dahlab de Blida, Algeria

Pr. Ahmed Abdelhafiz, Asiut Clinic for Gynecology and Obstetrics, Egypt
Pr. Ouahiba Hadjoudj, Hôpital Nafissa Hamoud (ex Parnet), Algeria
Dr. Muhammed Ajmal Shah, Government College University Faisalabad, Pakistan
Dr. Abdelkrim Meziane, CERIST, Algeria
Pr. Said Ghalem, University of Tlemcen, Algeria
Dr. Jude Hemanth, Karunya University, Coimbatore, India
Dr. Thierry Edoh, RFW-Universität Bonn, Germany
Pr. Boumedién Elhabachi, CHU Sidi Belabas, Algeria
Dr. Ralf Lohse, Underwriter, Hannover Reinsurance SE, Germany
Dr. Valeria Tananska, Medical University of Plovdiv, Bulgaria
Dr. Ana Claudia Mendes Seixas, PUC-Campinas, Brazil

Contents

Part I Medical Technologies for the Betterment of Humankind

- 1 Empathy and the Quest for Social Ethics: Their Relevance to Contemporary Healthcare – The European Perspective 3**
Valeria Tananska
- 2 Conceptual Model of Professional Supervision Study Based on Data Mining: A Study in the Regional Council of Nutritionists of the 4th Brazilian Region (Rio de Janeiro and Espirito Santo States). 11**
Anderson Luiz Ignacio de Lima, Rosane Justino de Sousa Lima, and Henrique Rego Monteiro da Hora
- 3 Building Bridges and Remediating Illiteracy: How Intergenerational Cooperation Foster Better Engineering Professionals 29**
M. A. de Jesus, Vania Vieira Estrela, R. J. Aroma, N. Razmjoooy, S. E. B. da Silva, A. C. de Almeida, H. R. M. da Hora, A. Deshpande, P. Patavardhan, Nikolaos Andreopoulos, Andrey Terziev, K. Raimond, Hermes J. Loschi, and Douglas A. Nascimento
- 4 Acoustic Contrast Between Neutral and Angry Speech: Variation of Prosodic Features in Algerian Dialect Speech and German Speech 41**
F. Ykhlef and D. Bouchaffra

Part II Medical Technologies Systems

- 5 Artificial Intelligence and Its Application in Insulin Bolus Calculators 55**
Abdelaziz Mansour, Kamal Amroun, and Zineb Habbas

6	Feature Extraction Based on Wavelet Transform for Classification of Stress Level	77
	Djamel Bouchaffra, Faycal Ykhlef, and Yamina Bennamane	
7	Packet Synchronization in a Network Time Protocol Server and ASTM Elecsys Packets During Detection for Cancer with Optical DNA Biochip	89
	Amina Elbatoul Dinar, Samir Ghouali, Boualem Merabet, and Mohammed Feham	
8	Particle Swarm Optimization with Tabu Search Algorithm (PSO-TS) Applied to Multiple Sequence Alignment Problem	103
	Lamiche Chaabane, Abdeldjalil Khelassi, Andrey Terziev, Nikolaos Andreopoulos, M. A. de Jesus, and Vania Vieira Estrela	
9	Extracted Haralick's Texture Features for Abnormal Blood Cells	115
	Abdellatif Bouzid-Daho, Naima Sofi, and Patrick Siarry	
10	Artificial Intelligence, Blockchain, and Internet of Medical Things: New Technologies in Detecting, Preventing, and Controlling of Emergent Diseases	127
	Akanksha Sharma, Rishabha Malviya, Rajendra Awasthi, and Pramod Kumar Sharma	
11	The Role of Vehicular Ad Hoc Networks in Intelligent Transport Systems for Healthcare	155
	Rabia Bilal and Bilal Muhammad Khan	
12	The Vedic Design-Carry Look Ahead (VD-CLA): A Smart and Hardware-Friendly Implementation of the FIR Filter for ECG Signal Denoising	185
	K. B. Sowmya, Chandana, and M. D. Anjana	
13	Implementation of an FPGA Real-Time Configurable System for Enhancement of Lung and Heart Images	199
	K. B. Sowmya, T. S. Rakshak Udupa, and Shashank K. Holla	
14	Adaptive Specular Reflection Detection in Cervigrams (ASRDC) Technique: A Computer-Aided Tool for Early Screening of Cervical Cancer	215
	Brijesh Iyer and Pratik Oak	
15	Implementation of Image Encryption by Steganography Using Discrete Wavelet Transform in Verilog	233
	K. B. Sowmya, Prakash S. Bhat, and Sudheendra Hegde	

**16 Nondestructive Diagnosis and Analysis of Computed
Microtomography Images via Texture Descriptors 249**
Sandro R. Fernandes, Joaquim T. de Assis, Vania Vieira Estrela,
Navid Razmjoooy, Anand Deshpande, P. Patavardhan, R. J. Aroma,
K. Raimond, Hermes J. Loschi, and Douglas A. Nascimento

**Correction to: Acoustic Contrast Between Neutral
and Angry Speech: Variation of Prosodic Features in Algerian
Dialect Speech and German Speech C1**

Index 263

Part I
Medical Technologies
for the Betterment of Humankind

Chapter 1

Empathy and the Quest for Social Ethics: Their Relevance to Contemporary Healthcare – The European Perspective



Valeria Tananska

1.1 Introduction

The present-day definition of personalized medicine is “the science of individualized anticipation of patients’ medical needs and therapy.” Even though physicians are opening up to the use of promising technologies such as nanorobotics, genetics-driven medicine, sequencing technology, health informatics, artificial intelligence, and computer science, the much anticipated big revolution is yet to come and pave the way to a stronger, better human being [4–10].

In a best-case scenario, technology assists physicians with more precise diagnosis, while ethical and empathetic healthcare professionals address the emotional, as well as the physical needs of their patients.

And nowadays patients are asking for such a personalized care (Fig. 1.1). They however view it only in light of more personal attention from and time spent with physicians. Most patients do not understand what Internet-integrated technology can do for them – access to more advanced software than the one their hospital can afford; better qualification of medical personnel via “in time” following of best practices instituted by larger, medical university hospitals; faster, more accurate analyses of patient’s condition through second opinion given by off-premise specialists; prevention of disease, based on global comparison with other similar cases; lowering the chance of professional mistakes and the synthesis of new medications, through the work of an AI; and improved security and longevity of stored individual medical test data.

The currently limited use of technology pinpoints additional areas of actual benefit for personalized healthcare, such as an easier access to computer-standardized medical test data from medical machinery vastly differing in its make, technological capabilities, and visualization format (Fig. 1.2) [10–12].

V. Tananska (✉)
Medical University-Plovdiv, Plovdiv, Bulgaria

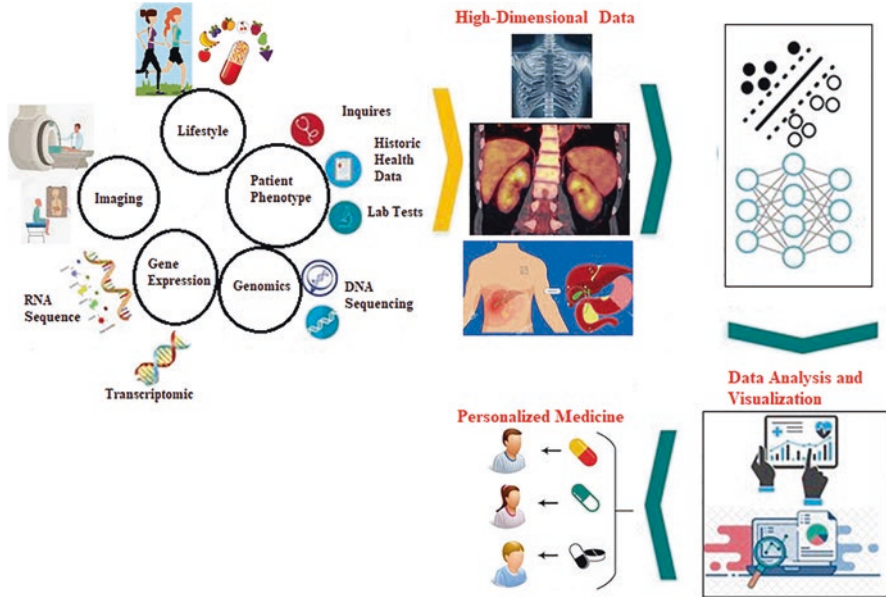


Fig. 1.1 Personalized healthcare [13]

All we need is open minds and the realization of concrete positive advantage.

Certain groups will undoubtedly oppose these proposals for change based on patient privacy concerns, the lack of advanced technical ability with healthcare providers, or the cost of implementing new technologies.

Yet, every issue has its solution. Evolution ensues from proactive involvement in technologies that would secure better medical service, more satisfied patients, and the future of our species as a whole.

With rising demands for individualized healthcare, personalized medicine is the route to take. It is the author's opinion that empathy and effective (rather than reptilian) listening to the patient are an integral part of the new way forward. As such, they must also be included into healthcare professionals' curricula, clinical practice, and counseling [1–3].

The next section discusses in greater debt the viewpoints of the author.

Finally, a conclusion section closes this manuscript.

1.2 Reflections on Empathy, Social Ethics, and Healthcare

Empathy is a type of one- or two-sided communication of emotion. Its practice requires a minimum of two people – an empath willing to relate to the transient mental plight of another and an empathee – the original source of such feelings.

Empathy is a product of necessity.

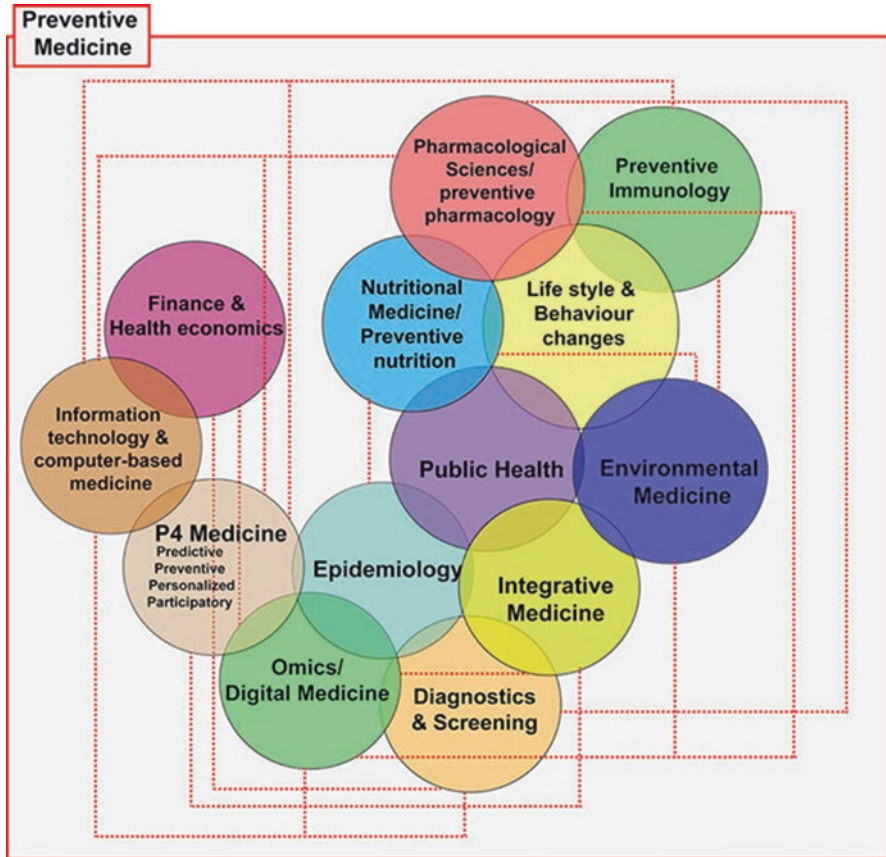


Fig. 1.2 Preventive medicine [14]

It stems from the evolutionary instinct to avoid danger and improve survival odds (while maximizing personal character growth) by steering away from self-capsulation, moving instead towards sharing resources and knowledge with others.

If history has shown us anything, however, it is that life with others is...well, complicated.

People have diverging needs, as well as a relentless desire to overcome and overpower all other egos. A hierarchical governing system, wars, and crime have been the obvious outcome.

To combat human nature and to survive in this world of our own making, we need higher guidance – a code of ethical conduct, supported by law and, in case of infringement, remediation.

Under the preeminent rule of a deity, God is the source of such guidance, as well as the objective adjudicator of its observance. He judges both the unrealized intent to do wrong (or advance one-self at the expense of others) and the actual deed to that effect. Non-compliance means just, perpetual punishment in the afterlife.

God is the only one that extends empathy. He does so solely to the deserving, the compliant, and the truly repentant. Everyone else must endure hardship – either because they have committed a sin, or because God tests the resolve of their character.

As He rarely communicates directly with his flock, God has chosen people qualified to interpret (the clergy) and implement (a ruling class) His word with the many.

But, in some realms in Europe, the interpreters lost their way. They sought to disbalance the system and usurp rulers' place. An additional irritant was the sale of indulgences, promising God's grace in writing off unethical or criminal behavior.

Widespread injustice to the many (committed not by God, but by fellow men) created pre-conditions for social upheaval. Fearing power displacement, the rulers reacted. With the inside help of like-minded religious reformers, they legislated an alternative view of God's ethics – their own.

Coded under the maxim *cuius regio, eius religio* ("whose realm, his religion"), rulers kept their judicial and executive privileges in the temporal world. Yet, they empowered themselves to connect directly to God and interpret His wisdom.

In so doing, rulers showed continuity. The new ethics incorporated God's teachings but applied them firmly to the needs of the state. Moral values were de-generalized and greatly expanded. Now they aimed at resolving frequently occurring social issues.

Within each realm, the resulting interpretation was not deemed a heresy, but acquired the power of law. Rulers' gave their subjects the new version of God's ethics in the vernacular.

The clergy got back to its preordained position of a repository of faith and ethical conduct.

Rulers and clergy worked together once more for the greater good of the many.

Desired stability however, was not achieved fast enough. To make matters worse, the former drivers of change (the rulers) got corrupted with power. They disregarded the ruled and degenerated into breaking their own ethical logic.

History repeated itself, only this time the opposing factions were different.

Lacking leadership qualities to incur change, the ruled joined effort with nobles-reformists. In some states, violent acts of divergence occurred (e.g., the French revolution). Defecting rulers were reminded of majority power. The many decided they would govern themselves.

The ensuing ethical shift sought to prevent further social injustice. Like its predecessor, it did not build from the start. It revised a previous version.

Governance was divided between a legislative, executive, and judicial branches, intended to balance each other out. Extreme forms of nepotism and ego-centrism were curbed through election to a temporary mid- and low-level governing position. The rise of a middle class began.

The Enlightenment (eighteenth century) and the Age of Reason (nineteenth century) followed. Both intellectual movements studied the individual in terms of creational impulse, physical and mental development, and health.

Europe's rapid industrialization, and several armed conflicts later, highlighted the next set of issues. Humanistic ideas had relaxed into hypocritical ranting.

Rulers and middle class enjoyed the comfort of their social position, while the rest of society struggled. Disease, death, and economic desperation run rampant. No longer would occasional acts of “noblesse oblige” (“nobility obligates”) towards the poor and the underprivileged suffice, when sustainable care was needed.

The poor took to the streets demanding their social justice.

Even with remedy in sight, society still lacked in equal representation. Economic outcasts were followed by women and people of color, who asked to join the electorate. Limited consideration was subsequently given to sexual orientation.

Which brings us to present day social life and its understanding of ethics.

Today, we, Europeans, believe that we have ethically evolved. Our social and personal acts are moved by God’s universal empathetic guidance. But we uphold it ourselves. We fight for our human rights. We do not expect that someone else will do it for us.

We would like to think that in so doing, we have broadened our mental horizons; that we have become more self-aware and considerate to each other.

Yet, an ethically driven society engineered in strife is never a done deal, rather a work in constant need of adjustment.

Below the surface, tensions persist, especially at the individual level.

The current bone of contention is that socio-political maneuvering around groups with common complaints has trampled personal value. Nowhere is it more ostensibly felt than in healthcare provision.

Patients increasingly claim that contemporary medicine has shifted in focus. It has abandoned pursuit for the holistic healing of individual people in favor of Fordist concerns like economy and efficient hospital stay turnover.

The result is limited bio-chemical testing culminating in treatment of illness types and inanimate clinical cases. To top it all, empathy for patient’s experience with the disease in a thus devolved healthcare system is totally missing.

The critics are correct, but only partially. Daily overload of responsibilities should not detract from empathetic professional treatment. Healthcare staff should be committed to patients’ mental as well as physical plight.

Yet, one should not forget that healthcare providers are (on occasion) themselves using the system. It would be wrong to point fingers solely at the medical corps, just because (in the absence of a concrete box punching bag) it means the front line for direct, emotional bashing.

A far more insidious culprit hides elsewhere.

We have been trapped in a whirlpool of continuous time discordance. Social ethics has evolved faster than the ability of the state to accommodate longer life expectancy with a shrinking healthcare- and tax-paying work force.

The latter (aged between 21 and 68, and the ceiling is ever rising) pays for the healthcare provision of:

- Themselves
- At least two retired live generations before them
- People with special medical needs
- The unemployed
- The incoming younger generation (at present – too young to socially contribute)

Ironically, state's work force has no right to be ill (at least, not for long). Sick leave exacerbates monetary losses – once, by using healthcare service and, second, time – by not making a full deductible towards it.

Breaching the gap between financial inflow and outflow in healthcare today is surely an uphill battle.

To resolve the predicament in times of external peace, policy-makers are faced with two choices: to borrow the outstanding amount from a bank (and indebt the work force of today and tomorrow) vs. to tap into annual taxation (and effectively charge the work force of today twice for the same service).

Unable to decide which option leads to the greater evil, most European states favor the third way – of a more ethical, hybrid option.

Yet, social justice has been breached. Some individuals take far more than their fair share from state's healthcare. Complaints are therefore raised of depleting resources.

Interestingly enough, not everyone who voices concern belongs to the health-care- and the tax-paying stratum.

Playing on the empathic nature of others, a group of social dependents have engaged in egocentric predatory practice. They demand more and free healthcare dividends.

The argument for the “necessary,” indeed “life-saving” handouts is a breach of contract with society, biology, and other states. The victims cannot lead productive lives due to lack of work opportunities, invalidation, or a repressive regime functioning elsewhere.

Any opposing opinion (or attempt at discussion) is met with immediate rebuttal.

Unfortunately, the rising trend of social extortion, based on the prevailing ethical norms in European states, is supplemented with another “bonus.”

Big hospitals are increasingly targeted by patients who, for the lack of a better term, “forget” all decorum, ethics, and civility. They jump the waiting line by faking stronger pain and a greater physical emergency.

Emotionally blackmailed into effective action, physicians prioritize by bringing forward the pushy, while leaving behind the socially compliant patients.

Another injustice is served. The rationale behind contemporary European ethics gets tested.

Will we ever reach a stable, universal, empathy-driven co-habitation?

The answer lies ahead. Until then, the social experiment continues.

1.3 Conclusions

This text tackles the concepts of empathy and ethics as they evolved throughout history and gradually became incorporated into the European healthcare sector. It also addresses current stresses on the thus created system.

The discussed issues impact all stakeholders – policy-makers, medical personnel, and patients [1, 2]. They can be resolved in two ways: first, through public

discourse and measures without compromise on European guiding ethical principles of social justice and, second, through technology – to streamline and widen data distribution and utilization, as well as improve patient survival outcomes, and telemedicine aimed at integrating remotely living patients, cut down on operational hospital costs and opportunist patient behavior therein.

Medicine is a profession guided by noble principles, but they must be reconciled not only downwards, with individual patient needs, but also upwards – with the politico-economic needs of the state, as substantial finances are needed to operate a state healthcare system. Since the latter often works at a loss (due to catering for unpaid emergency cases, rising prices of used goods and services, and general redundancies), it must receive direct contributions from the end beneficiaries (patients), pharmaceuticals (providing needed quality medicines in exchange for operating rights), and, ultimately, the manager/overseer of the healthcare system – the state.

References


1. K. Cornetta, C.G. Brown, Balancing personalized medicine and personalized care. *Acad. Med.: J. Associat. Am. Med. Coll.* **88**(3), 309–313 (2013)
2. V. Tananska, Medicine today – Strong systemization, zero empathy. Thoughts on necessary changes. *J. Bulgarian Med.* **5.3**, 33–37 (2015)
3. V. Tananska, Characteristics and pre-conditions for empathy: biology, reproduction, social environment, intellectual development & mindset. In Proc. the Annual Seminar “Interaction in the field of empathy”, Democritus University of Thrace, Xanti, Greece (2014). <http://elearning.didedra.gr/mod/resource/index.php?id=28>
4. V.V. Estrela, A.C. Monteiro, R.P. França, Y. Iano, A. Khelassi, N. Razmjoo, Health 4.0 as an application of industry 4.0 in healthcare services and management. *Med. Technol. J.* **2**(4), 262–276 (2019). <https://doi.org/10.26415/2572-004X-vol2iss1p262-276>
5. V.V. Estrela, E.G.H. Grata, Blade Runner 2049 and the quest for Industry 4.0. *Orient. J. Comp. Sci. Technol.* **10**(4) (2017). <https://doi.org/10.13005/ojst/10.04.01>
6. N.J. Zohar, Prospects for “genetic therapy” – Can a person benefit from being altered? *Bioethics* **5**(4), 275–288 (1991)
7. D.T. Wasserman, Better parenting through biomedical modification: A case for pluralism, deference, and charity. *Kennedy Inst. Ethics J.* **27**, 217–247 (2017)
8. C. Critchley, D. Nicol, G. Bruce, J. Walshe, T. Treleaven, B.E. Tuch, Predicting public attitudes toward gene editing of germlines: The impact of moral and hereditary concern in human and animal applications. *Front. Genet.* **9**, 704 (2018)
9. E.T. Juengst, Crowdsourcing the moral limits of human gene editing? *Hast. Cent. Rep.* **47**(3), 15–23 (2017)
10. E.T. Juengst, M. McGowan, J.R. Fishman, R.A. Settersten, From “personalized” to “precision” medicine: the ethical and social implications of rhetorical reform in genomic medicine. *Hast. Cent. Rep.* **46**(5), 21–33 (2016)
11. L. El-Alti, L. Sandman, C. Munthe, Person centered care and personalized medicine: Irreconcilable opposites or potential companions? *Health Care Anal.* **27**, 45–59 (2017)
12. J.D. Dagnone, Commentary: The physician as person framework: How human nature impacts empathy, depression, burnout, and the practice of medicine. *Can. Med. Educ. J.* **8**, e97–e98 (2017)

13. H. Fröhlich, R. Balling, N. Beerenwinkel, O. Kohlbacher, S. Kumar, T. Lengauer, M.H. Maathuis, Y. Moreau, S.A. Murphy, T.M. Przytycka, M. Rebhan, H.L. Röst, A. Schuppert, M. Schwab, R. Spang, D.J. Stekhoven, J. Sun, A. Weber, D. Ziemek, B. Zupan, From hype to reality: Data science enabling personalized medicine. *BMC Med.* **16**, 1–15 (2018)
14. www.dr-hempel-network.com/digital_preventive_healthcare/themes-preventive-medicine-deeper-look/. Accessed on Apr 13 2020

Chapter 2

Conceptual Model of Professional Supervision Study Based on Data Mining: A Study in the Regional Council of Nutritionists of the 4th Brazilian Region (Rio de Janeiro and Espirito Santo States)



Anderson Luiz Ignacio de Lima, Rosane Justino de Sousa Lima, and Henrique Rego Monteiro da Hora 

2.1 Introduction

A society provided by information technology is capable of producing a high amount of data, whose relevance grows at the same exponential pace [1–3], and it is no different in areas related to public health [4–6]. The availability of these large volumes of data, coupled with the application of artificial intelligence techniques, can solve health problems, hitherto not possible [7–9].

In this context, some studies present the use of mathematical tools for the treatment of data within the health area and report the achievement of satisfactory results. Bernstein et al. use statistics to compare the results of the statistical model versus clinical evaluation made by specialists for cases of unplanned readmission within 30 days after patient discharge and, thus, to estimate the risk, in addition to clinical intuition [10]. For the authors, the statistically driven model performed better than the clinically oriented model, helping to improve surgical quality and reduce costs.

Gibbons et al. [11] and Hautemaniere et al. [12] use mining techniques to monitor professional practice. Gibbons et al. use feedback text mining to assess variation in the professional performance of doctors in the United Kingdom [11], and Hautemaniere et al. use data mining to identify possible deaths from hospital infections [12]. Both concluded the applicability of the methods presented, indicating that their findings can inform future predictive models of performance and support the evaluation to improve the quality of professional practice.

A. L. I. de Lima (✉) · R. J. de Sousa Lima · H. R. M. da Hora
Instituto Federal de Educação, Tecnologia e Ciência Fluminense (IFF),
Campos dos Goytacazes, RJ, Brazil

Some of the purposes of the Regional Council of Nutritionists are to guide, supervise, inspect, and discipline the exercise of the profession, seeking the quality of services related to food and nutrition (Federal Brazilian Law N 6.583 [13]). In the inspection actions, one of the tools used by the inspectors is the technical visit scripts that were prepared based on the Resolution for the definition of the areas of activity of the nutritionist and their attributions (Resolution CFN N 380 [14]). These scripts are available at <http://www.crn4.org.br/fiscalizacaoroteiro-de-visita-tecnica.php> to permit the insertion of the data generated from the visits in a proprietary platform.

The set of data accumulated over the carried out inspections make up a precious material. Descriptive statistics can treat this information, and data mining techniques can expose behavior patterns of companies and supervised professionals. The resulting knowledge, if known and exposed, has excellent potential for use in the management of inspections and subsidizing future decision-making.

In this scenario, this article aims to generate useful information from the databases available in the information system of the Regional Council of Nutritionists of the 4th Region (CRN4), through data mining techniques, to expose behavior patterns of observed variables. This area comprises the states of Rio de Janeiro and Espírito Santo.

2.1.1 Data Mining

The vast amount of data available in the companies' databases hides much knowledge. Data mining transforms raw data into valuable information to assist decision-making [15].

According to Berson, Smith, and Thearling [16], data mining explores databases through tens of hundreds of different points of view. The difference between data mining and statistical techniques is in the use of the data itself for the discovery of patterns and not in the verification of hypothetical patterns.

Databases store knowledge that can help improve business, and traditional techniques only allow to verify hypotheses that are, approximately, only 5% of all the relationships found by these methods. Data mining can discover other unknown relationships: the remaining 95% [15].

Therefore, data mining is a set of techniques that involve mathematical methods, algorithms, and heuristics to discover patterns and regularities in large data sets.

2.1.2 Methodology

2.1.2.1 Research Classification

For its nature, this research is applied, because it uses techniques consolidated in the academy to solve problems and local realities. From its approach, the study is considered quali-quantitative. It is qualitative regarding data collection and composition of the variables of interest available in the form of the inspection script. Moreover, it is quantitative in the treatment of these variables when they are submitted to data mining algorithms [17].

For its objectives, the research is descriptive, since, from a set of data, it exposes the reality present in it without explaining its occurrence. Finally, for its procedures, the research is classified as a survey in data collection, bibliographic in its theoretical foundation, and case study, in the analysis of the object of study [18].

The research strategy was organized and structured in four sequential steps:

1. Definition and data collection
2. Data selection, pre-processing, and transformation
3. Data mining
4. Analysis and discussion of results

2.1.2.2 Definition and Data Collection

The data needed for the present research had identification restrictions, were made available, are the property of the Regional Council of Nutritionists of the 4th Brazilian Region (CRN4), and are the last of the inspections carried out by the CRN4 inspection team.

The research project was submitted to Plataforma Brasil, receiving the Certificate of Presentation for Ethical Appreciation under number 94572518.3.0000.5583, and obtained a substantiated opinion from the Research Ethics Committee, approving the project regarding ethical aspects. The CRN4 and the author signed the Institutional Cooperation Agreement Term sealing the commitment to exchange data and information to improve the inspection of professional practice, as well as working conditions, to promote policies in favor of the category.

All information and exclusive technical data, considered confidential by CRN4, provided under the agreement, were received and kept confidential. The collected data underwent treatment and anonymization not to allow the identification of the information holder.

The databases comprise the forms of the Technical Visit Routes (RVT) available at <http://www2.crn4.org.br/pg/fiscalizacao/visitasdefiscalizacao>, which are used in inspections and registered in the proper system for that purpose.

Technical visits are carried out with the nutritionist professional to guide and monitor professional practice.

The Technical Visit Routes are instruments developed to guide the visit of the Fiscal Nutritionist, enabling the gathering of information related to the professional practice and the support and guidance to the expert. They rely on the legislation of the CFN/CRN System that establishes the duties of professionals in the various areas of activity and on health legislation, seeking to contemplate the main mandatory aspects in a performance compatible with excellent quality standards [19].

This work uses the databases of four Technical Visit Routes, namely:

- Collective Feeding – Food and Nutrition Unit (FNU)
- School Feeding (SF)
- Clinical Nutrition – Hospital and Similar Institutions (HSI)
- Clinical Nutrition – Long-Term Institution for the Elderly (LTIE)

The records obtained and used are related to the results of the inspections carried out during the period from 2014 to 2018, covering the states of Rio de Janeiro and Espirito Santo.

2.1.2.3 Data Selection, Pre-processing, and Transformation

The stage of data pre-processing, according to [20], belongs to the Knowledge Extraction Process (KDD), where data mining is a critical stage. After data selection and before applying the data mining techniques, there is the selection and transformation stage. In this step, the original attributes of the database are converted and/or adapted to apply data mining.

In this step, the collected data are prepared for the mining process. They can be generalized and aggregated, or even new attributes can be created or deleted to understand the problem domain better. A typical procedure is the discretization or transformation of data into categories or quantitative ranges, for a better interpretation of the problem domain [21].

The database made available by CRN4 is presented in an Excel file. It comes in an unstructured form, requiring the use of a data dictionary for compatibility, use, and understanding of the data. After the application of the data dictionary, the variables “outcome” and “non-outcome” were identified, the necessary transformations were made, and then a comma-separated values (CSV) extension file was generated for reading by the analysis software. At the end of this stage, the database started to have a new configuration of attributes.

The analyzed RVTs also had a section with mandatory activities by the nutritionist, subdivided into Qualitative and Quantitative Indicators. Each indicator with the attributes that compose it with specific domain values for each indicator, namely, “Minimum Standard,” “Standard Target,” and “Does not reach minimum standard” for the attributes of the Qualitative Indicators and “Yes,” “No,” “Sometimes,” and “Not applicable” for the characteristics of the Quantitative Indicators. The attributes and domains were transformed, consolidating the attributes that make up the indicators into a single attribute for each indicator. In this way, the new attributes became

“Quantitative Indicators” and “Qualitative Indicators,” having as domains “Meets” and “Does not meet.”

To define the final outcome, it was considered as “Meets” only the cases in which all the original attributes have been met as “Minimum standard,” “Meta-standard,” or “Yes,” as the cases where only one attribute has been classified as “Does not reach the minimum standard,” “No,” or “Sometimes” indicates that the mandatory activities of the nutritionist are not being fulfilled.

Some specific attributes of each RVT were also transformed, which were replaced by intervals, taking into account the resolutions in force that deal with the minimum numerical parameters of reference for the nutritionist’s performance and the minimum numeric parameters within the scope of the School Feeding Program. For the Collective Feeding RVT – Food and Nutrition Unit (FNU), it was used as a domain of the attributes related to the number of meals, intervals according to the updated version (Resolution CFN N° 600, 2018). In this way, the number of small meals was converted into large meals, as directed in the Resolution, and only the large meal reference was utilized. The intervals became the same used as parameters of that Resolution.

The attributes of the School Feeding RVT, referring to the number of students, were also transformed, making them compatible with CFN Resolution No. 465 [22].

The number of beds referring to the RVT Clinical Nutrition – Hospitals and Similar Institutions was also transformed to adapt to the current Resolution (Resolution CFN No. 600 [23]). The quantities were considered according to its complexity, with the beds of medium complexity with intervals every 30 beds, and high complexity, with intervals every 15 beds.

The changes made regarding the RVT Clinical Nutrition – Long-Term Institution for the Elderly (LTIE) refer to the number of elderly people served. This quantity lists both the number of nutritionists per number of older people served and the necessary weekly technical workload, as CFN Resolution No. 600 [23].

2.1.2.4 Methodological Procedures and Analysis Techniques (Data Mining)

The algorithms were executed using the data mining tool Waikato Environment for Knowledge Analysis (WEKA), details in [24]; this has machine learning algorithms that can be used to extract relevant information from a database of data. The tool was adopted, according to the following reasons:

- (i) Open-source tool and free of cost
- (ii) Have several versions of algorithms used in data mining
- (iii) Availability of statistical resources to compare the performance of the algorithms and present several resources for data analysis

To assess the knowledge generated with the processing of the study base, data mining was performed using supervised learning for classification problems, and the classifier algorithm selected was J48 from WEKA, which offers a set of rules

that are easy to interpret by humans. The J48 algorithm is one of the most used in data mining, according to [25]. It uses machine learning with the divide-to-conquer scheme that decomposes a complex problem into simpler subproblems, and recursively the same strategy is applied to each subproblem [26].

As a result of the J48 algorithm application, the classifier outputs a precise model as a decision tree. The use of the decision tree serves to enhance and assist in making decisions more logically and rationally. The method assists in the decision process, as it allows the analysis of complex scenarios, and the graphic model favors the exploration of all the possibilities and results of a given decision, guiding in the best problem-solving.

The J48 algorithm employs the standard WEKA configurations with a tenfold cross validation test configuration to evaluate the model generalizability. Adjustments were made to the parameters “confidenceFactor” and “minNumObj,” to have better assertiveness in the results.

At the time of mining, for each RVT, two forms of data processing were performed, with the outcome of the attributes of the mandatory activities of the nutritionist, the first referring to the Qualitative Indicators and then the Quantitative Indicators. That is, in each processing, the decision trees were generated considering as an outcome the attributes of the mandatory activities of the nutritionist.

Regarding the period and region studied, this research used the RVTs registered between the years 2014 and 2018, in the states of Rio de Janeiro and Espírito Santo. Thus, all records that did not meet these criteria were discarded.

2.2 Discussion

In this section, the results obtained after applying the J48 classifier algorithm to the studied database are presented. The results were separated into topics with respect to their RVTs. The initial analyzes are done separately. In the end, a cross analysis between the RVTs is made, as well as a comparison with the works already published on the theme.

2.2.1 *Collective Feeding – Food and Nutrition Unit (FNU)*

In this subsection, the results obtained through data mining, performed on the “Collective Feeding FNU” basis between the years 2014 and 2018, in the states of Rio de Janeiro and Espírito Santo are presented. The results were obtained after the application of the J48 classifier algorithm consolidated on the studied database, considering both the Qualitative Indicators Outcome and the Quantitative Indicators Outcome.

2.2.1.1 Qualitative Indicators

Through the decision tree, it is possible to infer that the use of Standardized Operating Procedures (SOP) is a critical item, and its nonuse suggests that the establishment will also not comply with the mandatory activities of the nutritionist.

However, considering that the use of SOP occurs as a technical-administrative resource, attention is now focused on the use of technical reports/nonconformities, which, if unused, suggests that it will not comply with the mandatory activities of the nutritionist.

The number of sources of technical updates was also shown to be an essential factor in raising awareness, indicating that greater coverage in the information channels suggests a higher rate of compliance with mandatory activities (Fig. 2.1).

2.2.1.2 Quantitative Indicators

For the decision tree generated from the Quantitative Indicators, the indication is that if there is no supervision of the periodic control of rest-intake, then the monitoring and guidance of the nutrition trainees become the relevant factor, in which the cases where this monitoring occurs suggest that the mandatory activities of the nutritionist are being fulfilled. In contrast, with the supervision of the periodic control of rest-intake, the use of technical reports/nonconformities becomes the driver, where their nonuse indicates the nonfulfillment of mandatory activities.

The indicator of periodic control of rest-intake is presented as a complementary activity of the nutritionist at FNU in Resolution CFN No. 380 [14]; however, with

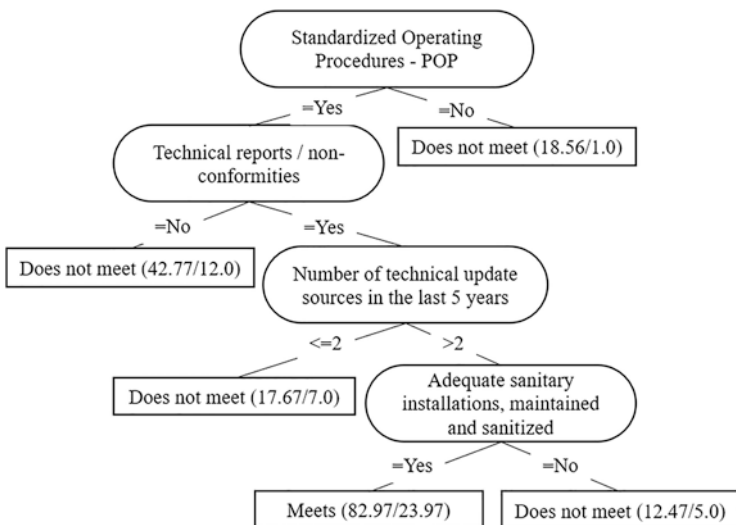


Fig. 2.1 Decision tree – FNU – qualitative indicators outcome

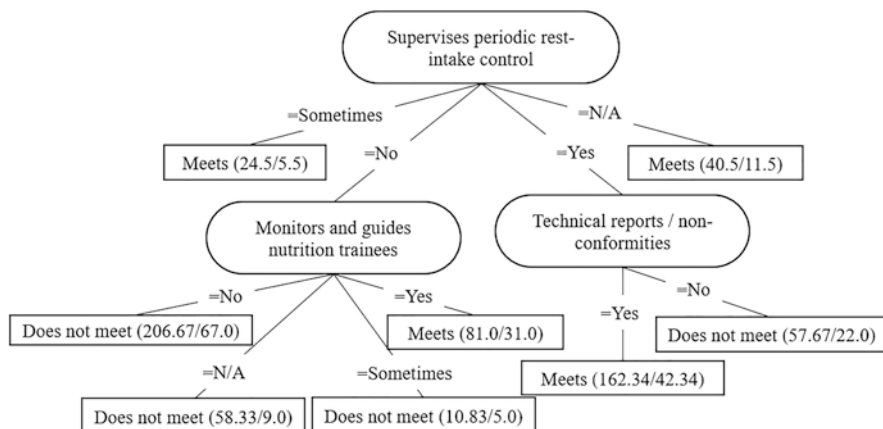


Fig. 2.2 Decision tree – FNU – quantitative indicators outcome

the update to Resolution No. 600 [23], this activity became mandatory. The result presented in the decision tree of the periodic control of rest-ingestion as root node of the tree corroborates and reinforces the importance of this activity, as also identified by the CFN itself, which is now considered a mandatory activity in the new version of the Resolution that defines the areas of activity of the nutritionist and their duties and indicates minimum numerical parameters of reference, by area of activity, for the effectiveness of the services provided to society (Fig. 2.2).

2.2.2 School Feeding

In this section, the results obtained through data mining, performed on the “School Feeding” basis, are presented.

2.2.2.1 Qualitative Indicators

The tree demonstrates that the use of specific computer programs helps in fulfilling the mandatory activities of the nutritionist, as it facilitates and streamlines the daily routine of the nutritionist.

For cases where specific programs are not used, the execution of the annual plan within the scope of the National School Feeding Program (PNAE) [27] becomes decisive, where only when executed does it present possibilities of fulfilling mandatory activities (Fig. 2.3).

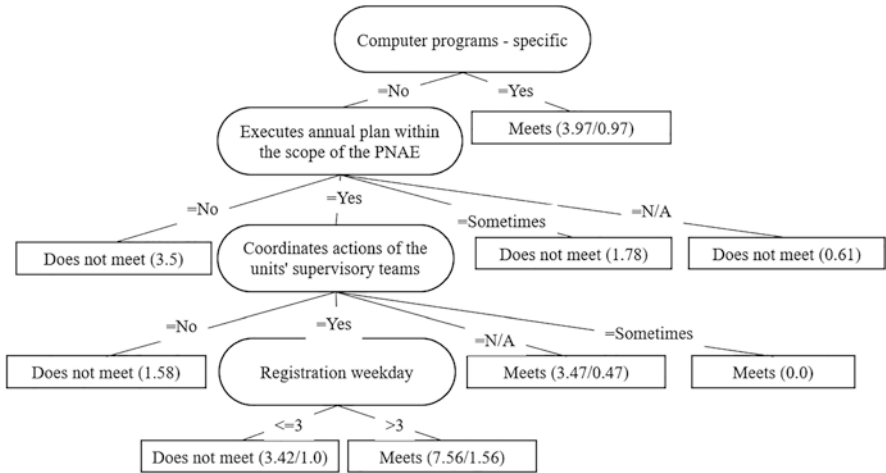


Fig. 2.3 Decision tree – school feeding – qualitative indicators outcome

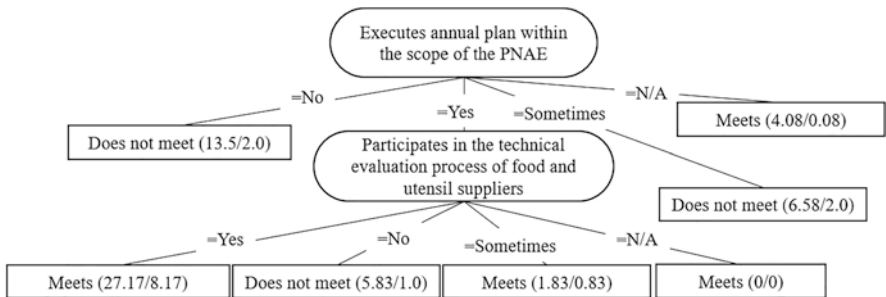


Fig. 2.4 Decision tree – school feeding – quantitative indicators outcome

2.2.2.2 Quantitative Indicators

The execution of the annual plan strongly influences the Quantitative Indicators within the scope of the PNAE since the decision tree generated, the situations where the execution of the plan was not carried out, showed tendencies in not meeting the outcome of the mandatory activities [27]. On the other hand, in case of implementing the plan, the item that becomes important is the participation in the process of technical evaluation of the suppliers of foodstuffs and utensils, where if there is no participation, it suggests that the requirement is not met (Fig. 2.4).

2.2.3 Clinical Nutrition – Hospital and Similar Institutions

In this section, the results obtained through data mining presented based on “Clinical Nutrition – Hospital and Similar Institutions” are presented.

2.2.3.1 Qualitative Indicators

The use of equipment for anthropometric assessment proved to be necessary for the conclusion of the qualitative outcome, because, when not used, they indicate that the mandatory activities of the nutritionist are also not being met. However, if anthropometric assessment equipment is being used, the fact that there is a technical supervisor indicates a higher incidence of compliance with mandatory activities. This fact can be explained by the presence of a superior accompanying the activities of the other nutritionists. If there is no technical supervisor, carrying out studies and research in your area of activity becomes of significant influence, suggesting that, when this fact is true, it also tends to meet the mandatory activities of the nutritionist (Fig. 2.5).

For the Quantitative Indicators, the most relevant item is the professional’s specialization. However, if the hospital/clinic is philanthropic, the suggested indication is that the mandatory activities are not being carried out. On the other hand, for situations with professionals without specialization, the time of drawing up became significant, with the evening period being the most favorable to verify the fulfillment of the mandatory activities of the nutritionist (Fig. 2.6).

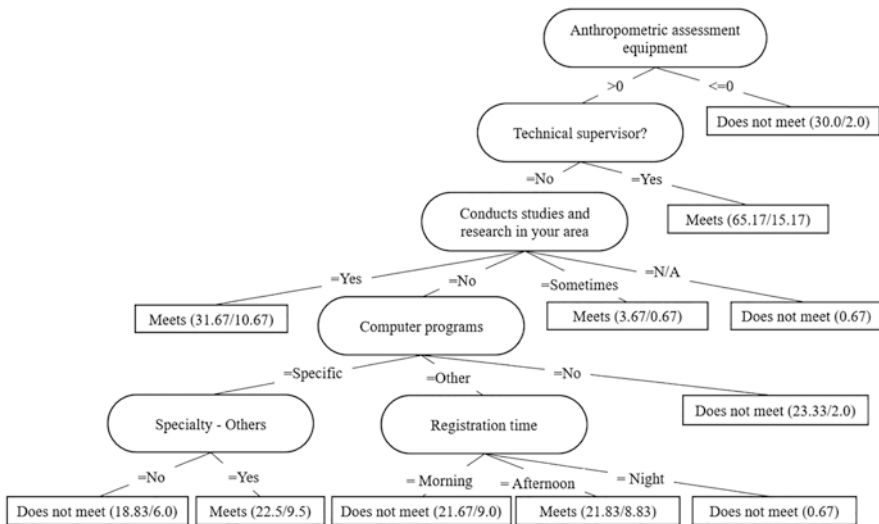


Fig. 2.5 Decision tree – hospitals and similar institutions – qualitative indicators outcome

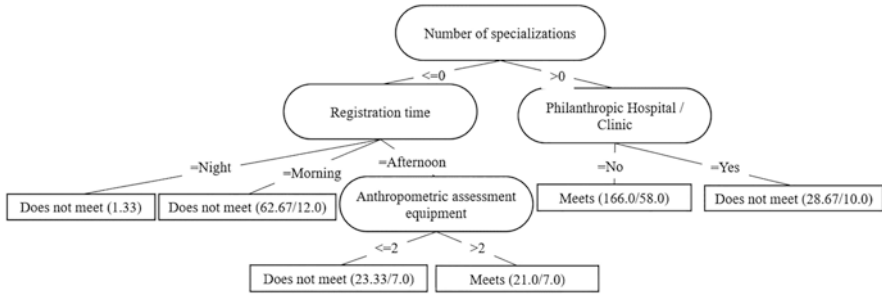


Fig. 2.6 Decision tree – hospitals and similar institutions – quantitative indicators outcome

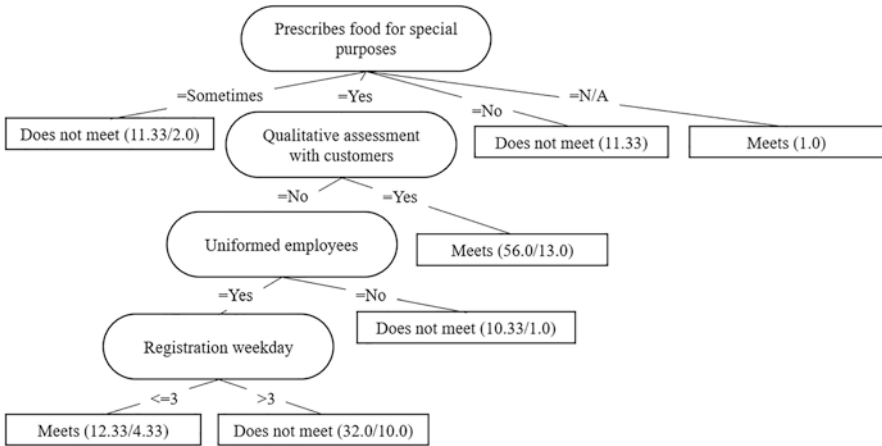


Fig. 2.7 Decision tree – LTIE – qualitative indicators outcome

2.2.4 Clinical Nutrition – Long-Term Institution for the Elderly (LTIE)

This section presents the results obtained through data mining, carried out based on “Clinical Nutrition – Long-Term Institution for the Elderly.”

2.2.4.1 Qualitative Indicators

The decision tree seen in Fig. 2.7 indicated as the most critical attribute of the prescription of foods for special purposes, suggesting that the nonprescription or inconsistency in the prescription causes the nonfulfillment of the mandatory activities of the nutritionist. Sequentially, the next attribute to observe is related to qualitative assessment with customers, suggesting that the execution of satisfaction surveys reflects the fulfillment of mandatory activities.

The prescription of food for particular purposes in the senile age group is a valuable item. This happens due to the natural and progressive decrease in muscle mass present in that age group, known as sarcopenia, indicating that the fulfillment of mandatory activities will provide information that will provide the identification and screening nutritional risk.

A study by Landi et al. indicates the high prevalence of sarcopenia among residents of Long-Term Care Institutions for the Elderly, identifying the nutritional risk and the decrease in muscle mass in these older people [28]. It reports the importance of dietary supplementation in this age group for the correction and prevention of sarcopenia. The study by Landi et al. confirmed the importance highlighted by the decision tree [28]. They indicate the prescription of food for special purposes as an attribute of greater relevance. This finding was also reported by Patronillo et al. [29]. Protein supplementation should be considered in elderly people at nutritional risk (or with sarcopenia already established), who do not reach the daily protein intake necessary to meet metabolic needs through dietary changes and without medical contraindications.

2.2.4.2 Quantitative Indicators

The quantitative outcome of Clinical Nutrition at LTIE has as its main attribute the qualitative assessment with clients, where the simple fact of carrying out a satisfaction survey with clients becomes an indicator of compliance with the mandatory activities of the nutritionist. However, failure to carry out the evaluation highlights the importance of using or not uniforms by employees, where nonuse suggests that mandatory activities are also unfulfilled. In the case of the use of uniforms, the next attribute to become relevant to the quantitative outcome is the existence of lavatories and aseptic products for handlers, emphasizing that the fulfillment of this attribute indicates a higher probability of fulfilling the mandatory activities of the nutritionist (Fig. 2.8).

2.2.5 Comparison between RVTs

Figure 2.9 shows the temporal distribution of the amount of RVT between the years 2014 and 2018, in the states of Rio de Janeiro and Espírito Santo.

The distribution of the number of RVTs over time is more concentrated between the years 2016 and 2017, wherein in 2016 there was a significant increase in the number of RVTs, growing a little more in 2017, but retreating again in 2018, but still at a level higher than the years 2014 and 2015.

The graph also shows a considerable difference in the number of RVTs related to Collective Food – FNU concerning the others, being higher than double the sum of the other three.

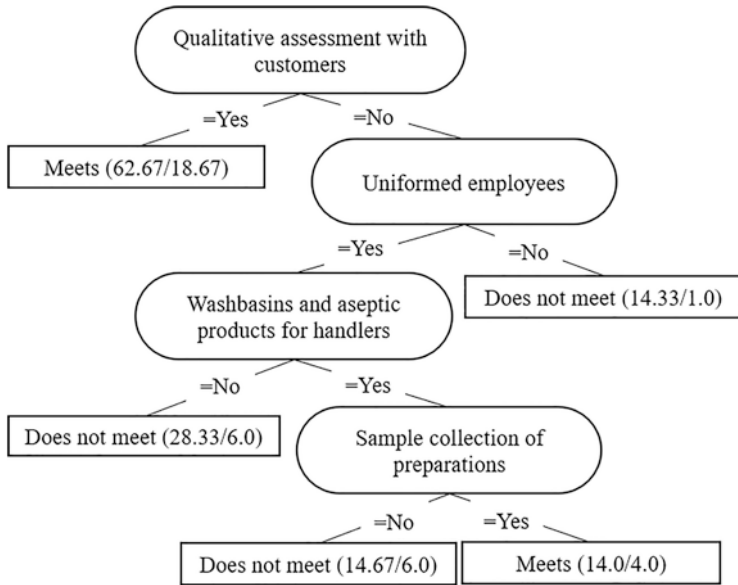


Fig. 2.8 Decision tree – LTIE – quantitative indicators outcome

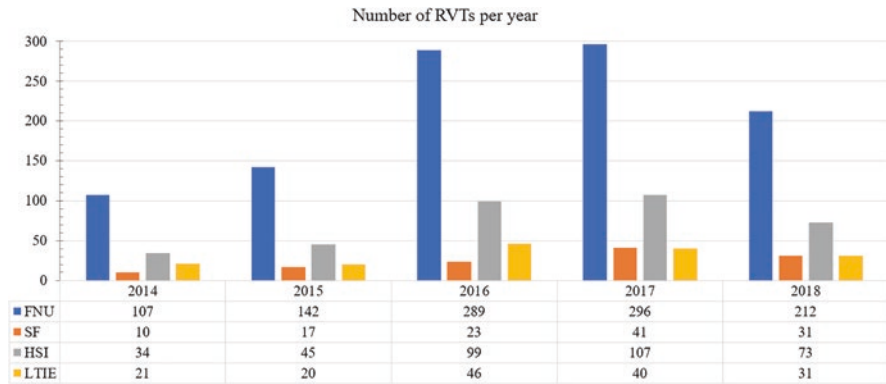


Fig. 2.9 Number of RVTs per year

Figure 2.10 shows the specifics of each RVT considering the attributes “Quantitative Indicator,” abbreviated in the Table (Fig. 2.10) as “Quant. Ind.,” and “Qualitative Indicator” abbreviated in the Table as “Qual. Ind..”

Through the results presented in Fig. 2.10, it can be observed that the precision for the classification “Does not meet” was superior to the accuracy for the classification “Meets” in all attributes of all RVTs. This is a decisive factor for the application and usability of the proposed decision-making model. This happens because these are tax actions and precision becomes more relevant for the definition of

	FNU		SF		HSI		LTIE	
	Quant. Ind.	Qual. Ind.	Quant. Ind.	Qual. Ind.	Quant. Ind.	Qual. Ind.	Quant. Ind.	Qual. Ind.
Does not meet	76,5	95	80,8	92,5	66,7	74,7	67,6	72
Meets	50,7	20,4	34,8	17,9	58,7	50,6	56,6	66,7
Weighted average	67,3	86,8	69,2	84,4	63,1	65,8	62,6	69,5

Fig. 2.10 Precision values for each outcome

noncompliance, particularly the classification “Does not meet” to the detriment accuracy to define compliance, in this case, the “Meets” classification.

This work presented a way of predicting the fulfillment of mandatory activities, using data from previous inspections, which are observations verified at the place visited through the Technical Visit Guide and carried out by a trained professional for inspection, thus helping and serving as a guide for future inspections.

Literature lack studies that use formal inspection data mining to verify the professional practice. What was found are works that use mining with the evaluation of comments in the open text, made by peer professionals as Gibbons et al. [11], or the database resulting from professional practice as presented by Hautemaniere et al. [12], which uses a mortality database from a university hospital, to verify professional conduct.

Other authors use statistics to compare the results of a statistical model versus clinical evaluation by specialists, as Bernstein et al. [30], in his work, which uses data from patients to make comparisons. Layzell [31] contextualizes the inadequate prescription of medications in postoperative patients, to identify, through an audit carried out during 5 weeks in a recovery ward, the delays suffered by patients for pain relief in the postoperative period and the reasons.

These works show undirected assessments and some even punctual, where there is no script or standard for verification or continuity, and may present biased or superficial results. In the past, none of them has sought to provide subsidies to official inspection bodies.

The work that comes closest to this goal is the study by [32] that uses online reviews from US restaurant consumers and introduces the vision of building a combined real-time inspection system with routine inspections by the public health department to prevent users from suffering foodborne illnesses. The authors explore analyses with sets of keywords that denote foodborne illnesses and use supervised learning techniques to classify the data to predict whether an assessment indicates foodborne diseases. In particular, they detect assessments that predict foodborne diseases, selected resources, and classification methods.

In view of the lack of specific studies involving data mining techniques and inspection of professional practice, this work contributes by presenting the feasibility of extracting strategic information from the Professional Council’s own database [33–35].

It is believed that the results obtained are of interest to CRN4 and to other Professional Councils and the method presented here can be reused in other

databases. For this reason, as future work, it is expected to use the present methodology in databases of other councils in the area, in order to serve as material for future inspection actions, directing and assisting in the prioritization of verification items when in inspection visits, helping to identify irregularities and nonconformities [36–41].

2.3 Conclusion

This research had the purpose of analyzing the behavior of the data resulting from the fiscal actions of the Regional Council of Nutritionists of the 4th Brazilian Region. The application of the J48 WEKA classifier algorithm returned satisfactory results, with classification accuracy for nonconformity, well above the classification accuracy for conformity, mainly for Qualitative Indicators, where it presented up to 95% accuracy for the classification “Does not meet,” which expresses the reliability of the information generated.

The high percentage values achieved in the accuracy parameters indicate that the level of reliability of the results obtained is satisfactory, which allows inferences consistent with the reality of the object of study.

According to the results obtained, we can conclude that it is possible to find a result trend and potential patterns in the proposed outcomes for the data mining process using the database from previous inspections [36–41].

For each RVT, the most critical and influential relative and specific attributes of the area in which the RVT itself operates are highlighted, such as (i) the execution of the annual plan under the PNAE for the School Feeding area and (ii) the prescription of food for special purposes for Long-Term Institutions, indicating the particularity of each region [27].

This study can serve as material for future inspection actions, directing and assisting in prioritizing verification items at the time of inspection visits, while helping to identify irregularities and nonconformities [42–44].

References

1. B. Neves, A. Raimundo, Z. Obermeyer, The quiet revolution of big data in medicine. *Med. Int.* **24**(4) (2017). <https://doi.org/10.24950/rspmi/Perspective/2017>
2. V.V. Estrela, A.C.B. Monteiro, R.P. França, Y. Iano, A. Khelassi, N. Razmjoooy, Health 4.0: applications, management, technologies and review. *Med. Tech. J.* **2**(4), 262–276 (2019). <https://doi.org/10.26415/2572-004X-vol2iss1p262-276.262>
3. V.V. Estrela, O. Saotome, H.J. Loschi, D.J. Hemanth, W.S. Farfan, R.J. Aroma, C. Saravanan, E.G.H. Grata, Emergency response cyber-physical framework for landslide avoidance with sustainable electronics. *Technologies* **6**, 42 (2018). <https://doi.org/10.3390/technologies6020042>
4. M.d.F. Pina, M.S. Carvalho, *GeoMed 2017: Visao mais profunda a partir de big data e pequenas areas.* *Cad. Saude Publica.* **33**(10) (2017). <https://doi.org/10.1590/0102-311x00172017>















5. C.E.V. Marinho, V.V. Estrela, H.J. Loschi, N. Razmjoooy, A.E. Herrmann, Y. Thiagarajan, M.P. Vishnevski, A.C.B. Monteiro, R.P. França, Y. Iano, A model for medical staff idleness minimization, in *Proceedings of the 4th Brazilian Technology Symposium (BTSym'18)*. *BTSym 2018. Smart Innovation, Systems and Technologies*, ed. by Y. Iano, R. Arthur, O. Saotome, V. Vieira Estrela, H. Loschi, vol. 140, (Springer, Cham, 2019)
6. L.M. Abreu, H.R.M. Hora, J.J.A. Rangel, M. Erthal Jr., N. Razmjoooy, V.V. Estrela, T. Edoh, G.G. de Oliveira, Y. Iano, A multi-criteria modelling for ranking CO2 emitting G20 countries from the Kaya and their impacts on elderly health, in *Proceedings of the 5th Brazilian Technology Symposium (BTSym'19)*. *BTSym 2019. Smart Innovation, Systems and Technologies*, ed. by Y. Iano et al., (Springer, Cham, 2020)
7. L.C. Lobo, *Inteligencia Artificial e Medicina*. *Rev. Bras. Educ. Med.* **41**(2), 185–193 (2017). <https://doi.org/10.1590/1981-52712015v41n2esp>
8. N. Razmjoooy, V.V. Estrela, H.J. Loschi, Entropy-based breast cancer detection in digital mammograms using world cup optimization algorithm. *Int. J. Swarm Intellig. Res. (IJSIR)* **11**(3), 1–18 (2020). <https://doi.org/10.4018/IJSIR.2020070101>
9. V.V. Estrela, J.M.R.S. Tavares, L. Wang, S. Fuqian, J. Hemanth, SPECIAL ISSUE: Soft Computing Techniques for Image Analysis in the Medical Industry – Current Trends, Challenges and Solutions, Editorial, *IEEE Access*, IEEE (2018)
10. D.N. Bernstein, A. Keswani, D. Ring, Perioperative risk adjustment for total shoulder arthroplasty: are simple clinically driven models sufficient? *Clin. Orthop. Relat. Res.* (2017). <https://doi.org/10.1007/s11999-0165147-y>
11. C. Gibbons, S. Richards, J.M. Valderas, J. Campbell, Supervised machine learning algorithms can classify open-text feedback of doctor performance with human level accuracy. *J. Med. Internet Res.* (2017). <https://doi.org/10.2196/jmir.6533>
12. A. Hautemaniere, A. Florentin, P. Hartemann, P.R. Hunter, Identifying possible deaths associated with nosocomial infection in a hospital by data mining. *Am. J. Infect. Control* (2011). <https://doi.org/10.1016/j.ajic.2010.04.216>
13. Federal Brazilian Law N 6.583. Cria os Conselhos Federal e Regionais de Nutricionistas, regula o seu funcionamento, e d'a outras providências. *Pub. L. No. LEI No 6.583* (1978)
14. Federal Resolution CFN N 380. Dispoe Sobre a Definicao das Areas de Atuacao do Nutricionista e Suas Atribuicoes, Estabelece Parametros Numericos de Referencia, Por Area de Atuacao, e da Outras Providencias. *Conselho Federal de Nutricionistas*. *Pub. L. No. RESOLUCAO CFN No 380* (2005)
15. D.C.C. Barbosa, M.A. Machado, Mineracao de Dados usando o software WizRule em Base de Dados de Compras de TI. *Revista Eletronica de Sistemas de Informacao* **6**(1) (2007). <https://doi.org/10.21529/RESI.2007.0601001>
16. A. Berson, S. Smith, K. Thearling, *Building Data Mining Applications for CRM* (McGraw-Hill, New York, 2000)
17. E.L. da Silva, E.M. Menezes *Metodologia da Pesquisa e Elaboracao de Dissertacao* (4th ed. rev. atual., Vol. 138) (2005)
18. A.C. Gil, *Metodos e tecnicas de pesquisa social* (Atlas, Sao Paulo, 2008)
19. CRN4. *Inspection (Fiscalizacao)*. *Visitas de Fiscalizacao* (2019). Available in: <http://www2.crn4.org.br/pg/fiscalizacao/visitasdefiscalizacao/>. Acessado em 08 Dec 2019
20. J. Han, M. Kamber, *Data Mining: Concepts and Techniques*, 3rd edn. (Elsevier, Burlington, 2011)
21. J.D.J. Costa, F.C. Bernardini, J. Viterbo Filho, A mineracao de dados e a qualidade de conhecimentos extraidos dos boletins de ocorrencia das rodovias federais brasileiras. *AtoZ: Novas praticas em informacao e conhecimento* **3**(2), 139 (2014)
22. Resolution CFN N 465. Dispoe sobre as atribuicoes do Nutricionista, estabelece parametros numericos minimos de referencia no ambito do Programa de Alimentacao Escolar (PAE) e da outras providencias. *Conselho Federal de Nutricionistas*. *Pub. L. No. RESOLUCAO CFN No 465* (2010)
23. Resolution CFN N 600. Dispoe sobre a definicao das areas de atuacao do nutricionista e suas atribuicoes, indica parametros numericos minimos de referencia, por area de atuacao, para a

- efetividade dos serviços prestados a sociedade e de outras providências. Conselho Federal de Nutricionistas. Pub. L. No. RESOLUC, AO CFN No 600 (2018)
24. E. Frank, M.A. Hall, I.H. Witten, *The WEKA Workbench. Online Appendix for Data Mining: Practical Machine Learning Tools and Techniques* (Morgan Kaufmann, San Francisco, 2016)
 25. X. Wu, V. Kumar, J. Ross Quinlan, J. Ghosh, Q. Yang, H. Motoda, D. Steinberg, Top 10 algorithms in data mining. *Knowl. Inf. Syst.* **14**(1), 1–37 (2008). <https://doi.org/10.1007/s10115-007-0114-2>
 26. J. Gama, *Arvores de Decisao* (2002). Last seen in 01/02/2020. <https://www.dcc.fc.up.pt/ines/aulas/MIM/arvoresdedecisao.pdf>
 27. Brazilian Ministry of Education, *Manual de apoio para as atividades técnicas do Nutricionista no âmbito do PNAE* (Fundo Nacional de Desenvolvimento da Educação, Brasília, 2018)
 28. F. Landi, R. Liperoti, D. Fusco, S. Mastropaolo, D. Quattrociochi, A. Proia, A. Russo, R. Bernabei, G. Onder, Prevalence and risk factors of sarcopenia among nursing home older residents. *J. Gerontol. Ser. A* **67A**(1), 48–55 (2012). <https://doi.org/10.1093/gerona/glr035>
 29. C. Patronillo, M.T. Verissimo, *Suplementos proteicos e Sarcopenia no idoso –Artigo de Revisão* (Faculdade de Medicina. Universidade de Coimbra, Coimbra, 2015)
 30. D.N. Bernstein, A. Keswani, D. Ring, Perioperative risk adjustment for total shoulder arthroplasty: are simple clinically driven models sufficient? *Clin. Orthopaed. Relat. Res.* **475**(12), 2867–2874 (2017). <https://doi.org/10.1007/s11999-016-5147-y>
 31. M. Layzell, Improving the management of postoperative pain. *Nurs. Times* **101**(26), 34–36 (2005)
 32. Z. Wang, B.S. Balasubramani, I.F. Cruz, in *ACM SIGSPATIAL Workshop on Smart Cities and Urban Analytics (UrbanGIS)*. Predictive Analytics Using Text Classification for Restaurant Inspections. Article No.: 14, pp. 1–4. <https://doi.org/10.1145/3152178.3152192> (2017)
 33. M.J.A. Berry, G. Linoff, *Data Mining Techniques: For Marketing, Sales, and Customer Relationship Management*, 2nd edn. (Wiley, Indianapolis, 2004)
 34. S.M. Weiss, N. Indurkha, *Predictive Data Mining: A Practical Guide* (Morgan Kaufmann Publishers, San Francisco, 1998)
 35. N.D. Hansen, *Web Data Mining for Public Health Purposes*. ArXiv, abs/1905.00829 (2019)
 36. A. Trajman, N. Assuncao, M. Venturi, D. Tobias, V. Tochi, V. Brant, A preceptoría na rede básica da Secretaria Municipal de Saúde do Rio de Janeiro: Opinião dos profissionais de saúde. *Rev. Bras. Educ. Med. Rio de Janeiro* **33**(1), 24–31 (2009)
 37. F.D. Silva, V.V. Estrela, L.J. Matos, Hyperspectral analysis of remotely sensed images, in *Sustainable Water Management in the Tropics and Subtropics-and Case Studies in Brazil*, ed. by C. Biblio, O. Hensel, J. F. Selbach, vol. 2, 1st edn., (University of Kassel, Kassel, 2011), pp. 398–423. ISBN: 9788563337214
 38. C.D. Leite, J.G. Rodrigues, T.D. Sousa, H.R. da Hora, *IT Services Management and ISO 20000: A Case Study in an IT Remote Support Company* (2014)
 39. G.T. Monteiro, H.R. Hora, *Pesquisa em Saúde Pública: como desenvolver e validar instrumentos de coleta de dados* (2014)
 40. M.D. Mussa, S.C. Souza, E.F. Freire, R.G. Cordeiro, H.R. da Hora, Business intelligence in education: An application of Pentaho software. *Revista Produção e Desenvolvimento* **4**, 29–41 (2018)
 41. L.R. Martins, L.D. Pereira, L.M. Almeida, H.R. da Hora, H.G. Costa, Study on the most appropriate scale for use in questionnaires: an experiment with Kano’s model. *Vértices* **13**(1), 73–100 (2011)
 42. N. Rosso, P.J. Giabbanelli, Accurately inferring compliance to five major food guidelines through simplified surveys: applying data mining to the UK National Diet and nutrition survey. *JMIR Pub. Health Surveill* **4** (2018)
 43. Y.E. Silva, C.G. Salgado, V.M. Conde, G.A. Conde, *Data Mining Using Clustering Techniques as Leprosy Epidemiology Analyzing Model* (DMBD, 2018)
 44. R. Valter, S. Santiago, R. Ramos, M.V. Oliveira, L.O. Andrade, I.C. Barreto, in *2019 IEEE International Conference on E-Health Networking, Application & Services (HealthCom)*. Data Mining and Risk Analysis Supporting Decision in Brazilian Public Health Systems (2019), pp. 1–6

Chapter 3

Building Bridges and Remediating Illiteracy: How Intergenerational Cooperation Foster Better Engineering Professionals



M. A. de Jesus , Vania Vieira Estrela , R. J. Aroma , N. Razmjoo ,
S. E. B. da Silva , A. C. de Almeida , H. R. M. da Hora , A. Deshpande ,
P. Patavardhan , Nikolaos Andreopoulos , Andrey Terziev ,
K. Raimond , Hermes J. Loschi , and Douglas A. Nascimento 

3.1 Introduction

Developing logical and arithmetic skills contributes significantly to improve senior citizens' mental capacity and avoid some health conditions. Distance education (DE) or long-distance learning alludes to training who are not physically at a classroom to accommodate their lives to societal and workforce fluctuations [1].

Dyscalculia is the math equivalent to dyslexia and independent from IQ. Nowadays, it hinders math literacy deterring people from using it in their lives and keeping their brains sharp by using this type of knowledge experiencing time, measurements, and spatial perception [2, 3].

Exploratory information was obtained from meetings with stakeholders: all either individually as each person works on the environment or through the

M. A. de Jesus · S. E. B. da Silva · A. C. de Almeida · A. Terziev
Universidade Estadual do Norte Fluminense (UENF), Campos dos Goytacazes, RJ, Brazil

V. V. Estrela (✉)
Department of Telecommunications, Federal Fluminense University (UFF),
Niterói, RJ, Brazil
e-mail: vania.estrela.phd@ieee.org

R. J. Aroma · K. Raimond
Department of Computer Science and Engineering, Karunya University,
Coimbatore, Tamil Nadu, India
e-mail: kraimond@karunya.edu

N. Razmjoo
Department of Electrical Engineering, Tafresh University, Tafresh, Iran

intercession of a tutor. The numerical information database (problem bank) about the four operations allows math training with decimal places. This database can be expanded altogether with only a guide conversing with the subjects (remotely or not), a group of learners and tutors, or learners alone.

3.1.1 Motivation

The elderly need math skills to perform everyday tasks like managing medicine dosages, doing income taxes, paying bills, time management, budget control, and preparing meals to exemplify and demonstrate the meaning and usefulness of math [4].

Technology keeps on delivering more and more gadgets to face these challenges that often eliminate mental calculations, critical thinking, and awareness of the self. However, calculations and estimations are essential for intuitive perception and critical concerns about the desired outcome. The relevance of mathematics skills for making decisions in everyday life (i.e., the propensity to recognize and solve quantitative issues in real-life situations) lacks adequate metrics and evaluation methods.

Emotions play a role in math anxiety, which is performance-based anxiety with symptoms akin to social anxiety, and it is related to situations demanding or anticipating performance [4, 5]. The mutual relationship between self-belief and math performance is essential, as well. High math confidence may favor its use. In daily life, mathematical reasoning may benefit medical and financial selections significantly but might be troubled in several ways.

H. R. M. da Hora
Instituto Federal de Educação, Tecnologia e Ciência Fluminense (IFF),
Campos dos Goytacazes, RJ, Brazil

A. Deshpande
Angadi Institute of Technology & Management, Belgaum, Karnataka, India

P. Patavardhan
Dayananda Sagar University, Bengaluru, Karnataka, India

N. Andreopoulos
Technological Institute of Iceland, Tæknigarður, Reykjavík, Iceland

H. J. Loschi · D. A. Nascimento
Universidade Estadual de Campinas, Campinas, SP, Brazil

Uniwersytet Zielonogórski, Zielona Góra, Poland
e-mail: eng.hermes.loschi@ieee.org; eng.douglas.a@ieee.org

3.1.2 *Distance Education*

The Internet of Things (IoT) and cloud-enabled solutions arrange for the prospect to shape new, attractive smart, connected distance education (DE) frameworks, assistive learning, collaborative caregiving, and healthcare systems [4, 6].

DE can be paced (PDE) and self-paced (SPDE). The PDE format resembles traditional classroom-based paradigms in which learners initiate and finish a class on a given subject at an equal time. SPDE is presently the most common style of DE delivery. Alternatively, some establishments offer SPDE programs that permit registration at any time, and a variable course duration set according to the learner's timing, abilities, and dedication levels. SPDE is generally asynchronous, whereas PDE can be either synchronous or asynchronous. Each delivery pattern has both benefits and drawbacks for learners, instructors, and institutions.

SPDE affords autonomy for learners to commence their revisions and training at any time. Nonetheless, they can also proceed with sessions speedily, if they want. Students often enter SPDE when they experience stress to finish programs or accomplish a particular task, cannot complete an orthodox course, require extra classes, or have some other hardship, which impedes standard study for any period. The SPDE nature of the virtual classrooms, though, is an intimidating education paradigm for a plentiful of learners and can incite procrastination besides course incompleteness. Although learning assessment can be a caveat as tests can happen on any day, allowing students to share test questions with subsequent loss of academic honor, this can be circumvented by having some random number generation. Ultimately, coordinating collaborative effort activities can be a hurdle. However, some schools have cooperative models relying on networked and connected SPDE pedagogies.

This manuscript comprises these parts: Section 3.2 describes the methodology, and Sects. 3.3 and 3.4 address, respectively, the discussions and conclusions of this project.

3.2 Methodology

The Dynamic System for Assemblage and Execution of Interactive Classes (SISDI) has as its primary objective to train individuals that struggle to perform mathematical calculations with decimal places. SISDI encompasses a set of choices for the learner to elect the intended content. Then, the SISDI employs this knowledge to mount and display an adequate class, and the student must choose the class development pace. The examples' varieties to be explored involve the quantity, detail level, and degree of difficulty and are pre-set by the instructor. The student solves cases interactively informing the data necessary to

- (i) Feed the learning engine
- (ii) Accomplish a particular task
- (iii) Go either to the subsequent step or try to resignify the content

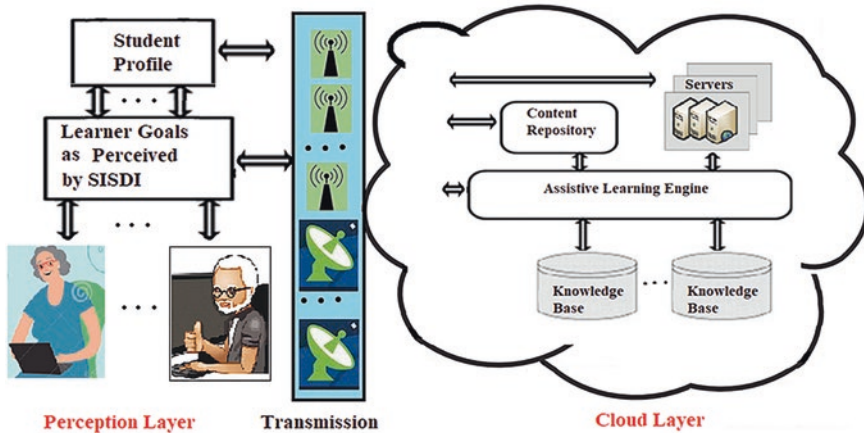


Fig. 3.1 SISDI perceived as a cyber-physical system

Figure 3.1 shows the cyber-physical system corresponding to the whole SISDI framework relying on a web-based environment comprising a content repository (CR) and the students' profile storage (SPS) [7–10]. This last module handles the information about the students, their behavior, and their goals. Each learner requires a knowledge evolution record identifying the necessary adaptation and a monitoring module providing tutors with data on the person's progression

The assistive learning engine (ALE) adapts the content displayed to the learner, the type of pedagogy, and the presentation to each student.

A typical object-oriented (OO) system has multiple layers [11–13], e.g., if the framework possesses three layers, (i) graphical user interfaces (GUIs), (ii) design of the application logic layer with domain objects, and (iii) the technical services layer, such as interfaces with database or registry error – usually independent of the application and reusable [13–15]. Creating layers breaks the complexity of software [13, 16, 17]. The SISDI analysis uses case diagrams and actors, and their associations appear in Fig. 3.2.

The use cases address the outer framework interface and specify many of the SISDI necessities to attain goals better. Figures 3.3 and 3.4 allude to the SISDI's Choose Example use case [14–17], where the user chooses an example to train. The SISDI's activity diagram demonstrates the accomplishments and changes starting from one activity to the next with the events happening in any part of the framework.

Sequence diagrams depict the flow of messages between different items, which are represented by dashed vertical lines with the name of the item on the top. The time axis is vertical at the same time expanding, so messages to be sent commence with one item and then onto the next as bolts with the activity and the names of the parameters, as the SISDI model example (Fig. 3.4). In implementing the SISDI, the case study was a division with decimal places by the fact that people find great difficulties in this type of mathematical operation. SISDI comprises several screens as follows (Figs. 3.5, 3.6, 3.7 and 3.8).

Fig. 3.2 Use case diagram

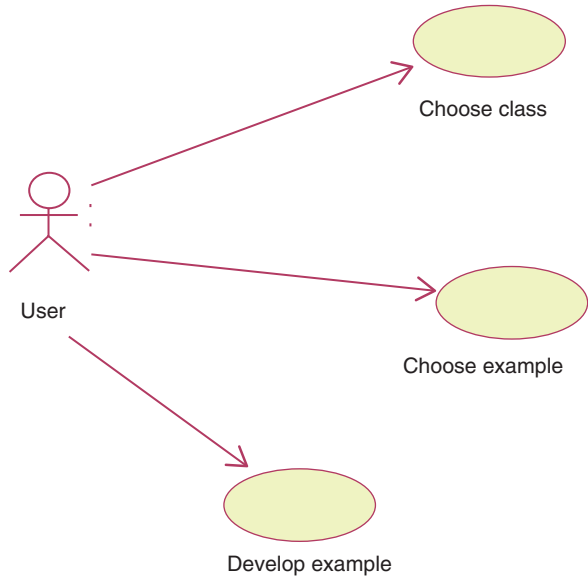
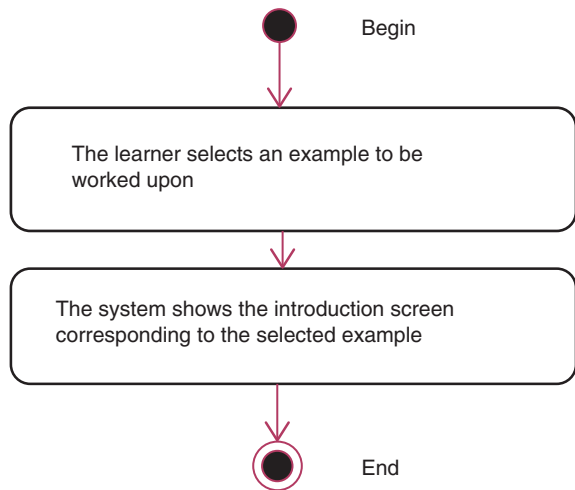


Fig. 3.3 Activity diagram: choose example



3.3 Discussion

A better semantic-based IoT engine would help to improve the system addressing these requirements:

- Interoperability among applications, even from heterogeneous domains
- IoT data interpretation
- Straightforwardness implementation and deployment of IoT applications
- Adaptivity to the different users' necessities (e.g., ensure privacy, interfaces to wearable/mobile devices)

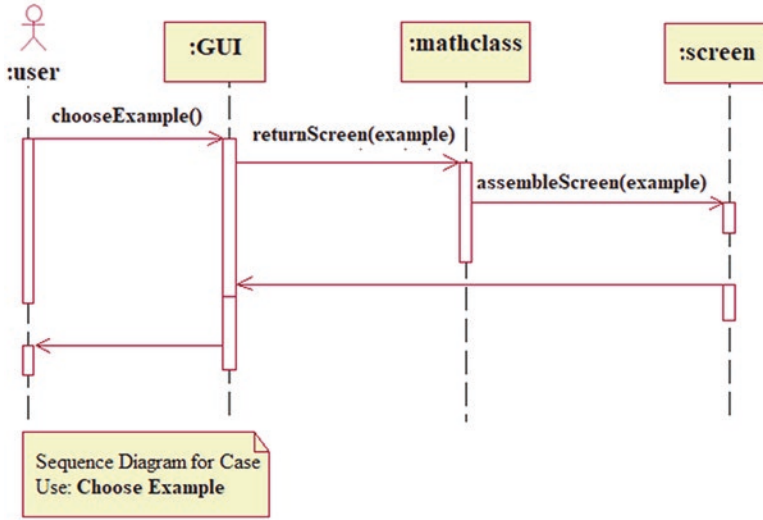


Fig. 3.4 Sequence diagram: choose example

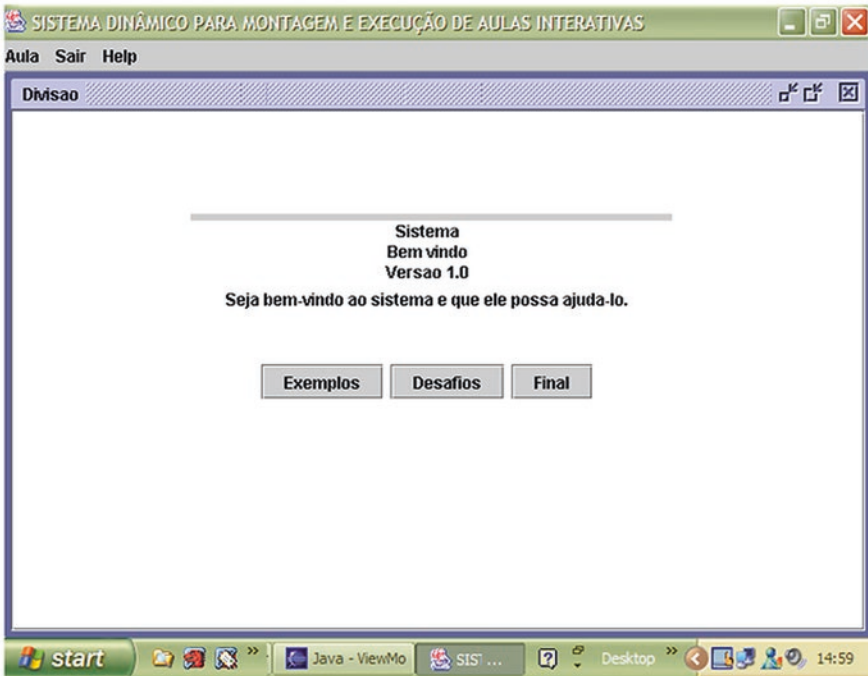


Fig. 3.5 Introduction screen: Allows the student to control the examples' difficulty degree

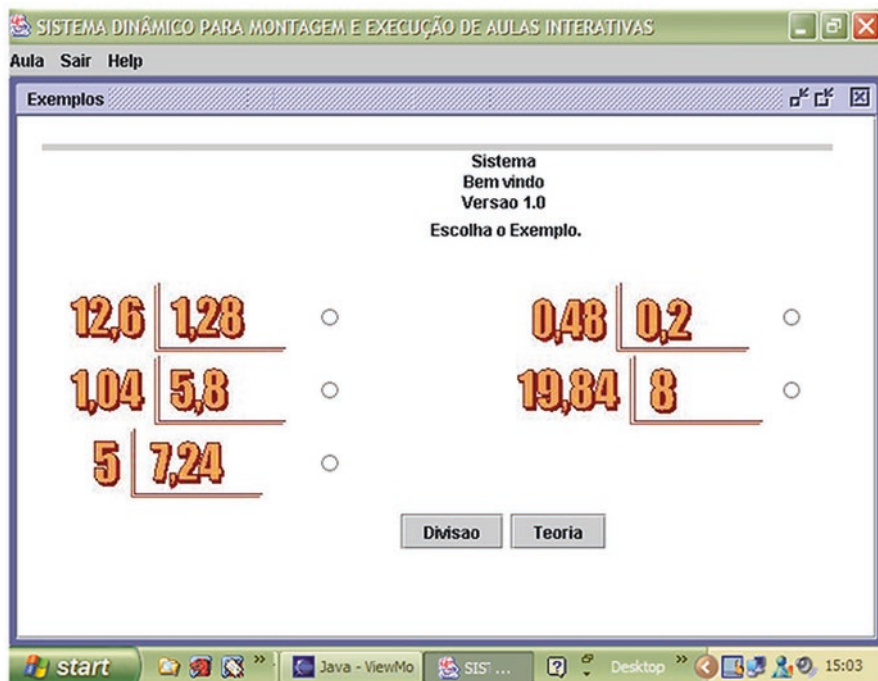


Fig. 3.6 Examples screen: permits the student to choose the example course of action

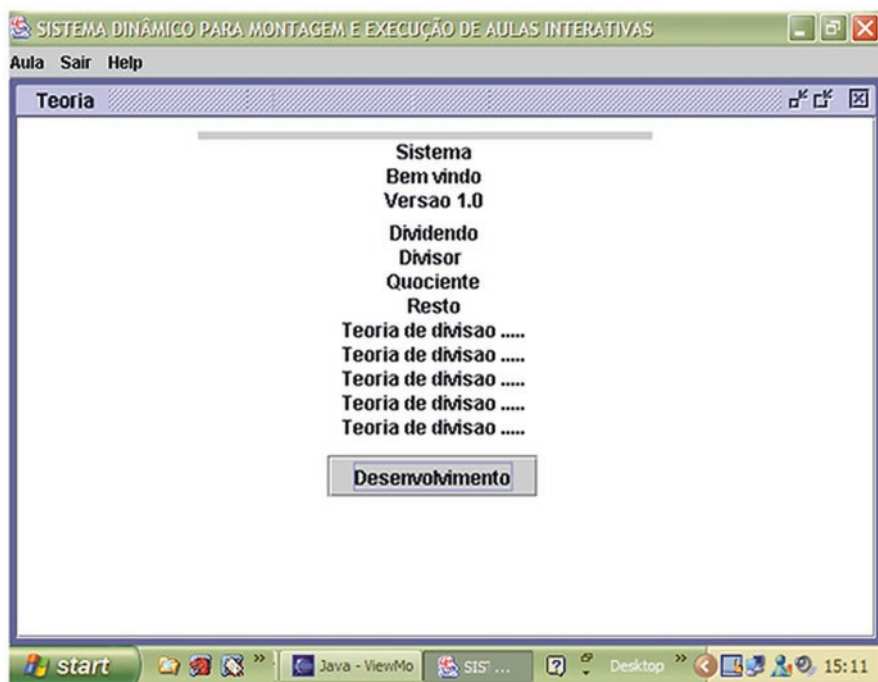


Fig. 3.7 Theory screen: allows the user to seek explanation and learn the concepts of division

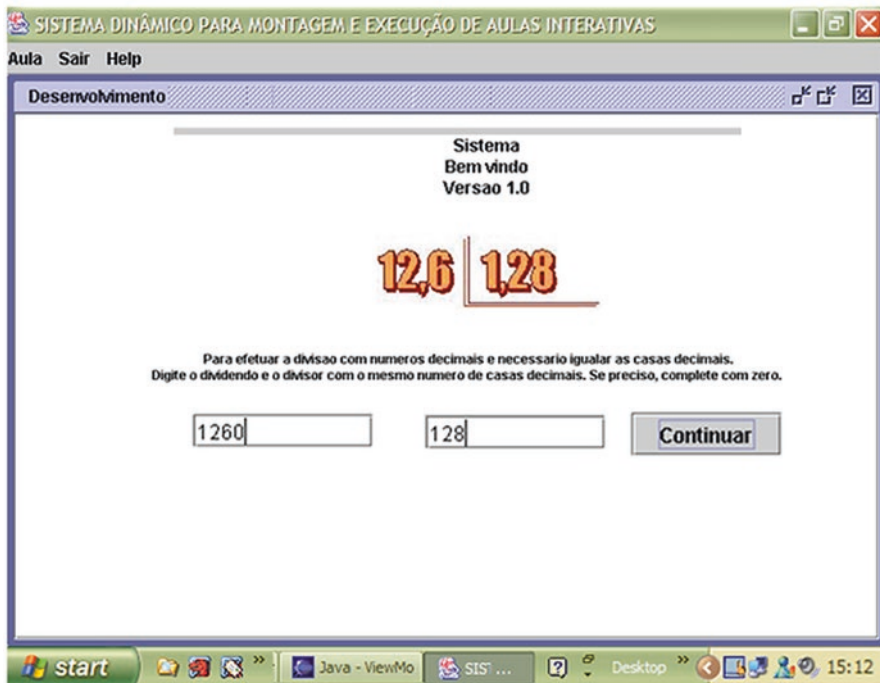


Fig. 3.8 Development screen: execution of tasks until the normal division

Replication with math anxiety questionnaires is necessary to include situations related to all respondents. Every day, math-related situations may vary from person to person. Likewise, the elderly deal with family responsibilities, medical conditions, and decisions that may use technology differently or even lack any technological help. Some examples have more common knowledge than an average real-life quantitative issue. Still, as the world changes, people will adjust their math use to technologies. For example, the amount of change in coins may decrease in the face of digital payments. Evaluation of full reliance on technology or mathematical thinking is still required.

A major challenge in the Cloud of Things (CoTs) handles the data created by too many IoT devices. Edge computing infrastructure, aka Edge of Things (EoT), solves problems by functioning as a middle layer connecting the IoT devices and cloud computing (CC). The Cognitive Internet of Things (CIoT) can deliver small-scale real-time storage and computing to guarantee low latency in addition to optimal IoT resource deployment. Still, the EoT has privacy issues, which is a noteworthy concern for systems with sensitive data. SISDI

necessitates an EoT computing framework for safe and smart tutoring as well as surveillance services with fully homomorphic encryption. The SISDI framework needs scalability to aggregate and analyze the large-scale and heterogeneous data in the distributed EoT devices independently before sending them to the cloud.

All over history, anthropological cognitive systems have been changed by the introduction of technology (e.g., primitive tools, oral communication, text, and math systems). The Internet reshaped human cognition with its multifaceted features and transformed people's thoughts and behaviors profoundly [18]. The elderly sense some rejection of DE when compared to generations that grow up with Internet technologies aka digital natives (DNs). Seniors tend to show shallow Internet behaviors with fast attention shifting and lesser deliberations.

Last, improving people's cognitive reserve augments the quality of their lives, preventing the onset of dementia or other cognitive impairment in aging [19].

3.4 Conclusions

SISDI helps people to perform calculations with decimal places. The repercussions of the analyses from meetings with stakeholders' pointed towards the transmedia aspect of the mediation conveyed enhancements to the learning encounters, together with a commitment in the application space that expanded understudy energy, content use over numerous media modalities, and interest in game-based learning [5, 20–22].

The whole route ought to be further ameliorated by combining quantitative methodologies, computational intelligence, and experience obtained. Reflections about the outcomes must converge towards the upgrading of fresh class designs and to amalgamate diverse subjects like biology [23], dance [24], geography [25], health self-care [26], and so forth.

This work is malleable enough to fit in a semantic engine either on the cloud, constrained devices, or gateways.

The present framework needs to incorporate concepts related to skills, emotional, and drive factors from everyday life, which has not been reported earlier in the literature. Individuals with prominent math skills are the ones that make use of math more habitually and are also more self-reliant concerning their math abilities. For women, math anxiety relates adversely to using math in ordinary life and to math expertise. Utilizing math routinely, taking into consideration skills, affective and motivational elements may strengthen and mutually stimulate each other [4].

References

1. T. Nguyen, The effectiveness of online learning: beyond no significant difference and future horizons. *Merlot. J. Online Learn. Teach.* **11**(2), 309–319 (2015)
2. Posner, T, *Dyscalculaic in the Making: Mathematical Sovereignty, Neurological Citizenship, and the Realities of the Dyscalculaic*. ProQuest. ISBN 978-1-243-99265-9 (2008)
3. M.D. Soares, P. Neelkamal, R. Dilip, Dyscalculia. *Int. J. Child Adolesc. Health* **8**(1), 15–26 (2015)
4. B.R. Jansen, E.A. Schmitz, H.L. Maas, Affective and motivational factors mediate the relation between math skills and use of math in everyday life. *Front. Psychol* **7**, 513 (2016)
5. L.S. Carreiro, V.V. Estrela, M.P. Vishnevski, W.D. Huacasi, A.E. Herrmann, H.J. Loschi, Y. Iano, N. Razmjoooy, Y. Thiagarajan, *POEMATHICS*, in *Proceedings of the 4th Brazilian Technology Symposium (4th BTSym)*, vol 140 (Springer, Cham/Zurich, 2019). https://doi.org/10.1007/978-3-030-16053-1_64
6. V.V. Estrela, A.C.B. Monteiro, R.P. França, Y. Iano, A. Khelassi, N. Razmjoooy, Health 4.0: applications, management, technologies and review. *Med. Tech. J* **2**(4), 262–276 (2019). <https://doi.org/10.26415/2572-004X-vol2iss1p262-269>
7. K. Zaheer, M. Othman, M.H. Rehmani, T. Perumal, A survey of decision-theoretic models for cognitive internet of things (CIoT). *IEEE Access.* **6**, 22489–22512 (2018)
8. P.-A. Cinquin, P. Guitton, H. Sauz on, Online e-learning and cognitive disabilities: a systematic review. *Comp. Educ., Elsevier* **130**, 152–167 (2019)
9. Z. Pirani, M. Sasikumar, Assistive e-learning system for the learning disabled. *Proc. Comp. Sci.* **45**, 718–727 (2015)
10. V.V. Estrela, J. Hemanth, O. Saotome, E.G.H. Grata, D.R.F. Izario, Emergency response cyber-physical system for flood prevention with sustainable electronics, in *Proceedings of the 3rd Brazilian Technology Symposium (BTSym 2017)*, (Springer, Cham/Zurich, 2019)
11. J. Dron, T. Anderson, *Teaching Crowds: Learning and Social Media* (AU Press, Edmonton, 2014)
12. J. Dron, T. Anderson, Three generations of distance education pedagogy. *Int. Rev. Res. Open Distrib. Learn.* **12**(3), 80–97 (2011)
13. C. Larman, *Utilizando UML e Padr es: Uma Introdu o   An lise e a Projetos Orientados a Objetos e ao Processo Unificado*, 2nd edn. (Bookman, Porto Alegre, 2004), pp. 34–35
14. R.S. Wazlawick, *An lise e Projeto de Sistemas de Informa o Orientados a Objetos*, 2nd edn. (Elsevier, Rio de Janeiro, 2004), p. 19
15. G. Booch, *The Unified Modeling Language User Guide*, 2nd edn. (Addison-Wesley, 2017)
16. C.S. Horstmann, *Core Java, Volume I – Fundamentals*, 11th edn. (Prentice-Hall, Upper Saddle River, 2019)
17. C.S. Horstmann, *Core Java, Volume II – Advanced Features*, 11th edn. (Prentice-Hall, Palo Alto, 2019)
18. K.K. Loh, R. Kanai, How has the internet reshaped human cognition? *Neurosci. Rev. J. Bring. Neurobiol. Neurol. Psychiat.* **22**(5), 506–520 (2016)
19. G. Arcara, S. Mondini, A. Bisso, K. Palmer, F. Meneghello, C. Semenza, The relationship between cognitive reserve and math abilities. *Front. Aging Neurosci.* **9** (2017)
20. G. Gadanidis, E. Simmt, G. Sterenberg, V. Tumanov, *Literature*, in *Proceedings of the 2004 Mathematics as Story: A Symposium on Mathematics through the Lenses of Art & Technology* (Faculty of Education, University of Western Ontario, 2004), pp. 62–65
21. A.E. Herrmann, V.V. Estrela, H.J. Loschi, M.P. Vishnevski, Some thoughts on transmedia communication. *OJCTST* **11**(4) (2018). <https://doi.org/10.13005/ojctst11.04.01>

22. E. McCarthy, M. Tiu, L. Li, Learning math with curious George and the odd squad: transmedia in the classroom. *Tech. Know. Learn.* **23**, 223 (2018)
23. S.E. Andrews, C.R. Runyon, M.L. Aikens, The math–biology values instrument: development of a tool to measure life science majors’ task values of using math in the context of biology. *CBE Life Sci. Educ* (2017)
24. P. Moerman, *Dancing, Math Teaching and Learning in the Interplay between Aesthetic and Mathematical Literacy* (2016)
25. R.I. Dorn, J.G. Douglass, G.O. Ekiss, B. Trapido-Lurie, M. Comeaux, R. Mings, R. Eden, C. Davis, E.R. Hinde, R. Ramakrishna, *Learning Geography Promotes Learning Math: Results and Implications of Arizona’s GeoMath grade K-8 Program* (2005)
26. M.I.P.O. Santos, M.R. Portella, Conditions of functional health literacy of an elderly diabetics group. *Rev. Bras. Enferm.* **69**(1), 144–152 (2016). <https://doi.org/10.1590/0034-7167.2016690121i>

Chapter 4

Acoustic Contrast Between Neutral and Angry Speech: Variation of Prosodic Features in Algerian Dialect Speech and German Speech



F. Ykhlef  and D. Bouchaffra 

4.1 Introduction

Emotion recognition (ER) can employ audio or image, and it is still thought-provoking for the reason that it can improve a number of interactional aspects among human beings in addition to the communication among them and their machines under real-life uncontrolled circumstances, e.g., data acquisition glitches, mutable/challenging lightning settings, modifications of indoor/outdoor conditions, sensor noise, blur due to movement, resolution issues, occlusions, and pose deviations, in addition to subjective elements that may impair conveying emotions [1–7].

This text ponders on speech ER, which is the most straightforward means to communicate human thoughts. Acoustic ER rely on low-dimensional data when compared to video ER. It expresses several clues linked to gender, age group, and linguistic levels, besides emotional information [8, 9]. ER is still a hot theme in speech/language processing.

Observing anger is paramount to ER [10] for medical psychology investigations and emotional health tracking. Moreover, it aids in the estimation of the level of stress, the detection of agents'/customers' mood swing in call center dialogs, the command of healthcare equipment (e.g., robots), as well as acknowledging frustration in day-to-day communications [11].

Voice activity detection (VAD) or speech detection distinguishes the presence or absenteeism of talking (differentiating dialog from nonspeech sections). VAD is

The original version of this chapter was revised. The correction to this chapter is available at https://doi.org/10.1007/978-3-030-57552-6_17

F. Ykhlef (✉) · D. Bouchaffra
Division Architecture des Systèmes et Multimédia, Centre de Développement
des Technologies Avancées, Algiers, Algeria
e-mail: fykhlef@cdta.dz; dbouchaffra@cdta.dz

imperative in audio-based applications, for the most part, in speech coding as well as recognition. There exist several VAD strategies in literature, relying on different rationales like abrupt alterations of spectral, energy, or cepstral distances. These changes fulfill different needs and entail various features, e.g., latency, sensitivity, accuracy, as well as computational cost.

The design and deployment of audio-based applications call for an in-depth comprehension of speech properties. Additionally, the acoustic and linguistic traits of emotional speech influence VAD performance. Without a doubt, prosody and voice quality are essential to discriminate emotions [9].

In particular, a higher pitch mean value, a higher intensity, a somewhat faster speaking rate, together with a breathy voice typify an angry speech compared to neutral talking. Moreover, pitch values belong to a longer interval and exhibit abrupt changes in line with investigative evidence from several idioms [9]. Yet, some of these characteristics may differ from a language to another. Besides, the precise amount of variation counts on the natural languages' properties and the type of corpora employed in the experiments. Plentiful of quite different results emerge in the literature as the following studies.

Oliveira Jr. et al. carried out a study on Brazilian Portuguese [12] whose speech anger rate is lower than the neutral one. This by-product is significant as it contradicts directly what literature regularly indicates for other languages.

G. Koolagudi et al. have classified sentiments from the Indian language speech [13]. Speech rate has been a significant feature to differentiate between emotions. The typical hostile speech duration is lesser than the average neutral talking length. The ER corpus, known as IITKGP-SESC, was the benchmark [13]. Indian actors have recorded simulated speech containing anger, disgust, fear, compassion, happiness, serenity, sarcasm, and surprise emotions.

S. Yildirim et al. conducted an ER acoustic study for the English language [14]. Professional actors simulated sadness, anger, happiness, and calmness in recorded speech data. This study has revealed that the duration of angry utterances is longer than the one of neutral utterances. Besides, silence duration between adjacent words is shorter. Moreover, it found that angry speech displays high values of both energy and pitch.

This text explores the variation of prosodic traits in Algerian dialect (AD) and likens the obtained results to German speech. The suggested methodology explores the set of prosodic traits, namely, pitch (F0), duration (D), and energy (E), to assess and separate anger and neutral states. The emphasis on AD rather than Standard Arabic (SA) happens for two main reasons:

- (i) The first reason is that the native language in the Arabic world and more precisely in Algeria is not SA. Algerians use their dialect more often to converse with each other than SA. For instance, the design of automatic software to infer the stress level in Algerian speakers employing audio waveform demands familiarity with the AD acoustic properties rather than the ones from SA.
- (ii) The second reason for focusing on dialects stems from the scarce availability of speech corpora. A speech corpus, which consists of the main linguistic clues of a given language, is indispensable to analyze emotional prosody acoustically.

There is no emblematic SA corpus for emotional speech detection as to the authors' awareness. However, the authors are presently building the first acted Emotional Speech Corpus of the AD (ESCAD). This novel corpus lets investigating the prosody variation in an emotional speech. The experimental outcomes obtained for the ESCAD were compared to those of the German language (GL) utilizing the German Corpus of Emotional Speech (EMODB). The authors compared AD to GL since the structural composition of the ESCAD resembles the EMOBDB organization. The authors scrutinized the variation of pitch (F0), energy (E), and duration (D) of utterances via the "Wilcoxon matched-pairs signed-rank" [15], which is an objective statistical test. The P-value quantifies the degree of statistical significance among the prosodic features pair extracted from neutral and angry speech waveforms.

The best feature set selection for speech ER depends on the language as it appears in [9]. For instance, if one opts for an acoustic element that separates flawlessly neutral and angry English speech, then this particular feature may not typify the indifferent and hostile Chinese speech suitably.

Prosodic features are amid the most excellent acoustic metrics for discerning between neutral and angry German speech [9]. Still, no findings emerged in the collected works for the AD as far as the authors are concerned. As a result, this study's outcomes will build a bridge between GL and AD while examining their differences and similitudes in terms of the prosodic features' variation. Then, the authors will discuss the potential of the prosodic features to classify neutral and angry AD speech. Furthermore, the authors will conduct an unpretentious and valid comparison between AD and GL while quantifying the separation degree. The investigational results will also pave the way for exploiting other alternatives on anger detection in GL and apply them to the AD.

Next, this work has the following parts: This study's materials and methods appear in Sect. 4.2. The essential results and discussions appear in that order, in Sects. 4.3 and 4.4. In conclusion, Sect. 4.5 closes the research and highlights future perspectives.

4.2 Materials and Methods

This section addresses the materials and methods that we relied on to investigate the acoustic contrast between irate and neutral speech employing the prosodic structures. The authors arrange for a brief description of feature extraction procedures and delineate the statistical separability proof between neutral and angry states. The authors describe in what way to use the P-value to quantify the degree of statistical significance between neutral and angry states. This study likens the AD and the GL. Detailed descriptions from [16, 17] tackle the phonetic composition of both AD and GL.

4.2.1 *Speech Corpora*

4.2.1.1 ESCAD

Emotional Speech Corpus of the AD (ESCAD) is a new simulated speech corpus that is being recorded at the Algerian Center for Development of Advanced Technologies [18]. A group of 25 males and 28 females took part in the recording of the speech corpus.

The simulated sentiments are (i) anger, (ii) happiness, (iii) disgust, and (iv) neutral. The speakers are uttering a set of 12 sentences that include the entire set AD phonemes [18]. The orators recorded the same sentence twice.

The data from this study include only anger and neutral states. Eleven referees evaluated these data subjectively. Only 10 speakers among the initial group of 53 are considered in our study. The selected speakers have shown a high Individual Evaluation of the Speaker (IES) score [18]. We restricted our selection to ten speakers to get a similar number of speakers as those available in the German corpus (EMODB). This investigation considered only one sentence repetition. The total number of angry sentences in the chosen subset is equal to 120. The same amount of neutral sentences comprise a set of paired observations. The picked subgroup guarantees that each pair of sentences (with neutral and hostile emotional undertones) has been uttered by the same speaker (Table 4.1).

4.2.1.2 EMODB

The department of communication science of Berlin University devised a database for emotional speech benchmarking christened EMODB [19]. It was recorded by five male and five female professional speakers to simulate seven emotional states: (i) anger, (ii) boredom, (iii) sadness, (iv) joy, (v) fear, (vi) disgust, and (vii) neutral. The speakers uttered ten sentences that include the phonetic components of the GL

Table 4.1 Overview of ESCAD and EMODB subsets

Properties/language	Algiers dialect	German language
Corpus type	Acted	Acted
Emotional states	Neutral (N) + angry(A)	Neutral (N) + angry(A)
# of speakers	10	10
# of sentences	12	10 (not for all speakers)
# repetitions	1	1
Total duration	365.11 (s)	384.34 (s)
Fs	44.1 kHz	16 kHz
# of files	120	77

[19]. Some speakers record repetitions of the same sentence. The data used in our study includes only anger and neutral states.

The number of angry recorded audio sentences within the EMODB corpus is equal to 77. Therefore, the authors selected only the set of neutral sentences corresponding to the same set of angry sentences to form paired observations (or groups). The process of file selection ensures that the same speaker (Table 4.1) uttered each pair of sentences with neutral and angry intonations.

4.2.2 Extraction of Prosodic Features

Each sentence (from the audio file of the sentence) has its F_0 and E contours appraised for the ESCAD and EMODB subsets via the following strategies (Fig. 4.1):

- (i) The Gonzalez technique [20] for the F_0 contour
- (ii) The Teager energy scheme [21] for the E contour

Sentence duration was estimated by merely computing the time interval of the speech waveform.

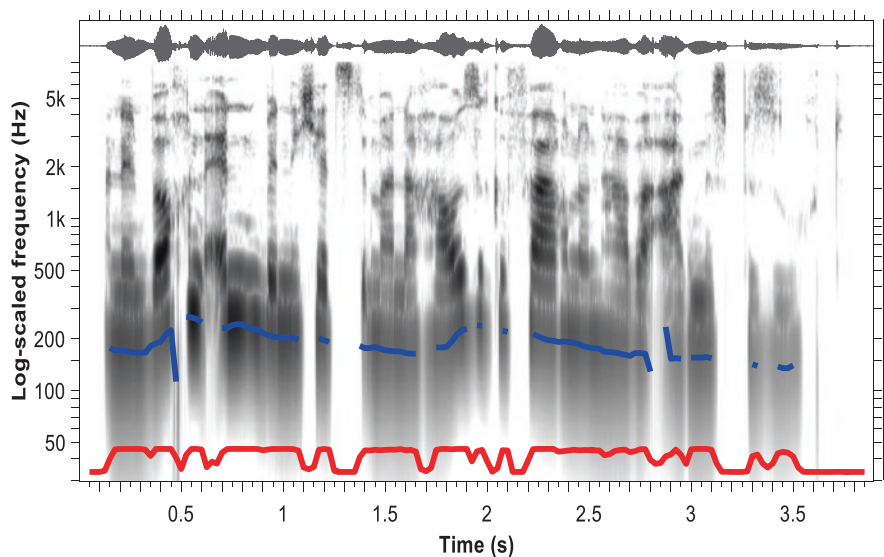


Fig. 4.1 Computation of the pitch and energy contours of the sentence “Your bill has not been paid,” (in AD: “فصل اخ شي هام كعانتن روتكفالف”) Lines color (red, energy; blue, pitch; black, speech waveform; gray, spectrogram)

4.2.3 Statistical Test

This study tries to disclose the acoustic contrast between neutral and angry speech through the analysis of prosodic variations. The quantification of the degree of separation between angry and calm emotional states using statistical hypothesis testing achieves this goal. This research work has utilized the nonparametric scheme named “Wilcoxon matched-pairs signed-rank test” from [15]. It aims at comparing the medians of two dependent (paired) observations. This statistical test takes place when one variable is present. In our study, the variable can be one of the three prosodic features, namely, (i) F_0 , (ii) E , or (iii) D . Therefore, the suggested practice applies the statistical test separately for each feature.

Three pairs of observations represent the two populations undergoing tests. Each pair corresponds to a single prosodic feature extracted from files containing neutral and angry speech samples. Usually, nonparametric testing is suitable for non-normally distributed data. Otherwise, parametric methods are used instead. The Anderson-Darling test [22] helped to check the non-normality of the data leading to the adoption of the “Wilcoxon matched-pairs signed-rank test.” The P -value worked appraises the separation between the two observations [23]. The test checks if the P -value is higher than or inferior to the significance level α , which in the present study is $\alpha = 0.05$, to either admit or throwaway the null hypothesis.

Nevertheless, the P -value magnitude provides extra information to quantify the degree of statistical significance [23]. The P -value designates the probability that the sample median difference among the two observations is zero at an α % significance level [15], given the null hypothesis is verified. Therefore, this study assessed the P -value for each prosodic feature utilizing two paired clusters (neutral and anger). The first cluster encloses three prosodic features (F_0 , D , and E) that extracted with neutral speech files. The succeeding cluster consists of the same set of features calculated through angry speech files.

These two clusters form our paired observations. This methodology treated the ESCAD and EMODB corpora employing the MATLAB IDE under a Windows platform to conduct these experiments.

4.3 Results

4.3.1 Feature Extraction

We applied a standard methodological approach to extract the prosodic features from our speech subsets. Our approach is composed of two main steps:

- (i) Selection of the speech subset SB (either ESCAD or EMODB)
- (ii) Clustering and extraction of information from SB

A detailed description of the second step is summarized as follows:

The speech subset is divided into two clusters C_1 and C_2 :

- C_1 includes “M” neutral speech files that encompass all phonemes of the speech material (AD phonemes if ESCAD is selected or GL phonemes if EMODB is selected). These speech files were uttered by “S” speakers. For each speech file, the mean value of the three prosodic features, namely, F_0 , E , and D , were computed. For the entire set of data files, the numerical values of the aforementioned features were saved in three different vectors: N_{F_0} , N_E , and N_D . The size of each vector is equal to “M.”
- C_2 includes “M” angry speech files that encompass all phonemes of the speech material (AD phonemes if ESCAD is selected or GL phonemes if EMODB is selected). The same speakers uttered these speech files as those selected in C_1 . The order of sentences and speakers is the same as in C_1 . For each speech file, the mean value of the prosodic features, namely, F_0 , E , and D , was calculated. Likewise, the numerical values of the aforementioned features were saved in three different vectors: A_{F_0} , A_E , and A_D . The size of each vector is equal to “M.”

C_1 and C_2 were used to form paired observations (N: *neutral* and A: *angry*) for each prosodic feature separately. For each subset, the couple of clusters was defined as:

- (i) $\{C_{1AD}; C_{2AD}\}$ for ESCAD
- (ii) $\{C_{1GL}; C_{2GL}\}$ for EMODB

Consequently, the prosodic features for each subset are expressed as follows:

- *ESCAD* (Fig. 4.2)
 - $F_{0_AD} = \{F0_C_{1AD}; F0_C_{2AD}\}$
 - $E_AD = \{E_C_{1AD}; E_C_{2AD}\}$
 - $D_AD = \{D_C_{1AD}; D_C_{2AD}\}$
- *EMODB* (Fig. 4.3)
 - $F_{0_GL} = \{F0_C_{1GL}; F0_C_{2GL}\}$
 - $E_GL = \{E_C_{1GL}; E_C_{2GL}\}$
 - $D_GL = \{D_C_{1GL}; D_C_{2GL}\}$

The number of neutral/angry files “M” and the total number of speakers “S” for each subset are given as follows (see Table 4.1 for more details):

- ESCAD: $\{M = 120, S = 10\}$
- EMODB: $\{M = 77, S = 10\}$

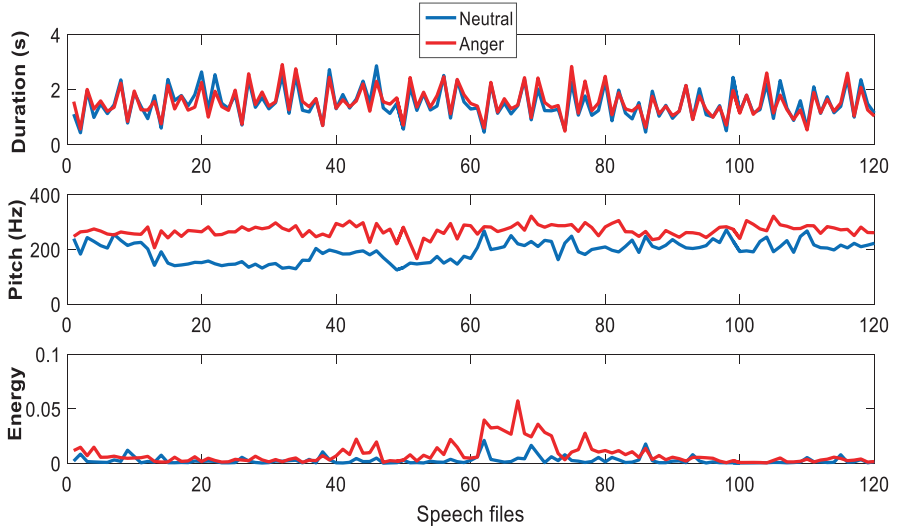


Fig. 4.2 Extraction of the AD prosodic features (ESCAD subset)

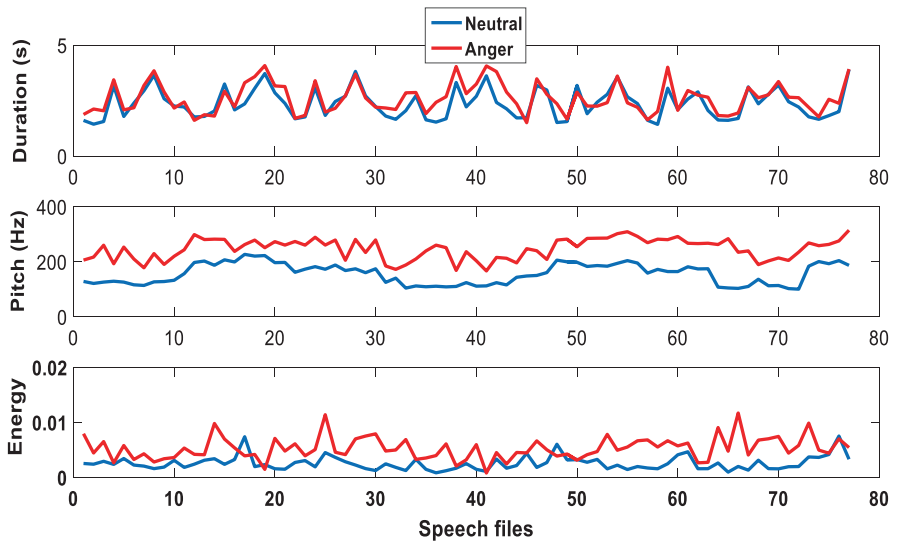


Fig. 4.3 Extraction of the GL prosodic features (EMODB subset)

4.3.2 Quantification of the Degree of Statistical Significance

Our goal consists of (i) providing statistical proof of the separation between neutral and angry prosodic features and (ii) quantifying the degree of this separation. We tested the separation of the three pairs of observations obtained in the previous section for both ESCAD (AD_{F_0} , AD_E , AD_D) and EMODB (GL_{F_0} , GL_E , GL_D)

subsets. We found that the null hypothesis of the Wilcoxon test was rejected for the three prosodic features (the P -value is less than 0.05).

This result proves that the separation between neutral and angry prosodic features is statistically significant in the AD and the GL as well.

The P -values obtained for each pair of observation is taken into account to quantify the degree of separation. The results obtained are depicted in Figs. 4.4, 4.5, and 4.6.

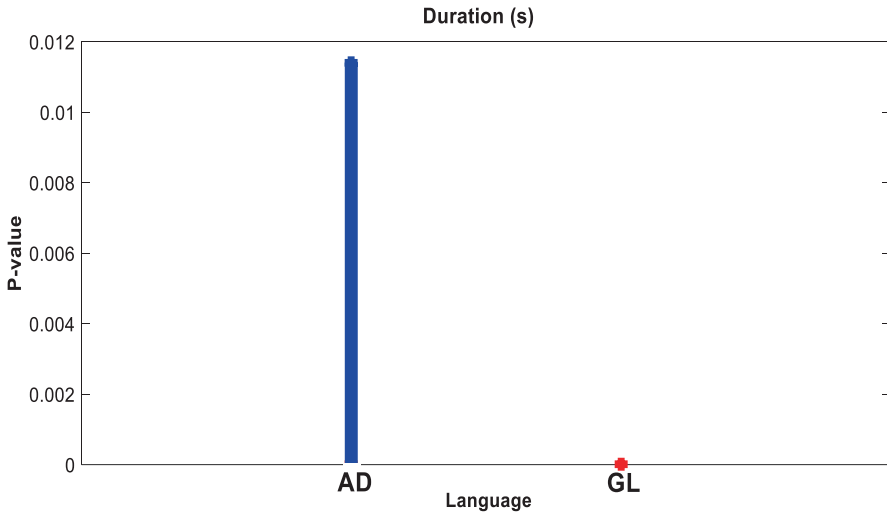


Fig. 4.4 P -value as measure of acoustic contrast in duration for AD and GL

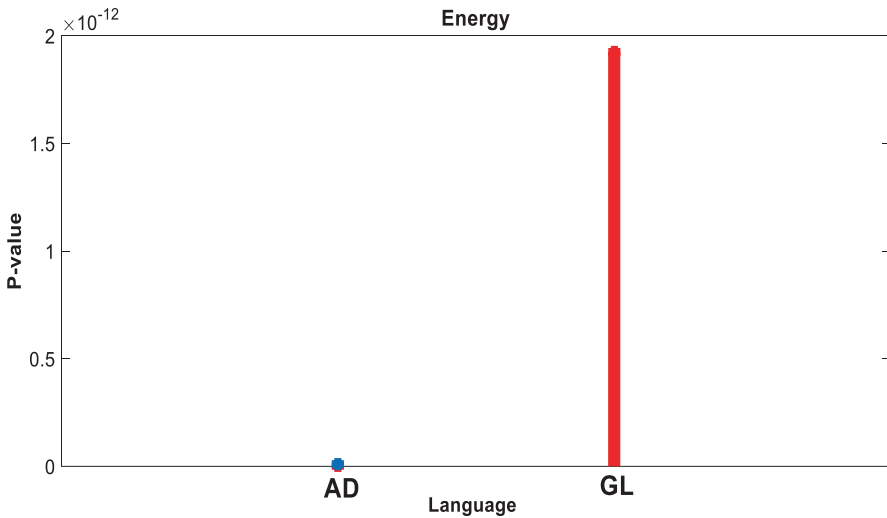


Fig. 4.5 P -value as a measure of acoustic contrast in energy for AD and GL

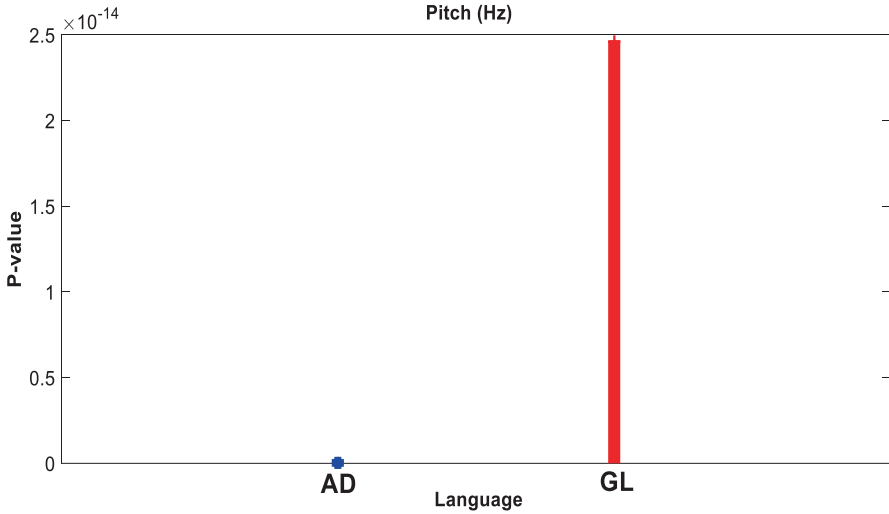


Fig. 4.6 P -value as a measure of acoustic contrast in pitch for AD and GL

4.4 Discussion

The obtained results show that for both languages, the mean values of F_0 and E measured using anger sentences are greater than those measured using neutral sentences. However, the opposite was found for the duration. The separation between neutral and angry prosodic features was proven to be statistically significant by the mean of the Wilcoxon test.

The P -value computed using GL sentences to test the separability between neutral and anger energies is much higher than the one obtained using AD sentences ($(P\text{-value_AD} = 1.18, 10^{-14}, P\text{-value_GL} = 1.92, 10^{-12})$) (Fig. 4.5). The same effect is exhibited for pitch values ($(P\text{-value_AD} = 2, 10^{-21}, P\text{-value_GL} = 2.46, 10^{-14})$) (Fig. 4.6). These findings mean that the energy contrast between neutral and angry states is much higher for AD than GL. The same behavior was observed for pitch. However, the opposite effect was observed for the duration ($(P\text{-value_AD} = 0.01, P\text{-value_GL} = 3.4365, 10^{-07})$) (Fig. 4.4).

4.5 Conclusion

This paper studied the acoustic contrast between neutral and angry speech by investigating the variations of prosodic features (i.e., pitch (F_0), energy (E), and duration (D)) in AD and GL. We proposed a methodology for testing and quantifying this contrast using the “Wilcoxon test” P -value. We provided statistical proof that the

three prosodic features of neutral and angry states are separable. Then, for both AD and GL, we have shown that the mean values of F_0 and E of angry utterances are much higher than those of neutral utterances. However, the opposite effect was observed for D .

This study proved the effectiveness of exploring prosodic features to discriminate neutral and angry emotions in Algerian speech. Furthermore, we discovered a significant difference in the variation of neutral and angry prosodic features between AD and GL.

We revealed that the contrast in E between neutral and angry states is much higher for AD than for GL. We showed the same results for F_0 variations. However, the opposite effect has been observed for D . Therefore, E and F_0 are very effective to detect AD angry speech.

Our next objective consists in investigating the variation of prosodic features between angry and neutral states by considering the gender and age of speakers.

Acknowledgments This research was funded by the ATRSS (Agence Thématique de Recherche en Science de la Santé) under grant n°: 64/DFPR/ATRSS/2017.

References

1. H. Kaya, F. Gürpınar, A.A. Salah, Video-based emotion recognition in the wild using deep transfer learning and score fusion. *Image Vis. Comput.* **65**, 66–75 (2017)
2. H.R. Marins, V.V. Estrela, On the use of motion vectors for 2D and 3D error concealment in H.264 AVC video, in *Feature Detectors and Motion Detection in Video Processing*, ed. by N. Dey, A. S. Ashour, P. K. Patra, (2017). <https://doi.org/10.4018/978-1-5225-1025-3.ch008>
3. A.E. Herrmann, V.V. Estrela, Content-based image retrieval (CBIR) in remote clinical diagnosis and healthcare, in *Encyclopedia of E-Health and Telemedicine*, ed. by M. M. Cruz-Cunha, I. M. Miranda, R. Martinho, R. Rijo, (2016). <https://doi.org/10.4018/978-1-4666-9978-6.ch039>
4. C. Su, W. Zhang, T. Feng, *Research on Extracting Facial Image for Bimodal Emotion Recognition Based on Speech Signal and Facial Expression*. *Int. J. Eng. Tech.* 4(1), 589–594, (2018)
5. V.V. Estrela, A.M. Coelho, State-of-the-art motion estimation in the context of 3D TV, in *Multimedia Networking and Coding*, ed. by R. A. Farrugia, C. J. Debono, (IGI Global, Hershey, 2013), pp. 148–173. <https://doi.org/10.4018/978-1-4666-2660-7.ch006>
6. B. Sun, Q. Xu, J. He, L. Yu, L. Li, Q. Wei, *Audio-Video Based Multimodal Emotion Recognition Using SVMs and Deep Learning* (CCPR, 2016)
7. J. Hook, F. Noroozi, Ö. Toygar, G. Anbarjafari, Automatic speech based emotion recognition using paralinguistics features. *Bull. Pol. Acad. Sci. Tech. Sci.* **67**(3) (2019)
8. J.S. Adelman, Z. Estes, M. Cossu, Emotional sound symbolism: Languages rapidly signal valence via phonemes. *Cognition* **175**, 122–130 (2018)
9. F. Vogt, *Real-Time Automatic Emotion Recognition from Speech* (PhD Thesis, University of Bielefeld, Germany, 2010)
10. J. Deng, F. Eyben, B. Schuller, F. Burkhardt, in *The 17th IEEE International Conference on Affective Computing and Intelligent Interaction Workshops and Demos*, Deep neural networks for anger detection from real life speech data (2017), pp. 1–6
11. F. Burkhardt, A. Paeschke, M. Rolfes, W.F. Sendlmeier, B. Weiss, in *The 9th European Conference on Speech Communication and Technology*. A database of German emotional speech (Lisboa, 2005)

12. M. Oliveira Jr, A.N. de Almeida, R.A. de Almeida, E.W. Silva, in *The 7th International Conference on Speech Prosody*. Speech rate in the expression of anger: a study with spontaneous speech material. (Dublin, 2014)
13. S.G. Koolagudi, S. Ray, K.S. Rao, in *The International Conference on Contemporary Computing*. Emotion classification based on speaking rate (India, 2010) pp. 316–327
14. S. Yildirim, M. Bulut, C.M. Lee, A. Kazemzadeh, Z. Deng, S. Lee, C. Busso, in *The 8th International Conference on Spoken Language Processing*. An acoustic study of emotions expressed in speech (South Korea, 2014)
15. J.D. Gibbons, S. Chakraborti, *Nonparametric Statistical Inference*, 5th edn. (Chapman & Hall/CRC Press/Taylor & Francis Group, Boca Raton, 2011)
16. S. Harrat, K. Meftouh, M. Abbas, W.K. Hidouci, K. Smaili, An Algerian dialect: Study and resources. *Int. J. Adv. Comput. Sci. Appl.* **7**(3), 384–396 (2016)
17. U. Ammon, *The Position of the German Language in the World* (Taylor & Francis Group, 2019)
18. F. Ykhlef, A. Derbal, W. Benzaba, R. Boutaleb, D. Bouchaffra, H. Meraoubi, Far. Ykhlef, in *The IEEE International Conference on Advanced Electrical Engineering*. Towards building an emotional speech corpus of Algerian dialect: criteria and preliminary assessment results. (Algiers, 2019)
19. F. Burkhardt, in *The 18th International Conference on Language Resources and Evaluation*. “You Seem Aggressive!” Monitoring anger in a practical application (Istanbul, 2012), pp. 1221–1225
20. S. Gonzalez, M. Brookes, PEFAC – a pitch estimation algorithm robust to high levels of noise. *IEEE Trans. Audio Speech Lang. Process.* **22**(2), 518–530 (2014)
21. R.C. Guido, Enhancing teager energy operator based on a novel and appealing concept: signal mass. *J. Franklin Inst.* **356**(4), 2346–2352 (2019)
22. T.W. Anderson, D.A. Darling, Asymptotic theory of certain “goodness-of-fit” criteria based on stochastic processes. *Ann. Math. Stat.* **23**, 193–212 (1952)
23. I.C. Marschner, *Inference Principles for Biostatisticians*, 1st edn. (Chapman & Hall/CRC Press/Taylor & Francis Group, Boca Raton, 2014)

Part II
Medical Technologies Systems

Chapter 5

Artificial Intelligence and Its Application in Insulin Bolus Calculators



Abdelaziz Mansour , Kamal Amroun , and Zineb Habbas 

5.1 Introduction

Diabetes mellitus is an increasingly common, chronic, and incurable disease. Worldwide, approximately 451 million adults had diabetes in 2017, and this number is expected to reach 693 million by 2045 [15]. It is associated with depreciated quality of life, disastrous complications, reduced life expectancy, and high healthcare costs. It occurs when the body cannot maintain healthy blood glucose (BG) levels due to an absence, a lack, or defect of the insulin, hormone secreted by the pancreas B cells. There are several types of diabetes. The most known are type 1 diabetes (T1D) and type 2 diabetes (T2D). Insulin production is almost nonexistent for T1D, whereas it is low or defective in the case of T2D. The authors in [5] review the classification of the different types of diabetes broadly.

T2D is the most common one, representing around 90% of the total diabetic population in the world [28]. The body produces almost no insulin in T1D. In T2D, the insulin produced either is not sufficient or is defective. The treatment depends on the type of diabetes and relies mostly on physical activity, healthy regimen, external injection of insulin, etc. The goal is to maintain BG levels within normal values to delay or prevent complications.

T1D treatment is based mainly on the external administration of insulin called insulin therapy. As part of treatment, T1D patients should inject insulin before each meal. The determination of the appropriate dose is a very challenging task because of the high variation in insulin requirements, influenced by multiple known and

A. Mansour (✉) · K. Amroun
Laboratoire d'Informatique MEDicale (LIMED), Faculte des Sciences Exactes,
Université de Bejaia, Bejaia, Algeria

Z. Habbas
LORIA, Université de Lorraine, Lorraine, France
e-mail: zineb.habbas@univ-lorraine.fr

unknown factors such as the amount of carbohydrate, protein, and fat contained in the meal, daytime, physical activity, stress, illness, etc. As a result, T1D patients have to consider many variables to perform actions, decisions, and diet adjustments in the daily routine.

Decision support systems called bolus calculators (BCs) assist them in determining the appropriate dose to help T1D patients in the decision-making process. Nowadays, these tools provide many advantages, and they contribute to T1D management. Some of them have received approbation in Europe and the USA [78], but they are not optimal and present some limitations related primarily to their modest adaptability to specific individual circumstances.

The development of these tools results from the collaboration between several fields of research, namely, medical, pathology, mathematical modeling in diabetes, control theory, and computer science. Over the past decades, artificial intelligence (AI) methodologies helped to develop BCs with promising results regarding glyce-mic control.

This paper explains the most knowledge needed by AI researchers to develop software tools. First, it provides a general overview of the elementary concepts and terminology definitions and terminology about diabetes frequently required for the development of BCs. Then, the authors exhibit how to determine the appropriate insulin dose that must be injected before the meal using a simple calculation. The “Bolus Calculators” section presents the main key terms related to this field, BC benefits, some BC algorithms based on AI techniques, how to estimate the meal content, and the evaluation BC algorithms using simulation and being in a real clinical environment. Finally, discussion and conclusions appear in the last section.

5.2 Diabetes

Some physiological variables such as body temperature, blood pressure, heart rate, and BG level must be kept within specific ranges of values despite body disturbances, thanks to a process of regulation called *homeostasis* that ensures the proper functioning of the organism.

These days, diabetes is an increasingly common, chronic, and incurable disease. It is a condition where the body can no longer maintain BG levels in normal range values, which means that *glucose homeostasis* is failing. An absence, a lack, or a defect of a hormone secreted by the pancreas B cells, called *insulin*, causes this. *Glucose homeostasis* is maintained by the actions of several hormones, essentially insulin and glucagon.

The glucose is the primary source of energy for body cells. Some types of cells, such as muscle ones, entail the presence of insulin, while others, e.g., the brain cells, do not require its intervention. These types of glucose use are called *insulin-dependent glucose uptake (IDGU)* and *insulin-independent glucose uptake (IIGU)*, respectively.

When no insulin is present in the body, the glucose is only consumed in an insulin-independent manner, which leads to an increase in the BG level (*hyperglycemia*) since the IDGU failed. In this case, the body looks for other energy sources to feed cells for which glucose consumption depends on insulin. This energy can be provided from different sources, for example, from fat cells that release a toxic substance called *ketone bodies* that makes the blood too acidic. This situation is known as a potentially life-threatening complication if not treated in time. It is *diabetic ketoacidosis*. In the long term, frequent hyperglycemia cause some complications especially in the eyes (retinopathy), kidneys (nephropathy), nerve (neuropathy), blood vessels, and heart, among other problems.

The treatment aims to normalize BG, i.e., maintain their blood glucose concentration (BGC) within a safe target range (70–180 mg/dL) as often as possible during the day, and to have an *HbA1c* (average blood glucose in the last 3 months) less than 7%. However, very low or very high blood glucose levels, called *hypoglycemia* and *hyperglycemia*, respectively, must be avoided. Several studies indicated that good glycemic control is effective in reducing the development and delaying the progression of long-term microvascular diabetic complications [19, 51, 79].

T1D treatment relies mainly on the administration of external insulin, which is often necessary for survival, called insulin therapy [52] utilizing two types of insulin: the *rapid-acting insulin* and *short-acting insulin*. They differ according to their onset and duration of action. The technical materials commonly used for its injection are the insulin pen and the insulin pump. For routine use, insulin is administered by T1D patients via the subcutaneous route (into the fatty tissues just beneath the skin). The BG measurement with BG meters (BGM) measures the BG from fingertip blood drop. Continuous glucose monitors (CGM) can also measure the interstitial glucose concentration in real time. Note that there is a time lag of BG value in these two places (capillary and interstitial glucose concentration) [65]. The use of insulin pumps and CGM avoids multiple uncomfortable injections and measurements, respectively.

The glycemic control can be achieved in T1D with an *intensive insulin therapy (IIT)*, i.e., by means of multiple daily BG measurements and insulin injections either with an insulin pen or pump, with a good adaptation of the doses. It is known that such therapy decreases the frequency or severity of diabetic complications [19].

The bolus-basal is the most common therapy in patients with T1D derived from *IIT*. It is proposed to mimic the normal physiological secretion of insulin. The injected insulin consists of *basal insulin* needed to provide glucose control between meals and overnight that reliably lasts at least 24 h and *bolus insulin* provided at times of eating to reduce postprandial glucose level caused by food intake. As an illustration, the body constantly needs insulin to allow the cells that use glucose in an insulin-dependent way to acquire energy, hence the main role of basal insulin. The use of an insulin pen involves the injection of short-acting insulin for basal needs and rapid-acting insulin for bolus needs. In the case of an insulin pump, only rapid-acting insulin is used. Clinicians generally adjust basal insulin dose in collaboration with patients during periodic visits. The treatment of T2D is based

essentially on lifestyle changes with a balanced diet, weight control, and regular practice of physical activity [12].

Diabetes self-management (DSM) for T1D patients is a therapeutic approach that leads to improve glycemic control and to prevent or delay the development of diabetes-related complications [70]. It includes mainly an education on carbohydrate counting and possibly fat and protein amount estimation to determine meal-time insulin dosing [6]. The calculation of the appropriate dose should not be a source of confusion. Errors can have a major deleterious effect on the quality of glycemic control achieved, i.e., risk of postprandial hypoglycemia or hyperglycemia. Hence, the interest of developing decision support systems (BCs) that assist T1D patients in the determination of the proper dose of insulin must be injected before the meal to cover insulin requirements of the postprandial period.

5.3 Determination of the Appropriate Bolus Dose

Optimal glycemic control in T1D requires control of both fasting plasma glucose levels (between meals and overnight) and postprandial glucose levels, by combining basal insulin and bolus insulin, respectively. The basal or bolus insulin doses must correspond to the specific needs of each patient. The basal insulin requirements are computed using formulas or determined empirically based on trial-and-error techniques [17, 22]. The insulin bolus dose is generally obtained using Formula (5.4). It consists of the sum of the insulin that will lower the BG owing to the intake of carbohydrate (CHO) and the insulin that will correct an unwanted glucose concentration level found before taking the bolus. If active insulin remains from the previous boluses called insulin on board (IOB), it should be subtracted from the total insulin bolus (see Formula (5.1)). Note that a good estimate of the basal dose is essential to succeed in the insulin bolus calculation.

The Formula (5.4) employs a patient-specific parameter that needs to be optimally estimated before being used. A correct preliminary estimate of the insulin-to-carbohydrate ratio (ICR) and insulin sensitivity factor (ISF) is essential. The ICR is the amount of carbohydrate covered by a single unit of insulin. The ISF determines the degree of glucose decrease caused by a single unit of rapid-acting insulin. The ICR and ISF are influenced by the insulin sensitivity (i.e., the ability of insulin to stimulate glucose utilization and inhibit glucose production [66]) of each individual. They are patient- and daytime-specific parameters that may vary during the day, in response to various factors such as lifestyle, physical activity, stress, illness, changes in weight, growth hormone, changes in gastrointestinal physiology throughout the day, circadian rhythms for cortisol, etc. They often need further adaptation and are usually determined by clinicians in collaboration with patients during periodic visits. The authors in [22, 62] provide a review on how ICR and ISF are determined using rules of thumb.

The insulin bolus (B) is equal to the meal insulin if there is no IOB, and the current blood glucose $G_{current}$ is close to G_{target} (see Formula (5.2)). G_{target} is a

patient-specific parameter that determines the glycemic goals of the individual patient. It can be either a specific value or a range of values, and it can be fixed or time-varying on each meal. If the meal does not contain carbohydrate (CHO) or in case of a need to correct hyperglycemia, insulin bolus corresponds only to the insulin correction (see Formula (5.3)):

$$B = \text{Meal insulin} + \text{Correction insulin} - \text{IOB}, \quad (5.1)$$

$$\text{Meal insulin} = \frac{\text{CHO}}{\text{ICR}}, \quad (5.2)$$

$$\text{Correction insulin} = \frac{G_{\text{current}} - G_{\text{target}}}{\text{ISF}}, \quad (5.3)$$

$$B = \frac{\text{CHO}}{\text{ICR}} + \frac{G_{\text{current}} - G_{\text{target}}}{\text{ISF}} - \text{IOB}. \quad (5.4)$$

In the literature, other abbreviations of the Formula (5.4) parameters can be found. For example, one can find ICR [36], CIR [62], or CR [68] to describe carbohydrate-to-insulin ratio; insulin sensitivity factor (ISF) [36]; correction factor (CF) [68]; bolus insulin on board (BOB) [78]; or insulin on board (IOB) [36].

Information on the carbohydrate content of different foods is necessary to make correct estimates of CHO in the meal. The American Diabetes Association (ADA) recommends including protein and fat estimations in diabetes management [6] as they lead to increased insulin requirements. A study regarding the postprandial glycemic impact of dietary protein alone without carbohydrate or fat in people with T1D indicates that large amounts of protein consumed alone cause delayed and sustained postprandial glycemic excursions 3–5 h after the meal [57]. It is also observed a significant HbA1c reduction results when taking fat and protein into account for insulin dose calculations [55].

The Diabetes Control and Complications Trial (DCCT) recommend the adjustment of the insulin dose to the food intake since it can reduce the HbA1c [23]. However, the estimation of bolus insulin dose is a complicated process in which all parameters of the Formula (5.4) must be determined every mealtime. To make this complex calculative process more effective and easier for the patient, new decision support systems that could assist patients in making decisions on their insulin doses before meals are developed. BCs will be explained next.

5.4 Bolus Calculators (BCs)

BCs are generally based on the Formula (5.4), and they are usually incorporated into glucose meters, smartphones, and insulin pumps (the first BC in an insulin pump was introduced in 2002 in the Deltec Cozmo pump) [68, 78]. They require

reliable estimates of Formula (5.4) parameters. Several studies have reported that BCs are promising tools that improve the accuracy of insulin therapy, and they are recommended by the ADA [6]. They have shown benefit when compared with mental calculation [71]. The authors in [2] have reported that a manual estimate of insulin bolus dose by 64% of T1D patients is incorrect, compared to 6% of those done using a BC. A clinical benefit of BCs in a pediatric population using insulin pumps has also been demonstrated [69]. They are effective in controlling postprandial glucose levels by reducing the number of correction boluses needed to correct hyperglycemia and the amount of carbohydrate needed to correct hypoglycemia [33]. The authors in [84] have reported that the frequent use of BC can improve glycemic control of pediatric T1D populations treated with an insulin pump. Studies about patient satisfaction, confidence, and ease of use of BCs have shown interesting results [33, 58, 67, 75]. A review of the current BCs can be found in [11, 25, 38].

Despite all these benefits, only a few BCs have received Food and Drug Administration (FDA) approvals in the USA, and the first phone application received Conformite Europeenne (CE) approval in the European market was in 2013 [78]. BC performance remains suboptimal since they require the user estimation of the parameters of Formula (5.4), especially ICR and ISF, which are exposed to change over time due to different factors cited above. The process of determination and adaptation of the parameters often requires the help of experts. To make these applications very effective, it is necessary to adapt them to the individual specific circumstances automatically. Hence, more dynamic, adaptive, and personalized systems are required. For this purpose, advanced algorithms have been developed to enhance their adaptability.

The development workflow of BCs passes mainly through four steps shown in Fig. 5.1. The first step is the proposition of an algorithm that provides insulin dose recommendation based on pre-defined inputs (see Sect. 5.4.6). The second step is the in silico evaluation based on computer simulation (see Sect. 5.4.4). The third step is the implementation of the algorithm on devices like smartphones and insulin pumps (see Sect. 5.4.6). The last step is the in vivo evaluation based on clinical trials (see Sect. 5.4.7).

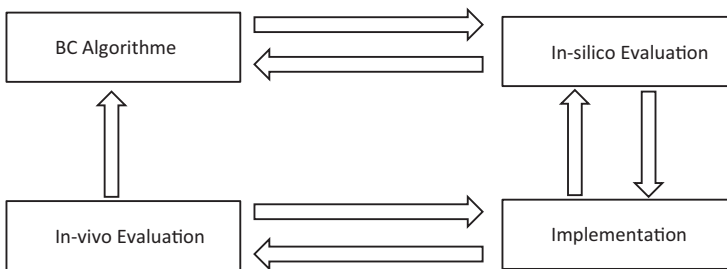


Fig. 5.1 Development workflow

5.4.1 Glossary and Key Terms

In this section, we present some concepts about BCs necessary to understand this field.

Closed-Loop

A closed-loop system is an automatic control system in which the glucose level is regulated by feedback. It links the CGM device and an insulin pump to a microprocessor, which uses mathematical algorithms to adjust the infusion rate. A closed-loop system is also called an artificial pancreas (as it does everything autonomously), but it is the preferred term in the healthcare world.

Open-Loop

An open-loop system is a control system where the delivery rate is preset, and there is no self-correcting action as there is in a closed-loop.

Run-to-Run Algorithms

The run-to-run (R2R) algorithms adjust the insulin bolus dose automatically on the basis of a performance measure for the same meal on the previous day(s). The run period is set equal to 24 h, which corresponds to the circadian rhythm of the subject's variation [72]. A preliminary study in [53] using R2R control for automatically adjusting the ICR parameter of a BC has shown promising results.

Case-Based Reasoning (CBR) Algorithms

CBR is an AI technique based on past problem-solving experiences to solve new ones [1]. It uses a knowledge base of past experiences. A case contains, basically, the description of the problem and its solution. This technique has proved its effectiveness in solving real-world problems, and it is widely applied in medicine [16, 37]. It can automate planning, diagnostic, design, and recommendation tasks. CBR originates from Kolodner's work based on Schank's idea of dynamic memory modeling and learning [41, 64]. It offers an interesting solution to deal with insulin sensitivity variations since it is capable of dealing with an unrestricted number of situations in which T1D patients can find themselves, considering that treating all of these possible situations can be very difficult because of the high combinatorial complexity.

Fuzzy Logic

Fuzzy logic is an extension of Boolean logic that enables a condition to be in a state more than true or false. It provides a precious flexibility for reasoning, which makes it possible to take into account inaccuracies and uncertainties. One advantage of fuzzy logic is its capability to describe rules in natural language to formalize human reasoning [24]. For example, in Boolean logic, a BG range >180 mg/dl is high, and a BG range <70 mg/dl is low. In fuzzy logic, one can say that 180 mg/dl is high but almost acceptable, while 300 mg/dl is very high and far from being acceptable; 70 mg/dl is low but almost acceptable but is very low and far from being satisfactory.

Artificial Neural Networks

They are systems inspired by the way biological neural networks process information. They are computational modeling tools that have emerged and found extensive acceptance in many disciplines for modeling complex real-world problems such as recognition, prediction, classification, optimization, etc. [7]. Recently, they become powerful and are one of the most popular machine learning models, especially when having massive datasets.

5.4.2 BC Algorithms Based on AI Techniques

The literature dealing with BCs presents several approaches based on artificial intelligence. CBR associated with R2R algorithms emerges as the favorite technique widely used in the literature. To our knowledge, the first CBR study for insulin recommender systems was proposed in [59]. In recent years, it is becoming an alternative to building BCs. Herrero et al. [36] have presented a new decision support algorithm that enhances standard BCs for T1D patients through the combination of R2R and CBR. The system exploits the data provided by CGM devices. ICR and ISF are updated daily according to a performance metric, presented by the distance between the minimum postprandial glucose concentration and the patient's target BG. It has been tested in silico using the UVA/PADOVA T1D simulator [43, 77] under realistic scenarios by emulating intra-subject insulin sensitivity variations, uncertainty in the capillarity measurements, and carbohydrate intake. Useful in silico results have been obtained. This study demonstrated a clear benefit of using CBR in combination with R2R instead of using R2R alone. In another study, the authors showed that the developed BC is safe for usage in T1D self-management [61].

The authors in [73] present "PepperRec," a BC-based CBR that accounts for missing values corresponding to factors that affect glucose metabolism, such as data about the physical activity. It calculates the ICR and ISF parameters from which the bolus is obtained. The BC is tested using the UVA/PADOVA T1D simulator. The achieved results demonstrate that "PepperRec" increases the number of times the users are in their target glycemic range and reduces the time spent below it while maintaining, or even reducing, the time spent above it. The authors in [11] proposed a novel approach that takes into account a temporal sequence of preceding events when computing the bolus insulin doses rather than looking at events in isolation. The authors in [74] propose a case-base maintenance methodology that decides which cases should be removed from the case base because they are redundant, old, etc. It combines case-base redundancy reduction and attribute weight learning. The proposed approach includes an algorithm for learning the relevance of the attributes, and it has been tested using the UVA/PADOVA T1D simulator. The authors in [74] present related literature in terms of CBR case-base maintenance algorithms and attribute weight learning.

The authors in [46] propose a bolus recommender system based on fuzzy logic, which simulation results for virtual subjects show that this system is effective and robust. The authors in [20] propose fuzzy decision support that suggests the appropriate bolus dose to be injected before the meal for T1D patients. This system takes into account the characteristics and the amount of the food, the preprandial glycemia, and the insulin resistance. Obtained results were promising compared to original doctor prescriptions.

The authors in [50] present the structure and the characteristics of an expert system to optimize the postprandial glycemia in T1D patients.

A neural network-based approach for optimization of bolus calculation using CGM was proposed in [13]. The system was tested *in silico* with the UVA/PADOVA T1D simulator, and results have shown a reduction in the BG risk index.

5.4.3 How Is the Meal Content Estimated Using AI Techniques?

The meal content is a paramount parameter in the determination of the pre-meal insulin dose. The success of the bolus calculation is significantly dependent on the correct estimation of the meal composition. In this context, some proposed systems attempt to recognize food and the amount of items present in meals automatically. Foltynski et al. [30] suggest insulin BC with automatic speech recognition, which estimates insulin dose based on the voice description of a meal. A study about the efficiency of automatic BC with automatic speech recognition in T1D patients has shown improvement in postprandial glucose control without increasing the time in hyperglycemia or hypoglycemia [29]. Authors in [56] presented an app that combines a nutrient database with the expert software named VoiceDiab for automatic speech recognition. Their study has been evaluated, with patients treated with continuous subcutaneous insulin infusion, in a crossover randomized controlled study made in 12 T1D adults, showing promising results.

Based on the k-means algorithm, LBP, and SVM AI techniques, the authors in [4] demonstrate the feasibility of a system that estimates carbohydrate amount based on its digital image. Therefore, it is possible to identify the food by taking a picture of the meal using a smartphone. Rhyner et al. [63] proposed GoCARB to support individuals with T1D during daily carbohydrate estimation. It hinges on computer vision techniques that automatically segment and recognize the different food items, and then the CHO content is calculated by combining the volume of each food item with the nutritional information provided by the Nutrient Database for Standard Reference (USDA).

5.4.4 *T1D In Silico Simulation Environment*

The term *in silico* refers to the usage of computer simulation to perform biological or medical experiments [54]. The *in silico* simulation is able to accelerate the evaluation process that is usually needed for expensive lab work and time-consuming in clinical experiments. It evaluates new treatments in diabetes, such as BC algorithms prior to their clinical application in humans. It allows performing some scenarios, which are too difficult, too dangerous, or not ethical in clinical experiments. Furthermore, it can provide valuable information about the safety, efficiency, and limitations of a newly developed algorithm [82].

The T1D *in silico* simulation environment, referred to as a simulator, is based essentially on mathematical models [14]. In its general scientific sense, a mathematical model in medicine is a formalization of a complex biological phenomenon by applying mathematical techniques and theories [14]. The literature dealing with mathematical modeling for different aspects of diabetes is abundant and is still an ongoing area of research [31].

The main components of these simulators are virtual T1D patient and virtual T1D population. A virtual patient incorporates a simulation model of the T1D patient physiology, which is characterized by a set of parameters that describe a specific patient. It can receive as inputs insulin delivery suggested by a BC algorithm, meals, etc. and provides as output the resulting glucose response. A virtual T1D population contains multiple virtual T1D patients. It utilizes multiple parameters set representing different virtual T1D patients that can be subdivided into different categories such as adults, adolescents, children, pregnant, etc. [81].

A T1D “virtual patient” is recently built from various sub-models. It includes a sub-model of the glucose kinetics and insulin action, a meal sub-model representing glucose absorption from the gastrointestinal tract, an exercise sub-model representing the effect of physical activity on glucose concentration [81], and sub-model of nocturnal glucose variability to describe the dawn phenomenon [72], among others. The number of other interacting physical sub-models depends on the input/output requirements of the material of treatment (insulin pumps, CGM, etc.). For example, in the case of testing a BC algorithm based on CGM and pump insulin, it is required to test it in a simulation environment that incorporates sub-models of subcutaneous glucose kinetics and the subcutaneous insulin kinetics, respectively [42, 81]. Figure 5.2 shows a schematic representation of an example of a T1D simulation environment.

A simulator is relevant if it provides a realistic testing scenario and grants to obtain the expected results observed in reality. Notwithstanding the significant progress made in the past years in the availability of large data from clinical trials and the new technologies of tracers and sensors, the simulation models, which compose those simulators, have some limitations. Thus, there is a need to refine these models to be more realistic and compassing on:

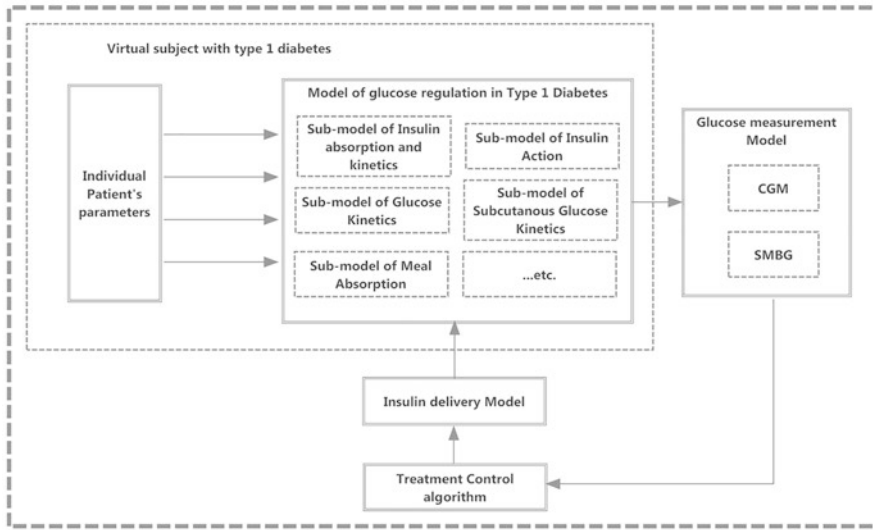


Fig. 5.2 A schematic representation of T1D virtual patient

- (i) The absorption of various kinds of food
- (ii) Physical activity
- (iii) The patient's behavior in making treatment decisions [76]
- (iv) Intra- and inter-day variability of insulin sensitivity
- (v) Intra- and intersubject variability of daily insulin sensitivity
- (vi) Dawn phenomenon
- (vii) Models of error affecting continuous glucose monitoring
- (viii) Self-monitoring BG devices, etc.

One of the most popular simulation environments is the commercial type 1 Diabetes Metabolic Simulator (T1DMS) UVA/PADOVA created by The Epsilon Group. The Food and Drug Administration (FDA) accepted it in 2013 as a substitute for preclinical animal trials in the testing of control strategies for T1D. It is implemented with Simulink/MATLAB and uses the mathematical model of Dalla Man et al. [21]. It is based on quantitative knowledge of glucose-insulin metabolism and data acquired from a large-population human subject study. There is an updated model published in 2014 [49] that included the effects of glucagon and refinement of insulin kinetics, taking into account increased insulin sensitivity during hypoglycemia.

The automated insulin dosage advisor (AIDA) is a simulation environment that incorporates a model of the glucose-insulin system in T1DM. It is used for patient and clinical staff education and is available as a free software download or online. It uses a knowledge-based system to make glycemic predictions and to generate insulin dosage adjustment advice [45]. Other simulation environments to support the development of glucose control algorithms can be found in [80].

5.4.5 *Statistical Measures for Evaluation of Bolus Calculators*

Assessment of BCs can be accomplished by analyzing the pattern of multiple BG samples drawn over time. The BG data provides the best representation from SMBG or CGM of the subject's well-being. Despite their inherent limitations [18], CGM devices produce complex and voluminous data interpreted by many statistical measures to evaluate the quality of BG, control algorithms. It is important to note that there is no clear consensus on the gold-standard statistical measures of glucose variability in clinical practice and research [32] that means that the interpretation of the data can be different from statistical measure to another. The choice of the performance metrics is a critical point, so the BC algorithms need to be assessed by appropriate performance metrics [72].

Several performance indices have been proposed to evaluate and compare the efficacy of the various algorithms.

Area Under the Curve

The glucose area under the curve (AUC), which is based on CGM data, is the definite integral in a plot of BG concentration over the postprandial period.

Times Within, Above, and Below Target Blood Glucose Level Range

Indicates the percentage of times the subject spends within, above, and below a pre-defined target range. A high percentage within the target range (e.g., [80–140]) is a good indicator of how the solutions provided are safe for the subject, contrary to a high percentage above and below target BG level range, which are not safe. However, this measure does not take into account the presence of extreme highs and lows of BG, which can be dangerous to the patient. The arbitrary definition of the BG target can be a disadvantage, as it is a patient-specific parameter [72].

Mean Blood Glucose Level

The mean of the blood glucose data is a simple indicator of the subject's overall well-being; it is calculated as the arithmetic mean of postprandial BG concentrations but does not aid in representing the variance, extreme lows, and extreme highs of BG levels. The optimal target means BG is dependent upon the subject's target BG level [27, 10].

Standard Deviation (SD)

It is a measure of the dispersion of data values around mean BG. The aim is to get low SD with minimal swings, which would reflect steady glucose levels. As an illustration, if the subject's BG levels are bouncing around between many highs and many lows on a given period, they will have a larger SD. If the subject's BG control is reasonable, he will have a lower SD. It is worth noting that a low deviation would indicate that the subject is consistently outside the safe zone if it is associated with low or high BG levels.

Low Blood Glucose Index, High Blood Glucose Index, and Blood Glucose Risk Index

The low blood glucose index (LBGI) and high blood glucose index (HBGI), which can be obtained both from SMBG and CGM data, are popular metrics used to quantify the risk of hypo- and hyperglycemia [27]. They represent the frequency and extent of low and high BG measurements, respectively. Higher LBGI or HBGI may indicate a large number of mild hypoglycemia/hyperglycemia, a small number of severe hypoglycemia or hyperglycemia, or a combination of both, respectively. The sum of LBGI and HBGI is the BG risk index (BGRI) which indicates the risk of experiencing extreme glycemic values [27, 32]. Some studies have shown the difference between LBGI and HBGI obtained based on SMBG and CGM [27].

The Control-Variability Grid Analysis (CVGA)

The overall performance in a population of T1D patients can be measured by using the control-variability grid analysis (CVGA). This method allows visualization of the minimum/maximum glucose values caused by a control algorithm in a population of patients either real or virtual, where each subject is represented by a single data point for any given observation period [47, 48]. For interested readers, a comprehensive presentation of CVGA can be found in [48].

5.4.6 Implementation

Once the in silico test phase of the proposed algorithm was completed with good preliminary results, the next step is to implement it on an insulin pump, glucometer, or smartphone to test it in vivo with human patients. The following points must be taken during the implementation:

- The acceptance of the BC by patients depends on the ease of use of human-machine interface (HMI) which must use the language, terminology, and lexicon familiar to patients.
- The application must be secure by password to avoid any tempting to do modification in the configuration.
- The automatic input of glucose readings to BCs results in usage simplification.

After the optimization and implementation of the algorithm, the application will be tested in a clinical trial.

5.4.7 In Vivo Evaluation

The definitive answer to how the performance of the developed BC is can only come from well-designed, randomized, controlled clinical trials. Thus, once the BC is implemented and incorporated to a smartphone, pump glucometer, or other devices,

the next step is testing it under real-life conditions with real patients; the results provided in this step determine the goodness of the developed BC. This step aims to validate the findings from the *in silico* evaluation; verify the safety, usability, efficacy, feasibility, and patient confidence to such tools; and ensure the consistency of dose recommendations. Before the first use, clinical guidance for patients on operating the BC is required, including how to select appropriate settings and how to adjust bolus recommendations when outside factors exist, such as physical activity. To obtain more credible results in the *in vivo* evaluation, it is essential to:

- Prepare the proper testing environment that includes the necessary human and physical means
- Test the BC behavior in routine and outlier situations
- Choose the target population based on diabetes self-management skills, gender, age, etc.

It is important to note the difficulty to isolate the benefit of BCs from other variables (such as carb counting skills, generally patient participating in the trial showing a high level of motivation, the inherent bias of algorithms related to food choices) that are determinants in the glucose control [68].

5.5 Discussion

Diabetes is a delicate disease that can have adverse health effects in the short and long term. There is a large diabetic population in the world, and research has not yet found an effective treatment. T1D treatment requires external insulin injections. A part of the treatment is based on the external injection of insulin before each meal. However, the determining of the appropriate dose is a complex decision task, which is depending on several factors such as meal content, mealtime, physical activity, stress, illness, daytime, etc. Note that optimal glycemic control in T1D requires control of both fasting plasma glucose and postprandial glucose levels. Hence, a reasonable estimate of the bolus dose depends on how correct is estimated the basal dose. Therefore, BCs are developed to assist T1D patients in the decision-making process. They are incorporated in some insulin pumps, glucometers, and smartphones, and they generally rely on the Formula (5.4).

BCs are helpful tools that are able to support diabetic patients in their therapy management. The determination of an optimal dose requires to user to define optimal values of each parameter of Formula (5.4), which are time-varying and patient-specific, particularly the ICR and ISF. Error in the estimation of a single parameter can lead to an error in the recommended insulin dose, which increases the risk of having postprandial hypoglycemia/hyperglycemia. Unfortunately, the methods for estimation of these parameters have not been fully optimized. Note that Formula (5.4) depends only on the carbohydrate nutrient.

Nevertheless, it has revealed in the literature that other macronutrients of meals, such as fat and protein, play an essential role in the postprandial glucose response,

which means that high-protein and/or high-fat meals lead to increased insulin requirements. Hence, the Formula (5.4) alone cannot return an optimal dose. Therefore, including the content of different foods (CHO, fat, and protein) is required when performing the calculation. Several works have proposed solutions that consider mixed meals containing fat and protein [8]. Note that all patients may not master these advanced assessments of meal composition. Additionally, BG meters need to be optimized to return values close to the real BG. Moreover, the patients' target BG should be regularly reviewed by an expert.

In the *in silico* evaluation step, algorithms must be tested under realistic scenarios that emulate intra-subject and intersubject insulin sensitivity variations, uncertainty in the glucose level measurements, and carbohydrate intake. To prevent insulin overdosing, setting safety constraints is recommended, such as avoiding an exaggerated update of the solution (ICR or ISF) and bounding the minimum and maximum values of the solution [36].

Many statistical measures exist for the assessment of BC algorithms. Note that there is no clear consensus on the gold-standard statistical measures of glucose variability in clinical practice and research [32], which means that the interpretation of the data analyses can be different from statistical measures to another.

The development of a closed-loop artificial pancreas (AP) is one of the main goals of diabetes management. It has the intent to eliminate the decision-making task. One could argue that achieving this goal will make BCs useless. However, there is still difficult work to achieve this goal satisfactory and accessible to everyone for different reasons, e.g., lack of acceptability, challenges of cost-effectiveness, and ethical issues [9, 60], among others. Indeed, AP uses a hybrid approach that requires the injection of a portion of the meal insulin dose in an open-loop manner before the meal [26] to compensate for the substantial absorption/action delay of insulin given by the subcutaneous route, which can lead to early postprandial hyperglycemia [26]. This dose can be computed using BCs. Hence, using this hybrid approach, which combines open-loop and closed-loop methods, remains valid in the future for T1D patients relying on basal-bolus insulin therapy. Therefore, any improvement of BCs by researchers will be welcome, as there is a need to improve their performance [35]. In this context, the authors in [34] present a new technique, based on CBR/R2R, to automatically adapt the meal-priming bolus within an AP. Improvement in glycemic control in T1D has been noticed compared to its non-adaptive methods.

There exist several possibilities that can empower BCs. However, numerous challenges arise from their developments. In the following, we describe some possibilities that can improve their ability to make decisions. Essentially, through the design of algorithms that:

- Automatically adjust the dynamics of ICR and ISF parameters.
- Accurately account for residual insulin activity from recent bolus doses to avoid overdoses of insulin.
- Take into account mixed meals (CHO, fat, and protein).

- Exploit the CGM measurements to obtain more information on the patients' status (e.g., trend, rate of change (ROC)) [35, 39].
- Remind the patient in case of forgetting to take the bolus. This can be achieved by proposing algorithms that can detect a meal based on changing glucose levels (e.g., as the time becomes longer between meals, the probability that a meal will be consumed in the near future increases) [44]. Alternatively, by the usage of wearable body sensors, for detecting intake gestures like intentional arm movements to bring food into the mouth, chewing sounds during food intake, and swallowing [3, 83].
- Automatically assess CHO content in a patient's diet, via smartphones' features such as their cameras and microphones (speech recognition) [4, 29, 30].
- Improve the ease of usage of BCs through the standardization of the user interface terminology to address issues related to ambiguity [78].
- Recommend carbohydrate intake needed to prevent or treat hypoglycemia when IOB is excessive.
- Recommend correction boluses, drug, or physical exercise to deal with hyperglycemia.
- Remind the patient using CGM or insulin pumps of certain behaviors linked to the use of BCs such as shutting off insulin delivery in advance of physical activities and periodically calibrating the CGM using a "finger-stick" glucometer [44].

It is important to realize that BCs are required to be sufficiently "safe" and "secure." As an illustration, modern commercial devices like CGM sensors can transfer data directly to smartphones [44]. Therefore, BCs must receive data from those devices without any form of data corruption. In addition, there is a necessity for any operating system update to not impact applications (BCs) safety, as reported by the US Food and Drug Administration (FDA) [40]. Another key point is the emerging technology of the Internet of things, which can significantly contribute toward the improvement of BCs, by enabling seamless integration of more data in BC algorithms. This integration increases security concerns with the mass deployment of connected objects involving sensitive or critical data.

5.6 Conclusion

Chronic diseases such as diabetes can benefit from the connectivity access of the Internet of things (IoT), cloud computing, and databases. Recently, the controlling of type 1 diabetes (T1D) prompted the development of new technologies and devices that could be of help in home care and healthcare facilities via the Internet, relying on wireless communications [85–92].

Our main aim in this paper is to provide to readers, especially the AI community, the necessary background for the development and improvement of BCs. Knowledge from different fields of research like medicine, diabetes, and mathematical modeling in diabetes is presented. In contemporary times, promising results have been

obtained using solutions based on AI techniques [16, 92–97]. These solutions tempt essentially to:

- Adapt the ICR and ISF values to the different situations in which T1D patients can find themselves
- Recognize the different items in a meal
- Try to spot other patients' features that can fine-tune the analysis

The evaluation of BC algorithms can require large clinical trials when performed in humans. Simulation environments that depend primarily on the mathematical models of the physiology of a diabetic patient and the associated treatment devices can accelerate the development of BCs.

The development of BCs requires skills from areas like diabetes, mathematical modeling, control theory, etc. Therefore, multidisciplinary research teams, including computer engineers and clinicians, mathematicians, etc., are necessary for cooperation in this field, in order to contribute to the improvement of BCs. Finally, a possibility to improve BCs is related to the availability of data obtained via different sensors, which allows creating large datasets that can be used by machine learning and deep learning techniques combined with security measures and energy-efficient designs [97–106].

References

1. A. Aamodt, E. Plaza, Case-based reasoning: foundational issues, methodological variations, and system approaches. *AI Commun.* **7**(1), 39–59 (1994)
2. A.J. Ahola, S. Ma Kimattila, M. Saraheimo, V.F. Mikkila, C. Orsblom, R. Freese, P.-H. Groop, F.S. Group, Many patients with type 1 diabetes estimate their prandial insulin need inappropriately. *J. Diabetes* **2**(3), 194–202 (2010)
3. O. Amft, *Automatic Dietary Monitoring Using On-body Sensors: Detection of Eating and Drinking Behaviour in Healthy Individuals* (ETH, Zurich, 2008)
4. M. Anthimopoulos, J. Dehais, S. Shevchik, B.H. Ransford, D. Duke, P. Diem, S. Mougiakakou, Computer vision-based carbohydrate estimation for type 1 patients with diabetes using smartphones. *J. Diabetes Sci. Technol.* **9**(3), 507–515 (2015)
5. S. Canivell, R. Gomis, Diagnosis and classification of autoimmune diabetes mellitus. *Autoimmun. Rev.* **13**(4–5), 403–407 (2014)
6. G. Rossi, Diagnosis and classification of diabetes mellitus. *Diabetes Care* **31**, S55–S60 (2008)
7. I.A. Basheer, M. Hajmeer, Artificial neural networks: fundamentals, computing, design, and application. *J. Microbiol. Methods* **43**(1), 3–31 (2000)
8. M. Błazik, E. Pankowska, The effect of bolus and food calculator diabetics on glucose variability in children with type 1 diabetes treated with insulin pump: the results of RCT. *Pediatr. Diabetes* **13**(7), 534–539 (2012)
9. C. Boughton, R. Hovorka, Is an artificial pancreas (closed-loop system) for type 1 diabetes effective? *Diabet. Med.* **36**(3), 279–286 (2019)
10. D. Brown, *Temporal Case-Based Reasoning for Insulin Decision Support*. PhD thesis (Oxford Brookes University, Oxford, 2015)
11. D. Brown, A. Aldea, R. Harrison, C. Martin, I. Bayley, Temporal case-based reasoning for type 1 diabetes mellitus bolus insulin decision support. *Artif. Intell. Med.* **85**, 28–42 (2018)

12. C. Burant, *Medical Management of Type 2 Diabetes* (American Diabetes Association, Virginia, 2012)
13. G. Cappon, M. Vettoretti, F. Marturano, A. Facchinetti, G. Sparacino, A neural-network-based approach to personalize insulin bolus calculation using continuous glucose monitoring. *J. Diabetes Sci. Technol.* **12**(2), 265–272 (2018)
14. S. Chevret, Modeles mathematiques utilises en medecine. *Reanimation* **16**(3), 240–244 (2007)
15. N. Cho, J. Shaw, S. Karuranga, Y. Huang, J. Da Rocha Fernandes, A. Ohlrogge, B. Malanda, IDF diabetes atlas: Global estimates of diabetes prevalence for 2017 and projections for 2045. *Diabetes Res. Clin. Pract.* **138**, 271–281 (2018)
16. N. Choudhury, S.A. Begum, A survey on case-based reasoning in medicine. *Int. J. Adv. Comput. Sci. Appl.* **7**(8), 136–144 (2016)
17. N. Chow, D. Shearer, H.G. Tildesley, J.A. Plaa, B. Pottinger, M. Pawlowska, A. White, A. Priestman, S.A. Ross, H.D. Tildesley, Determining starting basal rates of insulin infusion for insulin pump users: a comparison between methods. *BMJ Open Diabetes Res. Care* **4**(1), e000145 (2016)
18. C. Cobelli, E. Renard, B. Kovatchev, Artificial pancreas: past, present, future. *Diabetes* **60**(11), 2672–2682 (2011)
19. Control, D., and Group, C. T. R., The effect of intensive treatment of diabetes on the development and progression of long-term complications in insulin-dependent diabetes mellitus. *N. Engl. J. Med.* **329**(14), 977–986 (1993)
20. B. Cosenza, Off-line control of the postprandial glycemia in type 1 diabetes patients by a fuzzy logic decision support. *Expert Syst. Appl.* **39**(12), 10693–10699 (2012)
21. C. Dalla Man, R.A. Rizza, C. Cobelli, Meal simulation model of the glucose-insulin system. *IEEE Trans. Biomed. Eng.* **54**(10), 1740–1749 (2007)
22. P. Davidson, H. Hebblewhite, R. Steed, B. Bode, Analysis of guidelines for basal bolus insulin dosing: Basal insulin, correction factor, and carbohydrate-to insulin ratio. *Endocr. Pract.* **14**(9), 1095–1101 (2008)
23. L.M. Delahanty, B.N. Halford, The role of diet behaviors in achieving improved glycemic control in intensively treated patients in the diabetes control and complications trial. *Diabetes Care* **16**(11), 1453–1458 (1993)
24. F. Deroncourt, *Introduction to Fuzzy Logic* (Massachusetts Institute of Technology, 2013), p. 21
25. L. Eiland, M. Mclarney, T. Thangavelu, A. Drincic, App-based insulin calculators: current and future state. *Curr. Diab. Rep.* **18**(11), 123 (2018)
26. J. El Youssef, J. Castle, W.K. Ward, A review of closed-loop algorithms for glycemic control in the treatment of type 1 diabetes. *Algorithms* **2**(1), 518–532 (2009)
27. C. Fabris, S.D. Patek, M.D. Breton, Are risk indices derived from CGM interchangeable with SMBG-based indices? *J. Diabetes Sci. Technol.* **10**(1), 50–59 (2016)
28. O. Katherine, et al. IDF Diabetes Atlas: Global estimates for the prevalence of diabetes for 2015 and 2040. *Diabetes research and clinical practice* **128**(2017): 40–50
29. P. Foltynski, P. Ladyzynski, E. Pankowska, K. Mazurczak, Efficacy of automatic bolus calculator with automatic speech recognition in patients with type 1 diabetes: a randomized crossover trial: 1. *J. Diabetes* **10**(7), 600–608 (2018)
30. P. Foltynski, P. Ladyzynski, E. Pankowska, K. Mazurczak, M. Rachuta, B. Bonalska, J. Krzymien, Insulin bolus calculator with automatic speech recognition, in *EMBECC & NBC 2017*, (Springer, Singapore, 2017), pp. 603–606
31. K. Fritzen, L. Heinemann, O. Schnell, Modeling of diabetes and its clinical impact. *J. Diabetes Sci. Technol.* **12**(5), 976–984 (2018)
32. S. Frontoni, P. Di Bartolo, A. Avogaro, E. Bosi, G. Paolisso, A. Ceriello, Glucose variability: an emerging target for the treatment of diabetes mellitus. *Diabetes Res. Clin. Pract.* **102**(2), 86–95 (2013)
33. T.M. Gross, D. Kayne, A. King, C. Rother, S. Juth, A bolus calculator is an effective means of controlling postprandial glycemia in patients on insulin pump therapy. *Diabetes Technol. Ther.* **5**(3), 365–369 (2003)

34. P. Herrero, J. Bondia, O. Adewuyi, P. Pesl, M. El-Sharkawy, M. Reddy, C. Toumazou, N. Oliver, P. Georgiou, Enhancing automatic closed-loop glucose control in type 1 diabetes with an adaptive meal bolus calculator—in silico evaluation under intraday variability. *Comput. Methods Prog. Biomed.* **146**, 125–131 (2017)
35. P. Herrero, P. Pesl, J. Bondia, M. Reddy, N. Oliver, P. Georgiou, C. Toumazou, Method for automatic adjustment of an insulin bolus calculator: in silico robustness evaluation under intra-day variability. *Comput. Methods Prog. Biomed.* **119**(1), 1–8 (2015)
36. P. Herrero, P. Pesl, M. Reddy, N. Oliver, P. Georgiou, C. Toumazou, Advanced insulin bolus advisor based on run-to-run control and case-based reasoning. *IEEE J. Biomed. Health Inform.* **19**(3), 1087–1096 (2015)
37. A. Holt, I. Bichindaritz, R. Schmidt, P. Perner, Medical applications in case-based reasoning. *Knowl. Eng. Rev.* **20**(3), 289–292 (2005)
38. K. Huckvale, S. Adomaviciute, J.T. Prieto, M.K.-S. Leow, J. Car, Smartphone apps for calculating insulin dose: a systematic assessment. *BMC Med.* **13**(1), 106 (2015)
39. In Children Network (Direcnet) Study Group, D. R, Use of the Direcnet applied treatment algorithm (data) for diabetes management with a real-time continuous glucose monitor (the freestyle navigator). *Pediatr. Diabetes* **9**(2), 142–147 (2008)
40. D.C. Klonoff, D. Kerr, D. Kleidermacher, Now is the Time for a Security and Safety Standard for Consumer Smartphones Controlling Diabetes Devices (2017)
41. J. Kolodner, *Case-Based Reasoning* (Morgan Kaufmann, San Francisco, 2014)
42. L. Kovacs, G. Eigner, System engineering approach of diabetes treatment. *Int. J. Diabetes Clin. Diagn.* **3**(116), 1–6 (2016)
43. B.P. Kovatchev, M. Breton, C. Dalla Man, C. Cobelli, *In Silico Pre-clinical Trials: A Proof of Concept in Closed-Loop Control of Type 1 Diabetes* (2009)
44. T. Kushner, B.W. Bequette, F. Cameron, G. Forlenza, D. Maahs, S. Sankaranarayanan, Models, devices, properties, and verification of artificial pancreas systems, in *Automated Reasoning for Systems Biology and Medicine*, (Springer, Cham, 2019), pp. 93–131
45. E. Lehmann, T. Deutsch, E. Carson, P. Sonksen, Aida: an interactive diabetes advisor. *Comput. Methods Prog. Biomed.* **41**(3–4), 183–203 (1994)
46. S.-W. Liu, H.-P. Huang, C.-H. Lin, I.-L. Chien, Fuzzy-logic-based supervisor of insulin bolus delivery for patients with type 1 diabetes mellitus. *Ind. Eng. Chem. Res.* **52**(4), 1678–1690 (2013)
47. L. Magni, M. Forgione, C. Toffanin, C. Dalla Man, B. Kovatchev, G. De Nicolao, C. Cobelli, *Run-to-Run Tuning of Model Predictive Control for Type 1 Diabetes Subjects: In Silico Trial* (2009)
48. L. Magni, D.M. Raimondo, C.D. Man, M. Breton, S. Patek, G. De Nicolao, C. Cobelli, B.P. Kovatchev, Evaluating the efficacy of closed loop glucose regulation via control-variability grid analysis. *J. Diabetes Sci. Technol.* **2**(4), 630–635 (2008)
49. C.D. Man, F. Micheletto, D. Lv, M. Breton, B. Kovatchev, C. Cobelli, The UVA/PADOVA type 1 diabetes simulator: new features. *J. Diabetes Sci. Technol.* **8**(1), 26–34 (2014)
50. L. Nobile, B. Cosenza, M. Amato, V. Guarnotta, C. Giordano, A. Galluzzo, M. Galluzzo, Development of a fuzzy expert system for the control of glycemia in type 1 diabetic patients, in *Computer Aided Chemical Engineering*, vol. 29, (Elsevier, Burlington, 2011), pp. 1568–1572
51. Y. Ohkubo, H. Kishikawa, E. Araki, T. Miyata, S. Isami, S. Motoyoshi, Y. Kojima, N. Furuyoshi, M. Shichiri, Intensive insulin therapy prevents the progression of diabetic microvascular complications in Japanese patients with non-insulin dependent diabetes mellitus: a randomized prospective 6-year study. *Diabetes Res. Clin. Pract.* **28**(2), 103–117 (1995)
52. D.R. Owens, B. Zinman, G.B. Bolli, Insulins today and beyond. *Lancet* **358**(9283), 739–746 (2001)
53. C.C. Palerm, H. Zisser, W.C. Bevier, L. Jovanovic, F.J. Doyle, Prandial insulin dosing using run-to-run control: application of clinical data and medical expertise to define a suitable performance metric. *Diabetes Care* **30**(5), 1131–1136 (2007)
54. B. Palsson, The challenges of in silico biology. *Nat. Biotechnol.* **18**(11), 1147 (2000)

55. E. Pankowska, M. Błazik, L. Groele, Does the fat-protein meal increase postprandial glucose level in type 1 diabetes patients on insulin pump: the conclusion of a randomized study. *Diabetes Technol. Ther.* **14**(1), 16–22 (2012)
56. E. Pankowska, P. Ładzycki, P. Foltynski, K. Mazurczak, A randomized controlled study of an insulin dosing application that uses recognition and meal bolus estimations. *J. Diabetes Sci. Technol.* **11**(1), 43–49 (2017)
57. M. Paterson, C. Smart, P. Lopez, P. Mcelduff, J. Attia, C. Morbey, B. King, Influence of dietary protein on postprandial blood glucose levels in individuals with type 1 diabetes mellitus using intensive insulin therapy. *Diabet. Med.* **33**(5), 592–598 (2016)
58. P. Pesl, P. Herrero, M. Reddy, M. Xenou, N. Oliver, D. Johnston, C. Toumazou, P. Georgiou, An advanced bolus calculator for type 1 diabetes: system architecture and usability results. *IEEE J. Biomed. Health Inform.* **20**(1), 11–17 (2016)
59. C. Poerschke, *Development and Evaluation of an Intelligent Handheld Insulin Dose Advisor for Patients with Type 1 Diabetes*. PhD thesis (Oxford Brookes University, 2004)
60. A. Quintal, V. Messier, R. Rabasa-Lhoret, E. Racine, A critical review and analysis of ethical issues associated with the artificial pancreas. *Diabetes Metab.* **45**(1), 1–10 (2019)
61. M. Reddy, P. Pesl, M. Xenou, C. Toumazou, D. Johnston, P. Georgiou, P. Herrero, N. Oliver, Clinical safety and feasibility of the advanced bolus calculator for type 1 diabetes based on case-based reasoning: a 6-week nonrandomized single arm pilot study. *Diabetes Technol. Ther.* **18**(8), 487–493 (2016)
62. F. Reiterer, H. Kirchsteiger, A. Assalone, G. Freckmann, L. Del Re, Performance assessment of estimation methods for CIR/ISF in bolus calculators. *IFAC Papers OnLine* **48**(20), 231–236 (2015)
63. D. Rhyner, H. Loher, J. Dehais, M. Anthimopoulos, S. Shevchik, R.H. Botwey, D. Duke, C. Stettler, P. Diem, S. Mouggiakakou, Carbohydrate estimation by a mobile phone-based system versus self-estimations of individuals with type 1 diabetes mellitus: a comparative study. *J. Med. Internet Res.* **18**(5), e101 (2016)
64. R.C. Schank, *Dynamic Memory: A Theory of Reminding and Learning in Computers and People*, vol 240 (Cambridge University Press, Cambridge, 1982)
65. L. Schaupp, G. Brunner, H. Schaller, M. Bodenlenz, A. Wutte, P. Wach, T. Pieber, Glucose monitoring in the adipose tissue of type 1 diabetic patients using open-flow microperfusion and microdialysis, in *Diabetologia*, vol. 44, (Springer, 2001), pp. A46–A46
66. M. Schiavon, C. Dalla Man, Y.C. Kudva, A. Basu, C. Cobelli, Quantitative estimation of insulin sensitivity in type 1 diabetic subjects wearing a sensor augmented insulin pump. *Diabetes Care* **37**(5), 1216–1223 (2014)
67. S. Schmidt, M. Meldgaard, N. Serifovski, C. Storm, T.M. Christensen, B. Gaderasmussen, K. Nørgaard, Use of an automated bolus calculator in MDI-treated type 1 diabetes: the bolus-cal study, a randomized controlled pilot study. *Diabetes Care* **35**(5), 984–990 (2012)
68. S. Schmidt, K. Nørgaard, Bolus calculators. *J. Diabetes Sci. Technol.* **8**(5), 1035–1041 (2014)
69. B. Shashaj, E. Busetto, N. Sulli, Benefits of a bolus calculator in pre- and postprandial glycaemic control and meal flexibility of paediatric patients using continuous subcutaneous insulin infusion (CSII). *Diabet. Med.* **25**(9), 1036–1042 (2008)
70. S.R. Shrivastava, P.S. Shrivastava, J. Ramasamy, Role of self-care in management of diabetes mellitus. *J. Diabetes Metab. Disord.* **12**(1), 14 (2013)
71. A. Sussman, E.J. Taylor, M. Patel, J. Ward, S. Alva, A. Lawrence, R. Ng, Performance of a glucose meter with a built-in automated bolus calculator versus manual bolus calculation in insulin-using subjects. *J. Diabetes Sci. Technol.* **6**(2), 339–344 (2012)
72. C. Toffanin, R. Visentin, M. Messori, F. Di Palma, L. Magni, C. Cobelli, Toward a run-to-run adaptive artificial pancreas: in silico results. *IEEE Trans. Biomed. Eng.* **65**(3), 479–488 (2018)
73. F. Torrent-Fontbona, B. Lopez, Personalized adaptive CBR bolus recommender system for type 1 diabetes. *IEEE J. Biomed. Health Inform.* **23**(1), 387–394 (2019)

74. F. Torrent-Fontbona, J. Massana, B. Lopez, Case-base maintenance of a personalised and adaptive CBR bolus insulin recommender system for type 1 diabetes. *Expert Syst. Appl.* **121**, 338–346 (2019)
75. J. Van Niel, P.H. Geelhoed-Duijvestijn, Group, D. I. S, et al., Use of a smart glucose monitoring system to guide insulin dosing in patients with diabetes in regular clinical practice. *J. Diabetes Sci. Technol.* **8**(1), 188 (2014)
76. M. Vettoretti, A. Facchinetti, G. Sparacino, C. Cobelli, Type-1 diabetes patient decision simulator for in silico testing safety and effectiveness of insulin treatments. *IEEE Trans. Biomed. Eng.* **65**(6), 1281–1290 (2018)
77. R. Visentin, C. Dalla Man, B. Kovatchev, C. Cobelli, The university of Virginia/padova type 1 diabetes simulator matches the glucose traces of a clinical trial. *Diabetes Technol. Ther.* **16**(7), 428–434 (2014)
78. J. Walsh, G. Freckmann, R. Roberts, L. Heinemann, Bolus calculator safety mandates a need for standards. *J. Diabetes Sci. Technol.* **11**(1), 3–6 (2017)
79. P.H. Wang, J. Lau, T.C. Chalmers, Meta-analysis of effects of intensive blood-glucose control on late complications of type I diabetes. *Lancet* **341**(8856), 1306–1309 (1993)
80. M.E. Wilinska, L.J. Chassin, C.L. Acerini, J.M. Allen, D.B. Dunger, R. Hovorka, Simulation environment to evaluate closed-loop insulin delivery systems in type 1 diabetes. *J. Diabetes Sci. Technol.* **4**(1), 132–144 (2010)
81. M.E. Wilinska, R. Hovorka, Simulation models for in silico testing of closed-loop glucose controllers in type 1 diabetes. *Drug Discov. Today Dis. Model.* **5**(4), 289–298 (2008)
82. M.E. Wilinska, M. Nodale, An evaluation of “i, pancreas” algorithm performance in silico. *J. Diabetes Sci. Technol.* **3**(4), 857–862 (2009)
83. K. Zarkogianni, E. Litsa, K. Mitsis, P.-Y. Wu, C.D. Kaddi, C.W. Cheng, M.D. Wang, K.S. Nikita, A review of emerging technologies for the management of diabetes mellitus. *IEEE Trans. Biomed. Eng.* **62**(12), 2735–2749 (2015)
84. R. Ziegler, C. Rees, N. Jacobs, C.G. Parkin, M.R. Lyden, B. Petersen, R.S. Wagner, Frequent use of an automated bolus advisor improves glycemic control in pediatric patients treated with insulin pump therapy: results of the bolus advisor benefit evaluation (babe) study. *Pediatr. Diabetes* **17**(5), 311–318 (2016)
85. V.V. Estrela, J. Hemanth, H.J. Loschi, D.A. Nascimento, Y. Iano, N. Razmjoooy, Computer vision and data storage in UAVs, in *Imaging and Sensing for Unmanned Aircraft Systems*, ed. by V. V. Estrela, J. Hemanth, O. Saotome, G. Nikolakopoulos, R. Sabatini, vol. 1, (IET, London, 2020), pp. 23–46. ISBN 978-1-78561-642-6 Hardback, ISBN 978-1-78561-643-3 PDF
86. V.V. Estrela, A. Khelassi, A.C.B. Monteiro, Y. Iano, N. Razmjoooy, D. Martins, D.T.M. Rocha, Why software-defined radio (SDR) matters in healthcare? *Med. Technol. J.* **3**(3), 421–429 (2019). <https://doi.org/10.26415/2572-004X-vol3iss3p421-429>
87. V.V. Estrela, A.C.B. Monteiro, R.P. França, Y. Iano, A. Khelassi, N. Razmjoooy, Health 4.0: applications, management, technologies and review. *Med. Tech. J.* **2**(4), 262–276 (2019). <https://doi.org/10.26415/2572-004X-vol2iss1p262-276>
88. C.E.V. Marinho, V.V. Estrela, H.J. Loschi, N. Razmjoooy, A.E. Herrmann, Y. Thiagarajan, M.P. Vishnevski, A.C.B. Monteiro, R.P. França, Y. Iano, A model for medical staff idleness minimization, in *Proceedings of the 4th Brazilian Technology Symposium (BTSym'18). BTSym 2018. Smart Innovation, Systems and Technologies, 2019*, ed. by Y. Iano, R. Arthur, O. Saotome, V. Vieira Estrela, H. Loschi, vol. 140, (Springer, Cham, 2019)
89. L. Brazionis et al., An evaluation of the Tele-health facilitation of diabetes and cardiovascular care in remote Australian indigenous communities:-protocol for the Tele-health eye and associated medical services network [TEAMSnet] project, a pre-post study design. *BMC Health Serv. Res.* **17**(1), 13 (2017)
90. J. Miranda, J. Cabral, S.R. Wagner, C. Fischer Pedersen, B. Ravelo, M. Memon, M. Mathiesen, An open platform for seamless sensor support in healthcare for the internet of things. *Sensors* **16**(12), 2089 (2016)

91. G. Lanzola, E. Losiouk, S. Del Favero, A. Facchinetti, A. Galderisi, S. Quaglini, C. Cobelli, Remote blood glucose monitoring in mHealth scenarios: a review. *Sensors* **16**(12), 1983 (2016)
92. M.A. de Jesus, V.V. Estrela, An introduction to data mining applied to health-oriented databases. *Orient. J. Comput. Sci. Technol. (OJCST)* **9**, 177–185 (2016). <https://doi.org/10.13005/ojct/09.03.03>
93. N. Razmjoooy, V.V. Estrela, H.J. Loschi, *A study on metaheuristic-based neural networks for image segmentation purposes*, *Data Science Theory, Analysis and Applications* (Taylor and Francis, Abingdon, 2019)
94. N. Razmjoooy, V.V. Estrela, H.J. Loschi, W.S. Farfan, *A Comprehensive Survey of New Metaheuristic Algorithms* (Wiley, 2019)
95. N. Razmjoooy, V.V. Estrela, *Applications of Image Processing and Soft Computing Systems in Agriculture* (IGI Global, Hershey, 2019), pp. 1–300. <https://doi.org/10.4018/978-1-5225-8027-0>
96. G. García-Sález, J.M. Alonso, J. Molero, M. Rigla, I. Martínez-Sarriegui, A. Leiva, E.J. Gómez, E.M. Hernando, Mealtime blood glucose classifier based on fuzzy logic for DIABTel telemedicine system. *Artif. Intell. Med.* **5651**, 295–304 (2009)
97. C. Pérez-Gandía, A. Facchinetti, G. Sparacino, C. Cobelli, E.J. Gómez, M. Rigla, A. de Leiva, M.E. Hernando, Artificial neural network algorithm for online glucose prediction from continuous glucose monitoring. *Diabetes Technol. Ther.* **12**(1), 81–88 (2010)
98. B.F. Cruz, J.T. de Assis, V.V. Estrela, A. Khelassi, A compact SIFT-based strategy for visual information retrieval in large image databases. *Med. Technol. J.* **3**(2), 402–401 (2019). <https://doi.org/10.26415/2572-004X-vol3iss2p402-412>
99. A.C.B. Monteiro, Y. Iano, R.P. França, R. Arthur, V. Vieira Estrela, A comparative study between methodologies based on the Hough transform and Watershed transform on the blood cell count, in *Proceedings of the 4th Brazilian Technology Symposium (BTSym'18)*. *BTSym 2018*, Smart Innovation, Systems and Technologies, ed. by Y. Iano, R. Arthur, O. Saotome, V. Vieira Estrela, H. Loschi, vol. 140, (Springer, Cham, 2019)
100. A.A. Laghari, A. Khan, H. He, V.V. Estrela, N. Razmjoooy, J. Hemanth, H.J. Loschi, Quality of experience (QoE) and quality of service (QoS) in UAV systems, in *Imaging and Sensing for Unmanned Aircraft Systems*, ed. by V. V. Estrela, J. Hemanth, O. Saotome, G. Nikolakopoulos, R. Sabatini, vol. 2, (IET, London, 2020), pp. 213–242
101. A. Deshpande, P. Patavardhan, V.V. Estrela, N. Razmjoooy, Deep learning as an alternative to super-resolution imaging in UAV systems, in *Imaging and Sensing for Unmanned Aircraft Systems*, ed. by V. V. Estrela, J. Hemanth, O. Saotome, G. Nikolakopoulos, R. Sabatini, vol. 2, (IET, London, 2020), pp. 177–212
102. A. Arshaghi, N. Razmjoooy, V.V. Estrela, P. Burdziakowski, D.A. Nascimento, A. Deshpande, P.P. Patavardhan, Image transmission in UAV MIMO UWB-OSTBC system over Rayleigh channel using multiple description coding (MDC), in *Imaging and Sensing for Unmanned Aircraft Systems*, ed. by V. V. Estrela, J. Hemanth, O. Saotome, G. Nikolakopoulos, R. Sabatini, vol. 2, (IET, London, 2020), pp. 67–90. https://doi.org/10.1049/PBCE120G_ch4
103. M. Khera, Think like a hacker insights on the latest attack vectors (and security controls) for medical device applications. *J. Diabetes Sci. Technol.* **11**, 1932296816677576 (2016)
104. P. Burdziakowski, N. Razmjoooy, V.V. Estrela, J. Hemanth, Open source software (OSS) and hardware (OSH) in UAVs, in *Imaging and Sensing for Unmanned Aircraft Systems*, ed. by V. V. Estrela, J. Hemanth, O. Saotome, G. Nikolakopoulos, R. Sabatini, vol. 2, (IET, London, 2020), pp. 49–66
105. Z. Abbas, W. Yoon, A survey on energy conserving mechanisms for the internet of things: Wireless networking aspects. *Sensors* **15**(10), 24818–24847 (2015)
106. A.C.B. Monteiro, R.P. Franca, V.V. Estrela, S.R. Fernandes, A. Khelassi, R.J. Aroma, K. Raimond, Y. Iano, A. Arshaghi, UAV-CPSs as a test bed for new technologies and a primer to Industry 5.0, in *Imaging and Sensing for Unmanned Aircraft Systems*, ed. by V. V. Estrela, J. Hemanth, O. Saotome, G. Nikolakopoulos, R. Sabatini, vol. 2, (IET, London, 2020), pp. 1–22

Chapter 6

Feature Extraction Based on Wavelet Transform for Classification of Stress Level



Djamel Bouchaffra , Faycal Ykhlef , and Yamina Bennamane

6.1 Introduction

Traditionally, the definition of stress consists of a reaction from a restful state to an excited state in order to protect the cohesion of the organism. Classification of stress levels into different ranges (low, medium, and high) can be conducted using different sensors or instruments such as (1) galvanic skin response (GSR), (2) photoplethysmography (PPG), (3) electroencephalography (EEG), and (4) electrocardiogram (ECG). Sometimes, this task is also achieved through facial expression and speech. In the ECG domain, many approaches are proposed to classify stress. Most of these methods are based on P, QRS, and T waves due to the importance of characterizing the ventricular contractions in the human heart. The number of QRS complexes, the QRS durations, the RR distances, and the signal peak amplitudes have often been considered as relevant features for representing ECG signal. Discrete wavelet transform (DWT)-based heart rate (HR) detection algorithm is exploited for deriving HRV signals from the preprocessed ECG signal to improve stress detection (Karthikeya et al. 2013). Nimunkar et al. proposed an empirical mode decomposition (EMD) for R-peak detection [1]. A weighted total variation (WTV) denoising technique has been studied in [2] for QRS detection by preprocessing ECG signals. A regular grammar method for extracting QRS complexes has been laid out in [3]. A similar method based on DWT or identifying QRS waveforms has been introduced in [4]. The first derivative method-based Hamilton–Tompkins function and Hilbert transform for QRS identification are studied in [5]. The mother wavelet used in this latter context is the Haar function. To detect driver stress, multiple features have been utilized in [6] to achieve higher performance. In [7], after the signal

D. Bouchaffra (✉) · F. Ykhlef · Y. Bennamane
Division Architecture des Systèmes et Multimédia, Centre de Développement des
Technologies Avancées, Algiers, Algeria
e-mail: dbouchaffra@cdta.dz; fykhlef@cdta.dz; ybennamane@cdta.dz

denoising phase based on Savitzky–Golay filters, the authors relied on the isoelectric level, P wave, ST level, and QRS complex as main features for stress detection. In [8], statistical and frequency domain features of HRV have been combined seamlessly for classification of stress levels within a workplace. A sequential minimal optimization algorithm using EEG signals has been introduced in [9] to classify human stress with respect to music tracks. EEG signal-based maximum likelihood framework has also been exploited for the classification of stress at multiple levels in [10]. Another approach based on head pose features invoking different classification schemes (k-nearest neighbor, generalized likelihood ratio, and support vector machine classifiers) has been introduced in [11]. A fuzzy classifier is proposed in [12].

Furthermore, three levels of stress are detected through a fuzzy logic classifier based on features such as heart rate, skin conductance, and skin temperature information. Keshan et al. have devised different machine learning methods and algorithms to detect three levels of stress from ECG signals in automobile drivers [13]. The accuracy obtained in this latter design approaches 88.24%.

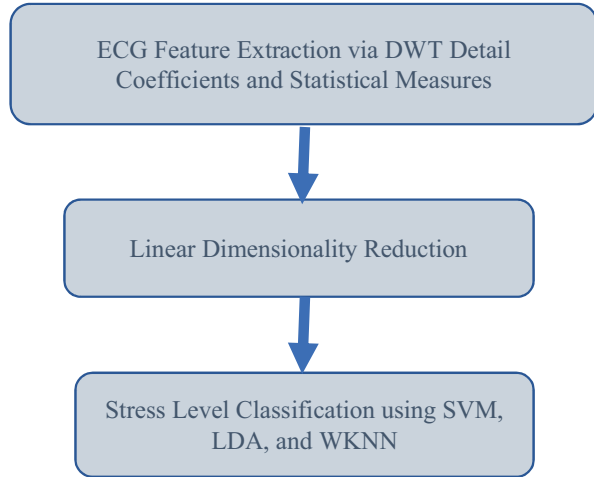
Unlike major traditional approaches cited above that are based on electrocardiogram specificities and clues such as QRS waves for feature extraction, our methodology relies on the seamless fusion of DWT analysis and statistical measures. It in fact captures the details of this type of signal. These details are indicators of abrupt changes in the ECG signals. Our approach for the classification of ECG physiological signals is novel. These latter signals represent an essential metric for getting feedback about a driver's state because they are often gathered continuously and without impeding the driver's task performance. To achieve this classification goal, we first removed noise from the original signals and then invoked discrete wavelet transform to extract a broad set of discriminative features based on the detail coefficients and statistical measures. We further applied principal component analysis (PCA) to perform feature space dimensionality reduction [14, 15]. This smaller set of features represents the input pattern to different classifiers, which are support vector machines (SVM), weighted k-nearest neighbors (WKNN), and linear discriminant analysis (LDA) for driver stress classification (refer to Fig. 6.1).

The logical organization of the manuscript is as follows: The materials and methods proposed in this research are laid out in Sect. 6.2. The obtained results and the discussion appear, respectively, in Sects. 6.3 and 6.4. Finally, Sect. 6.5 covers the conclusion and perspectives.

6.2 Materials and Methods

There are five steps that are performed to classify driver stress levels: (1) database collection, (2) signal preprocessing, (3) feature extraction, (4) feature dimensionality reduction, and (5) classification.

Fig. 6.1 The holistic flowchart of our methodology



Step 1. Database We have used the Stress Recognition in Automobile Drivers (SRAD) database, which is relevant for stress detection in drivers [6]. This dataset contains a set of several physiological reactions emanating from people driving on specified roads and highways, and in the following situations:

- a. Low stress state or when the driver is at rest
- b. Medium stressed state or when the driver is on the highway
- c. High stress state or when the driver enters the city

In this experiment, we have considered only ECG information. The total driving time varies from approximately 50 min to 1.5 h, depending on road conditions.

Step 2. Signals Preprocessing This step often includes the removal of different types of noises. It has to differentiate between pure and noisy data. Only pure data are left for further analysis. Cancellation of noise has been conducted using the Wiener filter. It is well known that Wiener filter achieves noise reduction with some integrity loss of the original signal. However, this loss is often not significant in our level of analysis.

Step 3. Feature Extraction We have considered features in different domains (time, frequency, time-frequency) through the use of linear or nonlinear methods. Features normalization is often performed to minimize the inter-driver variance. In our setting, a sampled ECG signal at 496 Hz and a segment of the 1-min duration ECG signal have been analyzed. We processed 120 signals for each class (class 1 represents low stress, class 2 represents medium stress, and class 3 denotes high stress). We applied DWT using the multiresolution method (MRA) on each signal, which is further decomposed into ten resolution levels. The mother wavelet that we have used is Daubechies 4 (db4). We have obtained coefficients of details and approximations. Next, we applied 12 statistical measures, which are mean, standard deviation, skewness, kurtosis, variance, root mean square, spectrum energy, Shannon

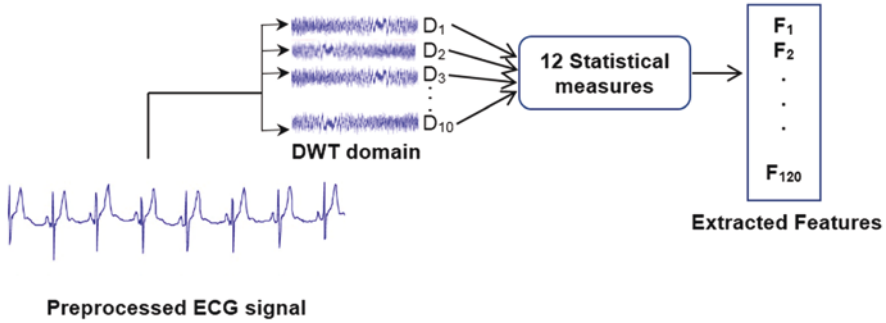


Fig. 6.2 Decomposition of the signal into ten levels using DWT: extraction of detail coefficients and statistical measures

entropy, log energy, form factor, and minimum and maximum value of wavelet coefficients. The set of detail coefficients capture abrupt changes in ECG signals (refer to Fig. 6.2).

We finally built a vector of $12 \times 10 = 120$ features for the ECG signals. These features are grouped and used as inputs for each classifier (refer to Fig. 6.3).

Step 4. Feature Dimensionality Reduction It often improves the performance of classifiers and minimizes computation time as well as energy costs. It is worth underscoring that some of the features we have selected are correlated: It is the role of dimensionality reduction algorithms such as PCA to recover from this issue.

Step 5. Classification After the selection of a validation set, a tenfold cross-validation is performed for prediction accuracy. This step allows predicting the class associated to a certain stress level of the driver and hence computing the global accuracy of our classifiers after averaging (refer to Fig. 6.4).

6.3 Results

As pointed out in Sect. 6.2, ECG signals used were collected from the dataset named “Stress Recognition in Automobile Drivers” available from the web repository. Training of classifiers is carried out in a MATLAB platform with a balanced dataset of 360 patterns partitioned into 120 patterns for each class (360 patterns for 3 classes). The SVM multiclass (one vs. one) is trained with the RBF kernel with optimal parameter values. Tenfold cross-validation is performed for all three classifiers SVM, WKNN, and LDA, and their accuracy is averaged within this fold. The following tables (Tables 6.1, 6.2, 6.3, 6.4, 6.5, and 6.6) depict the confusion matrices for the three classifiers with and without the application of PCA. Figures 6.5 and

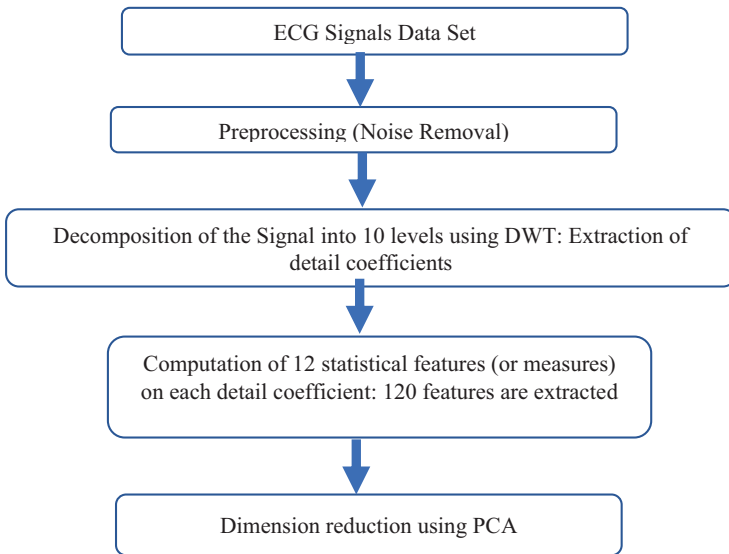


Fig. 6.3 Feature extraction flowchart

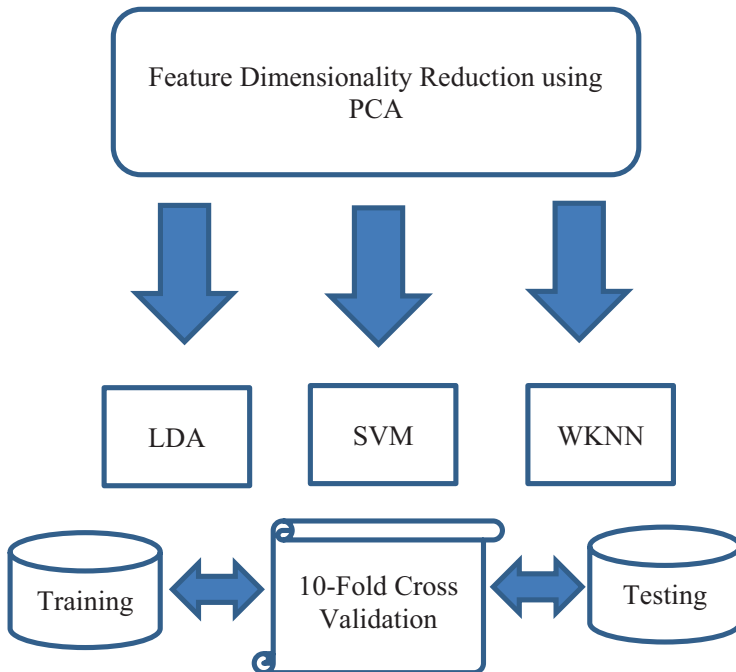


Fig. 6.4 Feature extraction and classification steps

Table 6.1 Confusion matrix of SVM with all 120 features showing an accuracy of 98.6%

	Predicted class			Rates		
		Low stress	Medium stress	High stress	TPR	FPR
True class	Low stress	118	1	1	98.3%	1.7%
		98.3%	0.8%	0.8%		
	Medium stress	1	117	2	97.5%	2.5%
		0.8%	97.5%	1.7%		
	High stress	0	0	120	100%	0%
				100%		
Accuracy		98.6%				

Table 6.2 Confusion matrix of SVM using PCA with 50 optimum number of components showing an accuracy of 95%

	Predicted class			Rates		
		Low stress	Medium stress	High stress	TPR	FPR
True class	Low stress	113	3	4	94.2%	5.8%
		94.2%	2.5%	3.3%		
	Medium stress	0	109	11	90.8%	9.2%
			90.8%	9.2%		
	High stress	0	0	120	100%	0%
				100%		
Accuracy		95%				

Table 6.3 Confusion matrix of LDA with all 120 features showing an accuracy of 98.6%

	Predicted class			Rates		
		Low stress	Medium stress	High stress	TPR	FPR
True class	Low stress	119	1	0	99.2%	0.8%
		99.2%	0.8%			
	Medium stress	2	118	0	98.3%	1.7%
			1.7%	98.3%		
	High stress	0	2	118	98.3%	1.7%
				1.7%		
Accuracy		98.6%				

Table 6.4 Confusion matrix of LDA using PCA with 65 optimum number of components depicting an accuracy of 98.6%

	Predicted class			Rates		
		Low stress	Medium stress	High stress	TPR	FPR
True class	Low stress	118	2	0	98.3%	1.7%
		98.3%	1.7%			
	Medium stress	1	118	1	98.3%	1.7%
			0.8%	98.3%		
	High stress	0	1	119	99.2%	0.8%
				0.8%		
Accuracy		98.6%				

Table 6.5 Confusion matrix of WKNN with all 120 features showing an accuracy of 98.6% with a number of neighbors equal to 3

	Predicted class			Rates		
		Low stress	Medium stress	High stress	TPR	FPR
True class	Low stress	118	2	0	98.3%	1.7%
		98.3%	1.7%			
	Medium stress	0	117	3	97.5%	2.5%
			97.5%	2.5%		
	High stress	0	0	120	100%	0%
				100%		
Accuracy (AC)		98.6%				

Table 6.6 Confusion matrix of WKNN using PCA with 40 components showing an accuracy of 89.2%

	Predicted class			Rates		
		Low stress	Medium stress	High stress	TPR	FPR
True class	Low stress	105	13	2	87.5%	12.5%
		87.5%	10.8%	1.7%		
	Medium stress	3	114	3	95.0%	5%
		2.5%	95.0%	2.5%		
	High stress	0	18	102	85.0%	15.0%
			15.0%	85.0%		
Accuracy (AC)		89.2%				

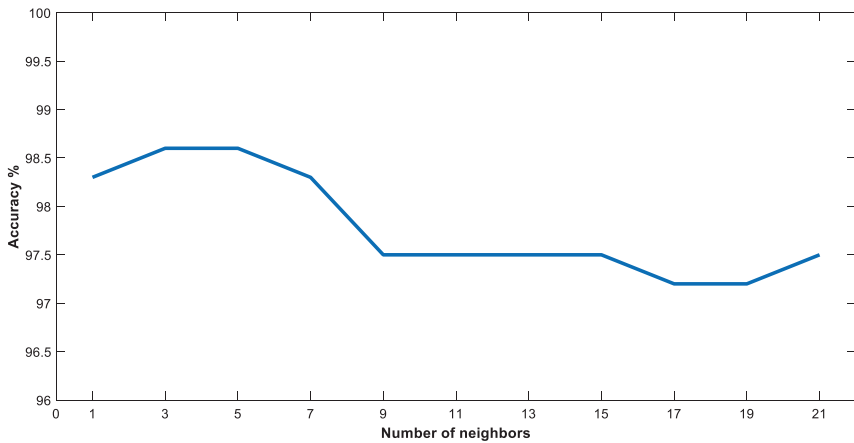


Fig. 6.5 Graph depicting the accuracy variation of WKNN classifier as a function of the number of neighbors (the accuracy is 98.6% when considering three neighbors)

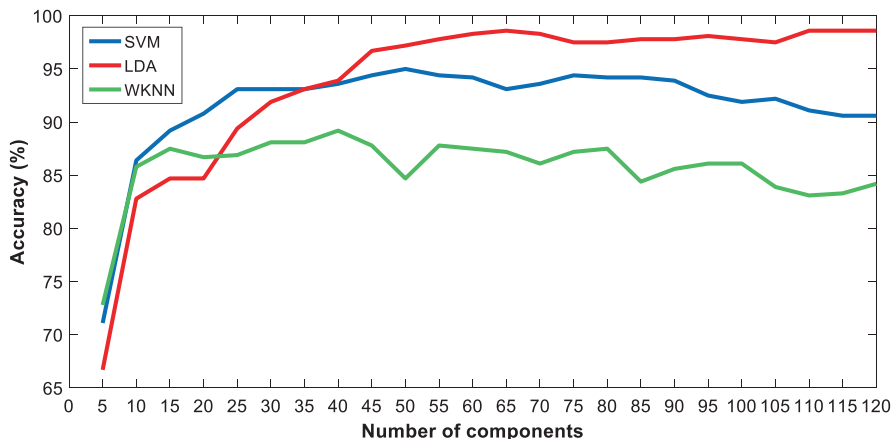


Fig. 6.6 Graph depicting the variation of the accuracy of all three classifiers (SVM, LDA, and WKNN) as a function of the number of PCA components

6.6 show the accuracy graphs with respect to some classifier parameters. The metrics used are defined as follows:

TP: True positive

TN: True negative

FP: False positive, **FN:** False negative

TPR: True positive rate

FPR: False positive rate

$$\text{Accuracy} = (\text{TP} + \text{TN}) / (\text{TP} + \text{TN} + \text{FP} + \text{FN})$$

6.4 Discussion

This research unravels several crucial clues related to stress classification. First of all, the accuracy obtained using all features is 98.6% with all three classifiers (refer to Tables 6.1, 6.3, and 6.5). This is quite a remarkable performance when compared to the major state-of-the-art techniques. Furthermore, it is important to underscore the effectiveness of the features we have generated. It is established in the machine learning literature that strong features contribute to a high accuracy independently of classifiers' strengths. Conversely, poor features contribute to a low accuracy even if the plugged classifier is strong. It is also clear that PCA degrades the performance in the case of SVM. The accuracy fell from 98.6% down to 95% (refer to Table 6.2).

We can also point out from these results that some features are linearly correlated since PCA with only 65 components (out of 120) has been capable of achieving an accuracy of 98.6% in the case of LDA (refer to Table 6.4). Moreover, the non-parametric classifier WKNN performed quite remarkably, with only three neighbors since it has achieved an accuracy of 98.6% (refer to Fig. 6.5). However, its performance degraded when applying PCA dimensionality reduction (refer to Table 6.6 and Fig. 6.6).

Finally, Fig. 6.6 shows starting from 40 PCA components and above, LDA has achieved the best performance among all classifiers. This result highlights the data linearity captured keenly by LDA. However, SVM appears to be less affected by the variation of the number of PCA components. Indeed, SVM performs better than the other two classifiers when the number of components is less than 30. SVM performance seems to degrade using PCA, but it remained stable and robust globally.

6.5 Conclusion

Our contribution to the field is twofold: (i) feature extraction and (ii) comparison between different types of parametric (LDA) and non-parametric (SVM, WKNN) classifiers [13, 16, 17]. It appears that the use of DWT in ECG signals is worth it, since abrupt signal changes are well captured and taken into account through detail coefficients. The application of statistical measures within DWT coefficients provides an efficient framework for feature extraction. This seamless fusion between two different types of information shows promise. In order to optimize the tradeoff between computation cost and performance in ECG stress classification, one can invoke LDA as the best classifier among SVM and WKNN. However, if computation resources are available, the three classifiers can be used interchangeably, since the three of them achieved the performance of 98.6%.

Our next future work consists of combining these three classifiers seamlessly in a single multi-classifier framework to improve the global accuracy further since these classifiers do not commit errors on the same signal instances individually.

Future works can also use independent component analysis (ICA) [18, 19]. Given the expansion of the Internet of Things in healthcare, the need to combine local and global knowledge to deliver better services, the proposed system needs to contextualize and converse with others according to the type of stress involved and the person's physical conditions [20–25].

Acknowledgments This research was sponsored by the Agence Thématique de Recherche en Science de la Santé (ATRSS) under grant n°: 64/DFPR/ATRSS/2017.

References

1. A.J. Nimunkar, W.J. Tompkins, R-peak detection and signal averaging for simulated stress ECG using EMD. *The 29th Annual International Conference of the IEEE Engineering in Medicine and Biology Society* (2007), pp. 1261–1264
2. T. Sharma, K.K. Sharma, QRS complex detection in ECG signals using locally adaptive weighted total variation denoising. *J. Comput. Biol. Med.* **87**, 187–199 (2017)
3. S. Hamdi, A.B. Abdallah, M.H. Bedoui, A robust QRS complex detection using regular grammar and deterministic automata. *Biomed. Signal Process. Control* **40**, 263–274 (2018)
4. C.M. Khamhoo, J. Rahul, M. Sora, Algorithm for QRS complex detection using discrete wavelet transformed. *Int. J. Electron. Eng.* **10**, 352–357 (2018)
5. N.M. Arzeno, Z.-D. Deng, C.-S. Poon, Analysis of first-derivative based QRS detection algorithms. *IEEE Trans. Biomed. Eng.* **55**(2), 478–484 (2008)
6. J.A. Healey, R.W. Picard, Detecting stress during real-world driving tasks using physiological sensors. *IEEE Trans. Intell. Transp. Syst.* **6**(2), 156–166 (2005)
7. S. Goel, G. Kau, P. Toma, A novel technique for stress recognition using ECG signal pattern. *Curr. Pediatr. Res.* **21**, 4 (2017)
8. S. Sriramprakash, V.D. Prasanna, O.R. Murthy, Stress detection in working people. *The 7th International Conference on Advances in Computing & Communications*, vol. 115 (2017), pp. 359–366
9. A. Asif, M. Majid, S.M. Anwar, Human stress classification using EEG signals in response to music tracks. *Comput. Biol. Med.* **107**, 182–196 (2019)
10. A.R. Subhani, W. Mumtaz, M.N.B.M. Saad, N. Kamel, A.S. Malik, Machine learning framework for the detection of mental stress at multiple levels. *IEEE Access* **5**, 13545–13556 (2017)
11. G. Giannakakis, D. Manousos, V. Chaniotakis, M. Tsiknakis, Evaluation of head pose features for stress detection and classification. *The IEEE EMBS International Conference on Biomedical & Health Informatics* (2018), pp. 406–409
12. A.G. Airij, R. Sudirman, U.U. Sheikh, GSM and GPS based real-time remote physiological signals monitoring and stress levels classification. *The 2nd International Conference on BioSignal Analysis* (2018), pp. 130–135
13. N. Keshan, P.V. Parimi, I. Bichindaritz, Machine learning for stress detection from ECG signals in automobile drivers. *The IEEE International Conference on Big Data* (2015), pp. 2661–2669
14. I.T. Jolliffe, Principal component analysis. *International Encyclopedia of Statistical Science* (2011)
15. A.M. Coelho, V.V. Estrela, EM-based mixture models applied to video event detection, in *Principal Component Analysis – Engineering Applications*, ed. by P. Sanguansat, (IntechOpen, London, 2012), pp. 101–124. <https://doi.org/10.5772/38129>
16. R. Varatharajan, G. Manogaran, P.M. Kumar, A big data classification approach using LDA with an enhanced SVM method for ECG signals in cloud computing. *Multimed. Tools Appl.* **77**, 10195–10215 (2017)
17. P. Karthikeyan, M. Murugappan, S. Yaacob, Detection of human stress using short-term ECG and HRV signals. *J. Mech. Med. Biol.* **13**(02), 1350038 (2013)
18. F.P. do Carmo, J.T. de Assis, V.V. Estrela, A.M. Coelho, Blind signal separation and identification of mixtures of images, in *2011 Conference Record of the Forty-Third Asilomar Conference Signals, Systems and Computers* (2011)
19. R. Favilla, V.C. Zuccala, G. Coppini, Heart rate and heart rate variability from single-channel video and ICA integration of multiple signals. *IEEE J. Biomed. Health Inform.* **23**, 2398–2408 (2019)
20. A. Khelassi, V.V. Estrela, J. Hemanth, Explainer: an interactive agent for explaining the diagnosis of cardiac arrhythmia generated by IK-DCBRC. *Med. Technol. J.* **3**(2), 376–394 (2019). <https://doi.org/10.26415/2572-004X-vol3iss2p376-394>
21. L. Ivonin, H.-M. Chang, W. Chen, M. Rauterberg, Unconscious emotions: quantifying and logging something we are not aware of. *Pers. Ubiquit. Comput.* **17**, 663–673 (2012)

22. V.V. Estrela, A. Khelassi, A.C.B. Monteiro, Y. Iano, N. Razmjoooy, D. Martins, D.T.M. Rocha, Why software-defined radio (SDR) matters in healthcare? *Med. Technol. J.* **3**(3), 421–429 (2019). <https://doi.org/10.26415/2572-004X-vol3iss3p421-429>
23. A. Kimmy, W. Chen, B. Lindsay, Smart photo frame for arousal feedback—Wearable sensors and intelligent healthy work environment, in *Proceedings of Workshop on Smart Offices and Other Workplaces of the 7th International Conference on Intelligent Environments*, Nottingham, UK (2011), pp. 685–696
24. E. Jovanov, A.O. Lords, D. Raskovic, P.G. Cox, R. Adhami, F. Andrasik, Stress monitoring using a distributed wireless intelligent sensor system. *IEEE Eng. Med. Biol. Mag.* **22**, 49–55 (2003)
25. A. Saidatul, M.P. Paulraj, S. Yaacob, N.N.F. Mohamad, Automated system for stress evaluation based on EEG signal: A prospective review, in *Proceedings of IEEE 7th International Colloquium on Signal Processing and Its Applications, Penang, Malaysia*, vol. 4–6 (2011), pp. 167–171

Chapter 7

Packet Synchronization in a Network Time Protocol Server and ASTM Elecsys Packets During Detection for Cancer with Optical DNA Biochip



Amina Elbatoul Dinar , Samir Ghouali , Boualem Merabet ,
and Mohammed Feham 

7.1 Introduction

Knowing in what manner to spot pathologies as early as possible has been and remains a challenge. The state of particular diseases (e.g., some cancers) at the diagnosis stage can be overly advanced for treatment. Then, new research has targeted discovering diseases earlier, knowing where and what to look for, improving treatments but also detection systems: better reliability, better performance, speed, etc. Man is once again pushing his limits.

Significant evolution has been made recently regarding patient comfort, to reduce the “heaviness” of treatments, or to speed up diagnosis. Still, the disease search always takes a long time. On average, the outcomes of a biopsy for cancer cells can call for up to 2 weeks (for a precise result: exact origin, sensitivity to antimetotics). Beyond the desire to cure the disease and, therefore, to take it at the least advanced stage possible, it is also necessary to respect the patient, his comfort, and his/her anguish. The disease treatment goes through several stages. The symptoms, first of all, lead to consultation and, if required, to tests to seek for traces of illness, infected cells, etc. Contingent on the results of the initial experiments (e.g., blood exams,

A. E. Dinar (✉) · B. Merabet
LSTE Laboratory, Faculty of Sciences and Technology, Mustapha Stambouli University,
Mascara, Algeria
e-mail: amina.dinar@univ-mascara.dz

S. Ghouali
Faculty of Sciences and Technology, Mustapha Stambouli University, Mascara, Algeria
STIC Lab, University of Tlemcen, Tlemcen, Algeria
e-mail: s.ghouali@univ-mascara.dz

M. Feham
STIC Lab, University of Tlemcen, Tlemcen, Algeria
e-mail: m_feham@mail.univ-tlemcen.dz

© Springer Nature Switzerland AG 2021

A. Khelassi, V. V. Estrela (eds.), *Advances in Multidisciplinary Medical Technologies — Engineering, Modeling and Findings*,
https://doi.org/10.1007/978-3-030-57552-6_7

CT, and ultrasound, to name a few), other more precise and more targeted examinations may follow.

There is a growing awareness in the improvement of analytical systems relying on DNA bioreceptor. A vital area in biological monitoring is the complex diagnosis of maladies, organisms, and living systems (e.g., bacteria, virus, or linked components) at ultra-trace levels in organic (as is the case with blood, tissues, and biological fluids) and environmental (from the soil, air, and water) samples. A biosensor is a device that must recognize and differentiate several biochemical elements for unambiguous identification and precise quantification in a real-life sample. Living structures possess sophisticated recognition features (e.g., enzyme, anti-body, and gene probes, among others), frequently denoted as bioreceptors for detailed identification of complex chemical and biological items.

Biosensors exploit the robust molecular recognition competency of bioreceptors. Gene probes exploiting surface-enhanced Raman scattering (SERS) can augment the selectivity and sensitivity of DNA biosensors while expanding biochip use.

Most existent DNA biosensors are made of fiber optic probes, glass, and silica plates, which function as the probe substrates to interface with particular detection systems. These detectors commonly embrace conventional detection devices like photomultipliers and charge-coupled devices (CCDs). Even though the probes are quite small (aka DNA chip or gene chip), they are still far from ideal for real-life usages. This happens because the detection structures employ relatively bulky confocal microscopes and CCDs suited for laboratory applications. Until now, there have been limited research and development efforts on a truly integrated and viable in large-scale biochip system with probes, samplers, detectors, amplifiers, and logic circuitry onboard them.

Biosensors are integrated circuit (IC) microchips relying on DNA bioreceptors capable of detecting genetic components in biological complex samples. These IC systems can consist of phototransistors and other technologies. Single phototransistors working as detectors may lack enough sensitivity for tracing elements. Nevertheless, other miniaturization technologies can investigate DNA.

7.1.1 DNA Biochips

A biopsy is necessary to be acquainted with the type and nature of cancer to use the appropriate treatment and medication, for example. Therapy comes after these tests encompassing the choice of drugs, solutions, and techniques to be considered as a viable cure for the patient as promptly and painlessly as thinkable at the border between photonics and biology and the forefront of biomedical technology. These innovations are rapidly expanding the field of diagnostic tools. Market analyses point toward photonics in the medical world to deliver minimally or non-invasive diagnostic tools. Likewise, the growth of microphonics medical chips, biophotonics, and their medical usages is also disposed to rise significantly in the future. These areas cover a broad range of uses from already established applications, such

as laser surgery, to new applications, such as DNA analysis [1–6]. A modern miniaturized high-tech tool, called a DNA biochip, has, in recent times, attracted the attention of the scientific community for its massive potential for biological diagnosis, the investigation into genetic mutations, and the development of new drugs. The agrifood and environmental sectors are also expected to be affected promptly [7–9]. The main reasons for micro- and nanoscale miniaturization are as follows:

- (i) Reducing the sensor element to the scale of the target species and hence providing a higher sensitivity of a single entity or even a molecule
- (ii) Reduced costs and associated reagent volumes
- (iii) Reduced result time due to small amounts and the possible usage of higher and effective concentrations
- (iv) Flexibility, portability, and ability to miniaturize entire systems
- (v) Point-of-care problem-solving/analyses
- (vi) The aptitude for multi-agent detection
- (vii) Potential for in vitro as well as in vivo use

The DNA biochips or merely biochip makes it plausible to all the while breaking down a few thousand diverse hereditary data. This technology resulted from merging biochemistry, combinatorial chemistry, molecular biology, microelectronics, computer science, and Big Data.

These DNA biochips are about to transform medical diagnosis and biological analysis in general. These systems' major advantage is their ability to sense an organic molecule in a sample that can hold millions – by specific affinity with a molecular probe in the chip. These miniaturized analysis supports (a few cm^2) can be fixed to a reader and a bioinformatics data processing system. The change of scale associated with this technology offers many advantages: time savings, smaller sample volumes, and a remarkable upsurge in parallel processing and, consequently, for data acquired.

The development of new biological analysis systems, for both medical and environmental diagnosis, requires good control [10]:

- On the one hand, the development of bimolecular buildings allowing the specific recognition of the desired mutations
- On the other hand, to utilize a high-performance reading technique (sensitive, specific, and low detection threshold) and, if viable, at low cost
- Real-time synchronization between the remote sample database server and the DNA biochip considering ASTM Elecsys packets traffic

In summary, integrated optics revealed itself as one of the most promising technologies in the context of the vast increase in optoelectronics. This matches the maturation of all the components essential to the design of an accomplished optoelectronic chain and the need for miniaturized photonic circuits at a very low cost. First, one can allude to the classic and apparent advantages of optical circuits:

- Due to the very high frequency of light, optical circuits designated as insensitive to electromagnetic noise.

- High level of reliability and, above all, security in data gathering and transferring within a strict framework.
- Ability to process data in real-time.
- Through the wavelength multiplexing scheme, there is an increase in the number of processed information transported in this way.
- Make non-contact measurements.
- One does not use local electrical power if one wants to build information processing devices or design measurement heads.

Thanks to integration techniques, the following advantages can be added:

- Optical circuits' simplification and miniaturization
- The disappearance of traditional alignment problems between components
- Possibility of deploying manufacturing techniques that can be assimilated and are compatible with mass production and low-cost objectives [11]

All the advantages mentioned above could only be achieved if one has adequate means at his/her disposal, such as efficient miniaturized light sources and highly trustworthy means of conveying the information.

7.1.2 Surface Plasmon Resonance (SPR) Imaging

The use of Surface Plasmon Resonance (SPR) imaging in optical DNA chip is very promising. This technique allows the follow in real-time and in parallel, without the use of markers. Different interactions taking place on a well-defined surface of the chip. This type of chip has been used to analyze DNA /DNA interaction for genetic diagnosis. Our contribution lies in creating a link between a server containing an integrated database and all the samples on the optical DNA chip via a protocol called NTP. This system will allow us to analyze simultaneously and especially in real-time several thousands of different genetic information with the least possible error. Thanks to this new tool, it is possible in parallel to identify and even measure a considerable number of DNA sequences contained in a biological sample. With the slightest error synchronization, our system will be able to predict the precise moment an identify the sample to be analyzed [12].

These SPRs are waves propagating at the interface amid two media of opposite permittivity like the one separating a dielectric and a metal. Summarizing, the surface plasmon is a collective longitudinal oscillation of free electrons in a metal. Then, it is a charge density fluctuation in time and space. According to established laws of electromagnetism, the surface electromagnetic wave, resulting from such fluctuation, has an exponential decrease on both sides of the interface, has a transverse magnetic polarization, and propagates [37]. The variation in reflectivity helps to encounter the mass and thickness of the layer deposited on the surface and, accordingly, the number of molecules attached. The change in light intensity helps

to perceive the influence of the variation in the dielectric index on the resonance situation of the surface plasmon. It can be visible by looking at a discrepancy of the different optical parameters of the light beam, such as spectrum, phase, and plasmon angle. Interferometry leads to knowledge about the phase. The absorbed wavelength results from spectroscopy, at a fixed angle, and then, thanks to this, the index variation comes from the spectral shift. The study of the plasmon angle offset inhibits real-time discovery because of an angular scanning that happens on a certain time [13].

Hence, one can use the physical SPR phenomenon to manufacture biochips. Many measurement methods are used where the best for biochips are (1) multi-sensor mounting in angular and spectral interrogation and (2) single-sensor mounting in angular and spectral probing. The authors selected the so-called single-sensor assembly. This mono-sensor angular probe permits real-time surveillance of interactions taking place on a single large surface. The resultant measurements correspond to an average value over a region with a width identical to the light beam reaching the surface. The authors use a He-Ne laser; the light beam passes through a blade that splits it into halves. One heads toward a reference photodiode to perceive fluctuations in the base beam and perform the necessary corrections. The second one passes through a half-wave blade to have a magnetic or electric transverse polarized transverse electromagnetic (TE) wave. Then, it illuminates an interface through a coupling prism. A measuring photodiode used to record kinetics and plasmon collects the reflected beam. The measuring photodiode and prism are each mounted on a turntable controlled by a computer program, which controls the synchronized rotation of the turntables and the signal acquisition. Considering the turntables' arrangement, the photodiode support plate rotates at a specific angle α , and the prism resting on a plate rotates at an angle $\alpha/2$. The biological elements to be tested are injected into a tank adjacent to the gold surface, using a specific pump. An added CCD camera receives the light intensity variations for each pixel; this one reflects the state of the area of which it is the image. When a biomolecular reaction takes place in this region, the dielectric index is disturbed; the observation angle of the surface plasmon shifts, in addition to the intensity reflected by this area, varies. Consequently, the CCD camera archives the spatial modulations of the reflected beam intensity.

Section 7.2 will address the proposed system. Section 7.3 displays and talks over experiments and their results. Conclusions appear in Sect. 7.4.

7.2 Materials and Methods

This study uses the UNIX Server platform and Network Time Protocol (NTP) to synchronize communication between servers and optical AND biochip automate server with consideration of ASTM Elecsys packets traffic.

7.2.1 Network Time Protocol

NTP is a protocol that allows computer time synchronization with that of a reference server and the possibility to correlate events from numerous systems via UDP to collect requests. Using an NTP server in network to synchronize other machines reduces bandwidth consumption due to NTP traffic [14–18]. The ntpq service implements NTP in Linux. Hence, it is possible to configure the service via a graphical interface on the machine with the default ntpq package installed. It is also possible to directly edit the file `/etc/ntp.conf`.

The service is configured through this file. The list of NTP servers and security rules are defined there. Two sections are available for safety:

- Access Control: The accesses of a machine or a range of IP addresses to the server can be defined; hence, it is possible to block certain addresses, as well as to choose the privileges of a machine on the server.
- Authentication: An authentication request for the NTP server can be placed to validate the weather change. Several possibilities exist for this system deployment, such as symmetric keys and public keys, besides others [17, 19].

7.2.2 ASTM Elecsys Communication Protocol

The low-level standard protocol for the E1381-91 depicts the way information is transmitted between the two frameworks alluding to the protocol subtleties. The high-level E1394-91 identifies the bundle substance and configuration of the sent information while regulating the sentence structure. Elecsys Type Protocol is in Table 7.1 [20].

[STX] FN text [ETB] CS1 CS2 [CR] [LF]

At the point when the last casing in a message or edge is a single casing, the low-level convention Protocol, E1381-91, depicts how the information is transmitted between hosts.

Table 7.1 Frame structure in ASCII [20, 21]

Field	Code ASCII	Content	Character	Note
[STX]	0x02	Start of text	1byte	
FN	–	Frame No.	1byte	1
text	–	Communication data	Max. 240 byte	2
[ETX]/[ETB]	0x03/0x17	End of text/end of communication block	1byte	3
CS1	–	Check sum	1byte	4
CS2	–	1byte		
[CR]	0x0d	Carriage return	1byte	
[LF]	0x0a	Line feed	1byte	

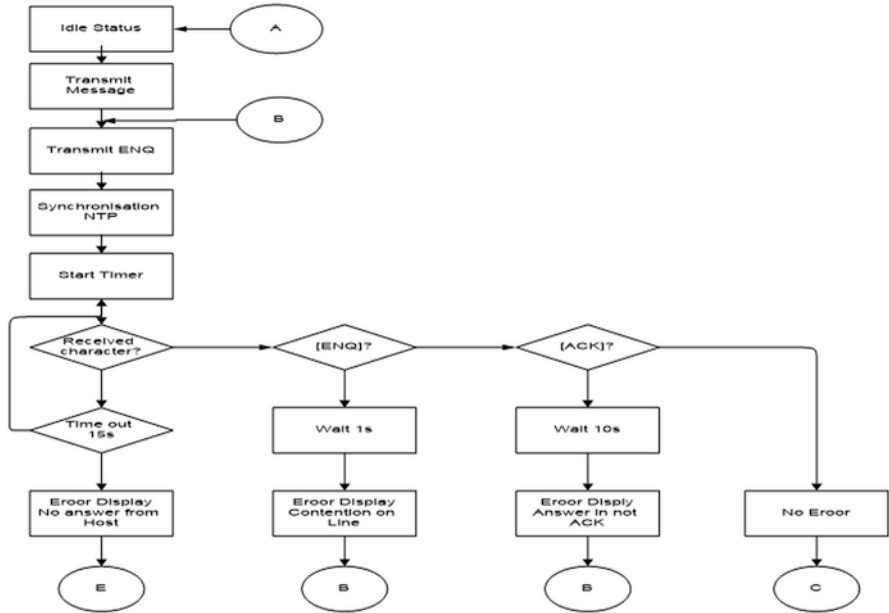


Fig. 7.1 Transfer Phase flowchart

[STX] FN text [ETX] CS1 CS2 [CR] [LF]

The main problem when using the ASTM Elecsys alone is the fact that it is asynchronous. For this reason, one seeks to integrate an NTP server to accomplish synchronization and play a strategic role in the variation of the waiting times as well as the time out. These decisions prevent losing information when sending or receiving ASTM Elecsys requests. Figures 7.1 and 7.2 allude to the flowcharts that offer a broad-spectrum idea of the different phases of sending and receiving.

The Transfer Phase reveals the flowchart of three kinds of reaction against casing correspondence. Section point C is chosen when the Establishment Phase is finished with no issue. Moreover, the passage point C is the re-emergence moment that the accompanying edge correspondence occurs. A passage point D is for retrying when [ACK] is not reacted. Section point E illustrates a change of the last phase of this layer (see Fig. 7.1).

Termination Phase: Both the sender and collector change their status into inactive in the Termination Phase. Possibly, this phase begins when the sender transmits the [EOT]. There is no reaction from the collector to this message. At the point when [EOT] is recognized at the beneficiary, it is gone to be inert, and the line is changes to unbiased (see Fig. 7.2).

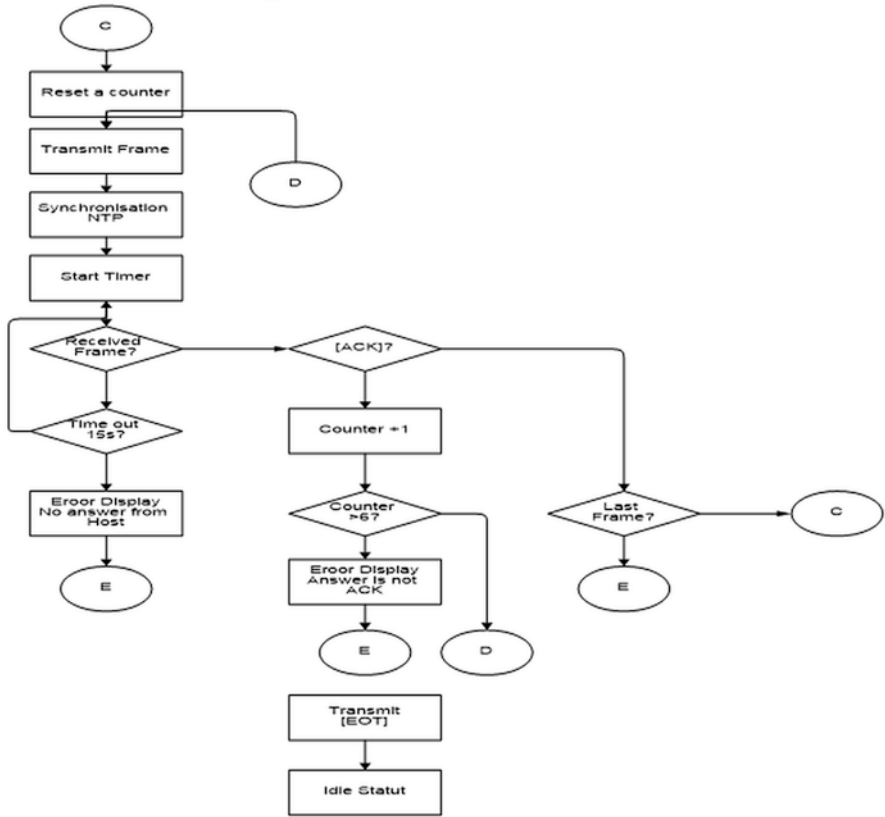


Fig. 7.2 Termination Phase flowchart

7.3 Results and Discussion

7.3.1 Using NTP to Synchronize the Server System

Synchronization is critical in today’s network environments. As different domains and the network services grow, their timing challenges and need for accuracy in their subsystems and applications also increase. There is no single standard policy for the device transient synchronization in networks [22–25]. Gigantic innovative research in many directions has been led previously. When all control stages finish, the writing features occur with two classes of synchronization components: wired and convention-based. Link solutions [26], which do not require the trading of data throughout a system, are mostly received because they can meet even the most stringent prerequisites. Then again, they need adaptability and, thusly, negatively affect working expenses during the establishment and support of the framework. Time synchronization must happen if a there is interfacing of the distributed devices

situated on the corresponding cyber-physical system arrangement, which does not occur in any case [34]. The way toward associating all optional change focuses on the organization's essential substations and control focus is as yet continuous in numerous nations. If the system framework is ready and the utilization of the time synchronization convention is practical, then both the standard and altered arrangements are proposed. Standard arrangements are broadly acknowledged and simple to execute, yet they can accomplish better execution with a particular situation. In terms of standard arrangements, the most well-known time convention is NTP, which is executed as a matter of course, in numerous correspondence stacks [27]. Largely, the precision of NTP synchronization depends carefully on the presentation of the hidden system framework: the better the system execution (and along these lines, the lower the correspondence inactivity and jitter), the lower the synchronization vulnerability.

In a committed neighborhood, NTP time synchronization could be in the request for several microseconds. At the same time, in a crossbreed organization, where various advances are received, ordinarily for associating hubs to a circulation framework, synchronization vulnerability can likewise arrive at many milliseconds [28–32]. There is a less mind-boggling NTP usage called Simple Network Time Protocol (SNTP) [35, 36] that uses similar system messages. However, it does not execute some complex NTP time following calculations. As a rule, it is appropriate for inserted gadgets since it requires fewer assets than NTP, yet offers lower synchronization exactness. The IEC61850-8-1 standard permits a synchronization framework dependent on SNTP. However, SNTP cannot fulfill the best synchronization classes characterized in IEC61850-5 [29]. The second standard answer for exact time synchronization on a system is PTP (Precision Time Protocol), otherwise called the IEEE1588 protocol [30, 33]. The convention gives nanosecond synchronization if all system gadgets support IEEE1588. As many systems are distributed over a network, NTP hosts (clients or servers) use messages to communicate. Here are the fields contained in an NTP package; the exchange of messages leading to synchronization follows the following procedure [18]:

- The system wishing to be synchronized first sends a packet in which it initializes at time t_0 the TT field “Transmit Timestamp” with its own system time.
- The server then stores the time of receipt of the packet in the “Receive Timestamp” field at $t + 1$ of the same packet.
- Then it performs a validity check of the package to ensure that it must perform the processing.
- Before returning the packet to the sender, the TT “Transmit Timestamp” field is copied into the OT “Originate Timestamp” field, and the TT “Transmit Timestamp” field is filled in at $t + 2$.
- The customer annotates the time of receipt of the response at $t + 3$ to allow the estimation of the travel time of the packet. Assuming that message transmission times are symmetrical, the travel time is half of the entire waiting time minus the handling time on the remote machine.

- The client also checks the answer validity to ponder if it should be taken into account.
- Then, the client system can estimate the offset of its clock in relation to the reference system.

The DNA database and the NTP timeserver will be installed on the same machine. The dependencies of these two actors are examined to decide which operating system will be deployed on the server. At the NTP server level, it can be Linux or Windows. For their installation, a Linux distribution is preferable. A dedicated server is set up for the NTP server and the log database. Certificates are integrated to allow mutual authentication of node implementation on the first server. The implementation can be threefold:

- Setting up the NTP server and configuring client
- Installation of the log database
- Generation of certificates and integration into the prototype

Every task of management, security, planning, and debugging a network needs to determine when events happen. Time is the critical element that allows an event on one network node to be mapped to a corresponding event on another. In many cases, the enterprise deployment of the NTP service overcomes these challenges. For healthcare facilities, a time synchronization system is particularly important to:

- (i) Ensure proper planning of medical teams
- (ii) Ensure proper administration of medication at the right time and in the right order of prescription
- (iii) Ensure the smooth running of surgical procedures [17–19]

Data centers need a time domain in the millisecond range for platform virtualization. The chronology of events also allows errors to be traced on the same millisecond scale: Traceability ensures a backup, or automatic backup, at night requiring accuracy of about 10 s. In Table 7.2, we show some UNIX commands for setting and synchronizing time.

Table 7.2 Common UNIX commands related to time

Commands	Description
date	Displays or sets the current system date and time
rdate	Sets the current system time from a remote host using the date protocol
adjtime()	Adjusts the system’s time of day clock gradually, to a specified value
set time of day()	Sets the system’s time of day clock instantly to a specified value sets the current systems
ntpdate	Traceability ensures a backup, or automatic backup, at night requiring accuracy of about 10 s
xntpd	NTP daemon
ntp-q	Monitor time synchronization

<p>rdate</p> <pre> asus@asus-X550LC:~\$ rdate Usage: rdate [-46acnpsv] [-o port] host -4: use IPv4 only -6: use IPv6 only -a: use adjtime instead of instant change -c: correct leap second count -n: use SNTP instead of RFC868 time protocol -o num: override time port with num -p: just print, don't set -s: just set, don't print -u: use UDP instead of TCP as transport -v: verbose output </pre>	<p>ntpdate</p> <pre> asus@asus-X550LC:~\$ ntpdate 29 Sep 02:27:46 ntpdate [7144]: asus@asus- X550LC:~\$ timedatectl Local time: dim. 2019-09-29 17:30:25 CET Universal time: dim. 2019-09-29 16:30:25 UTC RTC time: dim. 2019-09-29 16:30:25 Time zone: Africa/Algiers (CET, +0100) System clock synchronized: yes systemd-timesyncd.service active: yes RTC in local TZ: no </pre>
<p>ntpq -p</p> <pre> asus@asus-X550LC:~\$ ntpq -p remote refid st t when poll reach delay offset jitter ===== 0.ubuntu.pool.n .POOL. 16 p - 64 0 0.000 0.000 0.000 1.ubuntu.pool.n .POOL. 16 p - 64 0 0.000 0.000 0.000 0.ubuntu.pool.n .POOL. 16 p - 64 0 0.000 0.000 0.000 1.ubuntu.pool.n .POOL. 16 p - 64 0 0.000 0.000 0.000 2.ubuntu.pool.n .POOL. 16 p - 64 0 0.000 0.000 0.000 3.ubuntu.pool.n .POOL. 16 p - 64 0 0.000 0.000 0.000 </pre>	

7.4 Conclusion

At the beginning of the twenty-first century, we are reaching the limit of so-called “classical” technologies, and this is due to many parameters, including the fact that the size of the electron is about to be reached in engravings for the development of integrated circuits. Hence, researchers have turned to other perspectives. One of the most promising fields is the optical technology, which is vast and entails almost infinite possibilities and still poorly explored. Optical technologies have an immense potential exceeding that of classical techniques.

The desire for mutual aid between scientists outweighs the concern for profit and what better field than medicine to do so. We have therefore chosen among the various optical chips, the one dedicated to biomedical, is more precisely a DNA optical biochip whose role is the diagnosis of genetic diseases, and this with much higher efficiency than the usual procedures. The major problem in this type of diagnosis, especially when it comes to remote diagnosis, is the synchronization problem, so sometimes even the loss of data or overlap between them.

The use of NTP servers and the correct use of ASTM Elecsys Packets give us results that will allow us to perform a real-time and reliable diagnosis.

The ultimate goal of this research is to help others to save lives, prolong lives, have a real impact on society, and make science serve the public.

References

1. S. Cagnin, M. Caraballo, C. Guiducci, P.G. Martini, M. Ross, M. SantaAna, D. Danley, T. West, G. Lanfranchi, Overview of electrochemical DNA biosensors: New approaches to detect the expression of life. *Sensors (Basel, Switzerland)* **9**, 3122–3148 (2009)
2. K.E. Korhonen, S.P. Weinstein, E.S. McDonald, E.F. Conant, Strategies to increase cancer detection: review of true-positive and false-negative results at digital breast tomosynthesis screening. *Radiographics* **36**(7), 1954–1965 (2016)
3. I. Mannelli, V. Courtois, P. Lecaruyer, G. Roger, M.C. Millot, M. Goossens, M. Canva, Surface plasmon resonance imaging (SPRI) system and real-time monitoring of DNA biochip for human genetic mutation diagnosis of DNA amplified samples. *Sensors Actuators B Chem.* **119**(2), 583–591 (2006). <https://doi.org/10.1016/j.snb.2006.01.023>
4. M.G. Nair, S.S. Sandhu, A.K. Sharma, Cancer molecular markers: a guide to cancer detection and management. *Semin. Cancer Biol.* **52**(Pt 1), 39–55 (2018)
5. X. Zeng, Y. Yang, N. Zhang, D. Ji, X. Gu, J.M. Jornet, Y. Wu, Q. Gan, Plasmonic interferometer array biochip as a new mobile medical device for cancer detection. *IEEE J. Sel. Top. Quantum Electron.* **25**, 1–7 (2019)
6. J.A. Fee, F.P. McGrady, C. Rosendahl, N.D. Hart, Training primary care physicians in dermoscopy for skin cancer detection: A scoping review. *J. Cancer Educ.*, 1–8 (2019)
7. B. Han, Y.-L. Zhang, L. Zhu, X.-H. Chen, Z.-C. Ma, X.-L. Zhang, H.-B. Sun, Direct laser scribing of AgNPs RGO biochip as a reusable SERS sensor for DNA detection. *Sensors Actuators B Chem.* **270**, 500–507 (2018). <https://doi.org/10.1016/j.snb.2018.05.043>
8. V.V. Estrela, O. Saotome, H.J. Loschi, D.J. Hemanth, W.S. Farfan, R.J. Aroma, C. Saravanan, E.G.H. Grata, Emergency response cyber-physical framework for landslide avoidance with sustainable electronics. *Technologies* **6**, 42 (2018). <https://doi.org/10.3390/technologies6020042>
9. N. Razmjoooy, V.V. Estrela, *Applications of Image Processing and Soft Computing Systems in Agriculture* (IGI Global, Hershey, 2019), pp. 1–300. <https://doi.org/10.4018/978-1-5225-8027-0>
10. I. Mannelli, V. Courtois, P. Lecaruyer, G. Roger, M.C. Millot, M. Goossens, M. Canva, Surface plasmon resonance imaging (SPRI) system and real-time monitoring of DNA biochip for human genetic mutation diagnosis of DNA amplified samples. *Sensors Actuators B Chem.* **119**(2), 583–591 (2006). <https://doi.org/10.1016/j.snb.2006.01.023>
11. P. Liepold, H. Wieder, H. Hillebrandt, A. Friebe, G. Hartwich, DNA-arrays with electrical detection: A label-free low cost technology for routine use in life sciences and diagnostics. *Bioelectrochemistry* **67**(2), 143–150 (2005)
12. G. Kovacs, Optical excitation of surface plasmon-polaritons in layered media, in *Electromagnetic Surface Modes*, (Wiley, Boardman, 1982), p. 143
13. J. Homola, *Surface Plasmon Resonance Biosensors, in Optical Biosensors: Present and Future*, vol 207 (2002)
14. K. Vijayalayan, D. Veitch, Rot at the Roots? Examining Public Timing Infrastructure, in *Proceedings of the 35th Annual IEEE International Conference on Computer Communications* (2016), pp. 1–9
15. D. Matsakis, Time and frequency activities at the U.S. naval observatory, frequency control symposium and exposition. *Proceedings of the 2005 IEEE International* (2005), pp. 271–224
16. R.B. Warrington, P.T.H. Fisk, M.J. Wouters, M.A. Lawn, J.S. Thorn, S. Quigg, A. Gajaweera, S.J. Park, Time and frequency activities at the national measurement institute, Australia, Frequency control symposium and exposition, 2005. *Proceedings of the 2005 IEEE International* (2005), pp. 231–234
17. IEEE Std 1588-2008: IEEE standard for a Precision clock synchronization protocol for networked measurement and control systems[S]. IEEE1588-2008 standard (2008)
18. K.J. Zhao, A.I. Zhang, D.Y. Mning, Implementation of network time server system based on NTP. *Electron. Test* (7), 13–16 (2008)

19. D.L. Mills, Internet time synchronization: The network time protocol. *IEEE Trans. Commun.* **39**(10), 1482–1493 (1991)
20. <https://www.aggsoft.com/serial-data-logger/tutorials/astm.htm>, last accessed 2020/05/21
21. Roche Diagnostics Host Interface Manual – Version 1.4 (2013)
22. A.C.B. Monteiro, R.P. Franca, V.V. Estrela, S.R. Fernandes, A. Khelassi, R.J. Aroma, K. Raimond, Y. Iano, A. Arshaghi, UAV-CPSs as a test bed for new technologies and a primer to industry 5.0, in *Imaging and Sensing for Unmanned Aircraft Systems, Vol. 2, 1, 1–22*, ed. by V. V. Estrela, J. Hemanth, O. Saotome, G. Nikolakopoulos, R. Sabatini, (IET, London, 2020)
23. A. Arshaghi, N. Razmjoooy, V.V. Estrela, P. Burdziakowski, D.A. Nascimento, A. Deshpande, P.P. Patavardhan, Image transmission in UAV MIMO UWB-OSTBC system over Rayleigh channel using multiple description coding (MDC), in *Imaging and Sensing for Unmanned Aircraft Systems, Vol. 2, 4, 67–90*, ed. by V. V. Estrela, J. Hemanth, O. Saotome, G. Nikolakopoulos, R. Sabatini, (IET, London, 2020). https://doi.org/10.1049/PBCE120G_ch4
24. H.J. Loschi, V.V. Estrela, D.J. Hemanth, S.R. Fernandes, Y. Iano, A.A. Laghari, A. Khan, H. He, R. Sroufe, Communications requirements, video streaming, communications links and networked UAVs, in *Imaging and Sensing for Unmanned Aircraft Systems, Vol. 2, 6, 113–132*, ed. by V. V. Estrela, J. Hemanth, O. Saotome, G. Nikolakopoulos, R. Sabatini, (IET, London, 2020)
25. P. Ferrari, A. Flammini, S. Rinaldi, G. Prytz, Evaluation of time gateways for synchronization of substation automation systems. *IEEE Trans. Instrum. Meas.* **61**(10), 2612–2621 (2012)
26. K. Schneider, C.C. Liu, A proposed method of partially decentralised power system protection, in *Proceedings of CRIS 2004*, (2004)
27. F.A.-C. Figuerola, L.C. Graell, J.O. Enciso, Type an IP based, highly reliable telecommunications framework for advanced smart grid applications, in *Proceedings of 44th International Conference on Large High Voltage Electric Systems (2012)*, 7 p
28. D. Della Giustina, P. Ferrari, A. Flammini, S. Rinaldi, Experimental characterization of time synchronization over a heterogeneous network for smart grids, in *Proceedings of AMPS (2013)*, pp. 132–137
29. IEC Communication networks and systems for power utility automation, IEC 61850 Ed. 2 (2011)
30. M. Lombardi, J. Levine, J. Lopez, F. Jimenez, J. Bernard, M. Gertsvolf, et al., International comparisons of network time protocol servers, in *Proceedings of the 2014 Precise Time and Time Interval Systems and Applications Meeting*, 1–4 December, Boston, Massachusetts (2014), pp. 57–66
31. A. Novick, M.A Lombardi Comparison of NTP servers connected to the same reference clock and the same network, *Proceedings of the 2017 Precise Time and Time Interval Systems and Applications Meeting*, 30 January–2 February, 2017, Monterey, California (2017), pp. 264–270
32. S. Sommars, Challenges in time transfer using the Network Time Protocol (NTP), *Proceedings of the 2017 Precise Time and Time Interval Systems and Applications Meeting*, 30 January–2 February, 2017, Monterey, California (2017), pp. 271–290
33. LI X ZH, *Research on the Network Time Synchronization System Based on IEEE1588* (National Time Service Center, Chinese Academy of Sciences, 2011)
34. V.V. Estrela, J. Hemanth, O. Saotome, E.G.H. Grata, D.R.F. Izario, Emergency response cyber-physical system for flood prevention with sustainable electronics, in *Proceedings of the 3rd Brazilian Technology Symposium. BTSym 2017, Campinas, SP, Brazil*, ed. by Y. Iano, R. Arthur, O. Saotome, V. V. Estrela, H. J. Loschi, (Springer, Zurich, 2019). https://doi.org/10.1007/978-3-319-93112-8_33
35. Mills D.L. RFC1305 - NTPv3, <http://rfc-editor.org/>, last accessed 2020/05/21
36. D.L. RFC4330 - SNTPv4., <http://rfc-editor.org/>, last accessed 2020/05/21
37. M. Park, B. Kang, K. Jeong, Paper-based biochip assays and recent developments: A review. *Biochip J.* **12**, 1–10 (2018)

Chapter 8

Particle Swarm Optimization with Tabu Search Algorithm (PSO-TS) Applied to Multiple Sequence Alignment Problem



Lamiche Chaabane , Abdeldjalil Khelassi , Andrey Terziev , Nikolaos Andreopoulos , M. A. de Jesus , and Vania Vieira Estrela 

8.1 Introduction

Sequence alignment is paramount to molecular sequence analysis. It can help to build a phylogenetic tree of related DNA sequences or to predict the function/structure of unfamiliar protein sequences by aligning them with others whose function/structure is already acknowledged. Sequence alignment establishes an alignment of two or more sequences to maximize the similarities amid them [1]. This NP-hard problem [2, 3] can benefit from computational intelligence (CI) algorithms in reasonable processing time.

In recent years, metaheuristic procedures aided in producing approximate solutions for the MSA dilemma. Their primary rationale is to commence by an initial solution and ameliorate the MSA through a series of iterations until the solution does not become better any longer. This category of methods embraces tabu search (TS) [4], genetic algorithm (GA) [5], simulated annealing (SA) algorithm [6], ant colony (AC) algorithm [7], particle swarm optimization (PSO) [8], artificial bee colony (ABC) algorithm [9], and so on.

This research study brings in a hybrid line of attack named PSO-TS algorithm to devise an approximate solution to the MSA impasse combining the best characteristics of the PSO and the TS schemes.

L. Chaabane (Deceased)
Computer Science Department, University of M'sila, M'sila, Algeria

A. Khelassi (✉)
Abou Baker Belkaied University Of Tlemcen, Tlemcen, Algeria

A. Terziev · N. Andreopoulos · M. A. de Jesus · V. V. Estrela
Department of Telecommunications, Federal Fluminense University (UFF), RJ, Brazil
e-mail: vania.estrela.phd@ieee.org

The remainder of this document is organized as follows: Section 8.2 presents a brief literature review of the previous works pertinent to the PSO-TS framework. Section 8.3 depicts the basic concepts of the PSO and the TS metaheuristics. The details about the components of the PSO-TS algorithm are in Sect. 8.4. Simulation outcomes appear in Sect. 8.5, together with some discussions. Section 8.6 suggest improvements to the PSO-TS algorithm. Finally, this study ends with the comments from Sect. 8.7.

8.2 Literature Review

Among the significant multiple sequence approaches, some of them employ iterative alignment aligners. Rias et al. [4] applied a tabu search variant relying on the COFFEE objective function to find better results for the multiple sequences. In [5], the authors developed an amended GA with an intelligent selection strategy to resolve the multiple biological sequence dilemma. Proper alignments are obtained compared with those done by classical GA.

In Ref. [8], the authors applied PSO and Clustal X aligner to produce better results than those from Clustal X alone. An ABC algorithm for solving the MSA issue appears in [9]. In Ref. [10], V. Cutello et al. presented an immune-inspired algorithm (IMSA) to tackle the MSA dilemma utilizing ad hoc mutation operators. Simulation results on some BaliBASE v.1.0 instances show that IMSA is superior to other aligners such as PRRP, CLUSTAL X, SAGA, DIALIGN, PIMA, MULTIALIGN, and PILEUP8. An efficient method by using a multi-objective GA (MSAGMOGA) to discover optimal alignments is proposed in [11]. Experiments on the BaliBASE 2.0 database confirmed that MSAGMOGA obtained better results than MUSCLE, SAGA, and MSA-GA methods.

Recently, in [12], the authors announced a novel multi-objective evolutionary scheme called hybrid multi-objective ABC (HMOABC), which hinges on swarm intelligence for the MSA dilemma. Experimental results on some instances coming from the BaliBASE 3.0 database showed that the HMOABC is an auspicious approach for solving the MSA impasse. Reference [13] suggests a better-quality Chemical Reaction Optimization (CRO) algorithm for the MSA problem. In their work, the authors inserted an intelligent diversification mechanism in the initialization process to help the CRO algorithm to travel around the search space globally. Simulation results confirmed the superiority of this investigative effort over others.

8.3 Preliminaries

8.3.1 Particle Swarm Optimization (PSO)

Particle swarm optimization (PSO) is a metaheuristic (aka nature-inspired) optimization algorithm conceived by Kennedy and Eberhart [14] that had as its inspiration the bird flocking behavior. Rather than the hard optimization formulation, there is a new recast problem. This different formulation consists of a population of answers entitled particles, where the pair of features position and velocity characterize each particle. At each iteration, the particle's locus is updated in accordance with its personal best position and the best solution of the swarm. The subsequent equations govern the evolution of the population:

$$V^{(k+1)} = w.V^{(k)} + c_1.rand_1.(pbest^{(k)} - X^{(k)}) + c_2.rand_2.(gbest^{(k)} - X^{(k)}), \text{ and} \quad (8.1)$$

$$X^{(k+1)} = X^{(k)} + V^{(k+1)}, \quad (8.2)$$

where for each particle:

X is its position

V is its velocity

w represents the inertia weight

$pbest$ is its best place

$gbest$ is the global best position of the swarm

$rand1, rand2$ are random values within $[0, 1]$

$c1, c2$ are positive constants regulating the impact of the personal optimum as well as the global best solutions on the search course, respectively

k is the iteration number

The process stops after reaching a predefined number of iterations $Itmax$.

8.3.2 Tabu Search Optimization (TS)

TS appeared the first time in Glover's manuscript (1986) [15] to unravel a wide range of hard optimization problems. TS starts with a random tentative answer and appraises the fitness function for the given solution. Then all possible neighbors of the given solution are generated and evaluated. To overcome the local optimum limit, TS saves the better local neighbors (after searching, examining, and, if necessary, discarding them) in a Tabu List (TL). Moreover, TS can exploit an aspiration rule to make the whole search processing continue or to devise a diversified guided search tactic to other promising regions.

8.4 Proposed Method

PSO's main drawback is its premature convergence and local optimum problem. To evade this limit, TS is incorporated as a local search procedure to enrich the global best solution and to apply the diversification mechanism to guide the search to other promising regions of the search space. Then, the novel hybrid technique, called PSO-TS, consists of strong cooperation among PSO and TS. It makes full use of the exploration ability of PSO and the exploitation ability of TS.

In our MSA problem, PSO-TS works as follows:

1. PSO modifies both particle positions and velocities after establishing the initial population with the recommended swarm initialization strategy.
2. After that, a new global best solution ($gbest^*$) emerges from the improvement of the current global best solution ($gbest$) via the TS procedure.
3. This iterative process ends when a stopping condition is reached.

The PSO-TS hybridization strategy has a flowchart of is along these lines (Fig. 8.1):

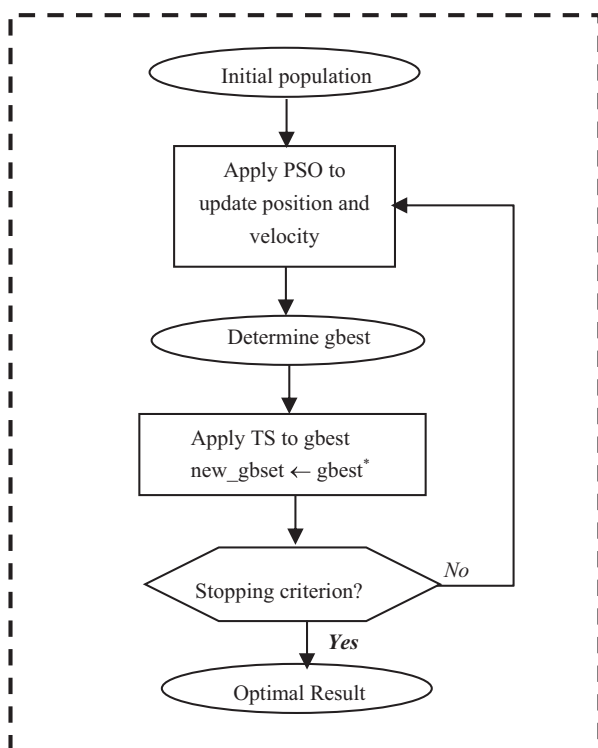


Fig. 8.1 PSO-TS algorithm flowchart

8.4.1 Components

Solution Encoding Each solution (particle) entails a set of vectors, whose elements indicate the position of the randomly interleaved gaps in the different sequences waiting for alignment. Here, the sequences should have the same length L (the typical L value is 1.2 times of the most prolonged sequences) [16]. Figure 8.2 brings in an example of this encoding scheme.

Swarm Initialization The multiple small-popsizes initialization strategy (MSPIS) [17] renders the initial population and ensures its diversity. Every time, there is a small number of chromosomes by a small-popsizes tactic. The best two individuals are selected into the initial population until the number of chromosomes equal to the present population size. A summary of the detailed MSPIS steps becomes.

- Step1.* Generate a small number of chromosomes through the small-popsizes initial method.
- Step2.* Calculate the mean value of the small number population fitness value, $Meanpop_i$.
- Step3.* All the chromosomes whose fitness values exceed $Meanpop_i$ go into the initial population.
- Step4.* Repeat steps 1–3 until the number of chromosomes equal to the present population size.

This initialization method delivers an approximate optimal solution as near as possible.

Objective Function Habitually, the objective function appraises the alignment quality in mathematical terms. For that, the score apportioned to each particle (alignment) consists of the summing of the scores (SP) of the alignment of each pair of sequences [18].

The score of each pair of sequences comprises the sum of the score assigned to the match of each pair of symbols. A substitution matrix, such as the PAM205 matrix, can achieve this effect. The objective function for an alignment A with k sequences is

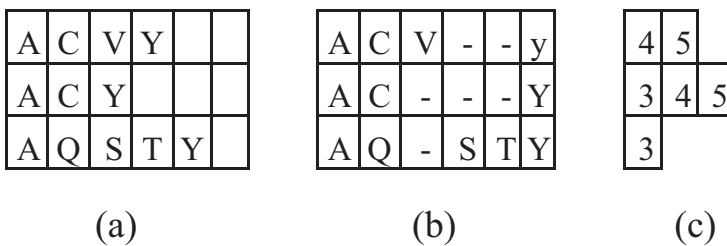


Fig. 8.2 Sequence alignment: (a) Set of sequences to align, (b) insertion of gaps, and (c) solution representation

$$\text{Score}(A) = \sum_{i=1}^{k-1} \sum_{j=i+1}^k S(A_i, A_j),$$

where $S(A_i, A_j)$ stands for the alignment score among two aligned sequences, A_i and A_j .

Particle Move Operator This operator is necessary to update the position of the particle in the search space. Each swarm element movement is contingent on its current location and the same as the leader. In this work, the distance between the particle and the leader amounts to the proportion of matching gaps in the sequences as

$$\text{Distance} = \frac{\text{matching gaps}}{\text{total gaps}}.$$

This research introduced the crossover operator from [16] to transport each particle toward the leader. It entails dividing the current alignment into two segments according to a randomly picked crossover point from the range $[1, \text{Distance} * L]$. After that, the best-produced child replaces the current particle.

8.4.2 TS Components of the MSA Problem

Cost Function It evaluates the quality of each candidate solution. In this research study, the authors retain the same one from the PSO algorithm.

Initial Solution In the suggested PSO-TS methodology, the TS works as a local search process to ameliorate the global best solution (*gbest*) yielded by the PSO algorithm. Then, the PSO output becomes an initial solution for the TS procedure.

Generation of Neighbors In order to generate a set of neighbors of the current solution, the authors apply a simple but effective strategy, which works as follows:

- (i) Firstly, it picks a random amino acid from a randomly chosen sequence in the alignment and checks whether one of its neighbors is a gap.
- (ii) If this is the circumstance, the algorithm swaps the elected amino acid with a gap neighbor.
- (iii) If both neighbors are gaps, then one of them is picked randomly [18].

Figure 8.3 portrays this mechanism.

Tabu List Update This list stores previously visited solutions to help the algorithm evade being trapped in local optima. Here, the user, depending on the size of the problem instances, predefines the tabu list length (TLL). Besides, the authors opted to modify the TLL value dynamically by increasing or diminishing it with a

A	C	N	-	K	T	V	Y
A	C	-	K	-	-	Y	-
A	Q	-	-	S	-	V	Y

A	C	N	-	K	T	V	Y
A	C	-	-	K	-	Y	-
A	Q	-	-	S	-	V	Y

Fig. 8.3 Neighbors generation strategy

prefixed constant X . Such a mechanism helps to attain some other solution and to overcome the cycling problem.

Stopping Condition The authors chose the most straightforward and most commonly used stopping criterion, i.e., to terminate upon reaching a predefined number of iterations.

The pseudo-code of our TS is given below:

Pseudo-code of TS algorithm

Step 0: Generate an initial alignment A_{init} .
 Initialize $ITMAX, N_s, TLL$
 Set $TL \leftarrow \emptyset, A_{curr} = A_{init}, A_{best} = A_{init}$

Step 2: Iterate the following steps for $ITMAX$ iterations

Step 2.1: Generate N_s neighboring alignments
 $A_i (i=1, 2, \dots, N_s)$ of A_{curr}

Step 2.2: $A_{best} \leftarrow Best_neighbor(A_1, A_2, \dots, A_{N_s})$
 If $(A_{best} \notin TL)$ and $S(A_{best}) > S(A_{curr})$ then
 $A_{curr} \leftarrow A_{best}$
 Else try next test alignment and go to step 2.1
 $TL \leftarrow TL \cup A_{curr}$
 If TL is full, remove the oldest solution from TL

Step 2.3: If $S(A_{curr}) > S(A_{best})$ then
 $A_{best} \leftarrow A_{curr}$

Step 3: Return A_{BEST} and $S(A_{best})$

After the description of both the PSO and TS algorithms, the global framework of the PSO-TS procedure is as follows:

8.5 Simulation and Results

The PSO-TS algorithm is implemented using JCreator version 3.5 and a personal computer with a 2.66 GHz Intel Pentium IV processor. A set of tests verified and validated the PSO-TS scheme, where the objective is to compare the PSO-TS method with other published works, including the IMSA approach [10] and the

PSO-TS Pseudo-code

1. Apply MSPIS strategy to generate an initial swarm
2. Fix NG value *// Number of generations*
3. Set $j \leftarrow 1$
4. While ($j \leq NG$) do
 - 4.1. Determine the leader particle value $gbest$
 - 4.2. For each particle in the population do
 - a) Evaluate the distance between $gbest$ and the particle
 - b) Select a crossover point randomly
 - c) Apply particle move mechanism
 - d) Assign to the current particle the best-produced child
 - End for
 - 4.3 Update $gbest$ *// Calculate the new leader particle gbest*
 - 4.4 $New_gbest \leftarrow TS(gbest)$ *// Apply TS to improve gbest*
 - 4.5 Insert New_gbest into the current population
 - 4.6. $j \leftarrow j + 1$
5. End while
6. Return $gbest$ value and its correspondent particle. *// Output the result.*

BPSO algorithm [19]. The BaliBASE SP score (SPS) results for both small and large datasets taken from the BaliBASE database [20] are portrayed in Tables 8.1 and 8.2.

The subsequent procedure provides the SP score [21]: for a candidate alignment (individual) of N sequences encompassing M columns, then the i -th column within the alignment becomes $A_{i1}, A_{i2}, \dots, A_{iN}$. A value of p_{ijk} characterizes each pair of residues A_{ij} and A_{ik} . If $p_{ijk} = 1$, it means that the candidate alignment residues A_{ij} and A_{ik} have been aligned with each other as far as the reference alignment is concerned. Otherwise, $p_{ijk} = 0$. Consequently, the score for the i -th column turns out to be

$$S_i = \sum_{j=1, j \neq k}^N \sum_{k=1}^N p_{ijk}.$$

For the candidate alignment, the overall SPS becomes

$$SPS = \sum_{i=1}^M \frac{S_i}{Mr},$$

with the number of columns in the reference alignment given by Mr while S_{ri} is the score S_i for the i -th column for the reference alignment. The values of SPS lie in the interval $[0.0, 1.0]$. High SPS values point toward closer likeness with the BaliBASE reference alignment [21].

Table 8.1 PSO-TS vs. IMSA: SPS comparative results for the BaliBASE test sets

Instance	N	IMSA [10]	PSO-TS
laboA	5	0.759	0.910
45lc	5	0.773	0.853
9rnt	5	0.954	0.948
kinase	5	0.644	0.716
2cba	5	0.754	0.754
lppn	5	0.987	0.989
2myr	4	0.285	0.433
left	4	0.880	0.928
ltaq	5	0.946	0.949
lubi	17	0.897	0.907
kinase	18	0.905	0.915
lidy	27	0.854	0.849
Average		0.810	0.846

Table 8.2 PSO-TS algorithm versus BPSO approach: SPS comparative results for the BaliBASE test sets

Instance	N	BPSO [19]	PSO-TS
lidy	5	0.7394	0.8492
45lc	5	0.7973	0.8532
lkrn	5	0.9984	0.9988
kinase	5	0.7064	0.7165
lpii	5	0.7987	0.7980
5ptp	5	0.9328	0.9410
lajsA	5	0.3528	0.3750
glg	5	0.8324	0.9241
ltaq	5	0.7633	0.9491
Average		0.7690	0.8227

From Tables 8.1 and 8.2, it is clear that comparing with IMSA and BPSO, the average SPS values of PSO-TS algorithm are more significant than or comparable with those obtained by the techniques stated above for the short, medium, and long sequences. In addition, significant improvements are observed in test cases with a large number of sequences, which shows that our approach can work well with large problem sizes.

8.6 Future Trends

Other metaheuristics and multi-objective optimization schemes can aid in unraveling this bioinformatics impasse [22–24].

As perspective innovations of this work, the authors contemplate (i) integration of other mechanisms within the neighborhood generation step or (ii) intensification/

diversification strategies in TS core to improve the quality of multiple alignments. In addition, the authors will use other powerful PSO variants as a part of this hybridization tactic to find a better solution for the MSA problem. A comparison of the proposed method with some other state-of-the-art techniques such as Clustal W, SAGA, or MULTALIGN, with other benchmarks, is possible to verify its enormous potential [25–27].

Deep learning (DL) has been in the spotlight as a potent tactic that makes noteworthy signs of progress when it comes to solving the issues plaguing the artificial intelligence. Nevertheless, numerous caveats, e.g., local minima trapping, inferior performance, and elevated computational time, still arise while applying DL to MSA. So, global optimization procedures like differential search algorithms can aid DL deployments to reach the best outcome and data [28–31].

8.7 Conclusion

The MSA problem is one of the primary techniques utilized in computational biology, e.g., genomic annotation, homology searches, gene regulation networks, protein structure prediction, and functional genomics, to name a few. Among MSA bottlenecks, there is the alignment of more than a pair of biological sequences, which is an NP-hard optimization problem.

This research showcases the PSO-TS approach, which is a novel hybrid algorithm constructed on metaheuristics developed to tackle the multiple sequence alignment (MSA) problem. The PSO-TS framework combines the PSO benefits, particularly its simplicity in implementation and its inexpensive computational processing time, with the best tabu search algorithm features, i.e., its local upgrading practice. These improvements enrich the global best solution by augmenting the diversification process. The results summarized in this paper show the superior capability of our hybrid approach compared to some other literature works.

References

1. J.D. Thompson, J.E. Thierry, O. Poch, Rapid scanning and correction of multiple sequence alignments. *Bioinformatics* **19**, 1155–1161 (2003)
2. T. Jiang, L. Wang, On the complexity of multiple sequence alignment. *J. Comput. BioI.* **1**, 337–378 (1994)
3. C.H. Papadimitriou, K. Steiglitz, *Combinatorial Optimization: Algorithms and Complexity* (Dover Publications, New York, 1998)
4. T. Riaz, Y. Wang, K.B. Li, Multiple sequence alignment using tabu search, in *Proceedings of 2nd Asia-Pacific Bioinformatics Conference (APBC)*, Dunedin, New Zealand, (2004), pp. 223–232
5. J.T. Hornig, L.C. Wu, C.M. Lin, B.H. Yang, A genetic algorithm for multiple sequence alignment, in *Proceedings of LNCS*, (2005), pp. 407–420

6. M. Hernández-Guía, R. Mulet, S. Rodríguez-Pérez, A new simulated annealing algorithm for the multiple sequence alignment problem. The approach of polymers in a random media. *Phys. Rev. E* **72**, 1–7 (2005)
7. L. Chen, L. Zou, J. Chen, An efficient ant colony algorithm for multiple sequences alignment, in *Proceedings of the 3rd International Conference on Natural Computation (ICNC '07)*, (2007), pp. 208–212
8. F. Xu, Y. Chen, A method for multiple sequence alignment based on particle swarm optimization, in *ICIC 2009, LNAI 5755*, (2009), pp. 965–973
9. X. Lei, J. Sun, X. Xu, L. Guo, Artificial bee colony algorithm for solving multiple sequence alignment, in *Proceedings of 2010 IEEE Fifth International Conference on BIC-TA*, (2010), pp. 337–342
10. V. Cutello, G. Nicosia, M. Pavone, I. Prizzi, Protein multiple sequence alignment by hybrid bio-inspired algorithms. *Nucleic Acids Res.* **39**(6), 1980–1992 (2011)
11. M. Kayaa, A. Sarhanb, R. Alhajj, Multiple sequence alignment with affine gap by using multi-objective genetic algorithm. *Comput. Methods Prog. Biomed.* **114**, 38–49 (2014)
12. R.L. Alvaro, A.V.R. Miguel, L.G.A. David, Hybrid multi-objective artificial bee colony for multiple sequence alignment. *Appl. Soft Comput.* **41**, 157–168 (2016)
13. R.K. Yadav, H. Banka, An improved chemical reaction-based approach for multiple sequence alignment. *Curr. Sci.* **112**(3), 527–538 (2017)
14. J. Kennedy, R. Eberhart, Particle swarm optimization. *Proc. IEEE Int. Conf. Neural Netw.* **4**, 1942–1948 (1995) Perth
15. F. Glover, Tabu search: Part 1. *ORSA J. Comput.* **1**(3), 190–206 (1989)
16. P.F. Rodriguez, L.F. Nino, O.M. Alonso, Multiple sequence alignment using swarm intelligence. *Int. J. Comput. Intell. Res.* **3**(2), 123–130 (2007)
17. C.Z. Ahn, R.S. Ramakrishna, A genetic algorithm for shortest path routing problem and the size of populations. *IEEE Trans. Evol. Comput.* **6**(6), 566–579 (2002)
18. C. Lamiche, A hybrid solver for protein multiple sequence alignment problem. *J. Bioinforma. Comput. Biol.* **16**(4), 1–20 (2018)
19. H.X. Long, W.B. Xu, J. Sun, W.J. Ji, Multiple sequence alignment based on a binary particle swarm optimization algorithm, in *Proceedings of Fifth International Conference on Natural Computation*, (2009), pp. 265–269
20. J.D. Thompson, F. Plewniak, O. Poch, A comprehensive comparison of multiple sequence alignment programs. *Nucleic Acids Res.* **27**(13), 2682–2690 (1999)
21. S.S. Sathya, S. Kuppaswami, K.S. Babu, Nomadic genetic algorithm for multiple sequence alignment (MSANGA). *Int. J. Adapt. Innov. Syst.* **1**, 44 (2009)
22. N. Razmjooy, V.V. Estrela, *Applications of Image Processing and Soft Computing Systems in Agriculture*. IGI Global. (2019). <https://doi.org/10.4018/978-1-5225-8027-0>
23. N. Razmjooy, V.V. Estrela, H.J. Loschi, A study on metaheuristic-based neural networks for image segmentation purposes, in *Data Science Theory, Analysis and Applications*, Taylor and Francis, Abingdon, UK, (2019)
24. M.A. de Jesus, V.V. Estrela, O. Saotome, D. Stutz, Super-resolution via particle swarm optimization variants, in *Biologically Rationalized Computing Techniques for Image Processing Applications. Lecture Notes in Computational Vision and Biomechanics*, ed. by J. Hemanth, V. Balas, vol. 25, (Springer, Cham, 2018). https://doi.org/10.1007/978-3-319-61316-1_14
25. C. Zambrano-Vega, A.J. Nebro, J. García-Nieto, J.F. Montes, Comparing multi-objective metaheuristics for solving a three-objective formulation of multiple sequence alignment. *Prog. Artif. Intell.* **6**, 195–210 (2017)
26. S. Chatterjee, P. Barua, M. Hasibuzzaman, A. Iftiea, T. Mukharjee, S.S. Nova, A hybrid genetic algorithm with chemical reaction optimization for multiple sequence alignment, in *2019 22nd International Conference on Computer and Information Technology (ICCIT)*, (2019), pp. 1–6
27. F. Naznin, R.A. Sarker, D. Essam, Progressive alignment method using genetic algorithm for multiple sequence alignment. *IEEE Trans. Evol. Comput.* **16**, 615–631 (2012)

28. Deshpande A, Patavardhan P, Estrela VV, Razmjooy N. (2020) Deep learning as an alternative to super-resolution imaging in UAV systems. In: Estrela V.V., Hemanth J., Saotome O., Nikolakopoulos G., Sabatini R. (eds), *Imaging and Sensing for Unmanned Aircraft Systems*, Vol. 2, 9, 177–212, Stevenage: The Institution of Engineering and Technology
29. R. Jafari, M.M. Javidi, M.K. Rafsanjani, Using deep reinforcement learning approach for solving the multiple sequence alignment problem. *SN Appl. Sci.* **1**, 1–12 (2019)
30. C. Zhang, W. Zheng, S.M. Mortuza, Y. Li, Y.A. Zhang, DeepMSA: Constructing deep multiple sequence alignment to improve contact prediction and fold-recognition for distant-homology proteins. *Bioinformatics* (2019)
31. S.N. Yousoff, A. Baharin, A. Abdullah, A review on optimization algorithm for deep learning method in bioinformatics field, in *2016 IEEE EMBS Conference on Biomedical Engineering and Sciences (IECBES)*, (2016), pp. 707–711

Chapter 9

Extracted Haralick's Texture Features for Abnormal Blood Cells



Abdellatif Bouzid-Daho, Naima Sofi, and Patrick Siarry 

9.1 Introduction

The purpose of the medical imaging is to create visual representation intelligible information of a medical nature. This problem fits more broadly in the framework of the scientific imaging and related technological cyber-physical systems [1, 2]. The objective is indeed to be able to represent a large amount of data from a multitude of sources in a format somewhat simple to a giving imaging mode or modes [3, 4]. In the multitude of medical images, the present investigation focuses on the characterization of the microscopic image by texture.

The texture is very often seen as disruptive as characterized by transitions but unattractive in terms of object contours. Various methods exist to extract the characteristics of image textures [5–9].

The texture, almost omnipresent in the images and, particularly, microscopic medical images (IMM), plays a paramount role in the analysis, segmentation, classification, representation, and characterization of imageries. Although it has interested many researchers and many of the works issued in recent years [10–12] tackled these issues, the knowledge area remains, still not fully exploited.

Feature extraction (FE) represents an image through a set of features (feature vector) with or without some dimensionality reduction. When the acquisition algorithm handles input data that are too bulky and contain redundancy, then the input can be transformed into a compact representation relying on a set of features. Hence, FE expresses the input data through a basis consisting of a set of image-related features. If the elements mined are chosen sensibly (this process is also known as

A. Bouzid-Daho (✉) · P. Siarry
Laboratoire Images, Signaux et Systèmes Intelligents (LISSI), Université Paris Est Créteil (UPEC), Créteil, France

N. Sofi
Centre Universitaire Naâma (CUN), Naâma, Algeria



Fig. 9.1 Depiction of the feature extraction process

handcrafted features), then the feature set will portray the relevant data from the input data satisfactorily. As a consequence, the sought after task can be performed with the reduced representation as a replacement for the full-size input. Features habitually encompass information about gray intensities, shape, texture, or context. One must initially extract some image features to categorize a picture object. The figure below depicts the processing stages of the proposed scheme [11–14] (Fig. 9.1).

The extracted blood cell features turn out to be the input to a classification stage that categorizes the cells according to hematological models automatically. The classification module should identify the blood cells relying on the extracted features from real images. When it comes to noisy images, this can impair the classification.

The statistical methods [15, 16] study the associations between each pixel and its neighbors. These procedures afford some adaptability of the study of the fine structures without apparent regularity. Three major statistical methodologies will be studied in this work: the first-order, second-order, and those of higher order. In this manuscript, the order of a technique [17] amounts to the number of pixels put into play during the assessment of each result [18].

The rest of the text is organized as follows. Section 9.2 overviews image analysis and the Gray-level co-occurrence matrix (GLCM) for textural analysis applied to the biomedical field. This section condenses the five main Haralick’s texture features calculated and employed the gray-level co-occurrence matrix for the bio-image textural analysis with a specific database of blood cell images. Section 9.3 details the main steps of the proposed analysis, arranges for experimental results, and discusses a comparative study. This part of the text scrutinizes the detection of abnormal blood cells that can be prospective cancerous cells. As a final point, a conclusion and future works emerge in Sect. 9.4.

9.2 Methods and Materials

Many applications are employing optical microscopy, including blood cancer cell detection. These applications require high-quality data for accurate cancer cell understanding and analysis. This work uses images provided by optical microscopy to identify pre-diagnoses abnormal blood cells using textural features to distinguish between the different grades of cancer cells (Fig. 9.2). An analysis of the textures and structures, present in the bio-images representing of samples, allows making a

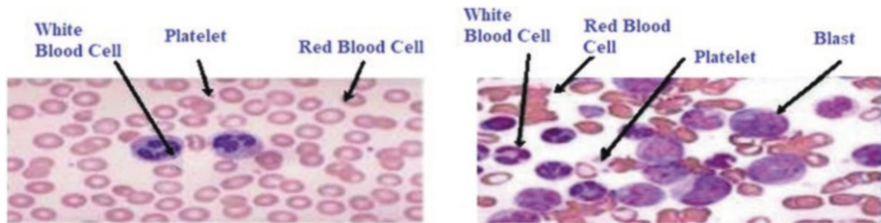


Fig. 9.2 Blood smear for normal cells (left) and cancerous cells (right) [9]

diagnosis of different degrees of cancers malignancy correspond to different structural patterns as well as apparent textures. We propose to apply the Haralick's texture features based on the GLCM in various types of blood cell images.

9.2.1 Textural Analysis Based on Gray-Level Co-occurrence Matrix (GLCM)

The authors consider the GLCM parameters as part of a statistical textural analysis study of bio-images to remove the different characteristics of texture [19]. The GLCM helps to relieve the burden of dealing with long feature descriptors [3, 4].

9.2.1.1 Gray-Level Co-occurrence Matrix (GLCM)

A statistical way of examining textures that may ponder on the spatial relationship of pixels is the GLCM, otherwise known as the gray-level spatial dependence matrix. The GLCM characterizes the texture of an image by evaluating how often pairs of pixels with particular numerical values and with a specified spatial connection happen in an image. These pieces of evidence aid in creating a GLCM and, then, identifying statistical metrics from this matrix. GLCM parameters described in texture analysis cannot provide information about shape contrariwise to the textural filter functions, i.e., the spatial pixel relationships within an image. The GLCM is an $N \times N$ square matrix, where N represents the gray level of the image. GLCM denotes the probabilities $P_{d(i,j)}$ of transition from a pixel of an i gray intensity to a pixel of a j gray intensity. The separation between i and j happens by a translation vector defined by the r direction and a d distance. The current values used are $r = 0^0; 45^0; 90^0; 135^0$ and $d = \{1,2,3,4\}$. The GLCM computation is widespread in texture depiction and hinges on the repetitive occurrence of some gray-level textural configuration, which varies fast with distance in fine textures and gradually for large textures. The GLCM definition is as follows:

$$P_{d(i,j)} = \left| \left\{ \left((r,s), (t,v) \right) : I(r,s) = i, I(t,v) = j \right\} \right|, \quad (9.1)$$

where

- $(r, s), (t, v)$ are the image coordinates with $(t, v) = (r + dx, s + dy)$.
- \mathbf{d} is the distance vector (dx, dy) .
- $|I|$ designates the cardinal of the whole

GLCM contains elements contingent on the image size. For instance, the authors found 256×256 elements for a 256-gray-level image, increasing the effort to manipulate GLCM.

In that way, the resolutions of images are often reduced to consider the gray-level coding of 8, 16, or 32 bits in practice. According to the GLCM, several calculated parameters characterize the spatial texture.

9.2.2 Haralick Parameters Extraction

GLCM contains lots of information complicated to exploit directly. Therefore, 14 parameters (as defined by Haralick [12]) can be calculated from GLCM, providing more easily the descriptive characters of the textures. The study's case only utilizes and computes the next five main Haralick's coefficients (or parameters) on GLCM for textural analysis: energy (ENE), contrast (CST), entropy (ENT), correlation (COR), and homogeneity (HOM) described as follows [19–21]:

1. **Energy:** It measures the texture uniformity. It has high values when the gray-level distribution is constant or periodic consistent with the expression below:

$$\text{ENE} = \sum_i \sum_j \left(Pd(i, j)^2 \right). \quad (9.2)$$

2. **Contrast:** This feature measures the image intensity contrast or the local variabilities present in an image to indicate the texture fineness. It is strongly uncorrelated to energy as illustrated by the next equation:

$$\text{CST} = \sum_i \sum_j \left((i - j)^2 Pd(i, j) \right). \quad (9.3)$$

3. **Entropy:** This parameter gauges the disorder within the image. It attains high values for a random texture and correlates strongly with the reverse of the energy. The succeeding expression defines this coefficient:

$$\text{ENT} = - \sum_i \sum_j \left(\log(Pd(i, j)) Pd(i, j) \right). \quad (9.4)$$

4. **Correlation:** This feature estimates the linear dependency (relatively to d) of the gray levels in the image. It is uncorrelated to energy and entropy parameters. The equation underneath specifies this parameter:

$$\text{COR} = \sum_{i,j=1}^N P_d(i,j) \left[\frac{(i-m_i)(j-m_j)}{\sqrt{\sigma_i^2 \sigma_j^2}} \right], \text{ with} \quad (9.5)$$

$$\begin{cases} m_i = \sum_{i,j=1}^N i(P_d(i,j)) \\ m_j = \sum_{i,j=1}^N j(P_d(i,j)) \end{cases} \quad (9.6)$$

and

$$\begin{cases} \sigma_i^2 = \sum_{i,j=1}^N P_d(i,j)(i-m_i)^2 \\ \sigma_j^2 = \sum_{i,j=1}^N P_d(i,j)(j-m_j)^2 \end{cases}. \quad (9.7)$$

5. **Homogeneity:** It returns a value corresponding to the closeness of the distribution of elements within the GLCM to the GLCM diagonal. The next equation states this coefficient:

$$\text{HOM} = \sum_i \sum_j \frac{P_d(i,j)}{1+(i-j)^2}. \quad (9.8)$$

All these attributes are defined for a displacement value d , which is very important [11] with regard to obtaining a significant result. Thereby, for each pixel, we define a vector of attributes v_i (energy, entropy, and so on).

9.2.3 Databases

The authors have handled images downloaded from [22] and a sample of blood cells. The results discussed in the next hand apply to the image from Fig. 9.3.

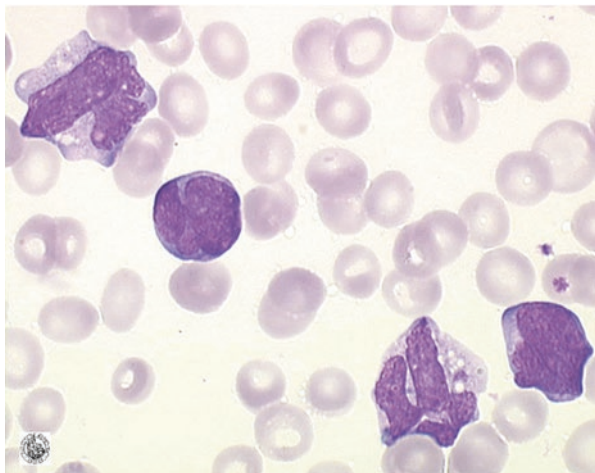


Fig. 9.3 Example of an input picture to the Haralick's FE process

Table 9.1 Representation of an 8×8 image window

204	210	219	226	220	205	191	184
209	209	208	206	205	206	205	202
198	205	205	198	198	204	201	192
185	203	209	196	189	193	189	177
179	202	209	190	178	185	189	182
168	193	206	194	184	186	185	175
176	191	197	189	181	176	161	143
205	199	184	166	158	154	137	118

9.3 Results and Discussion

The authors have treated the parameters of the co-occurrence matrix via Matlab R2012aa environment and tested on a typical PC Pentium (R) Dual Core CPU Processor 2.20 GHz with 4 GB RAM.

The analysis window size must fulfil two conflicting criteria, viz., be as small as possible to lessen the risk of blending different textures while the largest possible to extract statistics quite robust and significant. After several measures, the choice for the size of the window is 8×8 . First, the GLCM representation for each processed image pixel is below (Tables 9.1, 9.2, and 9.3):

The GLCM calculation for the previous image window occurs as in the following table:

The GLCM analysis results demonstrate that the summation of the coefficients $p(i, j)$ for any block of the same image remains equal. In this case, $S_p = \sum P(i, j) = 56$. The computation of the five criteria for 8×8 blocks with a displacement = 1 give the results below, where the following figures show the distribution of the results of five parameters under the form histograms (Figs. 9.4, 9.5, 9.6, 9.7, and 9.8).

Table 9.2 Calculates GLCM (8 x 8)

0	0	0	0	0	0	0	0
0	0	0	0	0	0	0	0
0	0	0	0	0	0	0	0
0	0	0	0	0	0	0	0
0	0	0	1	3	0	0	0
0	0	0	0	2	22	5	0
0	0	0	0	0	7	16	0
0	0	0	0	0	0	0	0

Table 9.3 Statistical comparison by texture indices of second order

	Healthy cell	Cancerous cell
Mean energy	1803.74	0
Mean contrast	3.46	4.26
Mean entropy	59.91	203.27
Mean correlation	0.13	0.54
Mean homogeneity	10.48	54.14

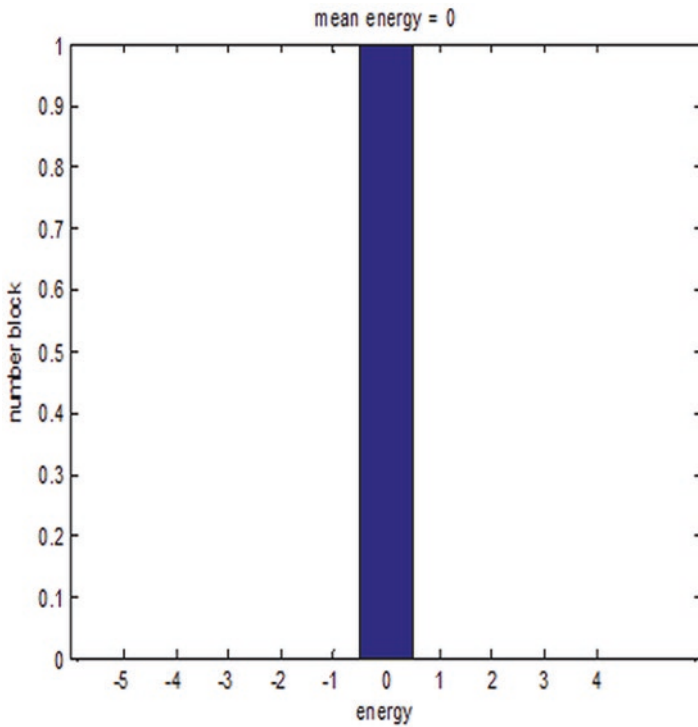


Fig. 9.4 Histogram of energy

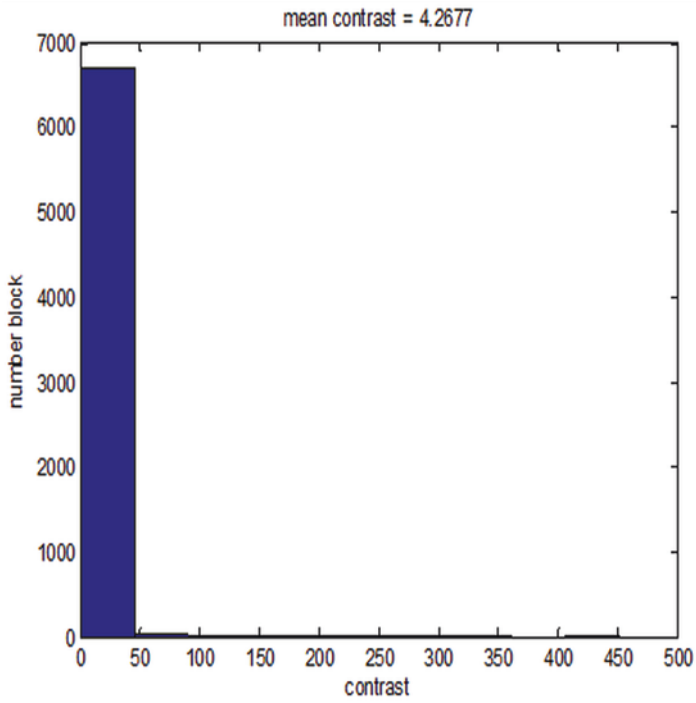


Fig. 9.5 Histogram of contrast

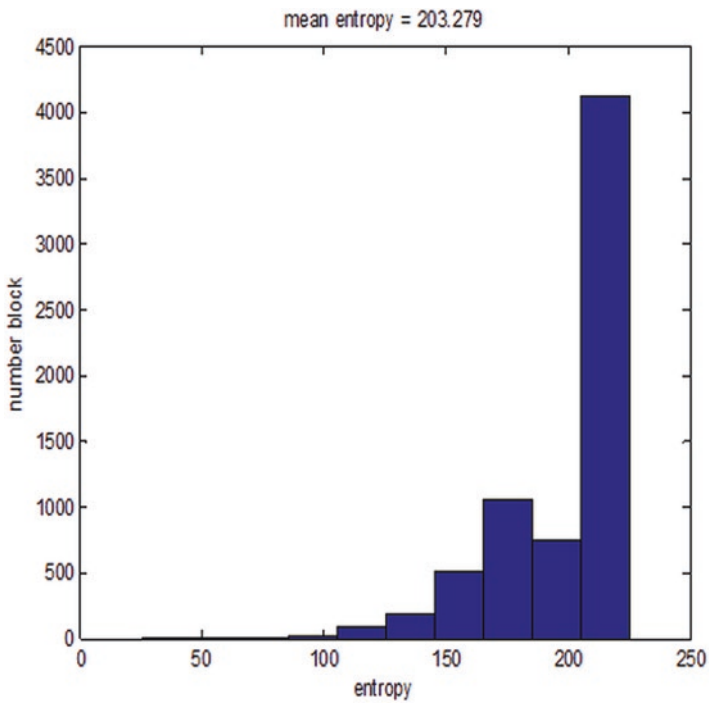


Fig. 9.6 Histogram of entropy

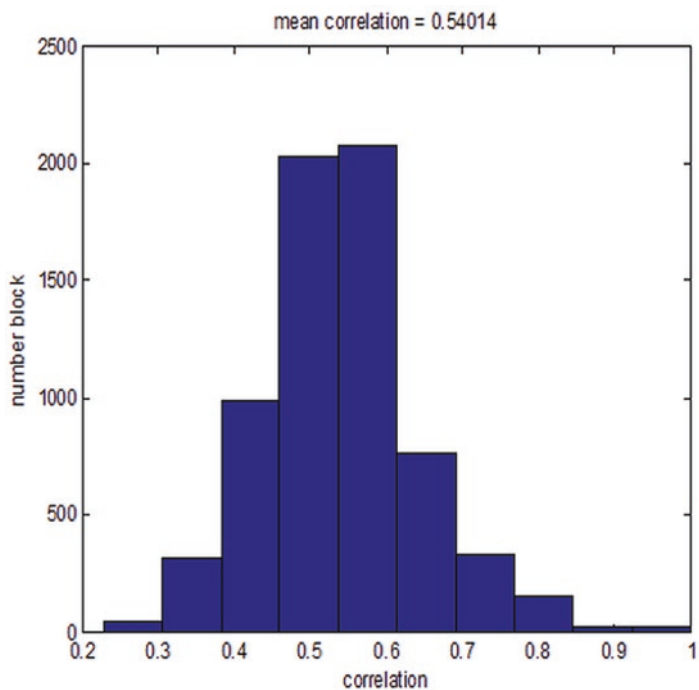


Fig. 9.7 Histogram of correlation

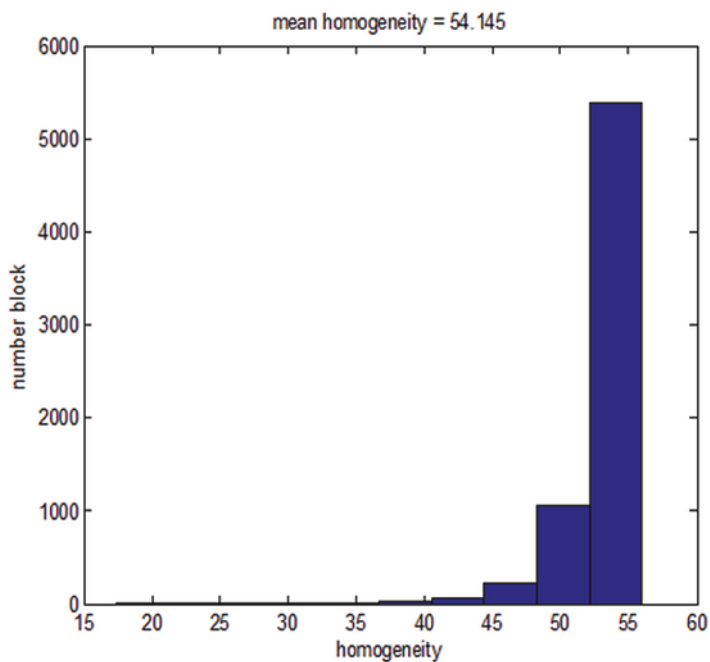


Fig. 9.8 Histogram of homogeneity

The results above relying on the representation of five parameters of the GLCM form histograms. The visual quality of the bio-image textures from the database improved a lot based on the evolution of pixel-based on gray levels for each index calculation. A table with a comparison between a healthy cell and other cancerous for abnormal regions detection confirms the effectiveness of the parameters' choice using the co-occurrence matrix as calculated before to form the histograms:

9.4 Conclusion

This work applies a method to make a bio-image textural analysis successfully and accurately, relying on a mathematical basis. The resultant feature vector has five entries: energy (ENE), contrast (CST), entropy (ENT), correlation (COR), and homogeneity (HOM). This software scheme employs a higher-order GLCM statistical method hinging essentially on the study of the relations between each pixel and its neighbors (to spot the fine textures) and the spatial distribution of the gray levels. This article only offers statistical information on the images, which is, therefore, considered as a higher order strategy. This happens because the methods allow quantifying nonvisible evidence (data that are incomprehensible by the humans) and, thus, augmenting the opportunity of interpreting more of the image data and in particular of the textured images. Although the GLCM scheme gives good results, it demands too many calculations. Each calculation is already relatively heavy. The results obtained are allowed to enrich the diagnostic of data thanks to the calculated parameters. The authors also suggest a hardware implementation. The FPGA technology speeds up the computation of features to attain both high performance and flexibility in fast computation in real-time processing [23]. Even though working with a reduced set of descriptors speeds up the diagnosis, in the future, a suspicious result can be directed to other stages of processing to additional analysis. Since the recommended method is simple and the feature vector contains only five entries, the algorithm has low dimensionality, and it is more proper for hardware implementations than some sophisticated deep learning realizations [24–31].

References

1. V.V. Estrela, O. Saotome, H.J. Loschi, D.J. Hemanth, W.S. Farfan, R.J. Aroma, C. Saravanan, E.G.H. Grata, Emergency response cyber-physical framework for landslide avoidance with sustainable electronics. *Technologies* **6**, 42 (2018). <https://doi.org/10.3390/technologies6020042>
2. C.E.V. Marinho, V.V. Estrela, H.J. Loschi, N. Razmjoooy, A.E. Herrmann, Y. Thiagarajan, M.P. Vishnevski, A.C.B. Monteiro, R.P. França, Y. Iano, A model for medical staff idleness minimization, in *Proceedings of the 4th Brazilian Technology Symposium (BTSym'18). BTSym 2018. Smart Innovation, Systems and Technologies*, ed. by Y. Iano, R. Arthur, O. Saotome, V. Vieira Estrela, H. Loschi, vol. 140, (Springer, Cham, 2019)

3. A.C.B. Monteiro, Y. Iano, R.P. França, R. Arthur, V. Vieira Estrela, V.V. Estrela, A comparative study between methodologies based on the Hough transform and Watershed transform on the blood cell count, in *Proceedings of the 4th Brazilian Technology Symposium (BTSym'18). BTSym 2018. Smart Innovation, Systems and Technologies*, ed. by Y. Iano, R. Arthur, O. Saotome, V. Vieira Estrela, H. Loschi, vol. 140, (Springer, Cham, 2019)
4. A.E. Herrmann, V.V. Estrela, Content-based image retrieval (CBIR) in remote clinical diagnosis and healthcare, in *Encyclopedia of E-Health and Telemedicine*, ed. by M. M. Cruz-Cunha, I. M. Miranda, R. Martinho, R. Rijo, (IGI Global, Hershey, 2016). <https://doi.org/10.4018/978-1-4666-9978-6.ch039>
5. S. Alférez, A. Merino, L. Bigorra, J. Rodellar, Characterization and automatic screening of reactive and abnormal neoplastic B lymphoid cells from peripheral blood. *Int. J. Lab. Hematol.* **38**(2), 209–219 (2016)
6. G.K. Chadha, A. Srivastava, A. Singh, R. Gupta, D. Singla, An automated method for counting red blood cells using image processing. *Procedia Computer Science* **167**, 769–778 (2020)
7. L. Puigví, A. Merino, S. Alférez, A. Acevedo, J. Rodellar, New quantitative features for the morphological differentiation of abnormal lymphoid cell images from peripheral blood. *J. Clin. Pathol.* **70**, 1038–1048 (2017)
8. X. Wu, M. Sikiö, H. Pertovaara, R. Järvenpää, H. Eskola, P. Dastidar, P. Kellokumpu-Lehtinen, Differentiation of diffuse large B-cell lymphoma from follicular lymphoma using texture analysis on conventional MR images at 3.0 Tesla. *Acad. Radiol.* **23**(60), 696–703 (2016)
9. M.D. Joshi, A.H. Karode, S.R. Suralkar, White blood cells segmentation and classification to detect acute leukemia. *Int. J. Emerg. Trends Technol. Comput. Sci.* **2**(3), 147–151 (2013)
10. D. Warude, R. Singh, Automatic detection method of leukaemia by using segmentation method. *Int. J. Adv. Res. Electron. Commun. Eng.* **5**(3), 495–498 (2016)
11. P. Suapang, M. Thongyoun, S. Chivapreecha, Automatic leukocyte classification based on microscope images, in *Proceedings of the 4th International Conference on Industrial Application Engineering* (2016), pp. 226–233
12. R.M. Haralick, K. Shanmugam, I. Dinstein, Textural features for image classification. *IEEE Trans. Syst. Man Cybern.* **3**(6), 610–621 (1973)
13. A. Merino, L. Puigví, L. Boldú, S. Alférez, J. Rodellar, Optimizing morphology through blood cell image analysis. *Int. J. Lab. Hematol.* **40**(Suppl 1), 54–61 (2018)
14. W. Xiao-ka, Intravascular large B-cell lymphoma with skin: a clinicopathologic analysis and review of literature. *Chin. J. Diagn. Pathol.* Vol. 32, N° 6, pp. 513–520 (2015)
15. S. Mishra, A.P. Deshmukh, Detection of leukemia using Matlab. *Int. J. Adv. Res. Electron. Commun. Eng.* **4**(2), 394–398 (2015)
16. A. Bouzid-Daho, M. Boughazi, B. Senouci, Multispectral images segmentation for biomedical applications diagnosis: K-means oriented approach, in *Proceedings of 2nd IEEE International Conference on Bio-engineering for Smart Technologies (IEEE BioSMART 2017)* (2017), pp. 1–5
17. A. Chaddad, C. Tanougast, A. Dandache, A. Bouridane, Classification of cancer cells based on morphological features from segmented multispectral bio-images, in *Proceedings of 4th International Conference on Biomedical Electronics and Biomedical Informatics* (2011), pp. 92–97
18. A. Bouzid-Daho, M. Boughazi, E. Petit, Detection of abnormal blood cells by segmentation and classification. *Int. J. Med. Eng. Inform.* **11**(1), 57–70 (2019) B.S. Dhruv, N. Mittal, M. Modi, Study of Haralick's and GLCM texture analysis on 3D medical images. *Int. J. Neurosci.* **129**, 350–362 (2019)
19. S.B. Tasdemir, K. Tasdemir, Z. Aydın, ROI detection in mammogram images using wavelet-based Haralick and HOG features, in *Proceedings of 17th IEEE International Conference on Machine Learning and Applications (ICMLA)* (2018), pp. 105–109
20. D. Baggett, M. Nakaya, M. McAuliffe, T.P. Yamaguchi, S. Lockett, Whole cell segmentation in solid tissue sections. *Int. Soc. Anal. Cytol. Cytometry.* **67A**, 137–143 (2005)

21. R. Hoofman, E.J. Benz, L.E. Silberstein, H. Heslop, J. Weitz, J. Anastasi, *Hematology: Basic Principles and Practice*, 6th edn. (Elsevier, Canada, 2013)
22. <http://hematocell.univ-angers.fr/index.php/banque-images> (Consulted: 10/01/2020)
23. A. Bouzid-Daho, M. Boughazi, C. Tanougast, O.B. Medjahed, Textural analysis of bio-images for aid in the detection of abnormal blood cells. *Int. J. Biomed. Eng. Technol.* **25**(1), 1–13 (2017)
24. N. Razmjooy, V.V. Estrela, *Applications of Image Processing and Soft Computing Systems in Agriculture* (IGI Global, Hershey, 2019). <https://doi.org/10.4018/978-1-5225-8027-0>
25. Z. Gu, J. Cheng, H. Fu, K. Zhou, H. Hao, Y. Zhao, T. Zhang, S. Gao, J. Liu, CE-Net: context encoder network for 2D medical image segmentation. *IEEE Trans. Med. Imaging* **38**, 2281–2292 (2019)
26. A. Deshpande, P. Patavardhan, Super resolution and recognition of long range captured multi-frame iris images. *IET Biom.* **6**, 360–368 (2017)
27. A. Deshpande, P. Patavardhan, Multi-frame super-resolution for long range captured iris polar image. *IET Biom.* **6**, 108–116 (2017)
28. R.J. Aroma, M. Kurian, A semantic web: Intelligence in information retrieval, in *2013 IEEE International Conference ON Emerging Trends in Computing, Communication and Nanotechnology (ICECCN)* (2013), pp. 203–206
29. R.J. Aroma, K. Raimond, A novel two-tier paradigm for labeling water bodies in supervised satellite image classification, in *2017 International Conference on Signal Processing and Communication (ICSPC)* (2017), pp. 384–388
30. S. Somasundaram, R. Gobinath, Current trends on deep learning models for brain tumor segmentation and detection – a review, in *Proceedings of 2019 International Conference on Machine Learning, Big Data, Cloud and Parallel Computing (COMITCon)* (2019), pp. 217–221
31. N. Dang, V. Saraf, A. Khanna, D. Gupta, T.H. Sheikh, *Malaria Detection on Giemsa-Stained Blood Smears Using Deep Learning and Feature Extraction* (2020) International Conference on Innovative Computing and Communications, pp. 789–803

Chapter 10

Artificial Intelligence, Blockchain, and Internet of Medical Things: New Technologies in Detecting, Preventing, and Controlling of Emergent Diseases



Akanksha Sharma , Rishabha Malviya , Rajendra Awasthi ,
and Pramod Kumar Sharma 

10.1 Introduction

Technologies such as artificial intelligence (AI), blockchain, and the Internet of Medical Things (IoMT) hold an unprecedented potential in the healthcare system when integrated for a specific disease condition. Together, these technologies impact the healthcare system when it comes to detecting, preventing, and controlling emerging diseases. This chapter will discuss the role of AI, blockchain, and the IoMT in the healthcare system for personalized medicine. Each technology has its advantages, limitations, challenges, and projections with special emphasis on the healthcare sector. Each of these technologies decreases the expenses of medication and save the time of both healthcare providers and patients. These technologies can also help in drug discovery and drug delivery and thus can be used in research and clinical trials. E-health services can be provided by using different mobile applications. It is expected that in the coming years, these technologies will deliver better health services and theragnostics (treatment and diagnostics) of various diseases. Figure 10.1 illustrates a schematic diagram of the new technologies used in the healthcare system.

A. Sharma · R. Malviya (✉) · P. K. Sharma
Department of Pharmacy, School of Medical and Allied Sciences, Galgotias University,
Greater Noida, Gautam Buddha Nagar, Uttar Pradesh, India
e-mail: rishabha.malviya@galgotiasuniversity.edu.in

R. Awasthi (✉)
Amity Institute of Pharmacy, Amity University Uttar Pradesh, Noida, Uttar Pradesh, India
e-mail: rawasthi1@amity.edu



Fig. 10.1 Schematic presentation of new technologies used in the healthcare system

10.1.1 Revolutions in Healthcare

Major healthcare revolutions are divided into four distinct stages, namely, Health 1.0, 2.0, 3.0, and 4.0. Health 1.0 was the old approach healthcare system. In Health 1.0, the patients read about the specific medical conditions or discuss it with their friends or family members to collect the information. Health 1.0 permitted only one doctor at one hospital to observe the patient record in that hospital. Health 2.0 was introduced in the mid-2000s. It permitted doctors from two or more hospitals to keep the patient record. In Health 2.0, patients can also access their health data. Healthcare 3.0 started in 2017 to overcome the limitations of Health 2.0. Health 3.0 compiled the data of all patients in the form of collective health record. Each individual has its full access permission. An individual is also permitted to add extra information through their account. Health 4.0 is the ultimate solution. It was derived Industry 4.0 concept. Health 4.0 is expected to overcome socioeconomic challenges by providing economic opportunities. Figure 10.2 illustrates consumer-centric care, which can be used in developing and implementing new healthcare technologies [1].

10.1.2 Personalized Medicine

Personalized medicine is the most widely and rapidly evolving healthcare area that contains specific clinical, genomic, genetic, and environmental details of each individual. It is an integrated, organized, and evidence-based approach used for individualizing patient treatment. In personalized medicine, a molecular understanding of the disease enhances preventive healthcare strategies. The predominant goal of personalized medicine is to improve medical treatment and outcomes for each client, resulting in unparalleled patient care customization [3].

Personalized medicine can connect the molecular and clinical profiles of the patient to enable the physicians to make the right decisions about patient care. Personalized medicine faces various changes in pharmaceutical and medical industries, which impacts on other aspects of society. More significantly, this would benefit the person whose safety is at stake [4].

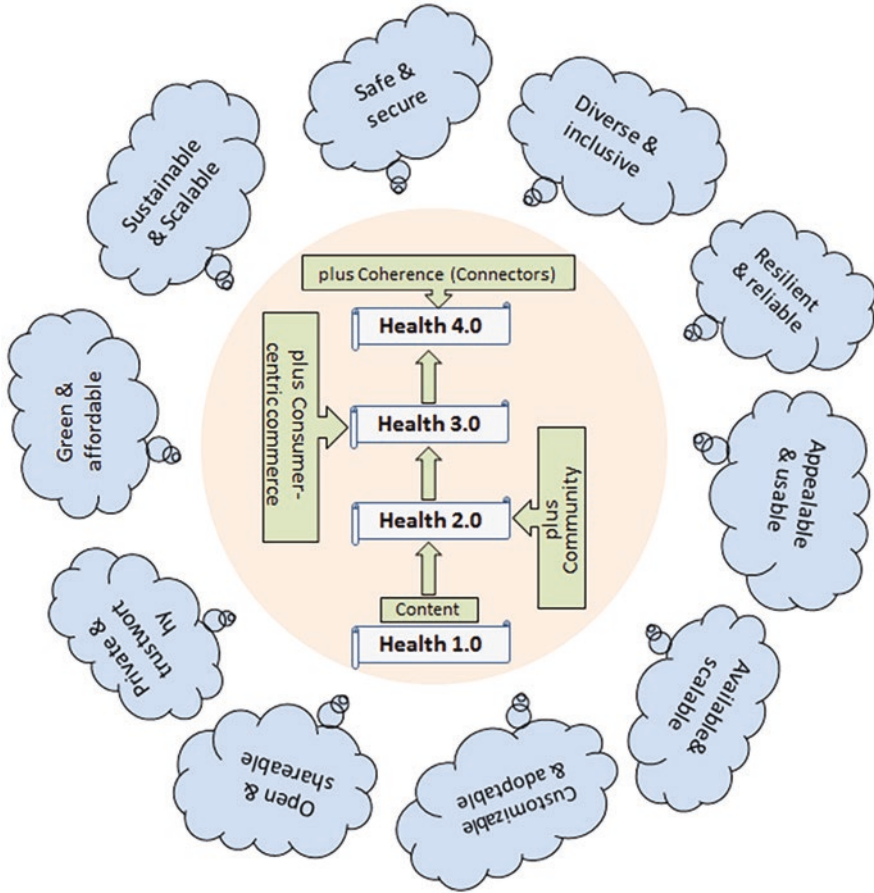


Fig. 10.2 Consumer-centric care in developing and implementing new healthcare technologies [2]

The success of personalized medicine depends on appropriate diagnostic tests that help in identifying patients for targeted therapies. Clinicians also often use diagnostics to assess the disease, such as how human breast cancer associated with overexpress the type 2 human epidermal growth factor receptor (HER2). It is associated with worse prognosis, but often predicts a better response to trastuzumab treatment. Along with the drug, test for HER2 is also recommended so that clinicians can better guide and care for their patients [5]. Personalized medicine relies on the use of multidisciplinary healthcare teams to encourage safety and well-being, patient awareness and satisfaction, custom disease prevention, diagnosis, and treatment [6].

Personalized medicine is not just about recognizing appropriate medications. Diagnostic tests also help to doctors in accessing the aggressiveness of tumor for certain cancers and eventually decide whether to conduct surgery or use less invasive

therapies. Clinical trials have shown that if a prostate cancer lacks the genes that cause aggressive cancer, the prostate gland may remain stable for a long time. Understanding of drug metabolism is essential for personalized medicine. It provides a piece of more accurate and detailed information about why people react to the same medication differently. Around 30 different enzymes, each composed of a single gene or group of genes, regulate how drugs are metabolized in the human body. A slight difference or absence of these genes will affect the therapeutic dosage without causing any adverse reaction [7].

10.1.3 Inpatient and Outpatient Personalized Care Within the Health 4.0

Inpatient medication is recommended for better management and care of patients with chronic diseases. Inpatient care specialists have played a significant role in urban hospitals in Great Britain and Canada. The purpose of such specialties has now been developed for areas where managed care predominates like San Francisco [8]. It has been observed that patients who receive structured inpatient treatment in a stroke unit are more likely to be cured and discharged from the hospital after 1 year of treatment. The organized stroke unit care in a hospital is provided by healthcare providers who are specialized in treating stroke patients [9]. Inpatient services are costly when compared to outpatient services to deliver healthcare. The urgent care clinics can also decrease the use of these high-cost inpatient services with sensitive ambulatory conditions [10].

The outpatient clinical decision support system induces a significant impact on critical aspects of diabetes care. The recent clinical decision support systems for diabetes care can be improved following prioritizing care guidelines, communicating treatment-related information to the patients. These systems are used for the planning and management of cases and incorporation of patient-reported data from remote devices into clinical decision interfaces and algorithms.

The optimal outpatient clinical decision support system recognizes the subset of patients with a disease like diabetes. It also recognizes the patient-specific non-target clinical domains; recommend patient-specific evidence-based treatment [11]. Outpatient therapy services include occupational therapy, physical therapy, and speech-language pathology. Outpatient services must be provided in terms of intensity, frequency, and duration [12].

Outpatient care for the child with a life-threatening illness is more supportive than treatment at other locations. Children spend more time in the company of familiar parents rather than the office of a pediatrician or a medical clinic where they have been cared for over time. Good communication within the child and clinicians will also help to establish a positive relationship that will continue during the child palliative care [13].

10.2 Artificial Intelligence in Healthcare

AI advances toward imitating the features of human intelligence. AI is applied in the healthcare sectors for patient administration, patient monitoring, healthcare interventions, diagnostics, and clinical decision support [14].

AI has been used in the treatment and diagnosis of diseases since 1970, with the advent of the MYCIN developed by Stanford University for the diagnosis of blood-borne bacterial infections. More recently, IBM's Watson has utilized a combination of machine learning and natural language processing abilities. AI-based methods can diagnose and treat disease with greater accuracy than humans. AI radiological image analysis involves various types of images, such as retinal scanning or genomic-based precision medicine [15].

DeepMind technology is a British AI company making a practical difference to patients, doctors, and nurses. It supports the National Health Service (NHS) and other healthcare systems. The FDNA startup is applying Face2Gene in facial analysis, AI, and genomic insights to improve the diagnoses and treatment of rare diseases. AI uses different algorithms to collect data from wearable sensors, such as fitness trackers. The Russian company Botkin.AI uses AI to handle medical images from computed tomography (CT) and magnetic resonance imaging (MRI) [16].

AI has many applications in the medical field, along with widespread use of EHR and rapid developments in various areas of life science such as neuroscience. In 2014, IBM announced the TrueNorth chip, which has the potential to revolutionize the computer industry by integrating brain-like capability into devices. China established its Next-Generation AI development in July 2017 to promote research and development. AI can provide active guidance to physicians in making clinical decisions. This also aids prediction, pathological investigations, imaging, and treatments. The Food and Drug Administration (FDA) of the United States granted marketing permission in 2018 to the first AI-based diagnostic system, namely, IDx-DR. It helps in detecting diabetic retinopathy and helps in deciding an AI algorithm after analyzing images of [17]. The Google AI system could improve breast cancer detection and can minimize the chances of false results by 20% in mammograms, which are commonly missed by radiologists.

10.2.1 *Role of Artificial Intelligence for Personalized Medical Application*

Personalized medicines is a new healthcare model used for the prevention and treatment of diseases based on individual conditions, including psychosocial characteristics, genetic information, environment, and lifestyles. This produces a vast amount of data that can be analyzed and integrated with AI technology. Deep Variant is a highly accurate genomic analysis system developed by Google Inc. It is based on deep neural network technology. AI technology has been employed to improve the quality of

radiological medical diagnosis due to a large number of medical image data. AI may play a vital role in stroke management through an individualized plan [18].

Personalized medicine uses practice and medical decisions to deliver customized healthcare services. The major function of personalized medicine is to predict the possibility of an individual developing a disease, achieve an accurate diagnosis, and optimize the best treatment available. The technology used by doctors, pharmacists, and nurses can deliver an efficient healthcare service as opposed to traditional techniques [19].

The broad availability of genetic information offered by next-generation sequencing technologies in the field of cancer genomics and rapid growth in the biomedical field has led to the advent of the big data era. Integration of AI approaches such as natural language processing, deep learning, and machine learning can quickly solve all the challenges of scalability and high dimensionality of data. It is also integrated into the transformation of big data into clinically actionable knowledge and become the infrastructure of personalized medicine. Personalized medicine tackles diseases by tailoring treatments based on the genomics, lifestyle, and environmental characteristics of each patient. Personalized medicine and the advancement of next-generation sequencing technologies are gaining popularity in genomic profiling of the patient for risk prediction, disease diagnosis, and targeted therapies [20, 21].

The Siri iOS application can appropriately direct an individual to the requested destination by identifying the current individual location and comparing it with the Google Maps database. An AI application in cardiac imaging can help physicians in interpreting cardiac images correctly. The physician can interpret results by comparing tomographic images with large age and sex matches. This can be done using a normal database that is specific for radiotracer and camera [22].

AI uses sophisticated algorithms to “learn” features from a large volume of data, which helps to obtain observations to assist clinical practice. An AI system can assist doctors by supplying up-to-date information from textbooks, journals, and clinical practices. An AI system can:

1. Reduce therapeutic and/or diagnostic errors that commonly occur in human clinical practice
2. Extract practical information from a large population to help in making real-time inferences for health risk alert/management and health outcome prediction [23]

AI systems execute planning strategies in collaboration with other systems to solve complex problems in a new environment. Planning strategies also help in the operational efficiency of AI and system by taking the current input state and executing different logic and rule-based algorithms to reach predefined goals [24].

10.2.2 Advantages of Artificial Intelligence

The use of AI in setting or building of personalized medicine is vital in terms of the accuracy and precision of disease recognition, drug administration, and treatment. The use of computers in hospitals and clinics to record medical activities or the use

of EHR systems nowadays provides medical knowledge and data that can be used as a standard to enhance medical service delivery [25]. AI applications typically handle a large amount of data for better decision-making. However, centralized data storage using data centers, clouds, and clusters constitute a significant constriction while developing a highly secure and privacy-preserving AI system [24, 26].

Machines with AI do not take rest, thus overcoming the inherent disadvantage of fatigue in humans. AI can also reduce the wastage of time throughout learning and passing knowledge to other humans [27]. It is used in the assessment of the risk of disease onset and in estimating treatment success before initiation. AI used to manage or reduce treatment complications. It helps to assist with patient care during active treatment. AI research focuses on the pathology or mechanism for the ideal treatment of disease [28].

AI uses sophisticated algorithms to learn features from the big data of healthcare records for interpreting results in clinical practice. AI can assist physicians by providing updated medical information from different sources such as textbooks, journals, and clinical practices to inform proper patient care. AI systems can also minimize common diagnostic and therapeutic errors in human clinical practices [23].

Among the healthcare data, images obtained from computed tomography, X-ray, magnetic resonance imaging, and ultrasound examinations also provide the most potential information for research and clinical applications. These data help to

- (a) Improve the automatic detection of diseases
- (b) Minimize human errors
- (c) Create study protocols
- (d) Ameliorate image quality
- (e) Decrease radiation dose
- (f) Lessen the MRI scanner time
- (g) Optimize staffing and scanner utilization

Thereby, these facts reduce costs and make expensive and time-consuming screening programs feasible in countries unable to afford those procedures [29]. Figure 10.3 shows the schematic presentation of applications of AI in healthcare.

10.2.3 Limitations of Artificial Intelligence

Data sparsity from highly dimensional and heterogeneous data impose a significant difficulty in integrative analyses. The impactful solution is not obtained due to the difficulty in getting statistically significant data from the patient outcome. Patient outcome data are personal health information that must be protected under the guidelines of the Health Insurance Portability and Accountability Act 1996 in the United States and General Data Protection Regulation in Europe. Regulation and sharing of data cannot be made lightly due to the critical security considerations in protecting sensitive data from being compromised [20, 30]. AI shows a lack of creativity in the responses. It may not be able to explain the logic and reasoning behind certain decisions. An AI system cannot predict the situation under certain conditions

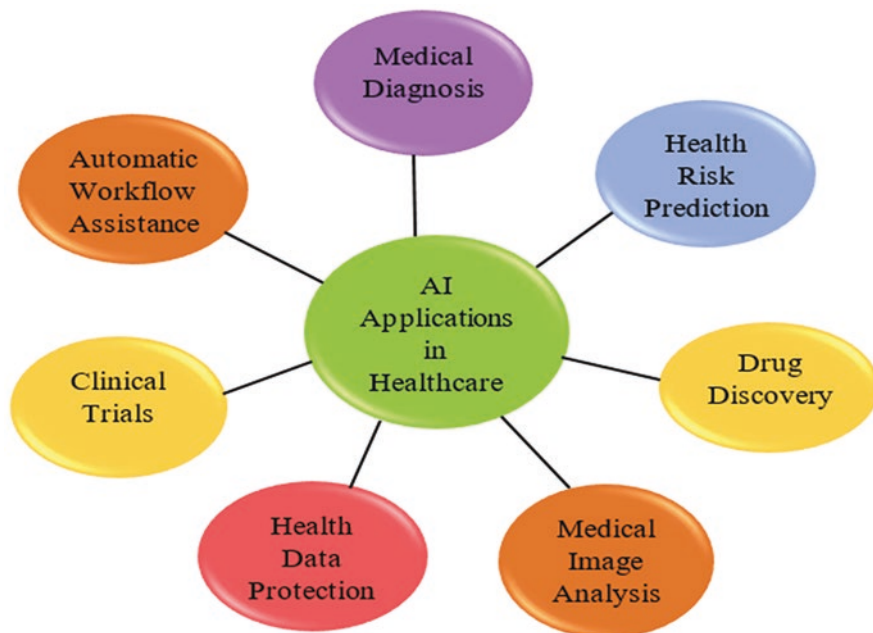


Fig. 10.3 Schematic presentation of applications of AI in the healthcare sector

where the solution to a particular problem is not available. Any malfunctioning can produce wrong solutions and since it cannot explain the reasoning behind its answer. Lack of common sense in the argument can also cause significant problems. It can cause mass-scale destruction if given in the wrong hands [27, 31].

AI algorithms are unable to perform a holistic approach to clinical scenarios [32]. AI may also cause bias due to the unwitting result from its decision-making criteria [33]. AI algorithms are essential to perform a holistic approach to clinical scenarios. These cannot take into the social and psychological aspects of human nature, which are also taken into account by a professional physician [34, 35]. In the clinical context, AI will be required for the widespread adoption of this technology [36]. The definitive collection of healthcare data depends on the consistency of data reporting and the use of electronic data records to avoid noisy data. There is a lag in the adoption of solely electronic medical records in emergency departments in Canada and the United States [37, 38].

10.2.4 Challenges and Future Perspective of Artificial Intelligence in Healthcare

The Center for Data Innovation regulates data sharing, data protection, and international standardization. The digital health program should ensure the safety and beneficial impact of AI on healthcare [20]. In dental science, the application of clinical

decision support systems is slow and limited due to the lack of formal evaluation of the systems, cost, challenges in developing standard representations, and practitioner doubt about the feasibility and value of clinical decision support systems. An information technology application for dental practice continues to create and contribute to reduce the mortality and morbidity of oral and maxillofacial diseases and, in turn, impact patient care [36].

AI techniques have sent enormous waves across the healthcare system, even inflame an active discussion of whether AI doctors will eventually replace human physicians in the future. Machines may not replace human physicians in the foreseeable short-term future. Still, AI can assist physicians in making better clinical decisions or even replacing human judgment in certain healthcare specialties (e.g., radiology). Followed by relevant clinical questions, powerful AI techniques can unlock the clinically relevant information hidden in a massive amount of data, which in turn can boost clinical decision-making [23, 37]. AI techniques in stroke imaging could markedly change the milieu during the diagnosis and management of stroke. Automated stroke diagnosis may be prevalent where fast thrombolysis and prehospital thrombolysis are recommended. Prediction of prognosis with AI techniques is widely used in stroke management. A well-constructed and extensive imaging database system is the fundamental prerequisite for the success of AI techniques in stroke-imaging analysis. This imaging database should be integrated and interpreted along with other large databases containing clinical and biological data [38, 39].

The AI use for better understanding and treating non-small cell lung cancer is proliferating. The execution of algorithms in clinical practice still faces hurdles. The AI guidelines and standards remain to be established. The FDA is evaluating the use of algorithms in clinical practices. The management of electronic health records can authorize patients by enabling access to their data. The recent fragmented, decentralized state of health records raises challenges for the implementation of algorithms in healthcare [40, 41].

10.3 Blockchain in Healthcare

Blockchain is a chain that covers information and maintains trust between individuals irrespective of the condition of how far they are. Scholars and scientists are interested in it for a broad range of domains in healthcare applications. Blockchain technology is used as Distributed Ledger Technology (DLT) for a peer-to-peer network for digital data transactions that may be privately or publicly distributed to all users, allowing storage of any type validly and reliably. The central concept of blockchain is the smart contract, which is a legally binding policy that consists of a customizable set of rules under which different parties agree to interact with each other in the form of decentralized automation [42]. Blockchain improves interoperability. Blockchain technology could develop patient-driven interoperability through the management of digital access rules. Blockchain enables a centralized and shared mechanism for the control of authorization and authentication of data [43].

Blockchain possesses various properties like decentralization, immutability, and transparency. It helps to potentially address issues in healthcare, including incomplete records at the point of care and demanding access to the patient's health information. An effective and efficient healthcare system requires interoperability, which allows software applications and technology platforms to communicate seamlessly and securely, data exchange, and use the exchanged data across health organizations and application vendors. Unfortunately, today's healthcare system suffers from fragmented and siloed data, delayed communications, and disparate workflow tools caused by the lack of interoperability. Blockchain provides the opportunity to enable access to complete, longitudinal, and tamper-aware medical records that are stored in fragmented systems in a secure and pseudo-anonymous fashion [44].

10.3.1 Role of Blockchain for Personalized Medical Application

Blockchain relies on open-source software and commodity hardware. These components facilitate faster and easier interoperability between systems and can efficiently scale to handle larger volumes of data and assisted the blockchain users. The architecture has built-in fault tolerance and disaster recovery. Data encryption and cryptography technologies are widely used and accepted as industry standards. In healthcare, blockchain is developed as open-source software [45, 46].

Blockchain technology has the potential to address the interoperability challenges present in current healthcare information technology systems and to be a technical standard that enables individuals, healthcare providers, healthcare entities, and medical researchers to securely share electronic health data. All medical data would be stored off-blockchain in a data repository called a data lake. Data lakes are a highly scalable tool for health research. They would be used for a variety of analyses, including mining for factors that affect outcomes, determine optimum treatment options based on genetic markers, and identify elements that influence preventative medicine to the key-value stores. Data lakes support interactive queries, text mining, text analytics, and machine learning. The information stored in a data lake would be digitally signed and encrypted to ensure the authenticity and privacy of information [47].

Blockchain is a distributed database that uses state machine replication with atomic changes to the database [48]. Modern society demands new tools such as distributed ledger and smart contracts for sharing data between patients and healthcare professionals by providing them controlled access over data and allowing more intelligent cooperation. In this situation, utilizing blockchain technology can resolve integrity, data privacy, security, and fraud issues. It can also increase patient autonomy and provide better service for patients and clinicians [49]. Blockchain technologies can [50]:

1. Optimize the pharmaceutical supply chain by improving traceability, transparency, and immutability
2. Enhance data sharing for medical research and primary care

Blockchain technology has gained considerable attention in the health management domain. It has been utilized in hospital activities, such as in maintaining medical records, disease surveillance, and insurance bills. The application of blockchain technology in the management of electronic health records is noteworthy, where vast information can be processed effectively. Its unique features can revolutionize the health databases and helps in improving access to medical records, archives of scanned images, prescriptions, and surveillance systems. Also, there can be built-in authentication controls that can minimize the risk of data theft [51].

10.3.2 Advantages of Blockchain

Blockchain technology offers many benefits for healthcare information technology. It is reliable and robust under fast-changing conditions that cannot be matched by closed, proprietary software. Open-source solutions also drive innovations in the applications market. Health providers and individuals would benefit from the full range of application choices and could select the option that can match their specific requirements. A blockchain runs on widely used and reliable commodity hardware. Commodity hardware provides a large amount of useful computation at a low cost. The hardware can employ open standards manufactured by multiple vendors. It is the most efficient and cost-effective technique for health and genomic research [45, 52].

Blockchain technology is a decentralized peer-to-peer architecture. Members in a distributed network record digital transactions into a shared ledger. Each member stores an identical copy of the shared ledger and changes it to the shared ledger, which is reflected in all copies. Blockchain technology offers many advantages to medical researchers, healthcare providers, caregivers, and individuals. Creation of a single storage location for all health data, tracking personalized data in real-time, and the security to set data access permissions at a granular level would fulfill the purpose of research and personalized medicine [47, 53]. The great advantage of blockchain technology in the healthcare field is that it allows the development of a stable and secure data set with which users can interact through various types of transactions. This environment supports the entry and operation of clinical data without compromising other sensitive data. The entire network in blockchain technology is decentralized, which is maintained by users. The blockchain code is open-source software and can be modified, used, and revised by its users [54].

Blockchain and critical public infrastructure develop patient-centric access control for electronic medical records, which is capable of providing security and privacy. The critical public infrastructure is used in some countries like Brazil to

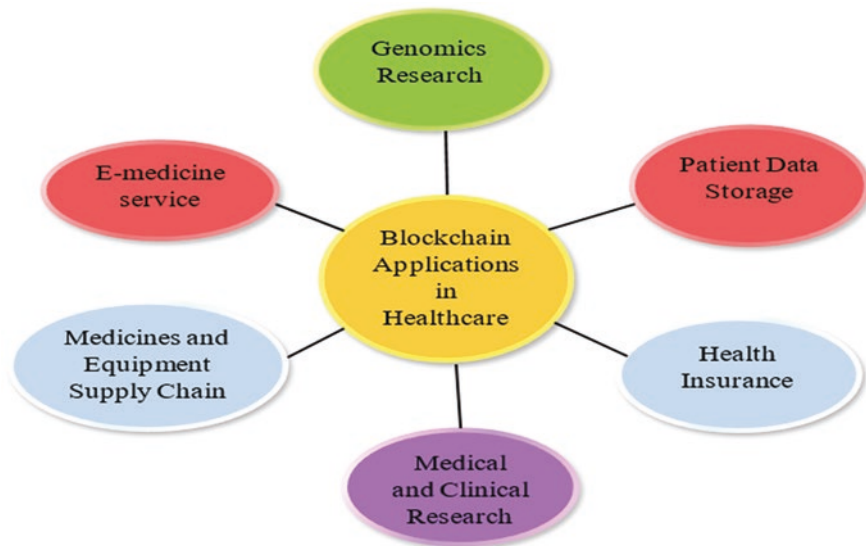


Fig. 10.4 Applications of blockchain in the healthcare sector

achieve a truly distributed electronic medical record having a high level of privacy for the patient health records. It keeps the secrecy between patient and physician due to the validation of all transactions that are added to the blockchain since revealing the patient's essential evidence between physicians is prohibited [55]. Blockchain provides a framework to amplify and support the integration of healthcare information across a range of uses and stakeholders. In healthcare, the unique advantages of real-time recordings and tamper resistance of blockchain can be reflected. Data stored can be shared across a group of people and organizations. A permissive blockchain can protect privacy while maintaining it by agreeing on where and by whom to be looking for deals and hiding the identities of all parties [56]. Traditional healthcare practices become more effective for the diagnosis and treatment of diseases due to more secure data sharing using blockchain tools. In the future, blockchain may provide an authentic, personalized, and reliable healthcare system by merging entire real-time clinical and presenting it in an up-to-date secure healthcare setup [57]. Figure 10.4 illustrates applications of the blockchain in healthcare.

10.3.3 Limitations of Blockchain

Data exchange is a chief blockchain problem in the healthcare field because of the high standards of data privacy and security needed. Data breaches in healthcare storage systems can be costly because of the Health Insurance Portability and Accountability Act fines and reputation losses [48, 58]. Blockchain technology

itself cannot guarantee data privacy and security. Thus, it has never been proposed as a stand-alone technology. However, it is recommended in combination with cryptographic techniques. Regardless of the number of existing prototypes of blockchain-based healthcare systems, due to the existing barriers to the adoption, such as social, technological, and legal limitations, there is a lacuna in the evaluation of real-world settings [50, 59].

OmniPHR was developed by Roehrs, Costa, and Righi to handle patient health records for providing unified patient health records stored across multiple healthcare providers. In an OmniPHR system, the data have to follow standards supported by the model. If the data is not supported, the scope of standards would not be shared. Also, the patient has to authorize to access the record. Only the patient and healthcare provider can access the data. The management of key and their recovery is also a problem that is not considered by OmniPHR when they get lost or leaked [60].

The MedRec Blockchain technology is a decentralized ERH system with some limitations, such as (a) it does not address the security of an individual database, (b) it attempts to solve digital rights management problems, and (c) the pseudo-anonymous nature allows the use of data forensics to infer the relationship between patients and providers.

Blockchain technology still fails to scale high transaction volume technology [60, 61]. Security risk with blockchain arises from intentional malicious attacks by criminal organizations or by government agencies that could compromise the privacy of the patients. The private key could be liable for the potential compromise, which results in unauthorized access to the stored health data [62, 63].

10.3.4 Challenges and Future Perspective of Blockchain in Healthcare

Blockchain data structures would work well for gathering data from wearable sensors and mobile applications and, thus, would contribute noteworthy information on the risks versus the benefits of treatments as well as patient-reported outcomes. Daily, personalized health data will likely engage a patient more in his healthcare and improve patient compliance. Moreover, the physician will be able to obtain more frequent data, such as daily blood pressures or blood sugar levels. Otherwise, it has only happened when a patient report for an appointment. It can improve individualized care with specialized treatment plans based on outcomes or treatment efficacy. Real-time access to data would improve clinical care coordination in emergency medical situations. Real-time data would also allow researchers to rapidly detect, isolate, and drive change in environmental conditions that impact public health [45, 64].

Blockchain can improve global health security and ensure the privacy of patient data. Epidemics of some re-emerging infectious diseases like Zika and Ebola have

raised health security concerns, which lead to the strengthening of surveillance systems. The focus of Global Health Security is to get alerts for global public health threats (both non-communicable and infectious diseases), strengthen the workforce, detect and respond effectively against disease threats, and elevate global health security as a priority. Blockchain has tremendous potential to overcome the limitations of current traditional approaches used in healthcare and disease surveillance projects [51, 65].

In the future, implications of the blockchain in the clinical field will drastically reduce processing time because the patient enrolls in the study, the complete collection of data will be available at once because of availability on the distributed ledger. The patient record on a blockchain network will lead people to connect with others all around the world with similar medical conditions. It will be beneficial for their health and also result in the patients feeling accepted and supported and to have strengthened will power to fight the disease [58].

The blockchain will be explored for the practical implementation of the cryptographic protocol model for the encrypted transaction and to attempt the evaluation of transactions and the performance of enhanced blockchain on the decentralized healthcare application. The performance measurements of enhanced blockchain will be conducted on transaction throughput, latency, resource consumption, and execution time [66]. In clinical trials, the blockchain data use Health Level Seven (HL7) international standards. HL7 consists of international standards for the transfer of administrative and clinical data between various healthcare providers using this software application. This provides a framework for the integration, exchange, retrieval, and sharing of electronic health information [67, 68].

10.4 Internet of Medical Things (IoMT)

IoMT describes various networks of actuators, sensors, processors, and computers connected to the Internet. The IoMT can deliver comprehensive patient care in multiple settings such as long-term (nursing homes), acute (in-hospital), and community-based (in-home). IoMT has the potential to accurately track people, specimens, equipment, supplies, and service animals and analyze the data captured. The patients get attached with sensors to measure vital signs and other biometric information. The problems can be easily diagnosed, and a better quality of care can be given using more efficient resources [69].

The integration of healthcare with the IoMT features into medical devices improves the effectiveness and quality of service. It brings high value for the elderly, patients with chronic conditions, and those who require consistent supervision. Intelligent systems and powerful algorithms are used to obtain an unprecedented level of real-time and life-critical data. Taking care of patient health at a meager cost is an essential factor. The primary purpose of applying IoMT in healthcare is to move out of the traditional area to visit hospitals, and thus the waiting will come to an end. It can sense and communicate with physical and biomedical parameters [70].

10.4.1 Role of the Internet of Medical Things (IoMT) for Personalized Medical Application

Personalized healthcare supports the sustainability of care. IoMT is a paradigm promising to manage the digital identity for personalized care services. Various types of equipment are being used in extra-wall healthcare and assistive services, which requires different sorts of objects to communicate and to make the omnipresent system. Extended entities and mixed roles are becoming interoperable [71, 72].

IoMT has the potential to promote various medical applications, for example, in remote health monitoring, physical fitness programs, Alzheimer's diseases, and elderly care. The IoMT healthcare system mainly tries to work with the existing wireless sensor networks, embedded device technologies, and pervasive computing. IoMT systems need to provide the services to anyone, anytime and anywhere. So, we need architecture to develop healthcare systems more efficiently and with less cost [73].

IoMT allows technologies to evolve from traditional hub-based systems to more personalized healthcare systems due to the rapid proliferation of wearable devices and smartphones. These healthcare systems use a set of interconnected devices to create an IoMT network. This performs healthcare activities, including monitoring, diagnosis, and remote surgeries. The sensing and wearable devices used for personalized medicine comprise signals from inertial sensors, global positioning systems, electrocardiograms, and electroencephalograms, among others. All are capable of observing and recording multiple types of health data, such as location, weight, blood pressure, heart rate, and user context information [74, 75]. Figure 10.5 shows the schematic diagram of the wearable devices used in the healthcare system.

IoMT will play an essential role in envisioning, developing, maintaining smart, connected, and personalized healthcare services. These can enable the patients to monitor their physical condition itself. By using this technology, an electronic health record is maintained, which allows the healthcare providers in better evaluation and better early detection of the physical conditions [76].

IoMT-based healthcare can congregate distributed devices, aggregate knowledge, analyze data, and communicate medical information to the cloud in real-time. Thus, it can collect, store, and analyze a large amount of data in several new forms and activate context-based alarms. This can allow ubiquitous and continuous health data access from any connected device over the Internet. The healthcare system implementation can monitor the physiological parameters of inpatients. Thus, IoMT empowered devices can simultaneously enhance the quality of care with regular monitoring and reduce the cost of care and actively engage in data collection and analysis [77]. IoMT solutions for healthcare in developing countries have brought revolutions to reduce the mortality rate and provide healthcare data at low cost. Smart IoMT-based healthcare applications play a vital role in tracking and monitoring patient healthcare information, their activities through powerful sensor technologies that enable clinical care to make smarter decisions [78].

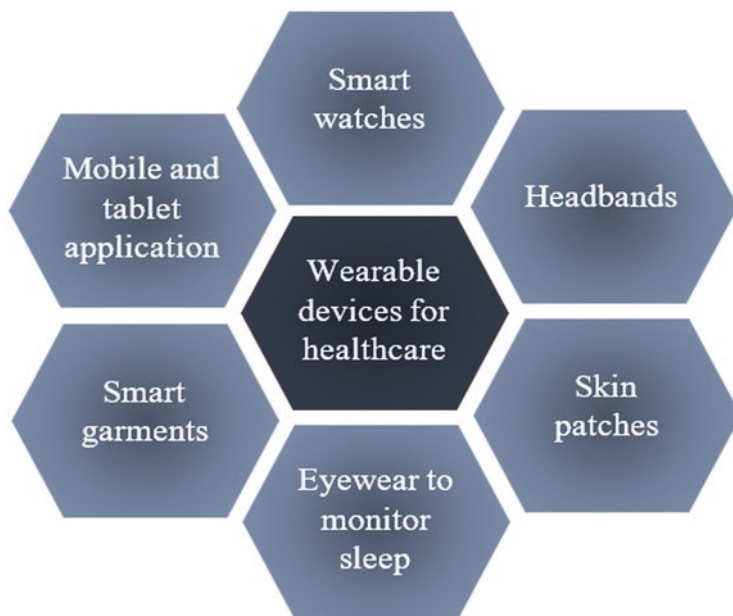


Fig. 10.5 Schematic diagram of the wearable devices used in the healthcare system

10.4.2 Advantages of Internet of Medical Things (IoMT)

IoMT can solve various healthcare interoperability problems. Organizations need not build a data bridge and translate it. They can easily connect to a central standard API “plug.” If done right, the aggregated data can form a base for high-speed and effective AI systems. IoMT is able to function in a real-time fashion [79, 80]. Advantages of healthcare IoMT are mobile medical applications or wearable devices that allow patients to record their health data. Hospitals use IoMT to keep tabs on the location of medical devices, personnel, and patients, which may make the patient more health-conscious. Through IoMT, doctors can use real-time location services and track the devices used for treating patients. Medical apparatus and devices like wheelchairs, scales, defibrillators, nebulizers, pumps, or monitoring equipment can be tagged with sensors and located easily with IoMT.

Apart from real-time location services, there are IoMT devices that help in environmental monitoring as well. With the intervention of the IoMT, clinicians can predict the arrival of patients who are recuperating in the post-anesthesia care unit. They can also monitor the status of patients in real-time and hand hygiene compliance in a healthcare worker and tighten budgets and improve the patient journey and remote monitoring [81]. Usak et al. reported various advantages of IoMT in the pharmaceutical industry. Poor-quality medicines or fake drugs can lead to serious health consequences, including death. Infrared and radio-frequency identification technologies are used to resolve such problems and to monitor medications without

physical contact. Doctors can handle all the legal health information of a patient using IoMT-enabled access [82].

IoMT renders a substantial contribution to the development of a smart healthcare system. In an intelligent healthcare system, the medical data are captured by sensors and transmitted to the cloud server to handle intelligent analytics through different types of IoMT networks. Various communication protocols are used based on the medical application requirements. The radio spectra allow a much easier and cheaper global broadband expansion of the smart healthcare 7Ps, including personalized, persuasive, predictive, participatory, preventative, programmable, and perpetual [83]. Recently, IoMT-based rehabilitation has been introduced to resolve the problem of scarce resources due to the aging of the population. It can be seen as a sub-system under a smart city. An IoMT-based healthcare system connects all available resources as a network to perform healthcare activities, which include monitoring, diagnosis, and remote surgeries over the Internet. IoMT framework has been dedicated to extending the healthcare services from hospitals and communities to homes [84]. Figure 10.6 shows the schematic presentation of applications of IoMT in the healthcare sector.

10.4.3 Limitations of the Internet of Medical Things (IoMT)

The most significant technical barrier to achieving a successful vision is the state of health data. Created by legacy electronic health record (EHR) systems, health data are largely fragmented into institution-centered. Current efforts are directed toward the exchange of individual records between silos using increasingly standardized vocabularies (code sets) and message formats. However, it does not entirely solve the problem of data fragmentation [79, 85].

Data from IoMT devices include a patient's vital signs, physical activity, or glucose levels, to name a few. On the other side, at home, this information does not typically travel to an EHR system and may not centralize or made readily available to the providers. With the lack of common security standards and practices, many health IT professionals have concerns about the risks associated with IoMT device tampering and data breaches [86, 87].

In a smart healthcare system, data size, irregularity, and sparsity may critically challenge data measurement and data processing, which generates a set of heterogeneous data that are fused satisfactorily at the data level. A priority controlling strategy must handle and resolve the critical data heterogeneity issue while keeping track of some quality metrics to guarantee that the output of the healthcare provider will be useful [83, 88].

IoMT does not maintain healthcare standardization, but it is desirable to enforce interoperability. Many manufacturers produce a diverse range of products and devices, and new vendors continue to join with technologies. IoMT devices have lower speed processors that must work with several sensors and actuators at a reasonable speed and with local and remote memory. IoMT must follow security protocols [89, 90].

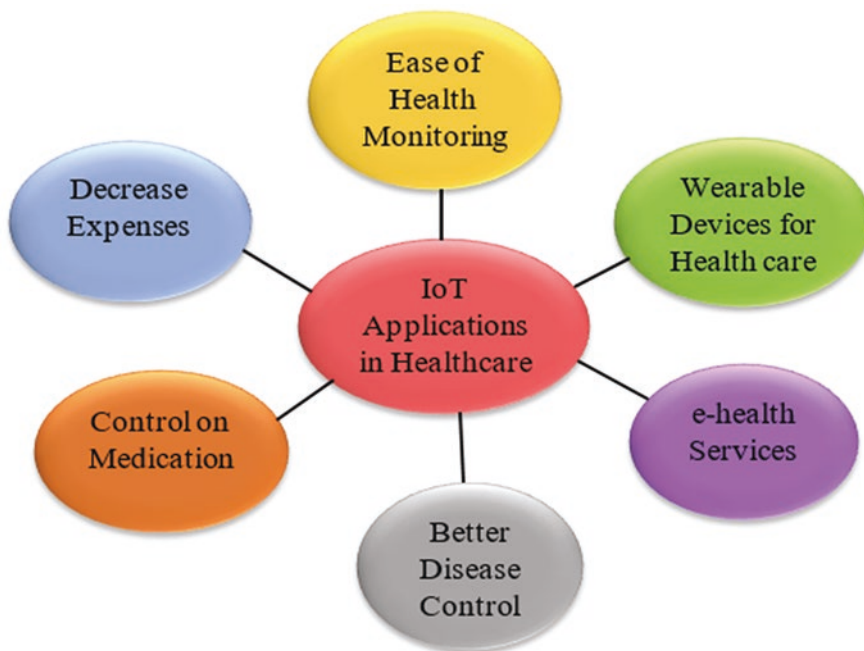


Fig. 10.6 Applications of the Internet of medical things in the healthcare sector

10.4.4 Challenges and Future Perspective of IoMT

The Pharma IoMT enables the patients and healthcare providers to use medicines using advanced sensor hardware and craft personalized care services. Wearable sensors are the example of pharma IoMT solutions, which provide medication management, improved patient outcomes, and quality of life in multiple sclerosis and Parkinson's disease patients. The pharmaceutical industries need to consider European Union data protection and privacy legislation, which controls the care data of a patient. The patient can transfer their care and health data to multiple service providers. This will lead to the emergence of totally new forms of service platforms and business models. It has been predicted that soon we will look at our smartwatch or phone to check our health outcomes more often than we do now to check our twitter, mail, WhatsApp, or Facebook accounts [79, 91].

IoMT enables new diverse and uncertain fields for exploration that will influence healthcare and rapidly changing society. In the future, studies will focus on new informatics methods in each layer of the IoMT ecosystem, seeking ways to empower IoMT [92]. IoMT-based applications and devices must contain important information related to private information communicating globally via networks, everywhere, and at any time.

Most likely, the use of knowledge and technology from smart cities, intelligent retail logistics, smart living, and intelligent environments would increase by IoMT [93]. IoMT has been used in the healthcare sector to improve the treatment and management of various diseases [94]. Since the IoMT can be hacked, it is essential to analyze and recognize its different characteristics regarding privacy and security, with its vulnerabilities, countermeasures, and security requirements [95].

10.5 Future Trends

10.5.1 *Ontologies for the IoMT*

For better flexibility and interoperability, Hachem et al. described a service-oriented middleware solution that can overcome the challenges associated with semantic technologies. The authors described future trends of sensor modeling approach with respect to different levels of details. The authors reported spatiotemporal and statistical correlation models to implement the plan and integrate their feasibility into the ontological analysis [96].

In ontology-inspired models, a formal definition of IoMT can be representative of real-world things and relationships. This methodology defines different cases of IoMT solutions and to promote potential extensions and upgrades. It is expected that in the future, IoMT will integrate with a crowdsourcing framework, which will save time and energy of potential users [97].

10.5.2 *Blockchain, Wearables, and Nanorobotics*

Distributed ledger technology (DLT) is gaining significant attention during the past two decades as one of the most disruptive technologies. It aims to change how people do business, monitor their goods, and handle their details. In 2009, DLT was first introduced as bitcoin. It gained considerable popularity during the last few years. Hyperledger Fabric is the first major private DLT system that started in December 2015 by the Linux Foundation. In the Fabric, a smart contract is packaged into chain codes. It is a computer program prepared on the ledger, which allows it to communicate with the ledger data. These chain codes can be written in Go or Java with other programming languages. In the recent IoMT-driven environment, both access control and blockchain technologies can be combined to integrate more advanced context conscious access control systems. It would work toward the potential blockchain-based access control implementations to ensure data sharing between various parties [98].

SymBiosis is a web browsing environment that makes a case for direct mutual profit sharing between censored users and uncensored users. The main idea is to transform the traditional voluntary one-way service into two-way anonymity supported interface between censored and uncensored users, making it a near-perfect method of circumvention with a ubiquitous relay deployment. SymBiosis can achieve all goals against the most sophisticated sensors as well as control mechanisms and provides functional output for everyday web browsing [99].

The wearable technology market demand is projected to increase from 15.74 trillion US\$ to 51.60 trillion US\$ between 2015 and 2022. Applications like health, entertainment, digital, and fashion are generally considered vertically within the framework of the consumer. The demand for devices is pushing wearable technology to grow [100].

Various research studies have been centered primarily on the application of blockchain technology to manage healthcare data. The blockchain-based gateway enables patients to own securely, monitor, and exchange their data without violating privacy. The cloud storage systems have been incorporated to obtain a solution for off-chain storage of massive biomedical data files. In modern blockchain applications, a special function called a data validator has been added in addition to the conventional data contributor/generator. The data validators will verify or certify the quality of data it has produced [101].

10.5.3 Security Benchmarks for IoMT

IoMT is a rapidly developing healthcare technology with much scope for security vulnerabilities. As other Internet-linked devices, IoMT is not safe from breaches. These breaches can affect device functionality, data protection, and privacy, which may cause life-threatening effects. A stakeholder centric approach can improve the reliability of IoMT wearables. The functioning of this system can be related to the collection of IoMT wearables security and privacy attributes, which are defined to measure security and privacy in those devices [102].

Many protection approaches for IoMT devices have been reported to secure a medical device theoretically. However, due to the size and power constraints, wearable and implantable devices may utilize limited resources and, thus, may not have sufficient resources to enforce these schemes. Ensuring safety and stability, these devices can cover the design space of human, cyber, and physical elements [106, 107]. In addition to the research efforts, a close collaboration must be established between academia, industries, and standard agencies to develop new methods, regulations, and standards to ensure the safety and privacy IoMT devices [103].

10.5.4 *Quality of Care*

IoMT solutions create trust in the security evaluation process. This includes answers for security evaluations, comprehensive and simple-to-use questions for IoMT. It also offers an evaluation tool for the IoMT solution with these evaluation criteria. This work educates the IoMT users who often have a low level of handling and security knowledge for IoMT. The IoMT solution providers may also benefit from this process in evaluating their products and comparing them to the other IoMT solutions. In the future, the IoMT solution will be adopted for rapid and continuous data analysis [104].

IoMT security assessment framework is a web-based application focused on a novel ontological scenario-driven approach to ensure security. IoMT security assessment framework innovation lies in its capacity to adapt to new stakeholders and emerging technologies, granularity, and compliance with standards. In some cases, system administrators are responsible for the security-related decision; this work will provide an excellent opportunity for the other stakeholders to gain practical experience in the cutting edge fields of IoMT. It will also promote healthy competition between IoMT solution providers by developing IoMT solutions to address the security measures to satisfy consumers [105].

10.6 Conclusions

This chapter focuses on the role of AI, blockchain, and the Internet of medical things (IoMT) for personalized medical applications, their advantage, and disadvantage, including prospects. Based on the available literature in context, different roles of these technologies in the healthcare sector have been described [108, 109]. This is an emerging area that can help to monitor patient health. It can also decrease expenses and time consumption during medication. At present, these technologies are also used in drug delivery and discovery processes. Shortly, these technologies will introduce new vistas for better health services by discovering mobile applications, diagnostic systems, and wearable devices by increasing the focus toward e-health services and the crescent usage of multimedia in healthcare [110–127].

Competing Financial Interests The authors declare no competing financial interests.

References

1. A.K. Lim, Virtualization of health care: the role of capacity building, in *Health 4.0: How Virtualization and Big Data are Revolutionizing Healthcare*, (Springer, Cham, 2017), pp. 125–153
2. Z. Pang, G. Yang, R. Khedri, Y.T. Zhang, Introduction to the special section: convergence of automation technology, biomedical engineering, and health informatics toward the healthcare 4.0. *IEEE Rev. Biomed. Eng.* **11**, 249–259 (2018)
3. I.S. Chan, G.S. Ginsburg, Personalized medicine: progress and promise. *Annu. Rev. Genomics Hum. Genet.* **12**, 217–224 (2011)
4. G.S. Ginsburg, J.J. McCarthy, Personalized medicine: revolutionizing drug discovery and patient care. *Trends Biotechnol.* **19**(12), 491–496 (2001)
5. M.A. Hamburg, F.S. Collins, The path to personalized medicine. *N. Engl. J. Med.* **363**(4), 301–304 (2010)
6. G.S. Ginsburg, H.F. Willard, Genomic and personalized medicine: foundations and applications. *Transl. Res.* **154**(6), 277–287 (2009)
7. M.G. Aspinall, R.G. Hamermesh, Realizing the promise of personalized medicine. *Harv. Bus. Rev.* **85**(10), 108 (2007)
8. R.M. Wachter, L. Goldman, The emerging role of “hospitalists” in the American health care system. *N. Engl. J. Med.* **335**, 514–517 (1996)
9. L. Govan, C.J. Weir, P. Langhorne, Organized inpatient (stroke unit) care for stroke. *Stroke* **39**(8), 2402–2403 (2008)
10. A. Khalsa, G. Liu, J.S. Kirby, Increased utilization of emergency department and inpatient care by patients with hidradenitis suppurativa. *J. Am. Acad. Dermatol.* **73**(4), 609–614 (2015)
11. P.J. O’Connor, J.M. Sperl-Hillen, C.J. Fazio, B.M. Averbek, B.H. Rank, K.L. Margolis, Outpatient diabetes clinical decision support: current status and future directions. *Diabet. Med.* **33**(6), 734–741 (2016)
12. A.A. Guccione, D. Avers, R. Wong, *Geriatric Physical Therapy-ebook* (Elsevier Health Sciences, St. Louis, 2011)
13. L.S. Gudas, G.P. Koocher, Palliative and end of life care for children and families, in *Developmental-Behavioral Pediatrics*, (WB Saunders, Philadelphia, 2009), pp. 355–365
14. S. Reddy, J. Fox, M.P. Purohit, Artificial intelligence-enabled healthcare delivery. *J. R. Soc. Med.* **112**(1), 22–28 (2019)
15. T. Davenport, R. Kalakota, The potential for artificial intelligence in healthcare. *Future Healthcare J.* **6**(2), 94 (2019)
16. O. Iliashenko, Z. Bikkulova, A. Dubgorn, Opportunities and challenges of artificial intelligence in healthcare, in *E3s Web of Conferences 2019*, vol. 110, (EDP Sciences)
17. J. Guan, Artificial intelligence in healthcare and medicine: promises, ethical challenges and governance. *Chin. Med. Sci. J.* **34**(2), 76–83 (2019)
18. J. Guo, B. Li, The application of medical artificial intelligence technology in rural areas of developing countries. *Health Equity* **2**(1), 174–181 (2018)
19. J. Awwalu, A.G. Garba, A. Ghazvini, R. Atuah, Artificial intelligence in personalized medicine application of AI algorithms in solving personalized medicine problems. *Int. J. Comput. Theory Eng.* **7**(6), 439 (2015)
20. J. Xu, P. Yang, S. Xue, B. Sharma, M. Sanchez-Martin, F. Wang, K.A. Beaty, E. Dehan, B. Parikh, Translating cancer genomics into precision medicine with artificial intelligence: applications, challenges and future perspectives. *Hum. Genet.* **138**(2), 109–124 (2019)
21. N.J. Schork, Artificial intelligence and personalized medicine, in *Precision Medicine in Cancer Therapy*, (Springer, Cham, 2019), pp. 265–283
22. S.E. Dilsizian, E.L. Siegel, Artificial intelligence in medicine and cardiac imaging: harnessing big data and advanced computing to provide personalized medical diagnosis and treatment. *Curr. Cardiol. Rep.* **16**(1), 441 (2014)

23. F. Jiang, Y. Jiang, H. Zhi, Y. Dong, H. Li, S. Ma, Y. Wang, Q. Dong, H. Shen, Y. Wang, Artificial intelligence in healthcare: past, present and future. *Stroke Vascular Neurol.* **2**(4), 230–243 (2017)
24. K. Salah, M.H. Rehman, N. Nizamuddin, A. Al-Fuqaha, Blockchain for AI: review and open research challenges. *IEEE Access* **7**, 10127–10149 (2019)
25. K.H. Yu, A.L. Beam, I.S. Kohane, Artificial intelligence in healthcare. *Nat. Biomed. Eng.* **2**(10), 719–731 (2018)
26. S. Iqbal, W. Altaf, M. Aslam, W. Mahmood, M.U. Khan, Application of intelligent agents in healthcare. *Artif. Intell. Rev.* **46**(1), 83–112 (2016)
27. P. Hamet, J. Tremblay, Artificial intelligence in medicine. *Metabolism* **69**, S36–S40 (2017)
28. A. Becker, Artificial intelligence in medicine: what is it doing for us today? *Health Policy Technol.* (2019)
29. F. Pesapane, C. Volonté, M. Codari, F. Sardanelli, Artificial intelligence as a medical device in radiology: ethical and regulatory issues in Europe and the United States. *Insights Imaging* **9**(5), 745–753 (2018)
30. W.N. Price II, Artificial Intelligence in Health Care: Applications and Legal Issues (November 28, 2017). 14 *SciTech Lawyer* 10 (2017); University of Michigan Public Law Research Paper No. 599
31. A.J. Bharucha, V. Anand, J. Forlizzi, M.A. Dew, C.F. Reynolds III, S. Stevens, H. Wactlar, Intelligent assistive technology applications to dementia care: Current capabilities, limitations, and future challenges. *Am. J. Geriatr. Psychiatry* **17**(2), 88–104 (2009)
32. R. Kapoor, S.P. Walters, L.A. Al-Aswad, The current state of artificial intelligence in ophthalmology. *Surv. Ophthalmol.* **64**(2), 233–240 (2019)
33. T. Ploug, S. Holm, The right to refuse diagnostics and treatment planning by artificial intelligence. *Med. Health Care Philos.*, 1–8 (2019)
34. K. Grant, A. McParland, Applications of artificial intelligence in emergency medicine. *Univ. Toronto Med. J.* **96**(1) (2019)
35. J.R. Baldwin, M. Rafiqzaman, The determinants of the adoption lag for advanced manufacturing technologies. *Statistics Canada Working Paper* **117**, 1–35 (1998)
36. S. Khanna, Artificial intelligence: contemporary applications and future compass. *Int. Dent. J.* **60**(4), 269–272 (2010)
37. A. Verghese, N.H. Shah, R.A. Harrington, What this computer needs is a physician: humanism and artificial intelligence. *JAMA* **319**(1), 19–20 (2018)
38. E.J. Lee, Y.H. Kim, N. Kim, D.W. Kang, Deep into the brain: artificial intelligence in stroke imaging. *J. Stroke* **19**(3), 277 (2017)
39. N.M. Murray, M. Unberath, G.D. Hager, F.K. Hui, Artificial intelligence to diagnose ischemic stroke and identify large vessel occlusions: a systematic review. *J. Neurointervent. Surg.* **12**(2), 156–164 (2020)
40. M. Rabbani, J. Kanevsky, K. Kafi, F. Chandelier, F.J. Giles, Role of artificial intelligence in the care of patients with nonsmall cell lung cancer. *Eur. J. Clin. Investig.* **48**(4), e12901 (2018)
41. J. Biot, How will clinical practice be impacted by artificial intelligence? *Eur. J. Dermatol.* **29**(1), 8–10 (2019)
42. S. Khezr, M. Moniruzzaman, A. Yassine, R. Benlamri, Blockchain technology in healthcare: A comprehensive review and directions for future research. *Appl. Sci.* **9**(9), 1736 (2019)
43. W.J. Gordon, C. Catalini, Blockchain technology for healthcare: facilitating the transition to patient-driven interoperability. *Comput. Struct. Biotechnol. J.* **16**, 224–230 (2018)
44. P. Zhang, D.C. Schmidt, J. White, G. Lenz, Blockchain technology use cases in healthcare. *Adv. Comput.* **111**, 1–41 (2018)
45. L.A. Linn, M.B. Koo, Blockchain for health data and its potential use in health it and health care related research, in *ONC/NIST Use of Blockchain for Healthcare and Research Workshop*, (ONC/NIST, Gaithersburg, 2016), pp. 1–10

46. A.A. Vazirani, O. O'Donoghue, D. Brindley, E. Meinert, Implementing blockchains for efficient health care: systematic review. *J. Med. Internet Res.* **21**(2), e12439 (2019)
47. K.J. Kim, S.P. Hong, A trusted sharing model for patient records based on permissioned Blockchain. *J. Internet Comput. Serv.* **18**, 75–84 (2017)
48. P. Mamoshina, L. Ojomoko, Y. Yanovich, A. Ostrovski, A. Botezatu, P. Prikhodko, E. Izumchenko, A. Aliper, K. Romantsov, A. Zhebrak, I.O. Ogu, Converging blockchain and next-generation artificial intelligence technologies to decentralize and accelerate biomedical research and healthcare. *Oncotarget* **9**(5), 5665 (2018)
49. S. Avdoshin, E. Pesotskaya, Blockchain revolution in the healthcare industry, in *Proceedings of the future technologies conference 2018 Nov 15*, (Springer, Cham, 2018), pp. 626–639
50. A. Dubovitskaya, P. Novotny, Z. Xu, F. Wang, Applications of blockchain technology for data-sharing in oncology: results from a systematic literature review. *Oncology*, 1–9 (2019)
51. V.K. Chattu, A. Nanda, S.K. Chattu, S.M. Kadri, A.W. Knight, The emerging role of blockchain technology applications in routine disease surveillance systems to strengthen global health security. *Big Data Cogn. Comput.* **3**(2), 25 (2019)
52. S. Angraal, H.M. Krumholz, W.L. Schulz, Blockchain technology: Applications in health care. *Circ. Cardiovasc. Qual. Outcomes* **10**(9), e003800 (2017)
53. R. Bhargava, Blockchain technology and its application: a review. *IUP J. Inform. Technol.* **15**(1), 7–15 (2019)
54. J.M. Roman-Belmonte, H. De la Corte-Rodriguez, E.C. Rodriguez-Merchan, How blockchain technology can change medicine. *Postgrad. Med.* **130**(4), 420–427 (2018)
55. M.T. de Oliveira, L.H. Reis, R.C. Carrano, F.L. Seixas, D.C. Saade, C.V. Albuquerque, N.C. Fernandes, S.D. Olabariaga, D.S. Medeiros, D.M. Mattos, Towards a blockchain-based secure electronic medical record for healthcare applications, in *ICC 2019–2019 IEEE International Conference on Communications (ICC)*, (2019), pp. 1–6
56. Y. Chen, S. Ding, Z. Xu, H. Zheng, S. Yang, Blockchain-based medical records secure storage and medical service framework. *J. Med. Syst.* **43**(1), 5 (2019)
57. A.A. Siyal, A.Z. Junejo, M. Zawish, K. Ahmed, A. Khalil, G. Soursou, Applications of blockchain technology in medicine and healthcare: challenges and future perspectives. *Cryptography* **3**(1), 3 (2019)
58. S. Alla, L. Soltanisehat, U. Tatar, O. Keskin, Blockchain technology in electronic healthcare systems. *IISE Annual Conference and Expo 2018* **2018**(1), 754–759 (2018)
59. A.D. Dwivedi, G. Srivastava, S. Dhar, R. Singh, A decentralized privacy-preserving healthcare blockchain for IoT. *Sensors* **19**(2), 326 (2019)
60. T. McGhin, K.K. Choo, C.Z. Liu, D. He, Blockchain in healthcare applications: research challenges and opportunities. *J. Netw. Comput. Appl.* **135**, 62–75 (2019)
61. J. Chanchaichujit, A. Tan, F. Meng, S. Eaimkhong, Blockchain technology in healthcare, in *Healthcare 4.0*, (Palgrave Pivot, Singapore, 2019), pp. 37–62
62. C.C. Agbo, Q.H. Mahmoud, J.M. Eklund, Blockchain technology in healthcare: a systematic review. *Multidisciplinary Digital Publishing Institute. Healthcare* **7**(2), 56 (2019)
63. R. Xu, S. Chen, L. Yang, Y. Chen, G. Chen, Decentralized autonomous imaging data processing using Blockchain. In *Multimodal Biomedical Imaging XIV 2019 Feb 27* (Vol. 10871, p. 108710U). International Society for Optics and Photonics
64. A. Dubovitskaya, P. Novotny, S. Thiebes, A. Sunyaev, M. Schumacher, Z. Xu, F. Wang, Intelligent health care data management using blockchain: current limitation and future research agenda, in *Heterogeneous Data Management, Polystores, and Analytics for Healthcare*, (Springer, Cham, 2019), pp. 277–288
65. L. Ponce, R. Kinoshita, H. Nishiura, Exploring the human-animal interface of Ebola virus disease outbreaks. *Math Biosci. Eng.* **16**(4), 3130–3143 (2019)
66. H.M. Hussien, S.M. Yasin, S.N. Udzir, A.A. Zaidan, B.B. Zaidan, A systematic review for enabling of develop a blockchain technology in healthcare application: taxonomy, substantially analysis, motivations, challenges, recommendations and future direction. *J. Med. Syst.* **43**(10), 320 (2019)

67. T.K. Mackey, T.T. Kuo, B. Gummadi, K.A. Clauson, G. Church, D. Grishin, K. Obbad, R. Barkovich, M. Palombini, 'Fit-for-purpose?'—challenges and opportunities for applications of blockchain technology in the future of healthcare. *BMC Med.* **17**(1), 68 (2019)
68. G. Carter, H. Shahriar, S. Sneha, Blockchain-based interoperable electronic health record sharing framework. In: 2019 IEEE 43rd Annual Computer Software and Applications Conference (COMPSAC) 2019 July 15 (Vol. 2, pp. 452–457)
69. P.A. Laplante, N. Laplante, The internet of things in healthcare: potential applications and challenges. *IT Prof.* **18**(3), 2–4 (2016)
70. Y. Bhatt, C. Bhatt, Internet of things in healthcare, in *Internet of Things and Big Data Technologies for Next Generation HealthCare 2017*, (Springer, Cham, 2017), pp. 13–33
71. M. Simonov, R. Zich, F. Mazzitelli, Personalized healthcare communication in Internet of things. *Proc. of URSI GA08* (2008)
72. M. Benchoufi, P. Ravaud, D. Altman, From clinical trials to highly trustable clinical trials: Blockchain in clinical trials, a game changer for improving transparency? *Front. Blockchain* **2**, 23 (2019)
73. K.U. Srekanth, K.P. Nitha, A study on health care in Internet of Things. *Int. J. Recent. Innov. Trends Comput. Commun.* **4**(2), 44–47 (2016)
74. J. Qi, P. Yang, G. Min, O. Amft, F. Dong, L. Xu, Advanced internet of things for personalised healthcare systems: A survey. *Pervasive Mobile Comput.* **41**, 132–149 (2017)
75. V. Neerugatti, A.R. Reddy, Secured architecture for Internet of Things-enabled personalized healthcare systems, in *Internet of Things and Personalized Healthcare Systems*, (Springer, Singapore, 2019), pp. 75–80
76. S.K. Datta, C. Bonnet, A. Gyrard, R.P. Da Costa, K. Boudaoud, Applying Internet of Things for personalized healthcare in smart homes. In 2015 24th Wireless and Optical Communication Conference (WOCC) 2015 Oct 23 (pp. 164–169). IEEE
77. R.K. Kodali, G. Swamy, B. Lakshmi, An implementation of IoT for healthcare. In 2015 IEEE Recent Advances in Intelligent Computational Systems (RAICS) 2015 Dec 10 (pp. 411–416). IEEE
78. B. Singh, S. Bhattacharya, C.L. Chowdhary, D.S. Jat, A review on internet of things and its applications in healthcare. *J. Chem. Pharm. Sci.* **10**(1), 447–452 (2017)
79. D.V. Dimitrov, Medical Internet of things and big data in healthcare. *Healthcare Inform. Res.* **22**(3), 156–163 (2016)
80. J. Gao, X. Wang, Y. Wang, Z. Yang, J. Gao, J. Wang, W. Tang, X. Xie, *Camp: Co-attention memory networks for diagnosis prediction in healthcare* (ICDM, 2019)
81. A. Gapchup, A. Wani, D. Gapchup, S. Jadhav, Health care systems using Internet of things. *IJIRCCCE* **4**(12) (2016)
82. M. Usak, M. Kubiakto, M.S. Shabbir, O. Viktorovna Dudnik, K. Jermstittiparsert, L. Rajabion, Health care service delivery based on the Internet of things: A systematic and comprehensive study. *Int. J. Commun. Syst.* **33**(2), e4179 (2020)
83. H. Zhu, C.K. Wu, C.H. Koo, Y.T. Tsang, Y. Liu, H.R. Chi, K.F. Tsang, Smart healthcare in the era of internet-of-things. *IEEE Consum. Electron. Mag.* **8**(5), 26–30 (2019)
84. Y.I. Yuehong, Y. Zeng, X. Chen, Y. Fan, The Internet of things in healthcare: An overview. *J. Ind. Inf. Integr.* **1**, 3–13 (2016)
85. M. Dauwed, A. Meri, IOT service utilisation in healthcare, in *IoT and Smart Home Automation*, (IntechOpen, 2019)
86. J. DeWitt Best Practices for Heterogenous Health IoT Integration into Electronic Health Records. 2019
87. M. Jacobs, L.J. Boersma, R. Swart, R. Mannens, B. Reymen, F. Körver, F. van Merode, A. Dekker, Electronic Health Record implementation in a large academic radiotherapy department: Temporarily disruptions but long-term benefits. *Int. J. Med. Inform.* **129**, 342–348 (2019)

88. M. Rath, Big data and IOT-allied challenges associated with healthcare applications in smart and automated systems, in *Data analytics in medicine: Concepts, methodologies, tools, and applications 2020*, (IGI Global, Hershey, 2020), pp. 1401–1414
89. S.R. Islam, D. Kwak, M.H. Kabir, M. Hossain, K.S. Kwak, The Internet of things for health care: a comprehensive survey. *IEEE Access* **3**, 678–708 (2015)
90. I.U. Din, H. Asmat, M. Guizani, A review of information centric network-based internet of things: communication architectures, design issues, and research opportunities. *Multimed. Tools Appl.* **78**(21), 30241–30256 (2019)
91. H. Kaur, M. Atif, R. Chauhan, An internet of healthcare things (IoHT)-based healthcare monitoring system, in *Advances in intelligent computing and communication 2020*, (Springer, Singapore, 2020), pp. 475–482
92. G. Bodur, S. Gumus, N.G. Gursoy, Perceptions of Turkish health professional students toward the effects of the Internet of things (IOT) technology in the future. *Nurse Educ. Today* **79**, 98–104 (2019)
93. A. Hussein, Internet of Things (IOT): research challenges and future applications. *Int. J. Adv. Comput. Sci. Appl.* **10**(6), 77–82 (2019)
94. A.M. Alqudah, The internet of things in healthcare: a survey for architecture, current and future applications, mobile application, and security. *JOIV: Int. J. Inform. Vis.* **3**(2), 113–122 (2019)
95. A.A. Mawgoud, A.I. Karadawy, B.S. Tawfik, A Secure Authentication Technique in Internet of Medical Things through Machine Learning. arXiv preprint. 2019; arXiv:1912.12143 [cs. CR]
96. S. Hachem, T. Teixeira, V. Issarny, Ontologies for the Internet of things. In: *Proceedings of the 8th middleware doctoral symposium*. 2011;1–6
97. F. Alsubaei, A. Abuhussein, S. Shiva, Ontology-based security recommendation for the internet of medical things. *IEEE Access* **7**, 48948–48960 (2019)
98. M.J.M. Chowdhury, M.S. Ferdous, K. Biswas, N. Chowdhury, A.S.M. Kayes, M. Alazab, P. Watters, A comparative analysis of distributed ledger technology platforms. *IEEE Access* **7**, 167930–167943 (2019)
99. M.J.M. Chowdhury, M.S. Ferdous, K. Biswas, N. Chowdhury, A.S.M. Kayes, P. Watters, A. Ng, Trust modeling for blockchain-based wearable data market. In *2019 IEEE International Conference on Cloud Computing Technology and Science*. CloudCom. 2019; pp. 411–417
100. M.A. Rasheed, White Paper: Blockchain for Wearable Devices. 2017
101. X. Zheng, R.R. Mukkamala, R. Vatrappu, J. Ordieres-Mere, Blockchain-based personal health data sharing system using cloud storage. In: *20th International Conference on e-Health Networking, Applications and Services (Healthcom) 2018*; pp. 1–6
102. S.R. Putta, A. Abuhussein, F. Alsubaei, S. Shiva, S. Atiewi, Security benchmarks for wearable medical things: stakeholders-centric approach, in *Fourth International Congress on Information and Communication Technology*, (Springer, Singapore, 2020), pp. 405–418
103. Y. Sun, F.P. Lo, B. Lo, Security and privacy for the internet of medical things enabled healthcare systems: a survey. *IEEE Access*. **7**, 183339–183355 (2019)
104. F. Alsubaei, A. Abuhussein, S. Shiva, A framework for ranking IoMT solutions based on measuring security and privacy, in *Proceedings of the Future Technologies Conference 2018 Nov 15*, (Springer, Cham, 2018), pp. 205–224
105. F. Alsubaei, A. Abuhussein, V. Shandilya, S. Shiva, IoMT-SAF: Internet of medical things security assessment framework. *Internet of Things*. **8**, 1–32 (2019)
106. V.V. Estrela, J. Hemanth, O. Saotome, E.G.H. Grata, D.R.F. Izario, Emergency response cyber-physical system for flood prevention with sustainable electronics, in *Proceedings of the 3rd Brazilian Technology Symposium. BTSym 2017, Campinas, SP, Brazil*, ed. by Y. Iano, R. Arthur, O. Saotome, V. V. Estrela, H. J. Loschi, (Springer, Zurich, 2019). https://doi.org/10.1007/978-3-319-93112-8_33

107. V.V. Estrela, O. Saotome, J. Hemanth, R.J.R. Cabral, Emergency response cyber-physical system for disaster prevention with sustainable electronics. Proceedings of the ACM PETRA 2017, Rhodes, Greece, 2017
108. H.J. Loschi, V.V. Estrela, D.J. Hemanth, S.R. Fernandes, Y. Iano, A.A. Laghari, A. Khan, H. He, R. Sroufe, Communications requirements, video streaming, communications links and networked UAVs, in *Imaging and Sensing for Unmanned Aircraft Systems*, ed. by V. V. Estrela, J. Hemanth, O. Saotome, G. Nikolakopoulos, R. Sabatini, vol. 2, (IET, London, 2020)
109. A. Arshaghi, N. Razmjoo, V.V. Estrela, P. Burdziakowski, D.A. Nascimento, A. Deshpande, P.P. Prashant, Image transmission in UAV MIMO UWB-OSTBC system over Rayleigh channel using multiple description coding (MDC) with QPSK modulation, in *Imaging and Sensing for Unmanned Aircraft Systems*, ed. by V. V. Estrela, J. Hemanth, O. Saotome, G. Nikolakopoulos, R. Sabatini, vol. 2, (IET, London, 2020)
110. V.V. Estrela, L.A. Rivera, P.C. Beggio, R.T. Lopes, Regularized pel-recursive motion estimation using generalized cross-validation and spatial adaptation, in *Proceedings of the XVI Brazilian Symposium on Computer Graphics and Image Processing (SIBGRAPI 2003)*, (2003). <https://doi.org/10.1109/SIBGRA.2003.1241027>
111. V.V. Estrela, N.P. Galatsanos, Spatially adaptive regularized pel-recursive motion estimation based on the EM algorithm. In: Proc. SPIE 3974, Image and Video Communications and Processing 2000, (19 April 2000), (2000). <https://doi.org/10.1117/12.382969>
112. V.V. Estrela, N.P. Galatsanos, Spatially-adaptive regularized pel-recursive motion estimation based on cross-validation. In Proceedings of the IEEE International Conference on Image Processing (ICIP 98), Chicago, IL, USA, IEEE. (1998). <https://doi.org/10.1109/ICIP.1998.723347>
113. H.R. Marins, V.V. Estrela, On the use of motion vectors for 2D and 3D error concealment in H.264 AVC video, in *Feature Detectors and Motion Detection in Video Processing*, ed. by N. Dey, A. S. Ashour, P. K. Patra, 1st edn., (IGI Global, Hershey, 2017). <https://doi.org/10.4018/978-1-5225-1025-3.ch008>
114. V.V. Estrela, A.M. Coelho, State-of-the-Art Motion Estimation in the Context of 3D TV, in *Multimedia Networking and Coding*, ed. by R. A. Farrugia, C. J. Debono, (IGI Global, Hershey, 2013), pp. 148–173. <https://doi.org/10.4018/978-1-4666-2660-7.ch006>
115. S.R. Fernandes, V.V. Estrela, H.A. Magalhaes, O. Saotome, On improving sub-pixel accuracy by means of B-Spline, Proceedings of the 2014 IEEE International Conference on Imaging Systems and Techniques (IST 2014), 68–72, 2014, <https://doi.org/10.1109/IST.2014.6958448> ISBN: 9781479952199
116. M.A. de Jesus, V.V. Estrela, A. Khelassi, R.J. Aroma, K. Raimond, S.R. Fernandes, S.E.B. da Silva, A.C. de Almeida, R.T. Lopes, *Motion Estimation Role in the Context of 3D Video. International Journal of Multimedia Data Engineering and Management (IJMDEM)* (IGI Global, Hershey, 2020)
117. N. Razmjoo, M. Ashourian, M. Karimifard, V.V. Estrela, H.J. Loschi, D. do Nascimento, R.P. França, M. Vishnevski, Computer-aided diagnosis of skin cancer: A review, in *Current Medical Imaging*, (Bentham Science Publishers, Sharjah, 2020). <https://doi.org/10.2174/1573405616666200129095242>
118. A. Khelassi, V.V. Estrela, J. Hemanth, Explainer: an interactive agent for explaining the diagnosis of cardiac arrhythmia generated by IK-DCBRC. *Med. Technol. J.* **3**(2), 376–394 (2019). <https://doi.org/10.26415/2572-004X-vol3iss2p376-394>
119. B.F. Cruz, J.T. de Assis, V.V. Estrela, A. Khelassi, A compact SIFT-based strategy for visual information retrieval in large image databases. *Med. Technol. J.* **3**(2), 402–401 (2019). <https://doi.org/10.26415/2572-004X-vol3iss2p402-412>
120. V.V. Estrela, A. Khelassi, M. ACB, Y. Iano, N. Razmjoo, D. Martins, R. DTM, Why software-defined radio (SDR) matters in healthcare? *Med. Technol. J.* **3**(3), 421–429 (2019). <https://doi.org/10.26415/2572-004X-vol3iss3p421-429>

121. V.V. Estrela, A.C.B. Monteiro, R.P. França, Y. Iano, A. Khelassi, N. Razmjoo, Health 4.0: applications, management, technologies and review. *Med. Technol. J.* **2**(4), 262–276 (2019). <https://doi.org/10.26415/2572-004X-vol2iss1p262-276.262>
122. A.M. Coelho, V.V. Estrela, F.P. Carmo, S.R. Fernandes, Error concealment by means of motion refinement and regularized Bregman divergence. Proceedings of the 13th international conference on Intelligent Data Engineering and Automated Learning, Natal, Brazil, 2012. https://doi.org/10.1007/978-3-642-32639-4_78
123. C. Luo, J. Nightingale, E. Asemota, C. Grecos, A UAV-Cloud System for Disaster Sensing Applications, In IEEE 81st Vehicular Technology Conference (VTC Spring), 2015:1–5, 2015. <https://doi.org/10.1109/VTCSpring.2015.7145656>
124. S. Gupta, R.B. Girshick, P.A. Arbeláez, J. Malik, Learning Rich Features from RGB-D Images for Object Detection and Segmentation. *Proc. 2014 ECCV*. 2014
125. Y. Zhou, H. Li, L. Kneip, Canny-VO: visual odometry with RGB-D cameras based on geometric 3-D–2-D edge alignment. *IEEE Trans. Robot.* **35**, 184–199 (2019)
126. S. Kosta, A. Aucinas, P. Hui, R. Mortier, X. Zhang, ThinkAir: Dynamic resource allocation and parallel execution in the cloud for mobile code offloading, *Proc. IEEE INFOCOM*, 2012:945–953
127. V. Namboodiri, T. Ghose, To cloud or not to cloud: A mobile device perspective on energy consumption of applications, *Proc. of the 2012 IEEE International Symposium on a World of Wireless, Mobile and Multimedia Networks (WoWMoM)*

Chapter 11

The Role of Vehicular Ad Hoc Networks in Intelligent Transport Systems for Healthcare



Rabia Bilal  and Bilal Muhammad Khan 

11.1 Introduction

11.1.1 Mobile Ad Hoc Networks (MANETs)

The arrival of the globally available computing and the designing of innovative, incredible, capable, handy computing gadgets have permeated wireless mobile communication and networking so that users avail from electronic services at any time, irrespective of their geographical location. There are two kinds of wireless networks: infrastructure-based and infrastructure-less (aka ad hoc networks).

An infrastructure-reliant network has the networking component (i.e., routers and gateways) and the nodes connected within the network range to the nearby base station that comes within its communication range. When a node exceeds the coverage area of that base station, it performs the handoff procedure so that it comes within the scope of the new base station. Cellular communication is a classic example of an infrastructure-based wireless network.

The infrastructure-less network or ad hoc network (AHN) where the Latin expression ad hoc designates literally “to perform something for a particular purpose.” AHN is a peer-to-peer (P2P), self-forming, and self-restorative kind of network.

Mobile ad hoc networks (MANETs) can immediately form a mobile node network, combined or segregated into discrete networks while in motion. The

R. Bilal

Department of Electrical Engineering, Usman Institute of Technology, Karachi, Pakistan
e-mail: rabilal@uit.edu

B. M. Khan (✉)

Department of Electronics and Power Engineering, National University of Sciences and Technology (NUST), Islamabad, Pakistan
e-mail: bmkhan@pnc.nust.edu.pk

© Springer Nature Switzerland AG 2021

A. Khelassi, V. V. Estrela (eds.), *Advances in Multidisciplinary Medical Technologies — Engineering, Modeling and Findings*,
https://doi.org/10.1007/978-3-030-57552-6_11

155

MANET's nodes depend on the networking requirement and vigorously handle the leaving or joining of network nodes. The main objectives of a MANET include reliability, availability, and scalability. The nodes in the network are self-governing processing devices with low capacity that are capable of moving freely, and due to this factor, the topology of the network changes swiftly, randomly, and periodically. Each network node can host or route (i.e., to transmit the data to other nodes). The achievement of communication is hugely reliant on the cooperation of the other nodes. Nodes are responsible for vigorously finding out the other nodes themselves for the communication in the wireless range. If MANET nodes keep on moving, then this results in a break in connection as well as the restoration capacity frequently. Moreover, the maximum number of nodes in a network has limited resources when it comes to battery power, as well as on computing ability, so the conventional computing routing protocols are not fit for MANET.

The devices, which are part of MANET, include handheld devices like smartphones, laptops, smartwatches, pocket PCs, or any wireless mobile devices. These devices are normally easy to carry and have batteries in them. Figure 11.1 shows an illustration of a heterogeneous mobile ad hoc network and its communication with different devices.

The extracted blood cell features turn out to be the input to a classification stage that categorizes the cells according to hematological models automatically. The classification module should identify the blood cells relying on the extracted features from real images. When it comes to noisy images, this can impair the classification.

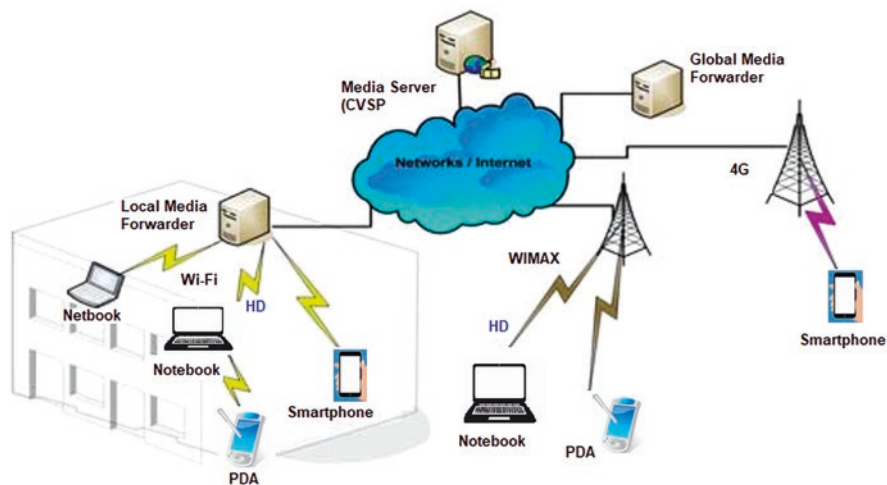


Fig. 11.1 Heterogeneous mobile ad hoc network (MANET)

11.1.2 Vehicular Ad Hoc Networks (VANETs)

Vehicular ad hoc networks (VANETs) have fully fledged out of the necessity to support the increasing amount of wireless products that can now be used in vehicles [1, 2]. Keyless entry devices, tablets, laptops, and smartphones are some of the wireless products. As mobile wireless devices and networks become more and more vital, the demand for vehicle-to-vehicle (V2V) and vehicle-to-infrastructure (V2I) communication will augment day by day [2]. VANETs can be used for an extensive range of safety and non-safety applications, e.g., automatic toll payment, traffic management, enhanced navigation, vehicle safety, location-based services, and search for the nearest place for service/entertainment (such as fuel station, restaurant, and motels) [3] as well as information applications employing the Internet. VANET's works are threefold and briefly described as follows:

Vehicle-to-Vehicle (V2V): It involves a Wireless Area Network (WAN) where vehicles converse through messages about the activities they are performing. This information includes many things like their speed, location, direction, braking, and loss of steadiness. DSRC (dedicated short-range communication) technology from V2V communication is a standard set by organizations like FCC and ISO. The frequency used in this communication is 5.9GHz, which is the same as the frequency of Wi-Fi, but calling it a Wi-Fi network is not appropriate. It can be called a Wi-Fi like a network. The range that is covered by the vehicles in this network is up to 300 m. The topology used in this network is mesh; it means that every node, it could be a car or a signal, can send, receive, and capture the signals. V2V network allows the vehicles to communicate with each other without depending on permanent infrastructure support and can be mostly used for safety, security, and dissemination applications (Fig.11.2).

Vehicle-to-Infrastructure (V2I) or On-Board Unit (OBU): It plays a vital role in the coordination of the vehicles. The radio transceivers are known as roadside unit (RSU), so that vehicle and the roadside transceiver communicate with each other for safety, security, and traffic management purpose. These networks collect the information of local signals and the road conditions and then impose some policies on the group of vehicles connected to the network for many useful purposes (Fig.11.3).

Vehicle-to-Vehicle-to-Infrastructure (V2V2I) or Hybrid Architecture: It merges both vehicle-to-vehicle and vehicle-to-infrastructure. In this type of communication, a vehicle can exchange the information with the roadside infrastructure either in a single hop or multi-hop manner, based on the distance, i.e., if it cannot approach the roadside unit directly or vice versa. It enables the vehicles to communicate with each other that are distant or allows a long-distance Internet connection for vehicles. V2V2I is a bit different from the other two types of communication that are discussed above (Fig.11.4).

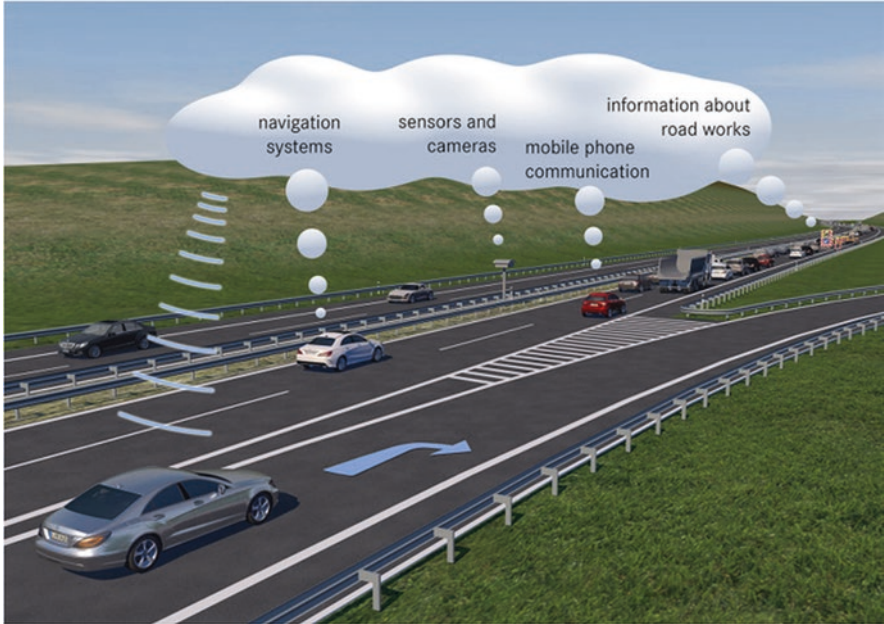


Fig. 11.2 Vehicle-to-vehicle (V2V) communication

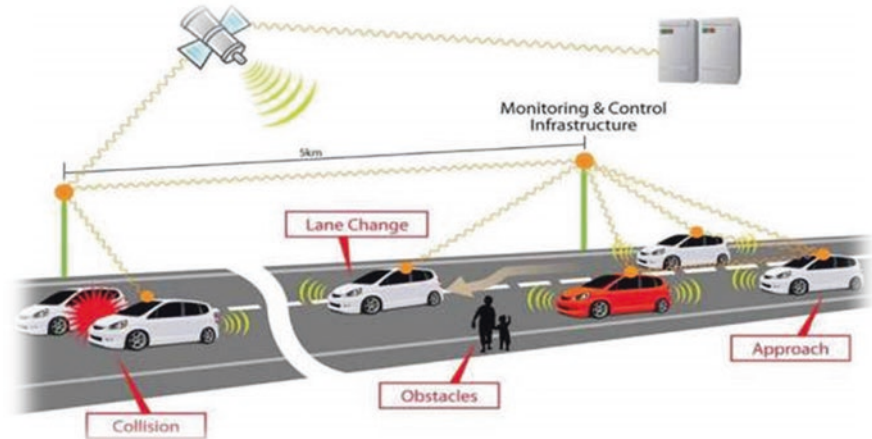


Fig. 11.3 Vehicle-to-infrastructure (V2I) communication

11.1.2.1 Distinguishing Features of VANETs

VANETs have become an important research area for developing countries by increasing their traffic situation day by day. VANETs which belong to the clan of mobile ad hoc networks (MANETs) have distinctive features when compared to

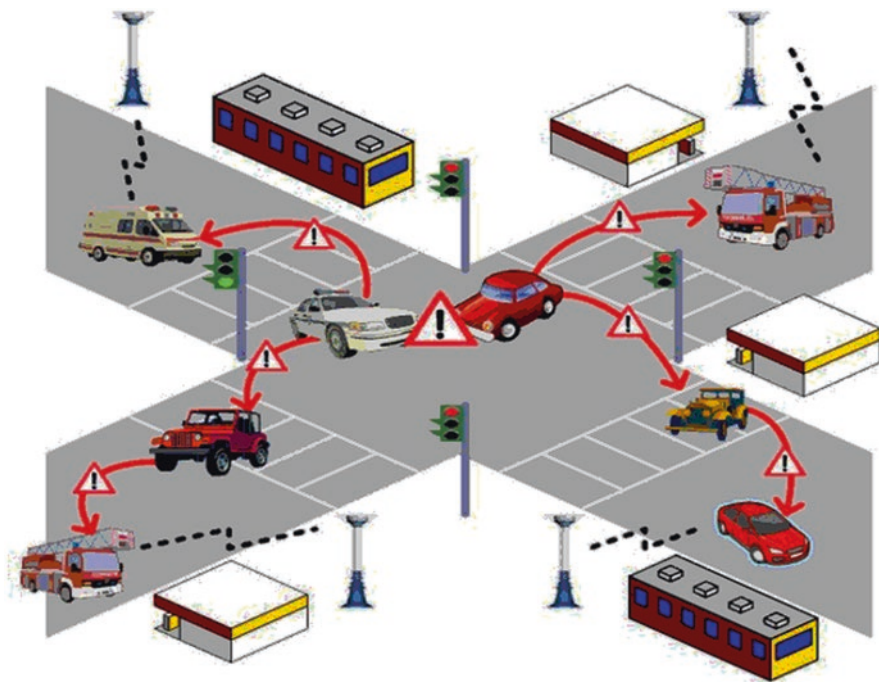


Fig. 11.4 Vehicle-to-vehicle-to-infrastructure (V2V2I) communication

MANETs, and some of them are as follows:

1. *High Computational Capability*: Nodes in the VANETs are vehicles with sufficient sensors and assets for processing, such as a Global Positioning System (GPS), processors, and large memory capacity. These resources are the most significant factor for the increasing capabilities of the nodes, which help in resulting the reliable communication by getting precise information about the vehicle direction, speed, and its current position [4, 5].
2. *Expected Mobility*: The mobility of VANETs is much more predictable than the one from MANETs. The last type of vehicular network node moves randomly, whereas in the VANETs the vehicles (nodes) usually follow the topology defined from the road in which they obey the traffic lights as well as the road signs, which results in the predictability of its movements [6–9].
3. *No Energy Problems*: Energy is not a big issue in VANETs as compared to MANETs because cars continuously provide enough power to OBU by the use of long-life battery [5, 7, 10].
4. *Variable Density in Network*: This factor only depends on the density of the traffic, and it can be low (as in residential traffic), or it can be very high (like during a traffic jam) [9, 10].
5. *Hefty Networks*: The network size in the VANETs varies from small to large such as rural areas, urban areas, highways, or a metropolitan city [9, 10].

6. *Immediate Alterations in Network Topology*: Vehicles traveling on the motorways with the high speeds can change the topology of the network instantaneously, and by this, the received information can affect the performance of the driver [8–10].
7. *Assurance of Harmless Driving*: This thing is only possible when the efficiency of the traffic is improved. The communication between the nodes is direct through VANETs, which allows the pack of applications that needs direct communication among the vehicle over the network. Additionally, these applications offer cautioning data to travelers moving along a similar course concerning the criticalness for quick hard breaking or about mishaps. In this manner, the driver needs to make a bigger picture of street topology ahead. Moreover, VANETs can likewise enhance voyager fulfillment and improve movement effectiveness by demonstrating data, for example, shopping malls, service station, climate, restaurants, and hotels [7].
8. *Time Critical*: The data in the VANET network must be delivered to the nodes at a particular time so that it will be easy for the node to make a quick decision and make some action rapidly.

11.2 Vehicular Network Challenges

11.2.1 Mobility

Evidently, in an AHN, each node is mobile, and it keeps on moving from one place to another within the coverage area. Still, mobility is restricted, but when it comes to VANET nodes, they possess high mobility. In this type of network, vehicles connect with other vehicles they never faced before. This connection may not stay as long as the time these vehicles travel their paths, and they may not meet each other again. So, it is a severe problem to secure the mobility challenge [11].

11.2.2 Volatility

The connectivity between the vehicles for communication can be extremely fugacious. This communication might not happen again as the nodes are traveling through their coverage area and build up its link with other nodes. These links/connections will be mislaid due to the high mobility of the vehicles, and they might be move in the opposite direction [11, 12]. Lacking the relatively long-life context will be found in these networks, so the private interaction from the customer's device to the hot spot will need long-life passwords, which seem to be unrealistic for the security of the virtual connection [13].

11.2.3 Verification in Terms of the Privacy

For the prevention of the different attacks on the network, the verification process of the node is vital, and unique or specific identity can be given to the individual vehicle to overcome this problem, but this is not the proper solution for most of the users. These users want to retain their info secure and private [11, 12].

11.2.4 Responsibility in Terms of the Privacy

For legitimate inquiry, responsibility will be an excellent option. This information cannot be repudiated by any user in case of collision and accidents [11]. Furthermore, it is imperative to keep the privacy of the user from others, and they can keep their personal information (ID, account number for toll collection, route, etc.) safe from other drivers as well [13].

11.2.5 Scalability

When it comes to scalability, these networks are vast enough, and their scalability is increasing day by day due to the increment of the vehicles. Moreover, another problem is this network has not any standards that govern by any authority or firm. The DSRC standards for each country vary from one another, and it also varies from vehicle to vehicle [13].

11.2.6 Routing Protocol

To create a new protocol that will be able to guarantee the delivery of packets in the small time frame with low packet drops will be considered as a severe issue for VANETs [14–17].

11.2.7 Trifling Operative Diameter

The small diameter results in a weak connection between the nodes during the communication. Hence, it is unfeasible to sustain the topology of the network global for any node [18].

11.2.8 Fading of Signals

Fading occurs due to the obstacles that are placed between the nodes, which are exchanging the information. The barriers can be static, like buildings and other moving vehicles. The effect is that these obstacles fade the signal and try to stop the signals to reach its desired destination [15].

11.2.9 Bandwidth Restrictions

This type of network does not have a centralized coordinator responsible for handling contention as well as bandwidth. Due to the limited range of frequency, the channel congestion probability is high when it comes to the high-density location.

11.2.10 Connectivity

High mobility is the main reason for the frequent disconnections in the network, and the required duration for exchanging the information would be enhanced. It is necessary to increase the transmission power to achieve this goal. Still, it will affect the degradation of throughput.

11.3 Architecture of VANETs

The population of vehicles is also increasing rapidly on roads, which results in the difficulty in driving and making it more dangerous and challenging day by day. Roads are packed with lots of vehicles, the rules that are speed and safety distance are rarely followed, and there is a lack of concentration in travelers while moving on the road. The following are the main objects present in VANET architecture.

11.3.1 On-Board Unit (OBU)

The first thing that comes in VANET architecture is OBU that is usually mounted on-board of a node. This device uses the wireless access in vehicular environment (WAVE) technology for the interchanging of information with other units or with roadside units (RSUs). Any OBU must include a user interface for storing and retrieving messages from memory. It processes all the same things a processor does while being a network sort of interface that creates a link with other OBUs. Last, it

is a wireless device for the short communication range that works on 802.11p protocol from the MAC standard for VANETs. A wireless channel is also needed for the connection between the different OBUs/RSUs, and this also works on the IEEE 802.11p standard, which is responsible for the interchanging of messages between OBUs/RSUs. The foremost responsibility of an OBU comprises information security, IP mobility, routing concerning geography, message transfer with reliability, and congestion control in the network [19].

11.3.2 Application Unit (AU)

AUs are gadgets inside the vehicle that utilize the administrations provided by the supplier by abusing OBU capabilities. AU can be any kind of PDA to associate with the Web or a gadget devoted to security applications. A wired or remote association is utilized to associate the AU to the OBU and may be kept in one physical unit with the OBU. The contrast between OBU and the AU is coherent.

11.3.3 Roadside Unit (RSU)

The roadside units (RSU) are the devices that use WAVE protocol, located in places like parking areas, signals, the road segment, or junctions. The RSU is equipped with a dedicated module for the short-range-based communication through radio within the network infrastructure. Different network devices may also be fitted out with RSUs, as shown in figures. The RSU primary operations, which are associated with congestion control communication consortium, are:

1. The enhancement in the range of the network can be achieved through the redistribution of the messages to different OBUs and relaying messages to RSUs so it can be transmitted to different OBUs.
2. It runs for safety purpose applications like accident warning, natural disaster warning, and work zone by using communication of V2I, which serves as a source of information.
3. The Internet connections are provided to OBUs through these units.

11.4 MANETs vs VANETs

The relationship between both types of ad hoc networks is that nodes are self-sustaining and can handle information by themselves without any infra. VANETs have some distinctive features, and it is a subclass of MANETs.

11.4.1 Quickly Variable Topology

In both kinds of network, topology changes swiftly as the nodes are mobilized and cannot stay in a network for long; however, in VANETs the speed of the nodes is comparatively high as compared to MANETs, so the network topology in VANETs is frequent and very fast. In VANETs, topology can be predictable as the vehicles follow the road path, while in MANETs, the nodes can be moved anywhere, and its topology is not that predictable.

11.4.2 Repeated Interruptions

Change in rapid topologies causes frequent interruption in the network. In VANETs, the probability of disconnections is very high as compared to MANETs because the connection between vehicles can disconnect very rapidly due to the high speed of the vehicles. The issue of interruptions becomes more inferior if the density of nodes varies.

11.4.3 Energy Constraint

In VANETs, the nodes do not have any energy restrictions as compared to MANET.

11.4.4 Production Cost

When it comes to implementing the cost to produce, the MANET network is much cheaper than the VANET as both networks have different types of nodes and their manufacturing cost of the equipment varies.

11.4.5 Reliability

When it comes to reliability, a VANET is much more reliable than the MANET because, in MANET, the security factor is much lower than the VANET. Further differences on which both networks differ from each other are mentioned in the below table (Table 11.1).

Table 11.1 Difference between MANETs and VANETs

S. No	Parameters	MANETs	VANETs
1	Production	Medium cost	High cost
2	Topology	Static	Highly variable
3	Mobility	Slow	Fast
4	Node density	Low number of nodes	High number of nodes
5	Bandwidth	Low rate	High rate
6	Range	Up to 100 m	Up to 500 m
7	Network active time	Depends on node energy	Depends on the vehicle condition
8	Multi-tier routing	Available	Weakly available
9	Reliability	Medium	High
10	Moving pattern of nodes	Random	Regular
11	Addressing scheme	Attribute-based	Location-based
12	Position acquisition	Using ultrasonic	Using GPS and RADAR

11.5 MAC Protocols for VANETs

For the improvement of transport systems, VANETs deliver safety as well as non-safety services to vehicles, and to attain this objective, vehicles need to communicate where there is no collision, and they can efficiently access the channel for communication. Numerous protocols are proposed for vehicular ad hoc networks, which specify the accessing of the channel by nodes in a different manner. Several problems are faced during the designing of this protocol like high mobility of vehicles, rapid change in the topology of the network, multi-channel separation, neighboring channel interference, and hidden node issues. MAC is categorized into three broad classifications, including contention-based, contention-free, and hybrid MAC protocols (Fig.11.5).

11.5.1 Routing Protocols for VANETs

Routing protocols in VANETs are categorized into five types, which include topology-based, cluster-based, position-based, broadcast, and geo-cast-based routing protocol. These protocols are characterized based on the types where their work and applications are more appropriate.

11.5.1.1 Topology Routing Protocol

This protocol uses information on the links in the network to forward the packets to the nodes. Further, they are divided into reactive and proactive protocols.

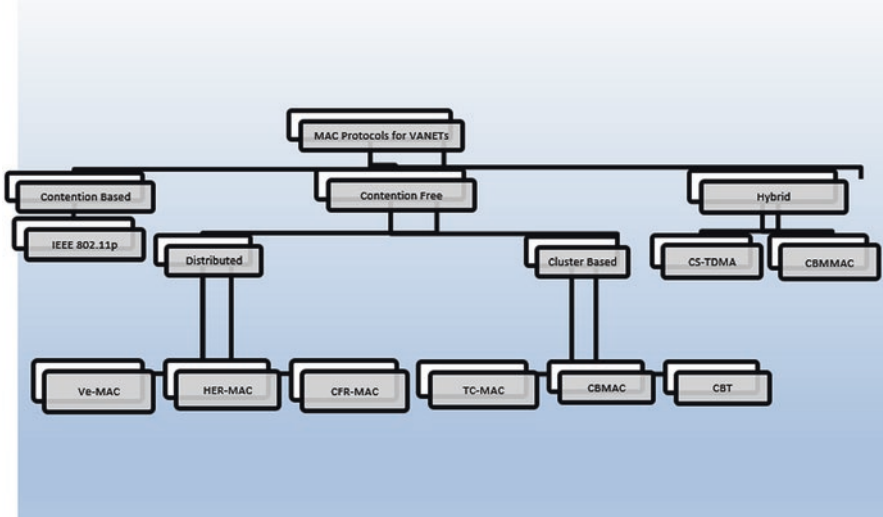


Fig. 11.5 Types of MAC protocols

Reactive Routing

In this type of protocol, the route for the node is only open when it is required for a node to communicate. It only retains the routes that are presently in use during routing, which decreases the burden of the network. This protocol discovers a route by flooding the network nodes and paths with a route discovery packet. This phase ends when the route from source to destination is found. The well-known reactive routing protocols are AODV, DSR, TORA, and PGB [20–23].

Proactive Routing

This routing protocol keeps the information about routing for the next hop in the background regardless of communication needs. As a benefit, this protocol lacks the route discovery phase for the next hop or destination that is saved in the background. Nevertheless, with this advantage comes a drawback of this protocol: for real-time applications, it provides low latency. The routing table is created and maintained in the node. Consequently, the next hop is already defined as the packet when it arrives at the node. Moreover, the protocol keeps the idle paths during communication, thus reducing the available bandwidth of the network. Well-known proactive protocols include DSDV, LSR, OLSR, and B.A.T.M.A.N[24–28].

Cluster-Based Routing Protocol

In this type of routing, a cluster is formed between the groups of nodes. From these nodes, one node becomes the head of the cluster that broadcasts the packets to other cluster heads and the gateway. Scalability can be achieved by using this protocol for large networks, but highly mobile network overhead and delays are experienced. Virtual infra must be formed in this protocol so that it can provide the scalability in the network. Well-known protocols are CBLR, RLSMP, AWCP, CBVANET, and COIN [29–31, 64].

Position-Based Routing

This class of routing algorithms shares geographical positioning properties to select the next hop to transmit the packet without any prior information on the neighborhood map. A neighbor is, by definition, one hop away, close to the destination node. These routing protocols are valuable as there is no requirement to create and maintain the communication path between the source and destination node. This protocol possesses two categories: delay-tolerant and position-based greedy V2V protocols. Examples of such protocols include GPCR, CAR, DIR, MOVE, VADD, and SADV.

Broadcast Routing Protocol

These types of protocols are commonly used in this network for traffic, weather, sharing, road conditions, and emergency between the vehicles and also for conveying broadcasts and commercials among the vehicles. Well-known protocols comprise DV-CAST, V-TRADE, BROADCAST, and UMB.

Geo-cast Routing Protocol

It is multicast routing based on the location. It sends the packets from a source to other nodes that are in the geographical range of the network, also known as the zone of relevance. Vehicles that are not in the range of ZOR are unable to get alerts so that the vehicles can avoid unwanted rapid response. In this routing, an origin zone forwards the flooding of packets. This flooding strategy diminishes congestion and message overhead of the network, which is caused by flooding the packets to the entire network. Unicast routing is performed in the destination zone for the forwarding of the packets. A drawback is the apportioning of the network and the hostile neighbors that can hinder the packet forwarding. Instances of this routing are IVG, Cached Geo-cast, abiding Geo-cast, DRG, ROVER, and DG-CastoR.

11.6 Theoretical Analysis of Routing Protocol for VANETs

In this segment, basic AODV will be discussed. Node movements in VANETs make them different from MANETs and corresponding routing protocols [32–34]. Nonetheless, these protocols will give a poor performance on directly applying to the VANETs due to differences in both networks [35]. In VANET networks, topologies changes dynamically and also lack the bandwidth resources, so it is not compulsory to sustain the route of each node. This frequent change of topology affects the effective timing of routing and also reduces the routing rate information. Thus, the protocols that are considered good for VANETs are on-demand routing protocol.

Protocols that come under the umbrella of on-demand follow two processes, i.e., route discovery and maintenance. The route discovery initialization process starts when the source node, which does not have any routing information in its table, needs to form a route to the destination—routing request packets flooded by the source node on the entire network through broadcasting. On the receiving of a route request packet, the destination node sends a route response packet to the source that creates a reverse-path between both nodes. The route maintenance process activates when the definite link of the activated path breaks or on the changing of the node. AODV [36–38], one of the most critical routing protocols in MANETs, also needs an improvement when applied to the VANETs.

11.6.1 Basic AODV

AODV is one of the most popular routing protocols among the ad hoc networks, and it is a reactive protocol. All the routes do not maintain in AODV all the time. When there is a need for the transmission route discovery of the process that starts by decreasing its overhead, the sequence number is used to make sure the freshness of the routes and is also a loop-free topology, which makes this protocol unique. This protocol embraces three phases: route discovery, data transmission, and route maintenance.

11.6.1.1 Data Transmission

After the course revelation stage, the information transmission stage takes put, and the parcels begin to transmit from the source hub to the goal through the same course built up prior. A few of the hubs may pull back themselves from the radio extend as the hubs are energetic and keep on moving, which causes the breakage in connect and transmission stops.

11.6.1.2 Route Maintenance

The course support prepare tries to repair the same interface or to set up a modern course to the goal hub. In this handle, the hub whose interface breaks produces a Course Blunder (RERR) bundle and sends back to the source. On the accepting of this bundle, the source hub looks in its directing table to see up the ancient route to the goal. If there's a course, the source chooses it and once more begins the transmission of information. Else, the source restores the other course to the goal hub and begins its transmission.

11.6.2 Basic AODV Drawback

In route discovery, the RREQ packets are forwarded to nodes adjacent to the source. Due to this process, the entire network is flooded by RREQ packets, which increases the routing overhead of the network as well as upsurges bandwidth consumption. Moreover, more than one route is found by the source node to the destination. The source node chooses a route with the newest sequence number or fewer hops though the route is not long-lasting to complete the transmission specifically in high dynamic VANETs.

11.6.3 Comparison Conclusions

Due to different features of MANETs and VANETs, the MANET protocol cannot be applied directly to the VANETs as it will give poor performance. As compared to other protocols, AODV performs better because of its quick reactiveness capability toward the changing network and establishing the route on demand. In [39], the method proposed by the authors is to add a packet header in the RREQ packet. The results of the simulation illustrate the smaller transmission delay, but there is a trade-off in the packet delivery rate. In [40], the speed and the position are used as information to assess the routes' lifetime and to select the longest lifetime route after evaluating the delivery of packets. Through this method, routes are stable, but in contrast, it increases the control overhead. In [41] the mechanism of route discovery is of two types: quick route discovery mechanism and traditional AODV mechanism. This protocol searches for the route through the first mechanism. If any path is not found, then it uses the second mechanism for the route discovery. On the traditional one, the entire network is flooded by the control packets, which increase the overhead of the network.

11.7 Simulation Results and Protocol Enhancement

This chapter discusses the outcomes of the simulation made for vehicular ad hoc network (VANET) protocol [42] in our designed network model for the performance parameters mentioned in Sect. 11.3.1. This chapter comprises two sections. The first section of the text shows a normal simulation mode of the WAVE [43] protocol in our designed network model. The second part shows the outcomes of enhanced WAVE protocol for VANET using cooperative communication.

11.7.1 802.11P Normal Simulation

Following are the parameters used for the normal simulation mode of 802.11p in our designed network model, as discussed in Sect. 11.3.3:

- (a) SNR point range = 10:20
- (b) MCS = 4
- (c) PSDU length = 10
- (d) No. of users = 20
- (e) No. of packets = 1000
- (f) No. of packet errors = 50

11.7.1.1 SNR (dB) vs PER Graph

This section gives the outcome in Fig. 11.6 as calculated Packet Error Rate (PER) concerning the number of signal-to-noise ratio (SNR) points simulated [44]. In this case, 1000 data packets are first created as discussed in Sect. 11.3.3 and then are passed through the additive white Gaussian noise (AWGN) channel to be simulated on SNR points mentioned. Here, packets are simulated from the SNR range between 10 dB and 20 dB with an interval of 1. Detailed results in the form of exact numeric values of Packet Error Rate (PER), number of packets correctly received at each SNR point, and number of error packets [45] are discussed and given as outcome received on MATLAB command window in Part 11.7.2.

11.7.1.2 Throughput in Percentage per User

This section gives throughput in the percentage of the network in Fig. 11.7. The throughput we are getting against each user/node is being simulated using standard/normal conditions of 802.11p protocol [46] against the packets transmitted at each SNR point. The percent throughput for each user decreases as the number of VANET users or nodes grows because of the increasing number of users sharing packets. This also shrinks the throughput. The exact value of throughput in percentage against each user is mentioned as MATLAB command window output in Sect. 11.7.2.

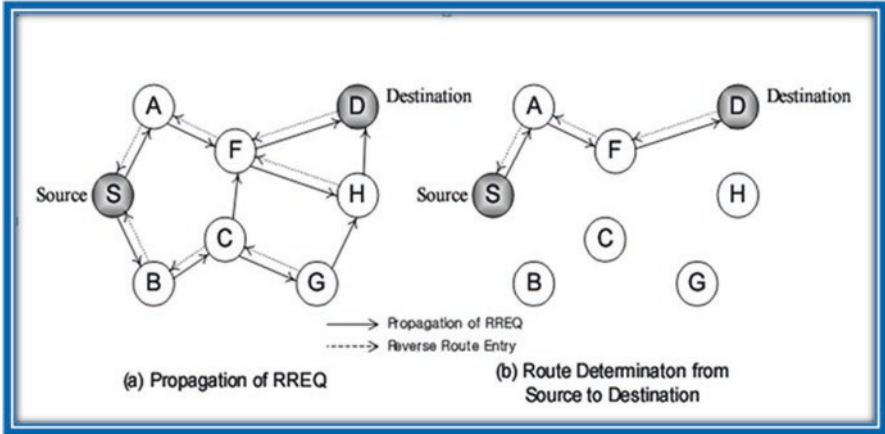


Fig. 11.6 Basic AODV routing protocol mechanism

11.7.1.4 Latency per User

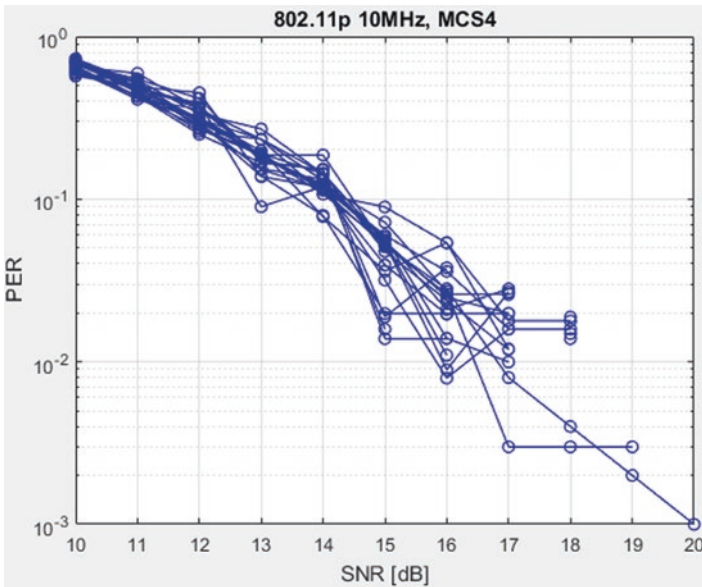


Fig. 11.7 SNR-PER Simulation at 802.11p normal mode

11.7.1.3 Bandwidth Utilization

This section shows the bandwidth utilization of the IEEE 802.11p protocol against the highest percentage of throughput received on the network. As 802.11p uses 10 MHz channel bandwidth in the frequency range of 5.85–5.925 GHz [47–49], the exact utilization of its 10-MHz band appears in Fig. 11.8.

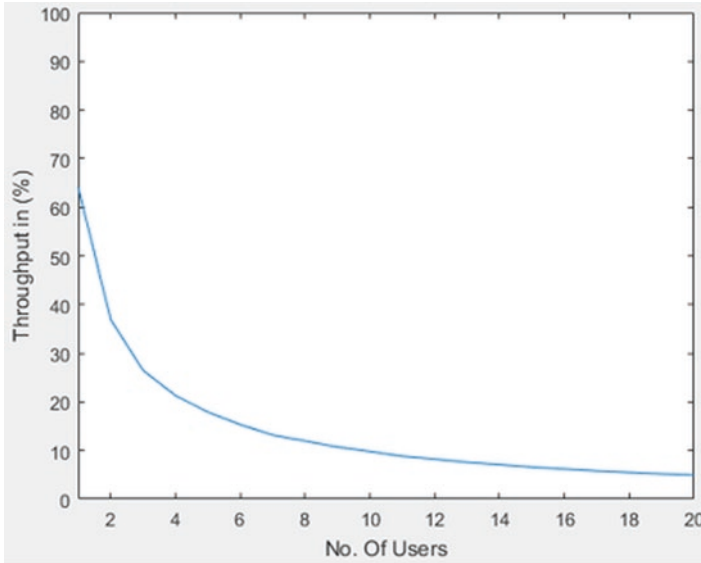


Fig. 11.8 Throughput in % per user for 802.11p normal mode

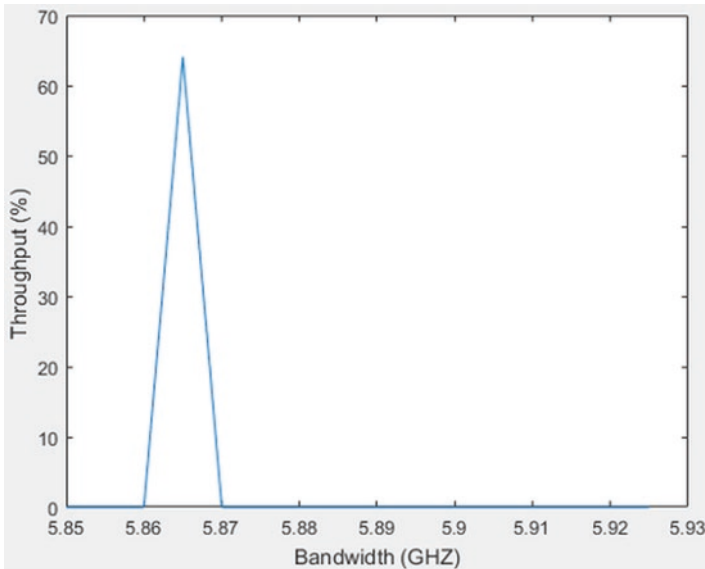


Fig. 11.9 Bandwidth utilization at the IEEE 802.11p normal mode

Network latency per user against the throughput received [50] on the network can be seen in Fig. 11.9. As the number of users on the network increases, the latency per user also grows, indicating that as the network gets busier with the number of

vehicular nodes rises, it will take more time to share data packets between them as throughput across each user decreases.

11.7.2 Data Results on the Command Window for the IEEE 802.11p Normal Simulation

This section explains the output waveforms of the first four sections. These values are obtained as the MATLAB command window outcome of normal simulation mode of 802.11p protocol. As discussed in the methodology of the subsection of 11.3.3, the values of how packets are transferred at each SNR point against each user can be seen below. As 1000 packets are transmitted with 50 error packets at an SNR range from 10 to 20, below-mentioned values give a complete simulation range of each user at every SNR point.

First, 72 packets were transferred with SNR = 10 dB, which gives a PER of 0.708 with 51 packets [51] received with error considering the below-mentioned outcome of USER 1. The PER is calculated by dividing the number of error packets by the number of packets correctly received [53]. It is to make clear that 72 packets are not transmitted due to the presence of 51 error packets. Hence:

$$N_{pcr} = N_{tp} - N_{ep},$$

where:

N_{pcr} = number of packets [52] correctly received

N_{tp} = number of total packets received at an SNR point

N_{ep} = number of error packets received at that SNR point

Therefore, here for the first value of USER 1 at SNR = 10 dB, the number of actually corrected packets received becomes $72 - 51 = 21$.

Means 21 packets are correctly received, and rest 51 are error packets [54], which are still present. Similarly, at SNR = 16 dB for USER 1, we can see that number of packets transferred has reached its maximum limit as 1001. But the number of error packets has started decreasing now to 28. This shows that still complete 1000 packets are not transferred properly through an SNR range, and correctly received packets at SNR = 16 dB using the same formula mentioned just above is $1001 - 28 = 973$ successfully received packets, and 27 packets are still left. From here on, the number of error packets that were maximum started decreasing to correctly transmit the total number of corrected packets [55] and at SNR = 20 dB. The number of error packet is reduced to 1, only mentioning that all 1000 packets are correctly transmitted now.

This is the reason for selecting the SNR range from 10 dB to 20 dB, because IEEE 802.11p packetsok at non-HT configuration objects start transmitting packets from SNR = 10 dB and almost complete its transmission at SNR = 20 dB.

The same mechanism goes for USER 2 and onward. The only change is that as the number of users increases, the total number of transmitted packets mutually shared between the users available on the network and its impact on the SNR of the simulated points grow.

11.7.3 802.11P Simulation with Cooperative Communication

The same parameters, as used in Sect. 11.4.1, are used here. But for enhancement of 802.11p in our designed network model, user cooperation is used adding relaying [56] concept reducing path length and delays as discussed in the previous section:

- (a) SNR point range = 10:20
- (b) MCS = 4
- (c) PSDU length = 10
- (d) No. of users = 20
- (e) No. of packets = 1000
- (f) No. of packet errors = 50

11.7.3.1 SNR-PER Graph

The response of user cooperation can be seen in Fig. 11.10 in the form of the SNR-PER graph as enhanced the IEEE 802.11p protocol is now simulated hereafter implementation of cooperative communication. We observe more packets received at each SNR point with the implementation of the technique from Sect. 11.7.2. A MATLAB command window interface displays the exact numeric values. The authors would like to explain that the same number of packets is simulated, even after incorporation of cooperative communication, with the same number of error packets, and the same simulated SNR points for a comparative analysis between the actual normal mode present simulation results of the IEEE 802.11p protocol and the enhancement made via user cooperation.

11.7.3.2 Throughput in Percentage per User

Figure 11.11 alludes to the network throughput [57] in percentage per user. The highest network throughput in normal simulation on a shared network was 64%, but this throughput considerably increases to more than 90% when the node/users cooperate with the relay nodes incorporated. The detailed numeric value results appear in Sect. 11.7.2.

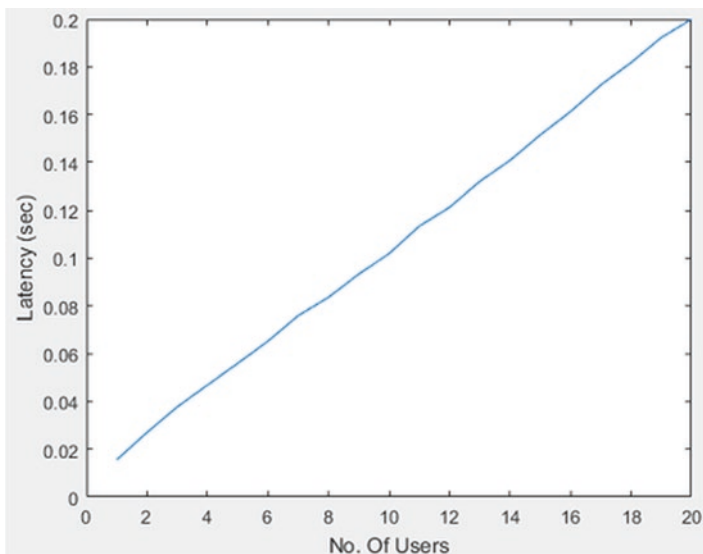


Fig. 11.10 Latency per user for 802.11p normal mode

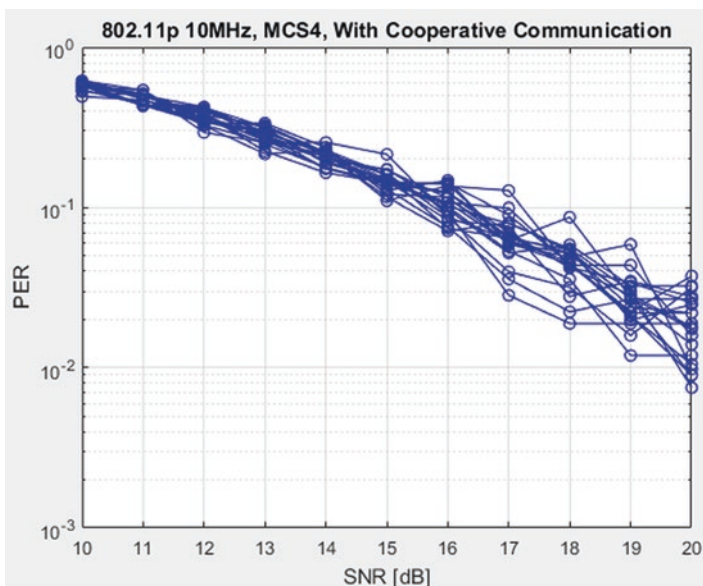


Fig. 11.11 SNR-PER simulation at the IEEE 802.11p with cooperative communication

11.7.3.3 Bandwidth Utilization

The enhancement in bandwidth utilization [58] due to better throughput received in that same 10 MHz channel of the IEEE 802.11p [59] appears in Fig. 11.12 with the incorporation of user cooperation. The channel in this scenario is also using that same range of 10 MHz between 5.86 GHz and 5.87 GHz for enhancement is in the form of better throughput against network usage.

11.7.3.4 Latency per User

The user cooperation clearly shows a fair decrease in network latency per user, as in Fig. 11.13 compared to Sect. 4.1.4. Likewise, the latency grows with an increase in the number of users on a network and a decrease in throughput [60], respectively. However, the users need not take a long time enough as earlier with the incorporation of cooperative communication and can be more quick and reliable with the help of relay nodes having better throughput on the enhanced protocol (Fig. 11.14).

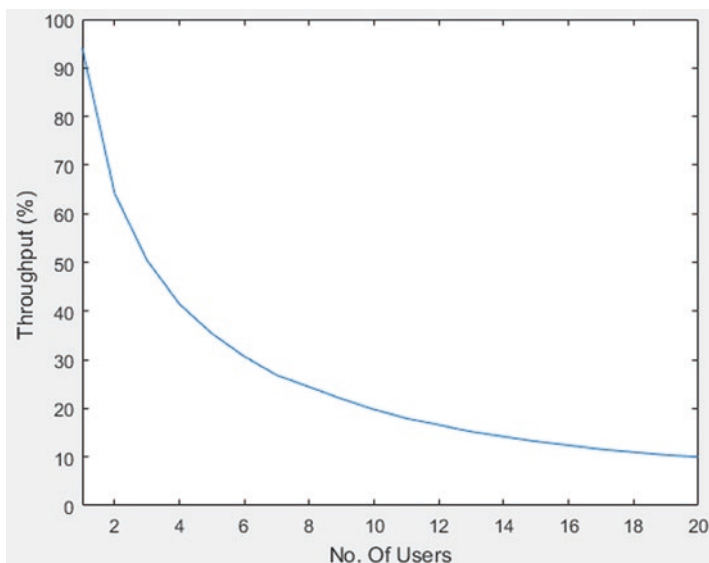


Fig. 11.12 Throughput in % per user for the IEEE 802.11p with cooperative communication

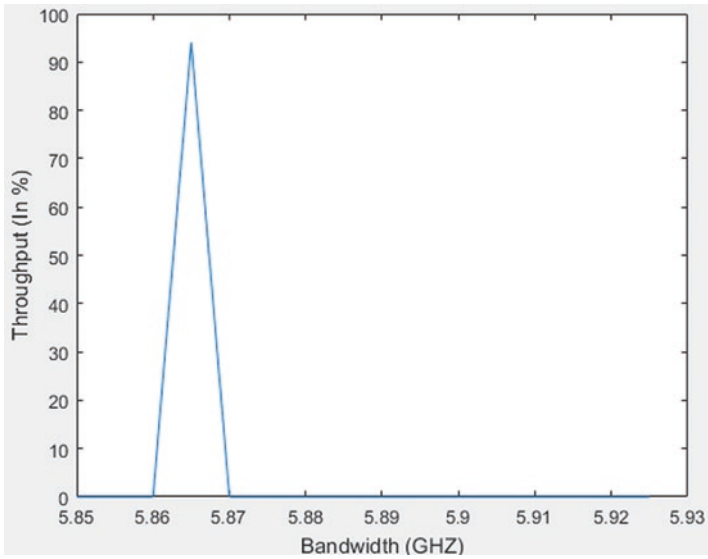


Fig. 11.13 Bandwidth utilization for the IEEE 802.11p with cooperative communication

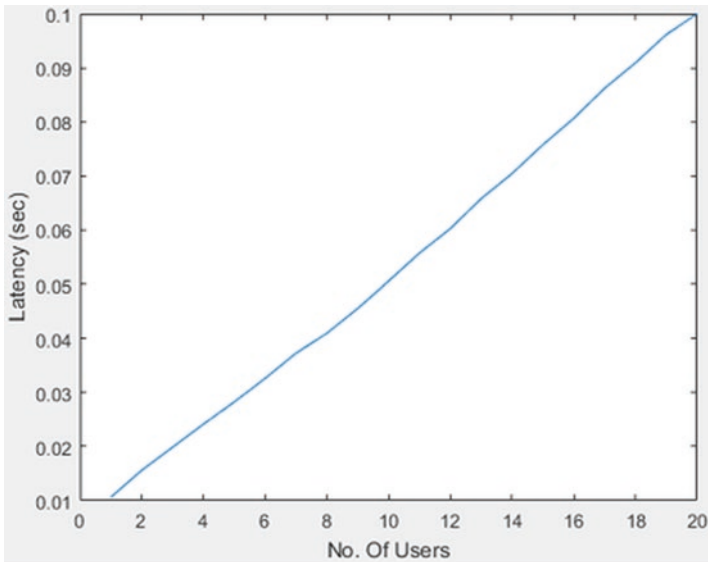


Fig. 11.14 Latency per user for the IEEE 802.11p with cooperative communication

11.7.3.5 Data Results on Command Window with the User Cooperation

After the implementation of cooperative communication for enhancement in the IEEE 802.11p standard protocol, the results in this subsection present exact numeric values obtained via the MATLAB command window interface, and they show a fair improvement [61] in the form of more packets transmitted at each SNR point. This can be checked and verified by observing any number of packets received at any SNR point for any USER below and comparing it with the ones received from Sect. 4.1.5 in normal simulation model using the IEEE 802.11p standard protocol.

11.8 Conclusion

The appropriate supervision of personal health-related data is paramount to healthcare. The foremost challenge for all stakeholders is to handle health records that will be available to all parts and the healthcare providers involved. In recent times, the utilization of wireless sensors and actuators in the medical arena has been augmenting tremendously due to the need to observe/follow patients and hazardous environments in real-time. An important topic is the deployment of healthcare-oriented vehicular ad hoc networks that converse with wireless sensor networks.

The implementation of the intelligent transportation system (ITS) [62] is a priority in all over the world due to the increased number of vehicles on roads, especially in a country like Pakistan, where the population is increasing day by day with limited resources to survive. Continuous jam-packed roads are prevalent nowadays, leading to an increase in travel time of vehicles from minutes to hours. Deadly accidents on highways due to smog or non-indication are no more any new thing that may suddenly have happened. This gives rise to the introduction of vehicular ad hoc networks (VANETs) in such type of traffic environment.

This research focuses on the protocol used for VANET, i.e., WAVE [63], which uses the IEEE WLAN protocol standard of 802.11p. A type of cooperative communication with modified functions is used on the designed network flow of 802.11p protocol to enhance its performance parameters and quality of service (QoS) [74] of a VANET [65]. This research contribution toward society may help in making intelligent transportation system (ITS) [66] even better, safer, and faster as mobile communication between vehicular nodes of a vehicular ad hoc network becomes more reliable [50].

In the future, more attention should be given to multimodality imaging that takes place on each vehicle [67–69]. When an environment and its constituents are mapped, several sources of information must be fused. Furthermore, augmented reality and the option to improve the resolution of regions of interest via, for instance, super-resolution will pose an overhead to the moving network nodes [70,

71]. Besides the issues mentioned in this manuscript, for fleets with a high number of vehicles subject to an intense working regimen, one needs to guarantee reliability, fast processing, and clever node assignment in case they need to make up for node failure and concurrent high-performance computing tasks [72, 73]. It should be stressed that healthcare and disaster mitigation call for a heavy computational load. Such substantial computational demand may call for lighter implementations using metaheuristics [73, 74].

Unmanned aerial vehicles (UAVs) can also serve as ambulance drones to reach the disaster-stricken regions speedier than any conventional rescue vehicles. Such strategy spares time and actions toward handling the unique wellbeing parameters and scenario changes. Flying ad hoc networks (FANETs) resemble MANETs and VANETs, despite their characteristics. UAVs when structured are FANETs, which are mission-based. Their mobility models are habitually determined by the mission purpose and the nature of the undertaking to be accomplished. Thus, FANET routing protocols should consider the types of applications and services involved and the associated mobility models. Nonetheless, routing protocols for FANETs are not an easy task because of the highly dynamic topologies and the flying restrictions they face [75–77].

References

1. M. Raya, J. Hubaux, The security of vehicular ad hoc networks. in Proceedings of the 3rd ACM Workshop on Security of Ad Hoc and Sensor Networks (SASN 2005), Alexandria, VA, 2005, pp. 1–11
2. C. Harsch, A. Festag, P. Papadimitratos, Secure position-based routing for VANETs. in Proceedings of the IEEE 66th Vehicular Technology Conference (VTC-2007), 2007, pp. 26–30
3. M. Gerlach, Full paper: Assessing and improving privacy in VANETs (2006). www.network-on-wheels.de/downloads/escar2006gerlach.pdf. Accessed 29 May 2010
4. S. Olariu, M.C. Weigle, *Vehicular Networks: From Theory to Practice*, 1st edn. (Chapman & Hall/CRC, Boca Raton, 2009)
5. M. Nekovee, Sensor networks on the road: The promises and challenges of vehicular ad hoc networks and grids. in Proceedings of the Workshop on Ubiquitous Computing and e-Research, 2005
6. J. Blum, A. Eskandarian, L. Hoffman, Challenges of intervehicle ad hoc networks. *IEEE Trans. Intell. Transp. Syst.* **5**(4), 347–351 (2004)
7. J. Jakubiak, Y. Koucheryavy, State of the art and research challenges for VANETs. in Proceedings of the 5th IEEE Consumer Communications and Networking Conference. CCNC 2008, 2008
8. F. Li, Y. Wang, Routing in vehicular ad hoc networks: a survey. *IEEE Veh. Technol. Mag.*, 12–22 (2007)
9. Y. Toor, P. Muhlethaler, A. Laouiti, Vehicle ad hoc networks: Applications and related technical issues. *IEEE Commun. Surv. Tutor.* **10**(3), 77–88 (2008)
10. S. Yousef, M.S. Mousavi, M. Fathy, Vehicular ad hoc networks (vanets): challenges and perspectives. in Proceedings of the 6th International Conference on ITS Telecommunications, 2006

11. P.I. Ofor, Vehicle Ad Hoc Network (VANET): Safety Benefits and Security Challenges. Nova Southeastern University (po125@nova.edu), 2012
12. S. Singh, S. Agrawal, VANET routing protocols: Issues and challenges. in Proceedings of the 2014 RAECs UIET Panjab University Chandigarh, 2014
13. S. Ghassan, W.A.H. Al-Salihy, R. Sures, Security Issues and Challenges of Vehicular Ad Hoc Networks (VANET). National Advanced IPv6 Center, Universiti Sains Malaysia Penang, Malaysia (2010)
14. W. Chen et al., A survey and challenges in routing and data dissemination in vehicular ad hoc networks. *Wirel. Commun. Mob. Comput.* **11**(7), 787–795 (2011)
15. H. Hartenstein, K. Laberteaux, A tutorial survey on vehicular ad hoc networks. *IEEE Commun. Mag.* **46**(6), 164–171 (2008)
16. Y. Lin, Y. Chen, S. Lee, Routing protocols in vehicular ad hoc networks: A survey and future perspectives. *J. Inf. Sci. Eng.* **26**(3), 913–932 (2010)
17. M. Zhang, R. Wolff, Routing protocols in vehicular ad hoc networks in rural areas. *Commun. Mag. IEEE* **46**(11), 126–131 (2008)
18. H. Hartenstein, VANET Vehicular Applications and Inter-Networking Technologies. Wiley Online Library (2009)
19. S. Olariu, M.C. Weigle, *Vehicular Networks: From Theory to Practice*, 1st edn. (Chapman & Hall/CRC, Boca Raton, 2009)
20. W.G. IEEE, IEEE 802.11pD2.01, Draft Amendment to Part 11: Wireless Medium Access Control (MAC) and Physical Layer (PHY) Specifications: Wireless Access in Vehicular Environments, March 2007
21. L. Zhang, Z. Liu, R. Zou, J. Guo, Y. Liu, A scalable CSMA and self-organizing TDMA MAC for IEEE 802.11 p/1609. x in VANETs. *Wirel. Pers. Commun.* **74**(4), 1197–1212 (2014)
22. V.D. Khaimar, S.N. Pradhan, Simulation based evaluation of highway road scenario between DSRC/802.11 p MAC protocol and STDMA for vehicle-to-vehicle communication (2013)
23. H.A. Omar, W. Zhuang, L. Li, VeMAC: a novel multichannel MAC protocol for vehicular ad hoc networks. in 2011 IEEE Conference on Computer Communications Workshops (INFOCOM WKSHPS), IEEE (2011), pp. 413–418
24. Y.-C. Lai, P. Lin, W. Liao, C.-M. Chen, A region-based clustering mechanism for channel access in vehicular ad hoc networks. *IEEE J. Sel. Areas Commun.* **29**(I), 83–93 (2011)
25. D.N.M. Dang, H.N. Dang, V.D. Nguyen, Z. Htike, C.S. Hong, HER-MAC: a hybrid efficient and reliable MAC for vehicular ad hoc networks. in 2014 IEEE 28th International Conference on Advanced Information Networking and Applications (AINA), IEEE (2014), pp. 186–193
26. M. Hadded, P. Muhlethaler, A. Laouiti, R. Zagrouba, L.A. Saidane, (2015) TDMA-based MAC protocols for vehicular ad hoc networks: A survey, qualitative analysis, and open research issues. *Commun. Surv. Tutor. IEEE* **17**, no. 4: 2461–2492
27. T.L. Sheu, Y.-H. Lin, A cluster-based TDMA system for inter-vehicle communications. *J. Inform. Sci. Eng.* **30**(1), 213–231 (2014)
28. L. Zhang, Z. Liu, R. Zou, J. Guo, Y. Liu, A scalable CSMA and self-organizing TDMA MAC for IEEE 802.11 p/1609. x in VANETs. *Wirel. Pers. Commun.* **74**(4), 1197–1212 (2014)
29. H. Su, X. Zhang, Clustering-based multichannel MAC protocols for QoS provisioning over vehicular ad hoc networks. *IEEE Trans. Veh. Technol.* **56**(6), 3309–3323 (2007)
30. A. Ahmad, M. Doughan, V. Gauthier, I. Mougharbel, M. Marot, Hybrid Multi-Channel Multi-hop MAC in VANETs (2010)
31. M.S. Almalag, S. Olariu, M.C. Weigle, TDMA cluster-based MAC for VANETs (TC-MAC). in 2012 IEEE International Symposium on World of Wireless, Mobile and Multimedia Networks (WoWMoM), 2012, pp. 1–6
32. D. Johnson et al., Dynamic Source Routing for Mobile Ad Hoc Networks, IETF MANET Draft (2003)

33. S. Jaap, M. Bechler, L. Wolf, Evaluation of routing protocols for vehicular ad hoc networks in city traffic scenarios, 11th EUNICE Open European Summer School on Networked Applications, Spain (2005)
34. E.M. Royer et al., (1999) A review of current routing protocols for ad hoc mobile wireless networks, *IEEE Pers. Commun.* 6 46–55
35. X. Sun, X. Li, Application of VANET to city road traffic management. *J. Shanxi Univ. Sci. Technol. (Natural Science Edition)* 26, 107–109 (2008)
36. C.E. Perkins, E.M. Royer, Ad-hoc on-demand distance vector routing, in *Proceedings of the 2nd IEEE Workshop on Mobile Computing Systems and Applications*, 1999, pp. 90–100.
37. C. Perkins, Ad hoc On Demand Distance Vector (AODV) routing, Internet-Draft, draft-ietf – MANET-aodv-00 (1997)
38. C. Perkins, E. Royer, S. Das, Ad hoc on-demand distance vector (AODV) routing. Internet Draft, Internet Engineering Task Force (2001)
39. B. Li, Y. Liu, G.X. Chu, Optimized AODV routing protocol for vehicular ad hoc networks. *Mobile Congress (GMC)* 2010, 1–4 (2010)
40. V. Namboodiri, M. Agarwal, L. Gao, A study on the feasibility of mobile gateways for vehicular ad-hoc networks, *Proceedings. ACM VANET* (2004)
41. Z. Kai, W. Neng, L. Ai-Fang, A new AODV based clustering routing protocol, 2005 IEEE International Conference on Wireless Communications, Networking and Mobile Computing (2005)
42. <http://omnet-tutorial.com/omnet-aodv-code/>. Accessed on 12 May 2020
43. A. Chakrabarti, A. Sabharwal, B. Aazhang, Cooperative communications. *Coop. Wirel. Networks Princ. Appl.*, (2006), pp. 29–62
44. H. Shan, W. Zhuang, Multi-hop cooperative communication for vehicular ad hoc networks. in 2011 6th International ICST Conference on Communications and Networking in China, 2011, pp. 614–619
45. A. Indra, R. Murali, Routing protocols for vehicular adhoc networks (VANETs): a review. *J. Emerg. Trends Comput. Inform. Sci.* 5(1), 56 (2014)
46. G. Marfia, M. Roccetti, A. Amoroso, M. Gerla, G. Pau, J.-H. Lim, Cognitive cars: constructing a cognitive playground for VANET research testbeds. in *Proceedings of the 4th International Conference on Cognitive Radio and Advanced Spectrum Management*, 2011
47. A. Amoroso, G. Marfia, M. Roccetti, G. Pau, Creative testbeds for VANET research: a new methodology. in 2012 IEEE Consumer Communications and Networking Conference CCNC'2012, 2012, pp. 477–481
48. A. Tomandl, D. Herrmann, K.P. Fuchs, H. Federrath, F. Scheuer, VANETsim: an open source simulator for security and privacy concepts in VANETs. in *Proceedings of the 2014 International Conference on High Performance Computing and Simulation, HPCS 2014* (2014), pp. 543–550
49. P.V.D. Khairnar, D.S.N. Pradhan, Comparative study of simulation for vehicular ad-hoc network. *Int. J. Comput. Appl.* 4(10), 15–18 (2010)
50. H. Dhawan, S.S. Waraich, A comparative study on LEACH routing protocol and its variants in wireless sensor networks: A survey. *Int. J. Comput. Appl.* 95, 21–27 (2014)
51. A.H. Abbas, L.M. Audah, N.A. Alduais, An efficient load balance algorithm for vehicular ad-hoc network. in 2018 Electrical Power, Electronics, Communications, Controls and Informatics Seminar (EECCIS) (2018), pp. 207–212
52. S. Kurkowski, W. Navidi, T. Camp, Discovering variables that affect MANET protocol performance*, *LOBECOM – IEEE Global Telecommunication Conference* (2007), pp. 1237–1242
53. H. Wahid, S. Ahmad, M.A.M. Nor, M.A. Rashid, Wireless networking: fundamentals and applications. *J. Ekon. Malaysia* 51(2), 39–54 (2017)

54. Z. Wang, H. Chen, L. Xie, K. Wang, Retransmission strategies of the generation-based network coding in packet networks. in 2009 15th Asia-Pacific Conference on Communication APCC 2009, no. Apcc (2009), pp. 745–748
55. M. Azfar Yaqub, S. Hassan Ahmed, D. Kim, Asking neighbors a favor: Cooperative video retrieval using cellular networks in VANETs. *Veh. Commun.* **11**(9), 551–511 (2017)
56. W. Fawaz, Effect of non-cooperative vehicles on path connectivity in vehicular networks: A theoretical analysis and UAV-based remedy. *Veh. Commun.* **11**, 12–19 (2018)
57. P. Ostovari, J. Wu, A. Khreishah, Network coding techniques for wireless and sensor networks, *Art Wirel. Sens. Networks Vol. 1 Fundam.*, no. January 2015 (2015), pp. 129–162
58. A.F. Santamaria, C. Sottile, Smart traffic management protocol based on VANET architecture. *Adv. Electr. Electron. Eng.* **12**(4), 279–288 (2014)
59. P.H. Ho, L. Peng, X. Jiang, A. Haque, Special issue on secure and privacy-preserving autonomous vehicle networks (AVNs). *Veh. Commun.* **11**, 32 (2018)
60. F. Mohammed et al. Efficiency evaluation of routing protocols for VANET, *IEEE Vehicular Technology Conference* (2014), pp. 410–414
61. M. Miao, Q. Zheng, K. Zheng, Z. Zeng, Implementation and demonstration of WAVE networking services for intelligent transportation systems. *IOV* (2014)
62. A.A.-R.T. Rahem, M. Ismail, A. Idris, A. Dheyaa, A comparative and analysis study of VANET routing protocols. *J. Theor. Appl. Inf. Technol.* **66**(3), 691–698 (2014)
63. A. Mahajan, D.R. Dadhich, Comparative analysis of VANET routing protocols using VANET RBC and IEEE 802.11p, vol. 3, no. 4 (2013), pp. 531–538
64. H. Teng, W. Liu, T. Wang, X. Kui, S. Zhang, N.N. Xiong, A collaborative code dissemination schemes through two-way vehicle to everything (V2X) communications for urban computing. *IEEE Access* **7**, 145546–145566 (2019)
65. C. Tripp-Barba, L. Urquiza-Aguilar, A. Zaldívar-Colado, J. Estrada-Jiménez, J.A. Aguilar-Calderón, M.A. Igartua, Comparison of propagation and packet error models in vehicular networks performance. *Veh. Commun.* **12**, 1–13 (2018)
66. A. Husain, R.S. Raw, B. Kumar, A. Doegar, Performance comparison of topology and position based routing protocols in vehicular network environments. *Int. J. Wirel. Mob. Networks* **3**(4), 289–303 (2011)
67. A. Arshaghi, N. Razmjoooy, V.V. Estrela, P. Burdziakowski, D.A. Nascimento, A. Deshpande, P.P. Prashant, Image transmission in UAV MIMO UWB-OSTBC system over Rayleigh channel using multiple description coding (MDC) with QPSK modulation, in *Imaging and Sensing for Unmanned Aircraft Systems*, ed. by V. V. Estrela, J. Hemanth, O. Saotome, G. Nikolakopoulos, R. Sabatini, vol. 2, (IET, London, 2020)
68. V.V. Estrela, A.C.B. Monteiro, R.P. França, Y. Iano, A. Khelassi, N. Razmjoooy, Health 4.0: Applications, management, technologies and review. *Med. Technol. J.* **2**(4), 262–276 (2019). <https://doi.org/10.26415/2572-004X-vol2iss1p262-276>
69. V.V. Estrela, O. Saotome, H.J. Loschi, D.J. Hemanth, W.S. Farfan, R.J. Aroma, C. Saravanan, E.G.H. Grata, Emergency response cyber-physical framework for landslide avoidance with sustainable electronics. *Technologies* **6**, 42 (2018). <https://doi.org/10.3390/technologies6020042>
70. A. Deshpande, P. Patavardhan, D.H. Rao, Super resolution based low cost vision system. in 2015 IEEE International Conference on Computational Intelligence and Computing Research (ICIC) (2015), pp. 1–6
71. A. Deshpande, P. Patavardhan, Super resolution and recognition of long range captured multi-frame iris images. *IET Biom.* **6**, 360–368 (2017)
72. H.J. Loschi, V.V. Estrela, D.J. Hemanth, S.R. Fernandes, Y. Iano, A.A. Laghari, A. Khan, H. He, R. Sroufe, Communications requirements, video streaming, communications links and networked UAVs, in *Imaging and Sensing for Unmanned Aircraft Systems*, ed. by V. V. Estrela, J. Hemanth, O. Saotome, G. Nikolakopoulos, R. Sabatini, vol. 2, (IET, London, 2020)
73. N. Razmjoooy, V.V. Estrela, *Applications of Image Processing and Soft Computing Systems in Agriculture* (IGI Global, Hershey, 2019), pp. 1–300. <https://doi.org/10.4018/978-1-5225-8027-0>

74. N. Razmjooy, V.V. Estrela, H.J. Loschi, W.S. Farfan, *A Comprehensive Survey of New Metaheuristic Algorithms* (Wiley, 2019)
75. Ghosal, P., Singh, S., Das, D., Mohiuddin, G., Pandit, S., Das, I. (2019). Ambulance Drone Using Raspberry Pi 3 in Emergency Healthcare
76. H.J. Loschi, V.V. Estrela, D.J. Hemanth, S.R. Fernandes, Y. Iano, A.A. Laghari, A. Khan, H. He, R. Sroufe, Communications requirements, video streaming, communications links and networked UAVs, in *Imaging and Sensing for Unmanned Aircraft Systems*, ed. by V. V. Estrela, J. Hemanth, O. Saotome, G. Nikolakopoulos, R. Sabatini, vol. 2, (IET, London, 2020), pp. 113–132
77. O.S. Oubbati, A. Lakas, F. Zhou, M. Günes, M.B. Yagoubi, A survey on position-based routing protocols for Flying Ad Hoc Networks (FANETs). *Veh. Commun.* **10**, 29–56 (2017)

Chapter 12

The Vedic Design-Carry Look Ahead (VD-CLA): A Smart and Hardware-Friendly Implementation of the FIR Filter for ECG Signal Denoising



K. B. Sowmya, Chandana, and M. D. Anjana

12.1 Introduction

Finite impulse response (FIR) filter implementations abound and play a major part in signal processing applications. The FIR filter (FIRF) delivers several benefits, and there exist many different realizations, such as designs using a system generator, normal FIRF, decimator FIRF, genetic algorithm (GA)-based, and parallel-based, among others. Most architectures utilize more hardware with less efficiency. Moreover, these existing architectures did not concentrate on and explored the applications' characteristics. The FIRF affords several paybacks like (i) computational efficiency in multi-rate frameworks, (ii) manageable linear phase response, and (iii) the desirable numerical ability to accomplish finite precision and fractional arithmetic. The digital multi-standard RFIR filter is implemented in wireless applications to decrease the bit error rate (BER). The discrete FIRF can render efficient designs with low-power consumption and high performance.

Earlier, hordes of research articles described different FIRF designs without handling signal denoising with an effective multiplier design.

Booth's algorithm performs multiplication by multiplying two signed binary numbers in 2's complement notation. The Booth multiplier (BM) overcomes the reduced area drawback, but it would not work with alternation of zeros and ones since it entails more additions and subtractions [1–3].

This problem is overcome by the modified BM (MBM), which contains half the number of partial product rows. It functions well regarding speed and power consumption. On the other hand, its main shortcoming is sloppy work for negative numbers [4, 5].

K. B. Sowmya (✉) · Chandana · M. D. Anjana
Department of Electronics and Communication Engineering, R.V. College of Engineering,
Bengaluru, India
e-mail: chandana.ec17@rvce.edu.in; anjanamahaveerd.ec17@rvce.edu.in

Hence, a nonconventional, nonetheless very efficient multiplier deployment. It relies on Vedic mathematics to deliver high performance because it deals mainly with several Vedic mathematical formulae and their applications for accomplishing bulky arithmetical operations smoothly. Vedic algorithms comprise 16 sutras (or algorithms) and are considered nature-inspired procedures. Among these, two sutras are for Vedic multiplication [3, 6, 7].

This project aims to overcome this hindrance through the Vedic design (VD)-Carry look ahead (CLA), aka the VD-CLA FIRF method.

Multipliers play a paramount role in FIRF design. A reduction of the area in chip occupied by multipliers implies a shrinkage in the total FIRF hardware utilization. Hence, the Vedic multiplier relying on the Urdhva tiryagbhyam Sutra findings augments the speed of operation and reduces the overall hardware utilization. In the accumulator module, carry look ahead (CLA) is used to accomplish the addition process. The Booth multiplier, constructed on a radix 4 encoding scheme, is presented in this work for low-power applications. This design arises as a good option for high-speed DSP applications, thanks to the usage of VD and CLA [8–23].

Section 12.2 of this manuscript brings in a literature examination. Section 12.3 contains the VD-CLA design methodology. Experimental results emerge in Sect. 12.4. Finally, Sect. 12.5 brings in conclusions and prospective improvements to the current design.

12.2 Literature Review

The dynamic system for researchers has suggested several FIR architectures. This section briefly evaluates some significant contributions to the field of FIR architecture (Table 12.1).

Next, the problem statement of FIR design and in what way the suggested methodology addresses shortcomings are explained. The concerns linked to FIR architectures are cited below [8–23]:

- Less efficient multipliers degrade the operation of the FIRF.
- Normal adders occupy larger hardware areas.
- After designing FIRF, no one focused on the specifics of the ECG signal, which is one of the major caveats.

12.3 Methodology

Figure 12.1 alludes to the overall block diagram of the VD-CLA FIRF. The MATLAB helps to read the ECG signal from the Internet available arrhythmia database. Then, white Gaussian noise (WGN) is added to that ECG signal. Here, noise density will be 0.1–0.5. In MATLAB, the `awgn` function adds the noise to the input

Table 12.1 Literature review

Work	Technique	Remarks
Reddy et al. [26]	Verilog HDL design and implementation of reconfigurable FIRF. Distributed arithmetic (DA) calculation employs a high request FIR channel	FIRF is consolidated with a MAC unit to increase the contribution of coefficients, to move, and after that to include them. However, the delay augments
Sumalatha et al. [25]	A low-power and low-area VLSI implementation of the VD FIRF for ECG signal denoising	Low-power and fast FIRF implemented using Vedic multiplier and 16-bit CLA adder for ECG denoising application
Doss et al. [22]	The pipelined architecture for adaptive FIRF design employed the DA algorithm with a high-throughput rate achieved by the updated LUT	The sampling period and area complexity were reduced. It used a faster bit clock for carrying save accumulation, but that used a very slower clock for remaining FIRF operations
Reddy et al. [24]	A low-power adaptive FIRF based on the DA algorithm	The least mean squares (LMS) algorithm reduced the mean squared error (MSE) between filter output and the desired response. This technique used a carry-save accumulator for FIRF architecture. It occupied more area in the FIRF design

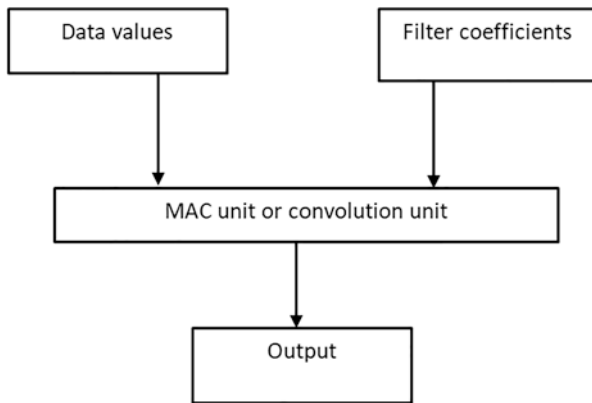


Fig. 12.1 Block diagram for the VD-CLA FIR filter architecture

signal. With the help of `dec2bin` MATLAB function, the ECG signals containing WGN are converted into the binary format. The associated binary signal is written in text file (Ex. `Noisy_ECG_signal.txt`). This `Noisy_ECG_signal.txt` file is given to the input of the Verilog. Normally, the input value has been generated randomly. This noisy binary value is considered as an input that is going to be stored in RAM, while the coefficient comes from the ROM. In the Verilog, the noise is reduced by using the Vedic design-carry look-ahead (aka VD-CLA) adder FIRF [8–14].

In this work, a VD-CLA FIRF architecture is designed. Every clock cycle accumulator result is stored in a text file (e.g., `Filter_output.txt`). By using the Verilog code, it aids to measure the FPGA performances (LUT, flip-flops, slices, and frequency). This `Filter_output.txt` file is given to the MATLAB for getting denoised ECG signals.

The block diagram of the VD-CLA FIRF architecture appears in Fig. 12.1, which consists of the data input block, filter coefficient block, and MAC unit. The coefficient data is stored in the ROM, and noisy data input is stored in the RAM. The input is read from the RAM, and the coefficient comes from the ROM to perform the filter operation. The noisy data value is considered as input (0, 255, etc.), which multiply with a coefficient (213, 18, etc.), and gives the FIRF results ($y = 0$). The coefficient is taken from MATLAB FDA tool. MAC unit consists of the Vedic multiplier and the CLA adder. In the accumulator, initially, the register contains zero. This register value is added with multiplier output stored in the same register. Finally, the output is delivered from the register [13–21]. The standard form of the N-tap FIR filter is given below:

$$y(n) = \sum_{k=0}^{N-1} h(k)x(n-k). \quad (12.1)$$

Here:

$n = 0, 1, \dots$

$y(n)$ represents the FIRF output.

$h(k)$ is the FIRF coefficient.

$x(n-k)$ is the input data to be filtered.

12.3.1 Vedic Multiplier

The proposed Vedic multiplier is designed using the Urdhva tiryagbhyam Sutra method (aka vertically and crosswise algorithm). In this algorithm, the partial product and sum are calculated in parallel, and because of this, the multiplier is independent of the clock frequency of the processor. The 16×16 multiplier is a portion of the convolution unit, as shown in Fig. 12.2. This block contains four 88 multiplier blocks and three 24-bit adder blocks [8–14].

The 8×8 Vedic multiplier employs four 4×4 Vedic multiplier blocks and three 12-bit adder blocks. The 4×4 Vedic multiplier comprises four 2×2 Vedic multiplier blocks and three 6-bit adder blocks. Figure 12.3 depicts the 2×2 multiplication with the Vedic multiplier.

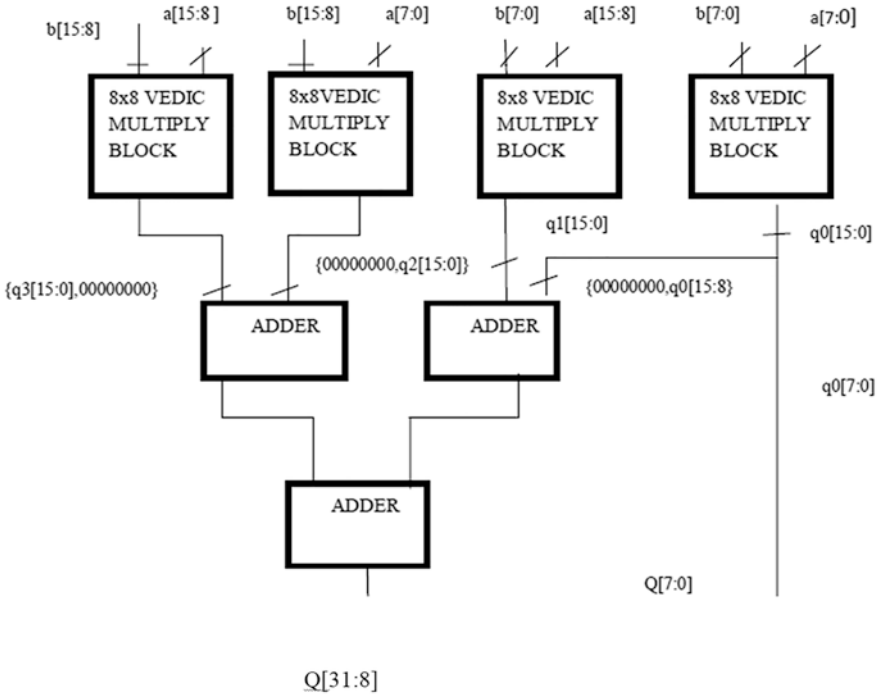


Fig. 12.2 16 × 16 Vedic multiplier

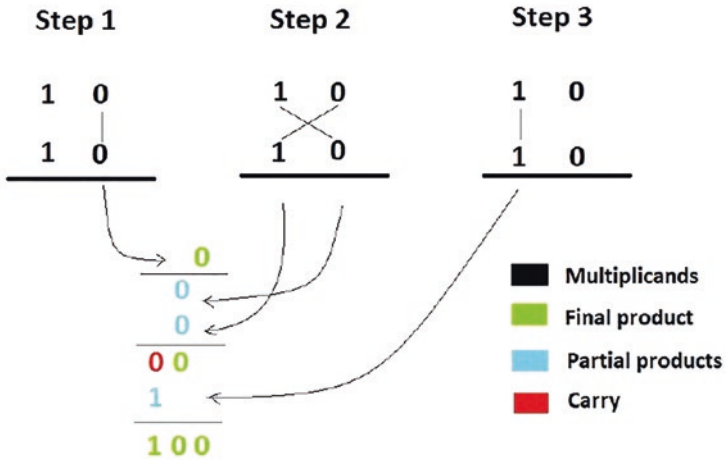


Fig. 12.3 Vedic algorithm for 2 × 2 multiplication

12.3.2 Compact Booth Multiplier

The Vedic multiplier, Wallace multiplier, and parallel multiplier, among other implementations, utilize only unsigned operands, while the BM handles the signed multiplication scheme. In the current techniques, radix 2-based recoding helps to design a Booth multiplier. The existing multiplier affords high complexity, highly optimized area, and low speed [13–21].

In the radix 2 encoding scheme, the number of addition/subtraction operations and the number of shift operations vary, which complicates the parallel multiplier design. The algorithm becomes inefficient and obsolete when there are isolated 1s. These limitations are remedied by using the modified radix 4 recoding technique. The novel BM is made of a finite state machine (FSM) and modified radix 4 BM to perform the multiplication of two numbers according to Fig. 12.4.

The number of shifts and adds is deficient in the proposed BM, where a compact partial product accumulation stage aids in shrinking the complexity of the recommended multiplier. In the radix 4 recoding scheme, it performs X, 1X, and 2X. Shift, addition, and subtraction are carried out to accomplish the sign multiplication hinging on the BM.

12.3.3 Carry Look-Ahead (CLA) Adder

The VD-CLA FIRF design employs a 32-bit CLA instead of the normal adder. In the accumulator module, this CLA adder boosts system performances with fast arithmetic operation in different types of data processing schemes, which reduces the circuit area and power dissipation. The CLA adders are implemented as a combination of 4-bit modules for designing higher-level modules. Figure 12.5 shows a detailed flowchart of the FIRF implementation for ECG signal denoising [13–21].

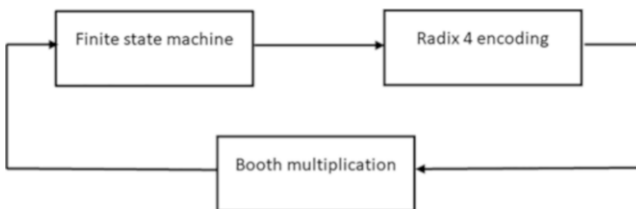


Fig. 12.4 Block diagram of the compact Booth multiplier

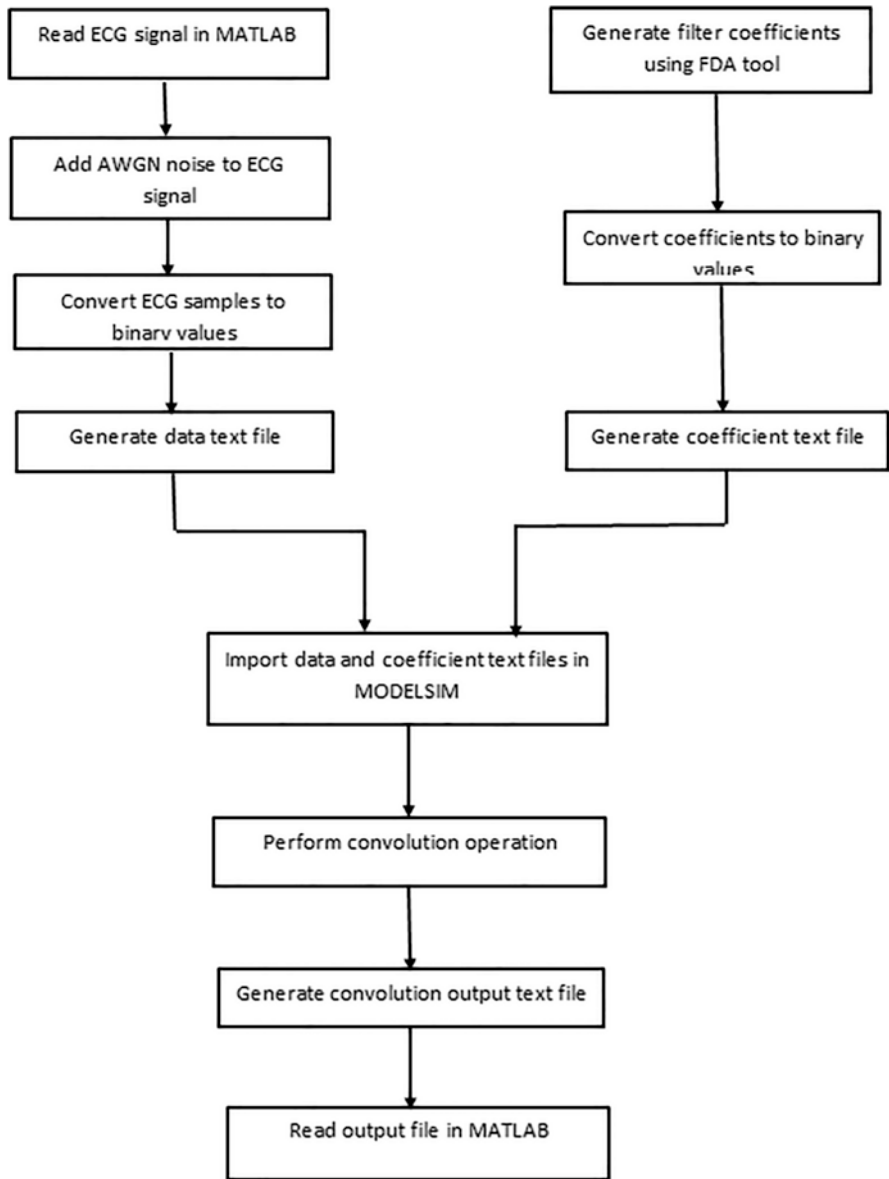


Fig. 12.5 Flowchart of the implementation of the VD-CLA FIR filter for ECG signal denoising

12.4 Analysis of the Results (Figs. 12.6, 12.7, 12.8, 12.9, 12.10, 12.11, 12.12, 12.13, 12.14, 12.15)

12.5 Conclusions

Multipliers are fundamental building blocks for numerous computational entities. The Vedic multiplier excels in performing faster multiplications because it leaves behind the nonessential multiplication phases. Consequently, the multiplication speed performance grows.

In this work, the Vedic design (VD)-carry look ahead (CLA), aka the VD-CLA, FIR filter (FIRF) built on the VD algorithm with the CLA adder and Booth multiplier was implemented in ModelSim by employing Verilog code. In any case, a MATLAB created code peruses the ECG signals, which can be influenced by AWGN. A text file stores the values of this noisy ECG signal, which feeds the Verilog module. The VD and the Booth procedures from this research project have accomplished the multiplications. The overall VD-reliant FIRF performed meritoriously, which removes the noise from the ECG signal. The Booth multiplier consumes less power than VD multiplier. Thus, the CLA adder can be replaced with a more efficient adder regarding power, circuit area, and speed.

Future works can explore the combination of Vedic sutras with the Karatsuba multiplier, for instance, to enrich results. Some hybrid strategies making use of that emerge in [27–29]. The performances of such hybrid multipliers can benefit from lessening the (i) spent power, (ii) total amount of gates, (iii) garbage outputs, (iv) constant inputs, (v) quantum cost, (vi) total reversible logic implementation cost

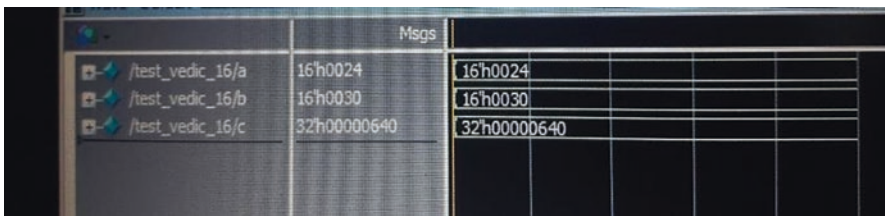


Fig. 12.6 Waveform obtained for 16 × 16 Vedic multiplier output

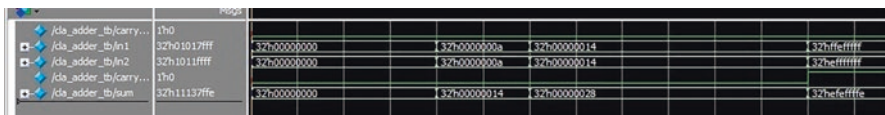


Fig. 12.7 32-bit carry look-ahead adder output

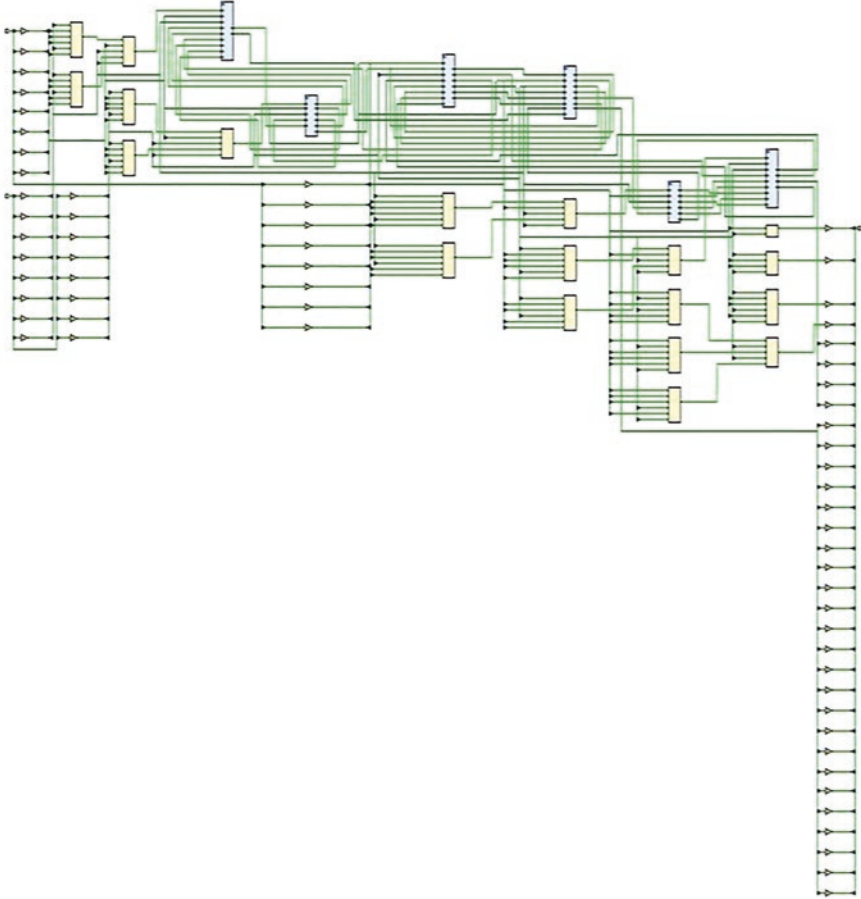


Fig. 12.8 RTL schematic for 16 × 16 Vedic multiplier

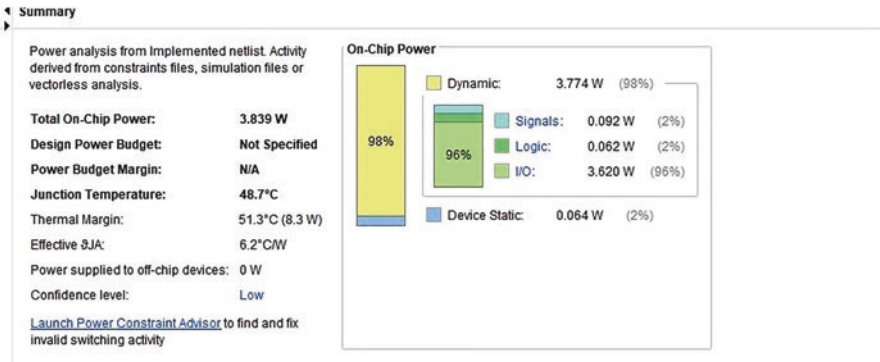


Fig. 12.9 Power analysis for the 4-bit Vedic multiplier



Fig. 12.10 Output from the 4-bit compact Booth multiplier

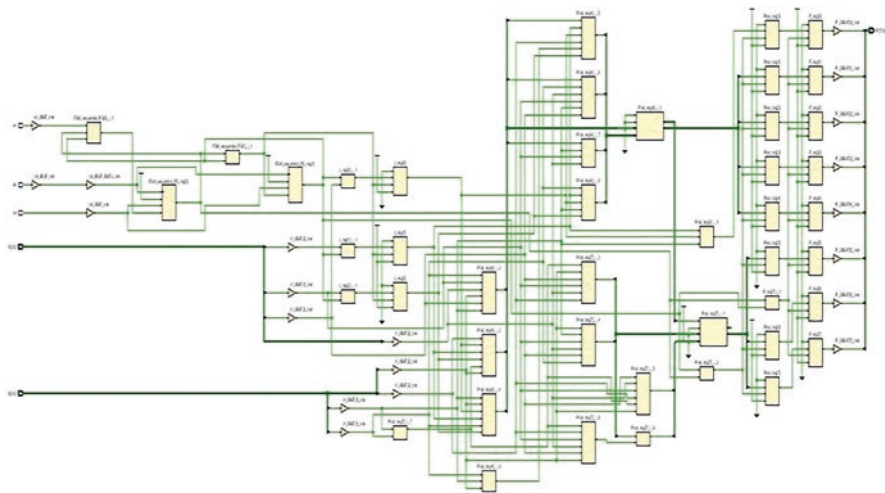


Fig. 12.11 RTL schematic for the compact Booth multiplier

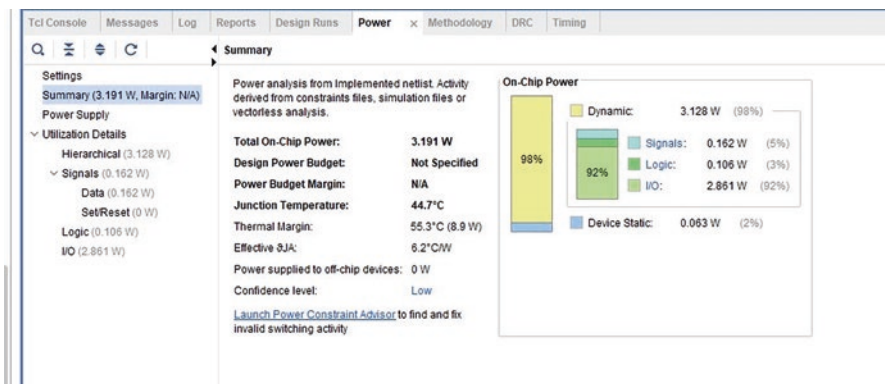


Fig. 12.12 Power analysis for the compact Booth multiplier

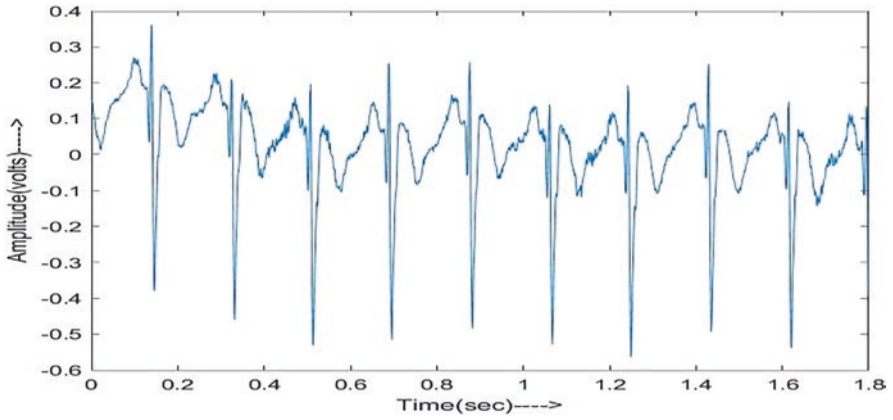


Fig. 12.13 ECG signal without adding noise

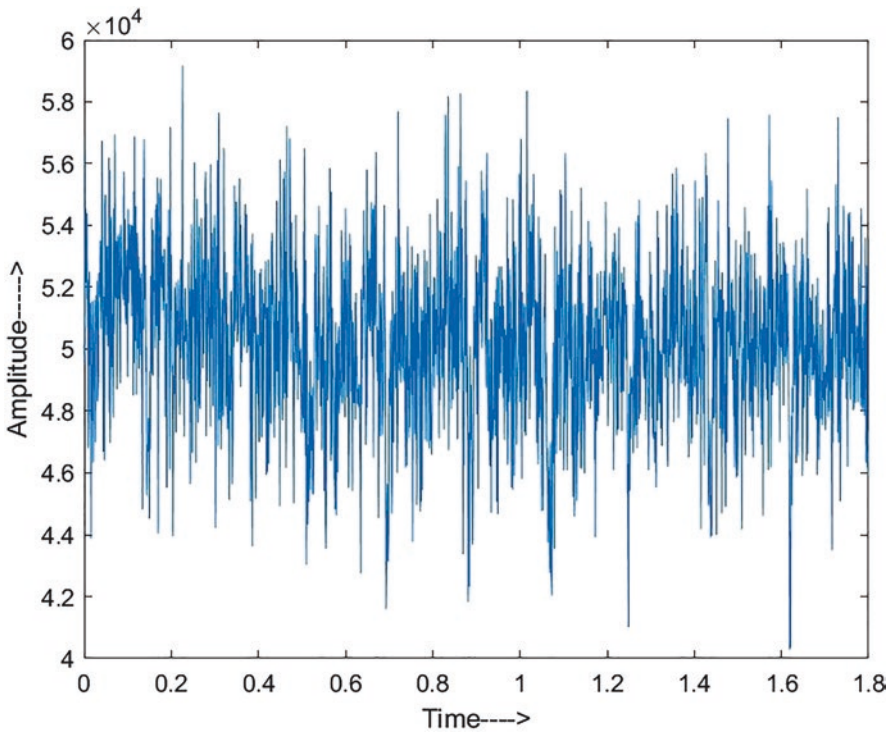


Fig. 12.14 ECG signal after adding noise

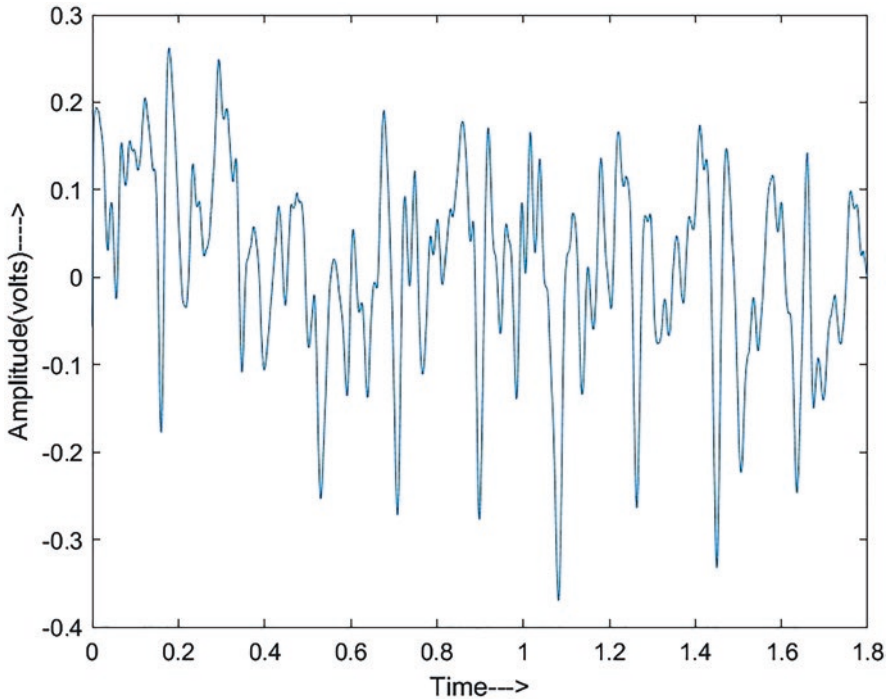


Fig. 12.15 VD-CLA FIR filter output after performing the convolution operation on the data input and filter coefficients

(TRLIC), and (vii) the usage of LUTs while ameliorating the speed of the computational units in contrast with other current multipliers.

Since Vedic math can speed up calculations and most metaheuristics rely heavily on multiplications and additions, the current design can augment the performance of existing deployments of FPGA-based signal processing noticeably [30–35].

This described VD-CLA structure can improve by taking a gander at other electronic system performance metrics to seek the best arrangement of attributes intended for a specific denoising application, e.g., mean squared error (MSE), signal-to-noise ratio (SNR), peak signal-to-noise ratio (PSNR), bit error rate (BER), and [25, 36–41].

References

1. A. Booth, A signed binary multiplication technique. *Q. J. Me. & Appl.* March **4**, 236–240 (1951)
2. C.S. Wallace, A suggestion for a fast multiplier. *IEEE Trans. Electron. Comput.* **13**, 14–17 (1964)

3. D. Chandel, G. Kumawat, P. Lahoty, V.V. Chandrodaya, S.K. Sharma, Booth multiplier: Ease of multiplication. *Int. J. Emerg. Technol. Adv. Eng. (IJETAEE)* **3**, 3 (2013)
4. M. Nicolaidis, R.D. Duarte, Fault-secure parity prediction Booth multipliers. *IEEE Des. Test Comput.* **16**, 90–101 (1999)
5. Wang, L., Jou, S., Lee, C. (2008) A well-structured modified Booth multiplier design. 2008 IEEE International Symposium on VLSI Design, Automation and Test (VLSI-DAT), 85–88
6. Mehta P., Gawali D. (2009) Conventional versus Vedic mathematical method for hardware implementation of a multiplier. In: *Proc. 2009 International Conference on Advances in Computing and Telecommunication Technologies*, 641–642
7. Ramya, K., Manvi, S.K. (2014). Design of a 4-bit Vedic multiplier using transistors. In: *Proc. 9th International Conference on Electrical Electronics and Computer Science (EECS 2014)*, 39–44
8. C.Y. Yao, W.C. Hsia, Y.H. Ho, Designing hardware efficient fixed-point FIR filters in an expanding subexpression space. *IEEE Trans. Circuits Syst. I* **61**(1), 202–212 (2014)
9. A. Bonetti, A. Teman, P. Flatresse, A. Burg, Multipliers-driven perturbation of coefficients for low-power operation in reconfigurable FIR filters. *IEEE Trans. Circuits Syst. I* **64**(9), 2388–2400 (2017)
10. J. Chen, J. Tan, C.H. Chang, F. Feng, A new cost-aware sensitivity-driven algorithm for the design of FIR filters. *IEEE Trans. Circuits Syst. I* **64**(6), 1588–1598 (2017)
11. J.L.M. Iqbal, S. Varadarajan, High performance reconfigurable FIR filter architecture using optimized multiplier. *Circuits Syst. Signal Process.* **32**(2), 663–682 (2013)
12. Xu C., Yin S., Qin Y., Zou H. (2013) A novel hardware efficient FIR filter for wireless sensor networks. In 2013 Fifth International Conference on ubiquitous and future networks (ICUFN), IEEE, 197–201
13. S. Madugula, P.V. Naganjaneyulu, K.S. Prasad, Implementation of FIR filter for low power and area minimization using shift-add method without multipliers. *Int. J. Intell. Eng. Syst.* **10**(6) (2017)
14. D. Shi, Y.J. Yu, Design of linear phase FIR filters with high probability of achieving minimum number of adders. *IEEE Trans. Circuits Syst. I* **58**(1), 126–136 (2011)
15. S. Bhattacharjee, S. Sil, A. Chakrabarti, Evaluation of power efficient FIR filter for FPGA based DSP applications. *Procedia Technol.* **10**, 856–865 (2013)
16. S. Harize, M. Benouaret, N. Doghmane, A methodology for implementing decimator FIR filters on FPGA. *AEU-Int. J. Electron. Commun.* **67**(12), 993–1004 (2013)
17. Y.C. Tsao, K. Choi, Area-efficient VLSI implementation for parallel linear-phase FIR digital filters of odd length based on fast FIR algorithm. *IEEE Trans. Circuits Syst. II* **59**(6), 371–375 (2012)
18. Meyer-Baese U, Botella G, Romero DE, Kumm M. (2012) Optimization of high speed pipelining in FPGA-based FIR filter design using genetic algorithm, In: *Independent Component Analyses, Compressive Sampling, Wavelets, Neural Net, Biosystems, and Nanoengineering X*, 8401, International Society for Optics and Photonics, 84010R
19. Khan S, Jaffery ZA (2015) Low power FIR filter implementation on FPGA using parallel distributed arithmetic, in: 2015 Annual IEEE India Conference (INDICON), IEEE, 1–5
20. B. Rashidi, B. Rashidi, M. Pourormazd, Design and implementation of low power digital FIR filter based on low power multipliers and adders on Xilinx FPGA, in: 3rd International Conference on Electronics Computer Technology (ICECT). *IEEE* **2**, 18–22 (2011)
21. Park SY, Meher PK. (2014) Efficient FPGA and ASIC realizations of DA-based reconfigurable FIR digital filter, *IEEE Transactions on Circuits and Systems-II: Express Briefs*
22. B. Doss, K. Soundararajamm, Y.N. Murthy, Low-Power and low-area adaptive FIR filter based on DA using FPGA. *Int. J. Sci. Res. Manag.* **3**(1) (2015)
23. S.Y. Park, P.K. Meher, Low-power, high-throughput, and low-area adaptive FIR filter based on distributed arithmetic. *IEEE Trans. Circuits Syst. II* **60**(6), 346–350 (2013)
24. K.S. Reddy, H.N. Suresh, A low power VLSI implementation of reconfigurable FIR filter using carry bypass adder. *Int. J. Intell. Eng. Sys.* **11**, 225–236 (2018)

25. M. Sumalatha, P.V. Naganjaneyulu, K.S. Prasad, Low power and low area VLSI implementation of Vedic design FIR filter for ECG signal denoising. *Microprocess. Microsyst.* **71**, 102883 (2019)
26. K.S. Reddy, S.K. Sahoo, An approach for fixed coefficient RNS-based FIR filter. *Int. J. Electron.* **104**, 1358–1376 (2017)
27. J.V. Suman, Design and Performance Evaluation of Hybrid Vedic Multipliers. *Int. J. Innov. Technol. Explor. Eng.* **8**, 1622–1626 (2019)
28. M.N. Angeline, S. Valarmathy, Implementation of N-bit binary multiplication using N – 1 bit multiplication based on Nikhila Sutra and Karatsuba principles using complement method. *Circ Syst* **07**, 2332–2338 (2016)
29. S. Mishra, M. Pradhan, Synthesis comparison of Karatsuba multiplier using polynomial multiplication, Vedic multiplier and classical multiplier. *Int. J. Comput. Appl* (0975–8887) **41**(9), 13–17 (2012)
30. N. Razmjooy, V.V. Estrela, Applications of image processing and soft computing systems in agriculture. *IGI Global* (2019). <https://doi.org/10.4018/978-1-5225-8027-0>
31. N. Razmjooy, M. Ramezani, V.V. Estrela, A solution for Dubins path problem with uncertainties using world cup optimization and Chebyshev polynomials, in *Proc. 4th BTSym (BTSym'18). Smart Innovation, Systems and Technologies*, ed. by Y. Iano, R. Arthur, O. Saotome, V. Vieira Estrela, H. Loschi, vol. 140, (Springer, Cham, 2019). https://doi.org/10.1007/978-3-030-16053-1_5
32. N. Razmjooy, V.V. Estrela, H.J. Loschi, Entropy-based breast cancer detection in digital mammograms using world cup optimization algorithm. *IJSIR* **11**(3), 1–18 (2020). <https://doi.org/10.4018/IJSIR.2020070101>
33. S. Raj, K.C. Ray, ECG signal analysis using DCT-based DOST and PSO optimized SVM. *IEEE Trans. Instrum. Meas.* **66**, 470–478 (2017)
34. R. Kar, Optimal designs of analogue and digital fractional order filters for signal processing applications. *CSI Trans. ICT* **7**, 1–6 (2019)
35. A. Verma, A. Gill, I. Kaur, Analysis and implementation of data mining algorithms for deploying ID3, CHAID and Naive Bayes for random dataset. *Indian J. Sci. Technol.* **9** (2016)
36. T.V. Padmavathy, S. Saravanan, M.N. Vimalkumar, Partial product addition in Vedic design-ripple carry adder design FIR filter architecture for electro cardiogram (ECG) signal denoising application. *Microprocess. Microsyst.* **76**, 103113 (2020)
37. A. Khelassi, V.V. Estrela, J. Hemanth, Explainer: An interactive agent for explaining the diagnosis of cardiac arrhythmia generated by IK-DCBRC. *Med. Technol. J.* **3**(2), 376–394 (2019). <https://doi.org/10.26415/2572-004X-vol3iss2p376-394>
38. A. Arshaghi, N. Razmjooy, V.V. Estrela, P. Burdziakowski, D.A. Nascimento, A. Deshpande, P.P. Patavardhan, Image transmission in UAV MIMO UWB-OSTBC system over Rayleigh channel using multiple description coding (MDC), in *Imaging and sensing for unmanned aircraft systems*, ed. by V. V. Estrela, J. Hemanth, O. Saotome, G. Nikolakopoulos, R. Sabatini, vol. 2, 4, (IET, London, 2020), pp. 67–90. https://doi.org/10.1049/PBCE120G_ch4
39. V.V. Estrela, J. Hemanth, H.J. Loschi, D.A. Nascimento, Y. Iano, N. Razmjooy, Computer vision and data storage in UAVs, in *Imaging and sensing for unmanned aircraft systems*, ed. by V. V. Estrela, J. Hemanth, O. Saotome, G. Nikolakopoulos, R. Sabatini, vol. 1, 2, (IET, London, 2020), pp. 23–46
40. N. Soni, I. Saini, B. Singh, A morphologically robust chaotic map based approach to embed patient's confidential data securely in non-QRS regions of ECG signal. *Australas. Phys. Eng. Sci. Med.* **42**, 111–135 (2018)
41. D.K. Atal, M. Singh, A dictionary matrix generation based compression and bitwise embedding mechanisms for ECG signal classification. *Multimed. Tools Appl.* **79**, 13139–13159 (2020)

Chapter 13

Implementation of an FPGA Real-Time Configurable System for Enhancement of Lung and Heart Images



K. B. Sowmya, T. S. Rakshak Udupa, and Shashank K. Holla

13.1 Introduction

Field-programmable gate arrays (FPGAs) are no longer challenging to use as logic arrangements, and they comprise the backbone of softcore processors [1, 2]. By softcore processor, the authors mean a software-defined microprocessor synthesizable in programmable hardware. Currently, they permit software designs with reconfigurable hardware platforms in terms of both logic wiring and algorithms. The fine-grained nature of FPGAs facilitates the parallelization, reconfigurability, and programmability of the system.

Regrettably, FPGAs may pose some caveats when it comes to practical programming. Hardware architectures with a fixed computational design, on the other hand, entail a high level of thought due to the need to respect architectural limitations. Therefore, an FPGA needs algorithms and the computational structures leading to a design that explores and conciliates several complexity levels. This fact, together with the complications of dealing with flexible parallel schemes and the extreme bandwidth concerns stemming from the high data volume related to images/video, resulted in a wide range of FPGA-based realizations for image processing systems.

This manuscript discusses how to implement and improve the real-time configurable system for image enhancement using the Verilog Hardware Description Language (HDL).

Image processing is used in various fields of modern society and especially in medical imaging and, recently, assists in the diagnosis of diseases. Image processing is a vast field that employs rigorous mathematical theory. Nowadays, image processing is an emerging biomedical tool that helps in the advancement of the healthcare sector. Recent image processing tools can perform image analysis, image

K. B. Sowmya (✉) · T. S. Rakshak Udupa · S. K. Holla
Electronics and Communication, RV College of Engineering, Bengaluru, Karnataka, India
e-mail: rakshakudupa.ec17@rvce.edu.in; shashankholla.ec17@rvce.edu.in

enhancement, noise reduction, image segmentation, geometric transformations, and image restoration.

Many motives give rise to blurry images. The finite size of the X-ray source focal spot and, therefore, the detector element within the computer tomography (CT) array, the imaging system owns an imperfect resolution, and image data lost throughout the image acquisition. Enhancements in imaging technology and algorithms have increased the clarity of medical images and contributed to a better diagnosis. Diminishing the blur enhances the overall picture quality.

The proposed arrangement is suited for various images. Different techniques we followed allow better tuning for threshold amount and less iteration involved in the enhancement process, causing faster, more efficient, and more accurate results. Our prototype consists of five enhancement stages that operate independently and without any interdependencies.

In Sect. 13.2 of this text, there is a literature review. The suggested methodology appears in Sect. 13.3. Section 13.4 shows the experimental results. Section 13.5 addresses some future ameliorations in the recommended framework, and, to finish, conclusions appear in Sect. 13.6.

13.2 Literature Survey

As image sizes and bit depths grow larger, software faces more challenges, and real-time hardware systems are options to achieve better results [3]. The planning and, consequently, the implementation of real-time hardware enhancements to speed up image processing for biomedical in the spatial domain on FPGA appear in [4]. A hardware design based on FPGA appears in [3] for image filtering. Contrast enhancement techniques allow displaying the details that are present in the lower dynamic range of the image. Operations like contrast enhancement and reduction or removal of noise improve the quality of the image. The local mean filter smoothes the image by taking the mean value of the pixels nearby the center pixel within the picture [5]. Direct application and improvement of the real-time configurable system for image improvement using the Verilog HDL and reconfigurable architecture are delineated in [6]. A comparative study of various enhancement techniques, such as inverting image operation, brightness control, segmentation (threshold), and contrast stretching, is administered to seek out the most straightforward procedure to reinforce a biomedical image on FPGA. These techniques treated images of hand veins using the Open Access Biomedical Image program. It was clear from the studies that brightness controlling techniques enhance the image and provide better information. Developing an efficient architecture by the application of minimum blocks for digital signal processing (DSP) tool, which integrates itself with the high-level, yet easy to use the graphical interface of MATLAB Simulink environment and removes the necessity of the textual HDL programming is described in [4]. Hardware-level filters have been proposed for image processing (edge detection,

sharpen operation, enhance contrast process, and brightness adjustment) to improve the quality of images and to support in diagnosis the medical specialist [6].

The DSP applications in medicine comprise signals of different dimensionalities and modalities, e.g., electroencephalogram (EEG), electrocardiogram (ECG), ultrasound, computerized axial tomography (CAT) scanners, magnetic resonance imaging (MRI), and holography among others as outlined in [7]. The analytic power, the problem-solving capabilities, and, therefore, the cost of the related systems are expanding continuously, as well as the dependence of recent medicine on them [7]. Thus, new types of filters are established at the hardware level for image processing (edge detection, sharpen operation, enhance contrast process, and brightness adjustment) to improve the quality of images and to support the medical diagnosis specialist [6, 8]. The results obtained with 512×512 images from [6] can be expanded to any size, as long as the FPGA memory has the necessary space to store the pictures. In [7], a new deblurring filter is proposed, which combines the Laplace filter and the Markov basis to boost the performance of colored images' processing. [9] offers a way to enhance real-time medical diagnosis using a dedicated computation engine to perform concentration index filtering, which is a kind of spatial filter optimized, aiming at full parallelism. To analyze the effect of applying a filtering technique on an image, [10] evaluates the filtering characteristics, by choosing a quality index. It speaks about how the application of special windows does image smoothing. [12] exploits concurrency at various levels in the implementation of the integration algorithm and general finite impulse response (FIR) filters to improve sampling/throughput rates.

13.3 Methodology

The process will first start by reshaping the given image to a binary sequence. Since any hardware device can only work on binary values, we can convert each layer (R-G-B) of the image into a binary sequence and feed it. The conversion of the image to a binary sequence can be easily done using Python, C++, or MATLAB. The implementation of various image processing techniques has been done using different filters. We have translated the kernel function to Verilog and implemented the convolution for a group of pixels surrounding a given pixel. The output after applying the filter is received back to reconstruct the image.

Each image pixel is represented by an 8-bit \times 3 RGB values. The entire image is then converted to a sequence of pixels that can be accessed by its row and column values. The brightness, invert, and threshold operations work on individual pixels, whereas for sharpening and blurring operations, the pixel is passed through a 3×3 kernel, as shown in Fig. 13.1. The nine filter entries depend on the type of filter (kernel) and the operation. Figure 13.2 shows the banking operation that separates even and odd pixels. This method of parallelism enables faster functioning. However, we have compromised speed with the area, i.e., to achieve faster performance, we have utilized better hardware, thus occupying more space.

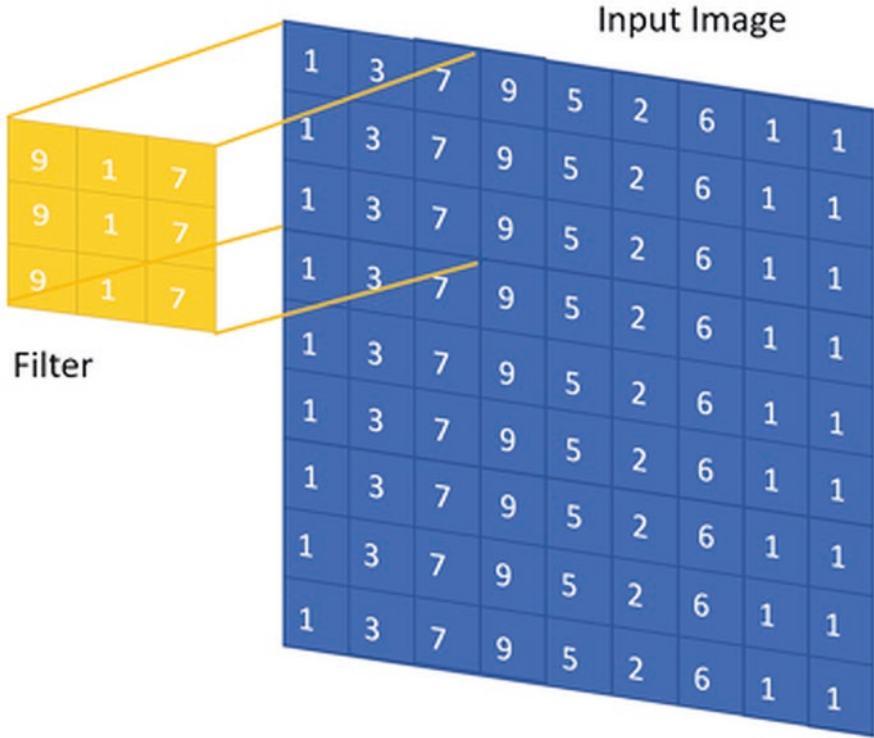


Fig. 13.1 Kernel application process

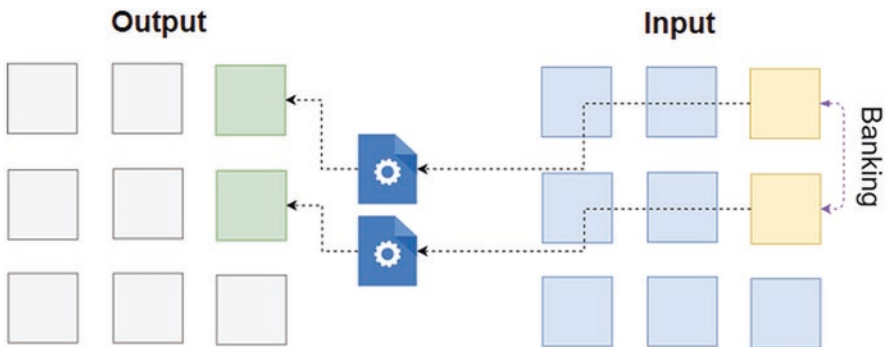


Fig. 13.2 Banking procedure used to improve performance

Image sharpening techniques are extensively employed to recover back the non-degraded image from its corrupted version and grant the image a sharper appearance because acquired images are considered as the degraded version of that view.

To blur an image, we use the blur filter, which looks like Fig. 13.3a. The rationale behind a filter like this is that blurring involves blending a pixel with its surrounding

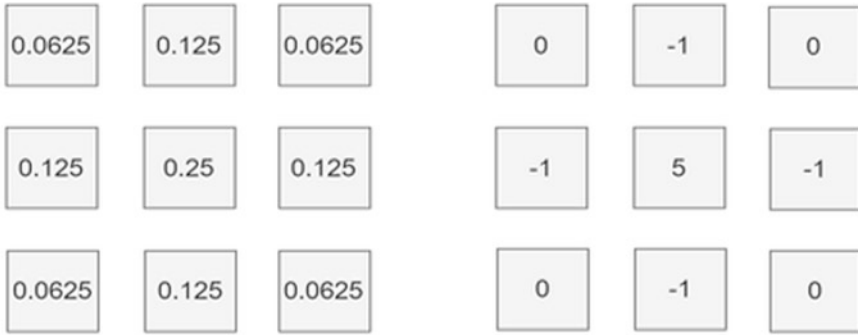
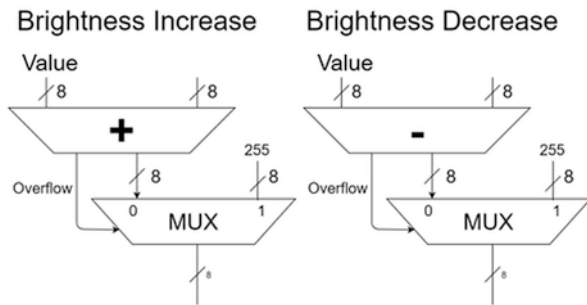


Fig. 13.3 (a) The blurring kernel and (b) sharpening kernel

Fig. 13.4 Brightness increase and decrease hardware illustration



pixels. Thus, it takes a weighted mean such that the current pixel is focused more, but is blended slightly with the immediately neighboring pixels. Moreover, for sharpening, we use the filter shown in Fig. 13.3b.

Image sharpening techniques are extensively employed to recover back the undergraded image from its corrupted version and grant the image a sharper appearance because acquired images are considered as the degraded version of that view. Many reasons led to having blurry images, for instance, the finite size of the X-ray source focal spot, the detector element within the CT array, the imperfect resolution of the imaging system, and the data loss throughout image acquisition. The implementation of a brightness augmentation circuit requires a multiplexer (MUX) and an 8-bit adder circuit.

The brightness can be increased to any desired value provided the value of the pixel does not go above 255. As shown in Fig. 13.4, the implementation of a brightness decrease circuit requires a mux and an 8-bit subtractor circuit. The intensity can be decreased to any desired value provided the value of the pixel does not go below 0. Application in the medical field involves focusing on certain tissue by increasing its brightness while decreasing the light intensity of the surrounding tissue.

Fig. 13.5 Thresholding operation hardware illustration

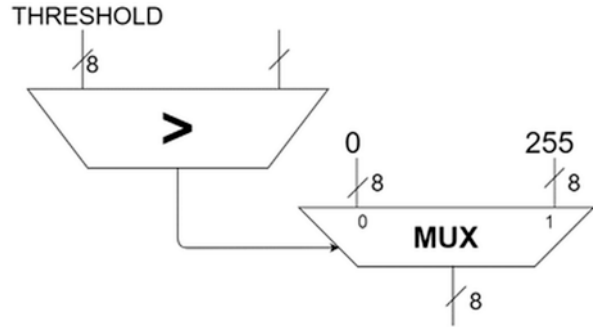
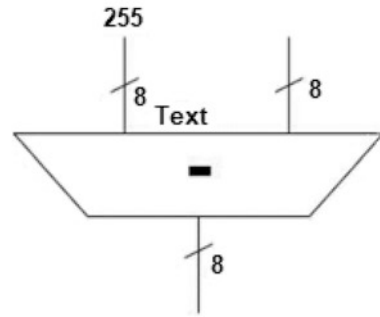


Fig. 13.6 Inversion operation hardware illustration



The threshold operation enhances an image by comparing the value of the pixel by a set threshold. Figure 13.5 shows this process. If the pixel value is greater than the threshold, the pixel is set to 255, else to 0. Here, 255 is white, and 0 is black.

Figure 13.6 illustrates the inversion operation implemented by a subtractor.

Certain tissues are usually surrounded by dark tissues, which makes it difficult to study them upon the inverting operation. The tissue we are interested in appears highlighted. The kernel is applied by multiplying each image pixel by its corresponding kernel pixel and supplied to an adder as described in Fig. 13.7. This adder acts as an accumulator that finally adds all the products and obtains the result for the pixel in question. Technically the kernel size can be modified to any size.

13.4 Experimental Results

A lung tissue sample image was taken and converted to a hexadecimal representation using MATLAB. It was then read into Verilog, and the image manipulation functions were applied. Figure 13.10 uses SEM alveoli in the lung [13] image to analyze the filters' output images outside the human lung [14]. A heart image is also analyzed [15].

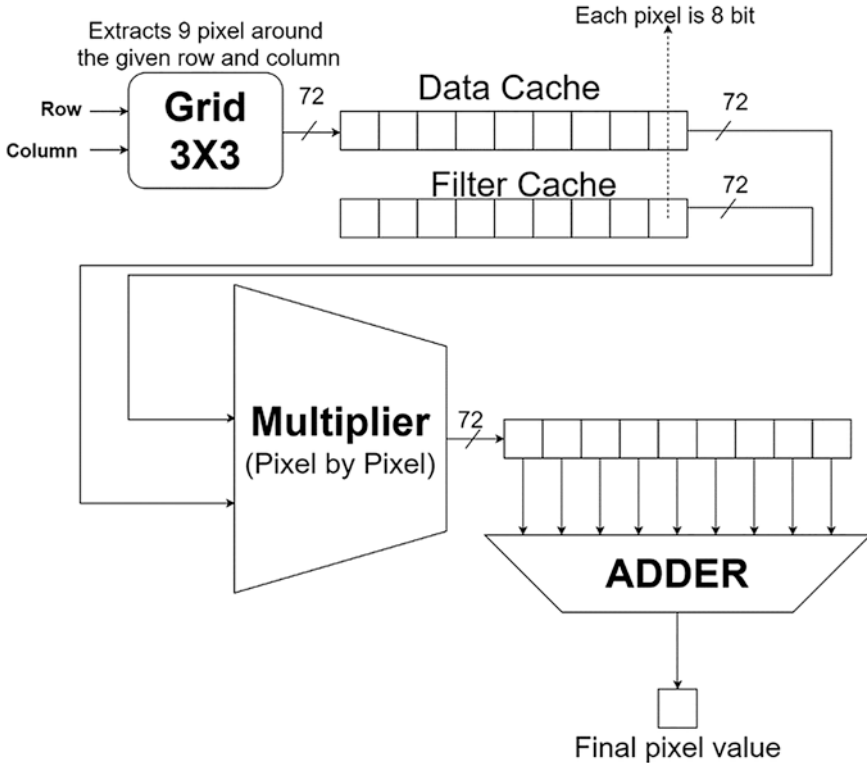


Fig. 13.7 Kernel application hardware illustration

The Verilog code yielded the image manipulation results seen in Figs. 13.8, 13.9, and 13.10 for brightness increase, inversion, threshold, blurring sharpening, gray-scale, and outline operations. The outputs of the Verilog-based filters and those from the equivalent MATLAB implementations have been compared for the same sets of images. The FPGA-based solution is better to obtain the given type of image manipulation at a faster rate.

Figure 13.10 compares the MATLAB and Verilog outputs. We can observe that the outputs are similar. However, the Verilog code can be synthesized into an ASIC hardware or dumped on to FPGA, and therefore we can expect improvement in speed. Figures from 13.11 to 13.14 display results for blurring, sharpening, inverting, and threshold operations, respectively, against the original image. The red in the graph indicates filtered image pixel intensities, whereas the blue shows the original image pixel intensities. The pixel intensities are plotted here to analyze how an image has been modified after the application of the filter. This helps us to understand the image enhancement process better. For example, the waveform of the blurred image is seen to be smoother and has lesser spikes when compared to that of the original in Fig. 13.11. One can also observe that the blurred image from

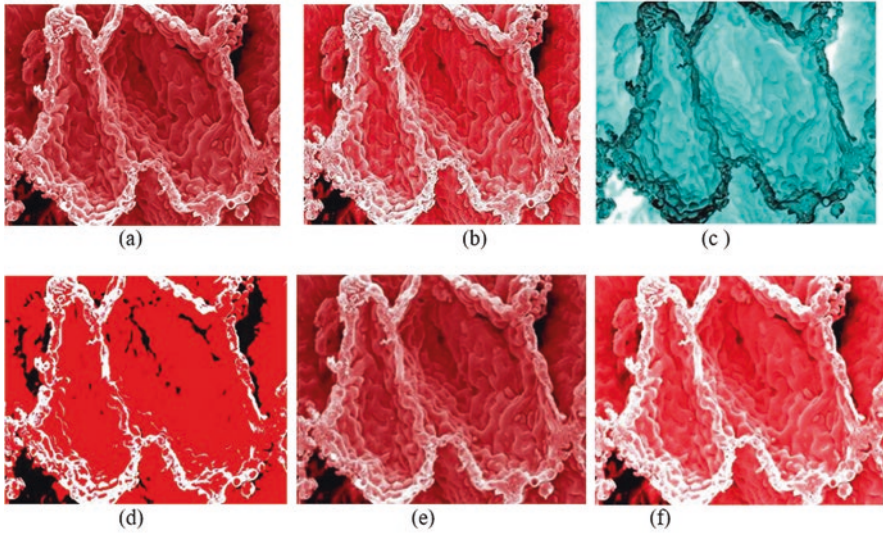


Fig. 13.8 Image of lung tissue: (a) original [11], (b) increased brightness, (c) inverted tissue, (d) threshold, (e) blur, and (f) sharpening

Fig. 13.12 shows that the sharpened image has flatter regions of pixel intensities when compared to the original image. In Fig. 13.13, one can observe the pixel values have been swapped in the inverted image when compared to that of the original image. In Fig. 13.14 one can understand that threshold operation can be used to remove noise from when cleverly applied to certain portions of the picture.

13.5 Future Work

FPGAs accelerate computationally demanding tasks, particularly in image processing and computer vision, where their processing acceleration has become common. This happens even more often within an embedded environment, like medical equipment and drones [16–18], where the power consumption and computational resources of orthodox processors fail to handle the data throughput, intensive communication, cloud computing access, and computational requirements for real-time uses.

Short computational times are paramount for quick and trustworthy biomedical diagnostics, but these requirements increase the computational demand for new and better-quality imaging procedures. FPGAs are an alternative to multi-core architectures and graphic cards that can also support alternative hardware paradigms that adjust the hardware to the problem [19, 20].

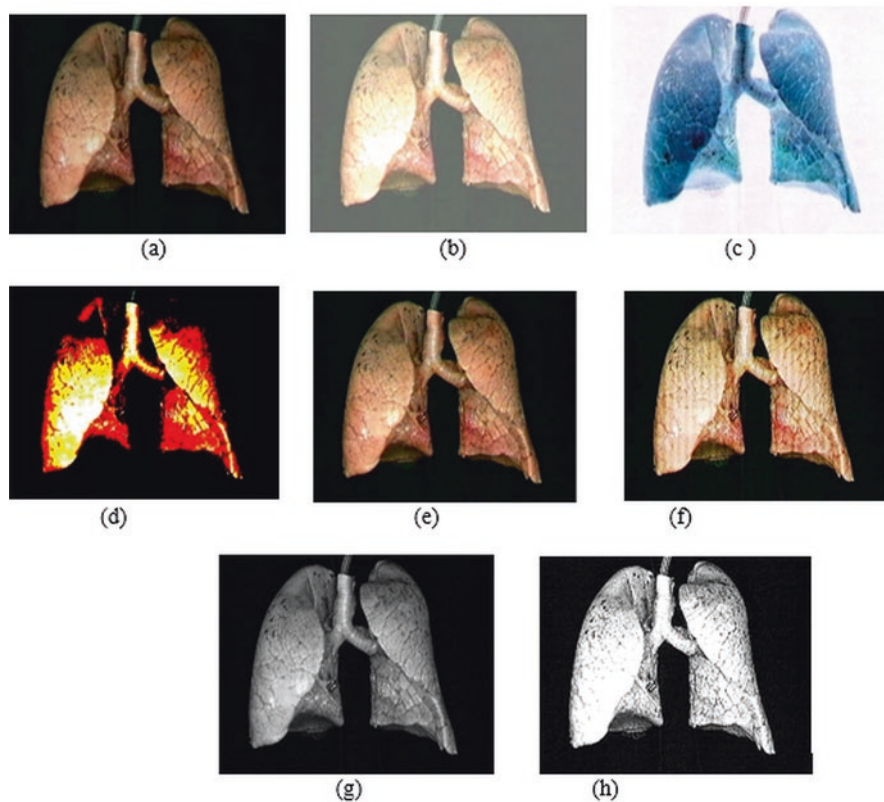


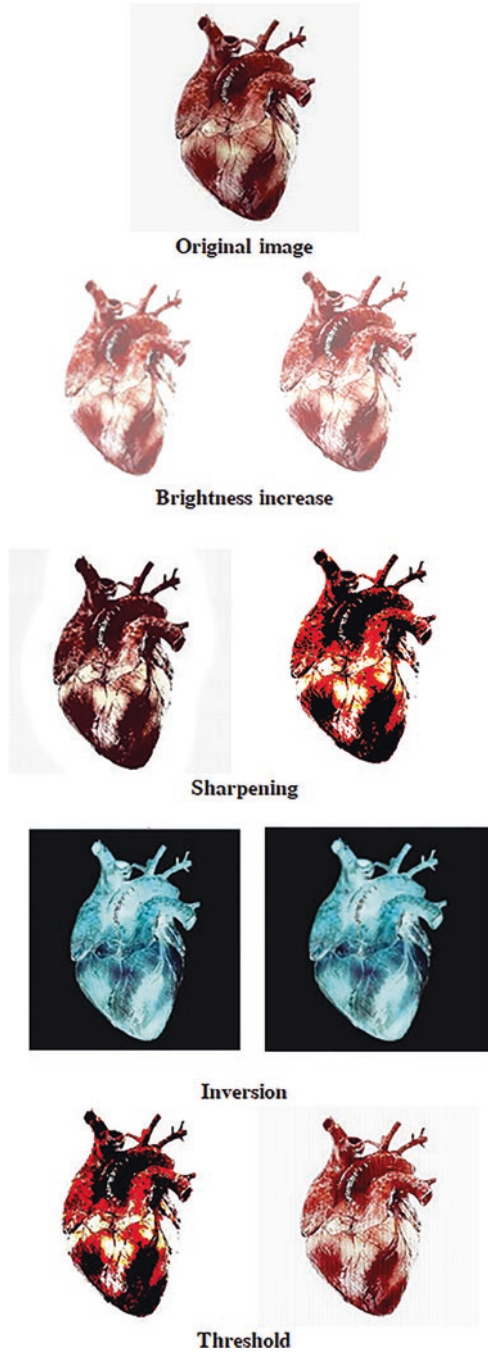
Fig. 13.9 Image of lungs: (a) original [11], (b) increased brightness, (c) inverted tissue, (d) threshold, (e) blur, (f) sharpening, (g) grayscale, and (h) outline

In the upcoming years, embedded Network-on-Chip (NoC) will be much faster to expand the FPGA's existing arrangements of biosensors, bioactuators, blockchain-enabled devices, wires, switches, and other items to support large medical applications. Flexible interfaces between FPGAs structures, wireless networks, and embedded NoCs will permit several levels of modularity and scalability [21–23].

The authors would like to point out that multimodality imaging techniques involve data acquired by different kinds of sensors and different representations. ECG is one-dimensional, while other diagnostic equipment can work with 2D, 3D, and 4D images. High-dimensional images pose arduous computational load hardware- and software-wise [24–30].

The fast-developing hardware technologies relying on computational intelligence allow the deployment of the recommended design of this text on small and portable FPGA-based equipment and, consequently, easy incorporation or adaptation into existing portable systems [31, 32].

Fig. 13.10 Comparison of MATLAB (left) and Verilog (right) image outputs



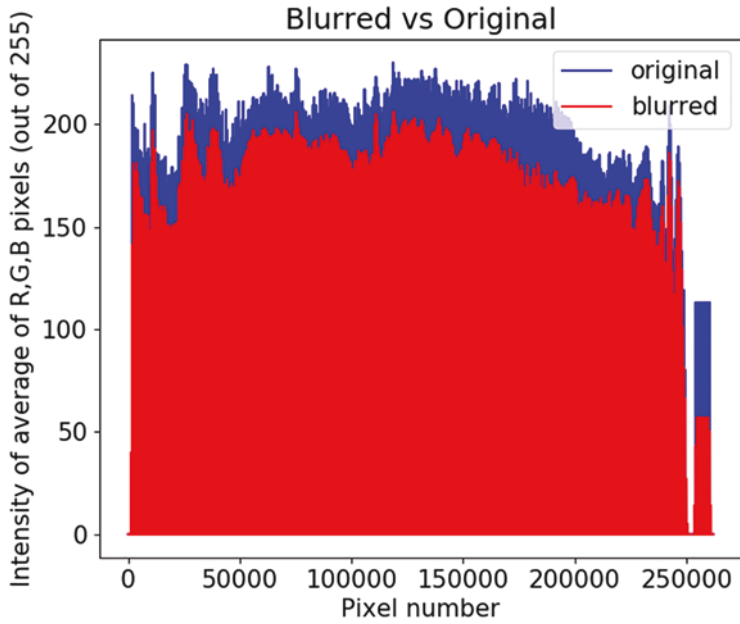


Fig. 13.11 Blurred vs original image pixel comparison

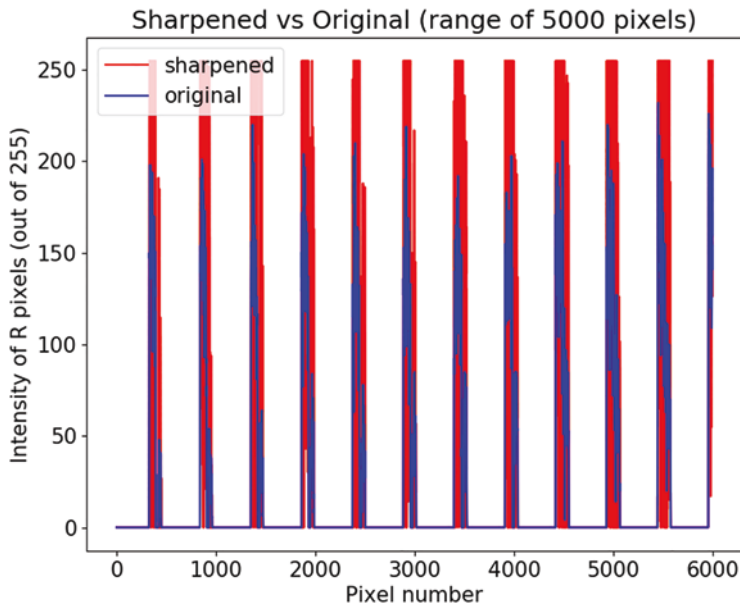


Fig. 13.12 Sharpened vs original images

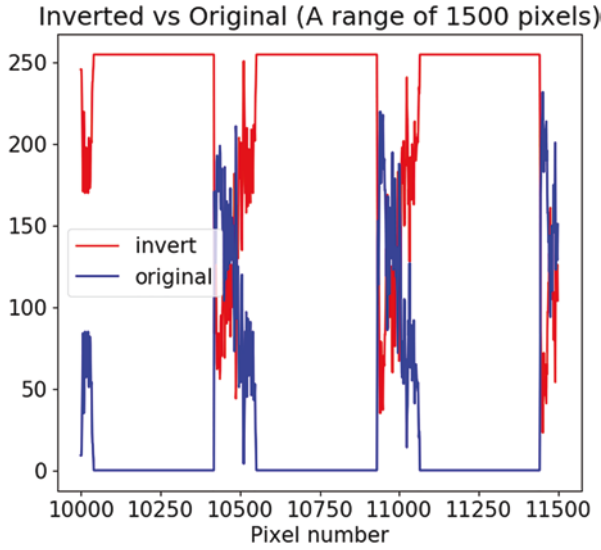


Fig. 13.13 Inverted vs original images

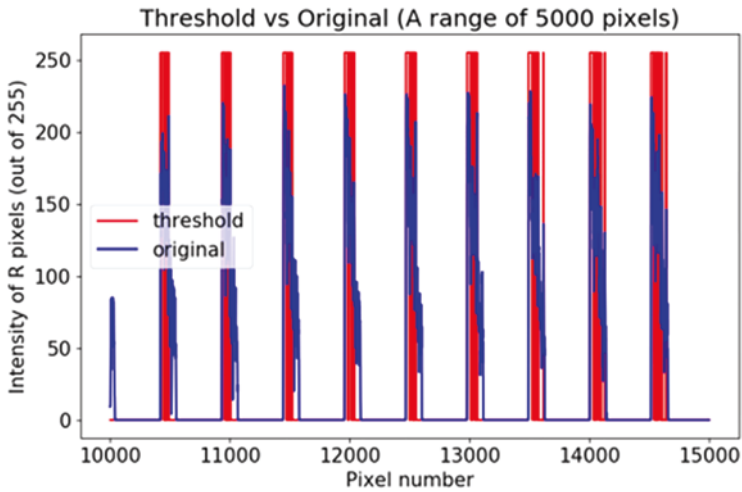


Fig. 13.14 Threshold vs original images

The authors are aware of the need to use objective metrics to evaluate the results, especially when working with different resolutions and zoom at the same time [33–37].

Optimization algorithms are frequently used in biomedical image processing, and they can handle mono-objective or multi-objective problems. Metaheuristic,

aka nature-inspired algorithms, originates from the reflections about natural behaviors. Medical imaging can benefit from implementations of computational intelligence procedures in FPGAs to advance communication, database handling, image retrieval, etc. The phenomenal growth in the uses of FPGA technologies in health-care occasioned several remarkable outcomes [38–43].

13.6 Conclusion

Embedded medical image processing designs built on FPGAs are ideal for delivering high performance with increasing picture resolutions and frame rates while permitting the addition of smart sensors/actuators, computer vision, and other novel technological innovations according to the cyber-physical system paradigm [44, 45].

FPGA improvement occurs due to the enormous speedup in the use and optimization given by hardware processing with excellent image quality. The FPGA realization leads to a better real-time performance in medical applications, where this can be used to improve the diagnosis speed and accuracy.

This work introduced a series of hardware-level filters for medical image processing to analyze the following operations: brightness adjustment, contrast enhancement, sharpening, blurring, grayscale, and outline. The present investigation relies on VLSI technologies because reconfigurable hardware devices provide higher speed than software implementations. The usage of a descriptive hardware language extends the field of circuitry to medical applications. Verilog Hardware Description Language (HDL) has opened the path toward the rapid hardware prototyping of further medical designs. Preliminary experimental outcomes for images of lungs and heart confirmed the benefit of employing softcore hardware.

References

1. D.G. Bailey, *Design for embedded image processing on FPGAs* (John Wiley & Sons, Singapore, 2011)
2. F.M. Siddiqui, S. Amiri, U.I. Minhas, T. Deng, R.F. Woods, K. Rafferty, D. Crookes, FPGA-based processor acceleration for image processing applications. *J. Imaging* **5**, 16 (2019)
3. S.Y. Singh, N. Singh, *Contrast enhancement and brightness preservation using global-local image enhancement techniques* (In Proc. 2016 Fourth International Conference on Parallel, Distributed and Grid Computing (PDGC), Waknaghat, 2016)
4. C. Li, Y. Zhang, Z. Zheng, Design of image acquisition and processing based on FPGA. *Int. Forum Inf. Tech. & Appl.* **2009**, 113–115 (2009)
5. M.I. Alali, K.M. Mhaidat, I.A. Aljarrah, Implementing image processing algorithms in FPGA hardware. 2013 IEEE Jordan Conference on Applied Electrical Engineering and Computing Technologies (AEECT), 1–5 (2013)
6. I. Chiuchisan, *An approach to the Verilog-based system for medical image enhancement* (2015 E-Health and Bioengineering Conference (EHB), Iasi, 2015), pp. 1–4

7. M.H. Zarifi, J. Frounchi, S. Asgarifar, M.B. Nia, FPGA implementation of a fully digital demodulation technique for biomedical application. CCECE, 001265–001268 (2008)
8. N. El Abbadi, E.J. Al Tae, Z. Abdulsamad, Improve image deblurring, 2018 International Conference on Innovative Trends in Computer Engineering (ITCE), 25–30 (2018)
9. T. Yokota, M. Nagafuchi, Y. Mekada, T. Yoshinaga, K. Ootsu, T. Baba, A scalable FPGA-based custom computing machine for a medical image processing, Proceedings 10th Annual IEEE Symposium on Field-Programmable Custom Computing Machines, 307–308 (2002)
10. S. Gedraite, M. Hadad, Investigation on the effect of a Gaussian blur in image filtering and segmentation, Proceedings ELMAR-2011, 393–396 (2011)
11. S. Sadangi, S. Baraha, D.K. Satpathy, P.K. Biswal, FPGA implementation of spatial filtering techniques for 2D images, 2017 2nd IEEE International Conference on Recent Trends in Electronics, Information & Communication Technology (RTEICT), 1213–1217 (2017)
12. B. Khurshid, R.N. Mir, A hardware intensive approach for efficient implementation of numerical integration for FPGA platforms, 27th International Conference on VLSI Design and 13th International Conference on Embedded Systems, 312–317 (2014)
13. SEM alveoli in the lung. Credit: David Gregory & Debbie Marshall. Attribution 4.0 International (CC BY 4.0)
14. Lung image from Acland's video atlas of human anatomy
15. Mohamed Nasir Bin Mohamed Shukor, Lo Hai Hiung and P. Sebastian, Implementation of real-time simple edge detection on FPGA, 2007 International Conference on Intelligent and Advanced Systems, Kuala Lumpur, 1404–1406 (2007)
16. V. Brea, D. Ginhac, F. Berry, R.P. Kleihorst, Special issue on advances on smart camera architectures for real-time image processing. *J. Real-Time Image Proc.* **14**, 635–636 (2018)
17. S. Vellas, G. Lentaris, K. Maragos, D. Soudris, Z. Kandylakis, K. Karantzalos, FPGA acceleration of hyperspectral image processing for high-speed detection applications. 2017 IEEE International Symposium on Circuits and Systems (ISCAS), 1–4 (2017)
18. V.V. Estrela, J. Hemanth, H.J. Loschi, D.A. Nascimento, Y. Iano, N. Razmjooy, Computer vision and data storage in UAVs, in *Imaging and sensing for unmanned aircraft systems*, ed. by V. V. Estrela, J. Hemanth, O. Saotome, G. Nikolakopoulos, R. Sabatini, vol. 1, (IET, London, 2020)
19. H. Engel, U. Keschull, F.R. Grull, High-level data flow description of FPGA firmware components for online data preprocessing (2014)
20. F. Grull, M. Kirchgessner, R. Kaufmann, M. Hausmann, U. Keschull, Accelerating image analysis for localization microscopy with FPGAs. 2011 21st International Conference on Field Programmable Logic and Applications, 1–5 (2011)
21. M.S. Abdelfattah, A. Bitar, V. Betz, Take the highway: Design for embedded NoCs on FPGAs. In Proc. of the FPGA '15 (2015)
22. G.J. García, C.A. Jara, J. Pomares, A. Alabdo, L.M. Poggi, F. Torres, A survey on FPGA-based sensor systems: Towards intelligent and reconfigurable low-power sensors for computer vision, control and signal processing. *Sensors* **14**, 6247–6278 (2014)
23. R.C. Barreto, J. Lobo, P. Menezes, Edge computing: A neural network implementation on an IoT Device. 2019 5th Experiment International Conference (Exp.At'19), 244–246 (2019)
24. N.F. Osman, J.L. Prince, Angle images for measuring heart motion from tagged MRI. Proceedings 1998 International Conference on Image Processing. SensorIIP98 (Cat. No.98CB36269) **1**, 704–708 (1998)
25. V.V. Estrela, N.P. Galatsanos, Spatially adaptive regularized pel-recursive motion estimation based on the EM algorithm, In: Proc. SPIE 3974, Image and Video Communications and Processing (2000), <https://doi.org/10.1117/12.382969>
26. R. Mosqueron, F. Capita, L. Bolomey, I. Gomez, New noise reduction method based on FPGA for a stereoscopic video system. International Conference on Quality Control by Artificial Vision (2019)

27. J. Park, H. Lee, B. Kim, D. Kang, S.O. Jin, H. Kim, H. Lee, A low-cost and high-throughput FPGA implementation of the Retinex algorithm for Real-Time Video Enhancement. *IEEE Trans. VLSI Sys.* **28**, 101–114 (2020)
28. Y. Kim, J. Choi, M. Kim, A real-time convolutional neural network for super-resolution on FPGA with applications to 4K UHD 60 fps video services. *IEEE Trans. Circuit. & Sys. Vid. Technol.* **29**, 2521–2534 (2019)
29. M.A. de Jesus, V.V. Estrela, A. Khelassi, R.J. Aroma, K. Raimond, S.R. Fernandes, S.E.B. da Silva, A.C. de Almeida, R.T. Lopes, Motion estimation role in the context of 3D video. *International Journal of Multimedia Data Engineering and Management (IJMDEM)* (2020)
30. H. Kim, Y. Kim, H. Ji, H. Park, J. An, H. Song, Y.T. Kim, H. Lee, K. Kim, A single-chip FPGA holographic video processor. *IEEE Trans. Ind. Electron.* **66**, 2066–2073 (2019)
31. R. Wang, Z. Fang, J. Gu, Y. Guo, S. Zhou, Y. Wang, C. Chang, J. Yu, High-resolution image reconstruction for portable ultrasound imaging devices. *EURASIP Journal on Advances in Signal Processing* **2019**, 1–12 (2019)
32. M. Amiri, F.M. Siddiqui, C. Kelly, R.F. Woods, K. Rafferty, B. Bardak, FPGA-based softcore processors for image processing applications. *J. Signal Process. Sys.* **87**, 139–156 (2017)
33. A. Deshpande, P. Patavardhan, Super resolution and recognition of long range captured multi-frame iris images. *IET Biom.* **6**, 360–368 (2017)
34. A. Deshpande, P. Patavardhan, Survey of super resolution techniques. *ICTACT J. Image & Vid. Process.* **9**, 1927–1934 (2019)
35. Y. Marin, J. Miteran, J. Dubois, B. Heyrman, D. Ginjac, An FPGA-based design for real-time super-resolution reconstruction. *J. Real-Time Image Process.*, 1–17 (2020)
36. G.W. Cook, J. Ribera, D. Stolzitzka, W. Xiong, 85-4: A subpixel-based objective image quality metric with application to visually lossless image compression evaluation. *SID Symp. Dig. Tech. Paper, Soc. Inf. Disp.* **49**(1), 1163–1166 (2018)
37. C.H.B. Elliott, T.L. Credelle, S. Han, M.H. Im, M.F. Higgins, P. Higgins, Development of the PenTile Matrix™ color AMLCD subpixel architecture and rendering algorithms. *J. Soc. Inf. Disp.* **11**(1), 89 (2003). <https://doi.org/10.1889/1.1831725>
38. N. Razmjoo, V.V. Estrela, H.J. Loschi, *A study on metaheuristic-based neural networks for image segmentation purposes* (Data Science Theory, Analysis and Applications, Taylor and Francis, Abingdon, 2019)
39. O. Kerdjijdj, A. Amira, K. Ghanem, N. Ramzan, S. Katsigiannis, F. Chouireb, An FPGA implementation of the matching pursuit algorithm for a compressed sensing enabled e-Health monitoring platform. *Microprocess. Microsyst.* **67**, 131–139 (2019)
40. A. Deshpande, P. Patavardhan, V.V. Estrela, N. Razmjoo, Deep learning as an alternative to super-resolution imaging in UAV systems, in *Imaging and sensing for unmanned aircraft systems*, ed. by V. V. Estrela, J. Hemanth, O. Saotome, G. Nikolakopoulos, R. Sabatini, vol. 2, 9, (IET, London, 2020), pp. 177–212. ISBN 978-1-78561-644-0 Hardback, ISBN 978-1-78561-645-7 PDF
41. H.H. Issa, S.M. Ahmed, FPGA implementation of floating point based Cuckoo search algorithm. *IEEE Access* **7**, 134434–134447 (2019)
42. P.P. Cespedes, G.A. Gimenez, L.S. López, J.L. Vázquez, H. Legal-Ayala, D.P. Pinto-Roa, Inpatient multimodal medical image registration of brain CT-MRI 3D: An approach based on metaheuristics. *Symposium on Medical Information Processing and Analysis* (2018)
43. S. Kockanat, N. Karaboga, *Medical image denoising using metaheuristics. Metaheuristics for medicine and biology* (Springer, Berlin, 2017), pp. 155–169
44. M.M. Nair, A.K. Tyagi, R. Goyal, Medical cyber physical systems and its issues. *Procedia Comput. Sci.* **165**, 647–655 (2019)
45. V.V. Estrela, O. Saotome, H.J. Loschi, D.J. Hemanth, W.S. Farfan, R.J. Aroma, C. Saravanan, E.G.H. Grata, Emergency response cyber-physical framework for landslide avoidance with sustainable electronics. *Technologies* **6**, 42 (2018). <https://doi.org/10.3390/technologies6020042>

Chapter 14

Adaptive Specular Reflection Detection in Cervigrams (ASRDC) Technique: A Computer-Aided Tool for Early Screening of Cervical Cancer



Brijesh Iyer  and Pratik Oak

14.1 Introduction

Cervical cancer (CC) is the fourth most recurrent women's cancer worldwide. In line with the WHO health report, every fifth woman in the world will be impacted by it in 2050 [1]. Nearly 90% of the 270,000 deaths from CC in 2015 took place in low- and middle-income countries. Noteworthy progress in disease screening and treatment supports prevention, and prompt diagnosis may drastically reduce the CC mortality rate [1].

CC begins with abnormal modifications in the cervical tissue. The risk of having these unusual changes is concomitant with infection by the human papillomavirus (HPV). Moreover, early sexual interaction, manifold sexual partners, usage of oral contraceptives (birth control pills), unhygienic lifestyle, and misinformation are the critical factors for spreading this disease. If spotted early, CC can be cured reasonably. The most prevalent CC detection method is the Pap smear.

Nonetheless, it has inherent limitations such as sample quality, slide quality, and effectiveness of screeners. The CAD systems can help to treat this disease by analyzing an input image and, with the assistance of various image-processing algorithms, predict or detect abnormalities. The earliest and challenging step in medical image exploration is to pre-process the input image for the uncovering and removal of noise. Specular reflection (SR) is a variety of prominent noise that appears in photography and medical imaging. Once a ray of light strikes the surface, a portion of the ray is straightaway reflected from the interface amid the surface and the air, thanks to their different refractive indices. This reflected light is called SR [2]. The humidity on the cervix surface engenders the SR, which hampers early CC

B. Iyer (✉) · P. Oak
Department of E&TC Engineering, Dr. Babasaheb Ambedkar Technological University,
Lonere, India
e-mail: brijeshiyer@dbatu.ac.in

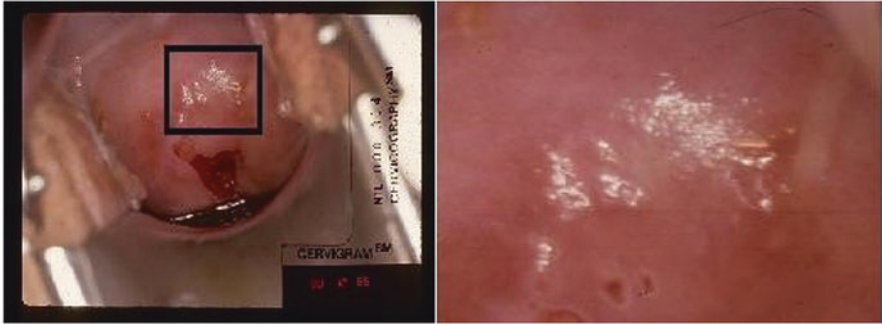


Fig. 14.1 Example of an SR affected cervix image with cropped SR region

detection by computational systems [3]. Figure 14.1 illustrates the initial cervix image with the SR region (black box in the middle) and cropped SR region near it so that these regions undergo automatic detection, correction, and deletion according to the specialist's needs.

The rest of the manuscript goes as follows: Sect. 14.2 talks over the state-of-the-art methods for SR detection and its removal. Section 14.3 describes the components of the ASRDC scheme. The experimental outcomes appear in Sect. 14.4. Section 14.5 closes this work with remarks on the ASRDC methodology and its future.

14.2 State-of-the-Art Technology

Automatic recognition and removal of SR experimented a few contributions lately. The correlated literature generally embraces four categories as (i) the dichromatic reflection model (DRM) usage, (ii) kernel filtering, (iii) SR cast as classification, and (iv) thresholding procedures.

The DRM principle states that a reflection combines specularly and diffusion linearly. Yoon et al. appraised the value of the specularly-invariant pixels as well as their ratio to set apart diffuse components. Still, this maneuver suits textured imageries, and approximation in the normalization procedure bounds the accuracy of SR detection [4]. Tao et al. introduced a new metric termed line consistency for depth estimation of specular regions. They had estimated colors from multiple light sources. However, this strategy failed to distinguish saturated specularly [5]. J Suo et al. applied the DRM rationale perceiving the problem as a signal separation for SR detection and removal.

In contrast, the procedure overlooked smooth color alterations, and it failed to discern the pixels with identical hue and different saturation [6–8]. Das et al. advised kernel-based filters for SR detection and exclusion, e.g., filling, dilation, multiscale morphology, and IS-histogram [3]. Kudva et al. utilized morphological kernels as

filters to acquire features from color images [9]. Xue et al. predefined the structuring element (SE) as a kernel. The top-hat transform treated the intensity image I (whose entries hold brightness values within some range) of input cervigrams [10]. Yet, all these schemes rest on the size and shape of the kernel applied to the database. Gao et al. proposed SR detection as a classification problem using SVM classifiers. This method's caveat is the requirement of training every time for SR detection [11].

Zimmerman et al. suggested multiplying S and I by an arbitrary constant where S is the saturation component, which shows how much the white color taints a given color. The S component belongs to the range $[0, 1]$ within the HSI plane. The gradient image outputs on these multiplied regions are SR pixels [12]. Akbar et al. computed the SR pixel via a chaotic clonal selection procedure [13]. The image specular degree can function as a thresholding parameter to separate diffused images and for SR detection [2, 14]. The choice of arbitrary constants throughout automatic detection of SR pixels may be contingent on the database under experimentation. However, the detection system must be entirely automated and independent of the database. Therefore, any imaging modality calls for automatic threshold selection. Table 14.1 relates the state-of-the-art SR discovery approaches and the ASRDC concept. Automatic thresholding fits in fivefold groups according to the information content they rely upon, viz.:

- (i) Histogram-based schemes analyze the primary intensity, decimation in intensity range, and nonlinear nature of the smoothed histogram.
- (ii) Clustering-related strategies split the gray levels from the input image into the background and foreground pixels.
- (iii) Entropy-based methods employ local entropy, cross-entropy of the foreground and background regions, original and binary images, etc.

Table 14.1 State-of-the-art SR detection categories

Sr. No.	Category	Working principle	Remarks
1.	Dichromatic reflection model [4–7]	Reflection is a linear combination of specular and diffuse components	Limits the identification of saturated specularity
2.	Use of kernel as a filter [3, 9, 10]	Applying a specific mask on an input image as a filtering operator	The inappropriate selection of size and shape of the kernel affects the accuracy
3.	SR as a classification problem [11]	Feature extraction and training a system with predefined labels as SR pixels	Requires a training system every time for SR detection
4.	Thresholding [2, 3, 12, 13]	Collection of pixels falling below the predefined threshold value, as SR pixels	Arbitrary selection of constant makes the system database dependent
5.	ASRDC method	SR detection using automatic thresholding and quality enhancement of low-resolution images	Fully automatic system, which is independent of size and shape of kernel and selection of arbitrary constant, no need for separate training

- (iv) Object attribute-based methods focus on the similarity between the gray level and its black and white versions.
- (v) Statistical relation-founded schemes rely on higher-order moments and/or the correlation among pixels for threshold selection [15].

These threshold-picking strategies can be either bi-modal or multi-modal. Nonetheless, the application demands to get SR pixels, which are always bright. Hence, bi-modal distribution is the best choice, along with a histogram-based approach. Table 14.2 abridges a review of automatic threshold determination practices built on histograms.

In 2004, Sezgin and Sankur reviewed the performance of thresholding techniques using five quality measures, viz., misclassification error (ME), edge mismatch (EMM), relative foreground area error (RAE), modified Hausdorff distance (MHD), and region nonuniformity (NU). They calculated the average score of each scheme, ranked individual quality measures, and, finally, concluded that Kittler and Kapura were the superlative adaptive thresholding procedures [15]. Donald Bailey also investigated adaptive thresholding techniques for performance analysis and

Table 14.2 State-of-the-art SR detection categories

Author	Criteria function	Significance	Remarks
Calvard and Riddler [16]	Starts with the histogram mean Updates the threshold with the average of the lower and upper means of the histogram. Stops if the lower and upper threshold difference is zero	Simple and speedy Detected threshold is useful for foreground separation	SR intensities are always brighter Not suitable for SR detection
Otsu [17]	Use of kernel [3, 9, 10], minimizing intra-class variance between the left and right regions of the histogram	Best suitable for histograms with a clear valley between the modes	Not suitable for histograms where objects and b/g are not well separated
Kapura [18]	Maximization of entropy between two regions	Works on actual information extraction of two modes	SR detection does not require to know average information of lower-intensity pixel region
Kittler [19]	Minimum error thresholding for the standard deviation of both sub-histograms	Moderate threshold selection. Suitable for proper foreground detection	Some changes in partitioning required for high-intensity threshold selection
Carlotto [20]	Histogram represented as the combination of Gaussian mixtures of different modes	Approximation of histogram is dependent for the selection of the number of modes	Computationally complex
Patra [21]	Calculated energy of pixel over a 3×3 neighborhood	Proposed energy curve behaving similar to a histogram with valleys and peaks	Applicable for spatial contextual information inappropriate for multilevel histogram

found that Kittler's minimum error is the best [20]. The ASRDC methodology overcomes the limitations above due to:

- (a) Its complete independence on size and shape of the kernel
- (b) No requirement for the training process
- (c) Fully automatic threshold calculations

The catchline features of the ASRDC methodology are:

1. Use of the lightness as a no-reference quality measure for selection of appropriate algorithm
2. Automatic selection of threshold by a modified Kittler's method
3. Automatic enhancement of low-quality images before the SR treatment

14.3 The ASRDC Methodology

The ASRDC block diagram appears in Fig. 14.2. The section further describes the threefold contribution of the chapter.

14.3.1 Selection of Optimum Threshold Detection Technique

The authors picked the Kittler minimum error thresholding scheme for automatic SR detection [19] from the approaches talked over in Sect. 14.1.

14.3.2 Automatic SR Detection

A histogram exemplifies the distribution of the pixel intensities, where an SR is a bright spot on an image, which agrees with the maximum part of the intensity range (close to white). Nevertheless, few non-SR pixels may also possess high brightness. SR pixels occur at the dark side of the S in addition to the bright side of the I images

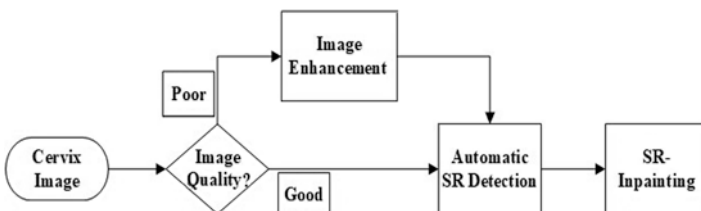


Fig. 14.2 Block diagram of the ASRDC system

[14]. As a consequence, the SR occurrence in the intensity saturation (IS) histogram is a foremost ASRDC concern. The automatic SR recognition is carried out by a simple variant of the Kittler method to attain the optimum threshold on the S and I images. The modified Kittler method (MKM) understands the threshold (T) differently from the original tactic. This work considers the span going from minimum to maximum intensity (i.e., over complete dynamic range) as opposed to starting with a random T . An optimum threshold matches the minimum Jaccard Index (JI) value (aka criteria function) of the MKM.

The Jaccard Index J is a statistic that explains the similarities between finite sample sets. J is defined properly as

$$J = \frac{|A \cap B|}{|A \cup B|} = \frac{|A \cap B|}{|A| + |B| - |A \cap B|}, \quad (14.1)$$

i.e., the size of the intersection $|A \cap B|$ divided by the size of the union $|A \cup B|$ of the sample sets A and B .

The ASRDC methodology employs half of the intensities for two different inputs. The thresholds, starting from 1 to 128, assist in calculating the minimum error with the MKM criterion function and are known as the left-side threshold (TL). Similarly, the right-side threshold (TR) results from all combinations of pixels from 128 to 256. The modified algorithm is given below.

The MKM Algorithm

1. Go through every possible threshold (T), i.e., grey level from 1 to 128 or from 128 to 256.
2. Consider the groups (i) 1 or T , and (ii) 2 or $(T+1)$, i.e., highest intensity.
3. Compute the histograms of these groups and mark their sums as $P1$ and $P2$.
4. Determine the mean and standard deviation for the histograms.
5. Compute the Jaccard Index (J) criterion function for all possible T .
6. The finishing threshold is the position with minimum J .

Thresholds generated from step 6 (TL and TR) work on saturation (S) and intensity (I) images, respectively. The SR pixels as given below.

$$SR = (S(i,j) < TL) \&\& (I(i,j) > TR) \quad (14.2)$$

where (i, j) symbolizes the pixel location (for row i and column j) in an picture and “&&” is the logical AND.

14.3.3 *Image Quality Assessment (QA)*

The overall input image condition dramatically impacts any algorithm performance. Therefore, the input image quality assessment (QA) is vital to the deployment of an adaptive system. The objective QA of the examined picture consists of the computation of the threefold quality metric categories, viz., full reference (FR), reduced reference (RR), and no reference (NR). As ground reality images are not available when it comes to cervigrams, the NR metric is preferred in input quality testing. Several investigators commended many color quality parameters or attributes for NR-based QA like brightness, colorfulness, sharpness, contrast, and entropy. The colorfulness illustrates the color information perceived by the human eye. The sharpness gives the amount of preservation of edges. The contrast addresses the emphasis on the foreground and background association. The average image information corresponds to the brightness measures, whereas the lightness promotes the distortion in intensities of pixels [22].

It is essential to use quality measures related to distortion for SR detection. Hence, the ASRDC scheme takes account of the lightness parameter together with colorfulness (C1), contrast (C2), and sharpness (C3). Their grouping forms a quality measure if and only if they are correlated, which, consequently, leads to the calculation of the correlation between the lightness and the three attributes. The validation of the null hypothesis can confirm the possibility of this combination, i.e., the lightness is uncorrelated with all three attributes. The Pearson correlation coefficient (p-value) gives the acceptance probability of the null hypothesis. In general, the significance level of the p-value is 0.05, namely, if the p-value is less than 0.05, attributes are correlated with the refutation of the null hypothesis [23]. The tryouts from Sect. 14.4 (B) substantiate the dominance of lightness features among the color attributes to deal with an eventual image enhancement. The experimental investigation of the ASRDC method indicates that if the lightness is greater than 1, then image quality amelioration is required.

The low-quality images must be enhanced before applying the ASRDC methodology. This scheme has a histogram-based automatic threshold selection (Sect. 14.3 (B)) that also enhances pictures by altering the histogram shape.

Most prevalent histogram-centered measures to enhance pictures are histogram equalization (HE) [17], bi-HE (BHE) [24], adaptive HE (AHE) [32], contrast-limited AHE (CLAHE) [33], and brightness preserving BHE (BBHE) [24]. Among these approaches, the BBHE scheme preserves the image characteristics after pre-processing. Hence, this work treated low-quality images with BBHE before employing the ASRDC method to manage SR in an input image adaptively as:

- (a) Initial quality check of the input picture utilizing the lightness parameter
- (b) Low-quality image enhancement through BBHE
- (c) Application of the ASRDC technique to the input image

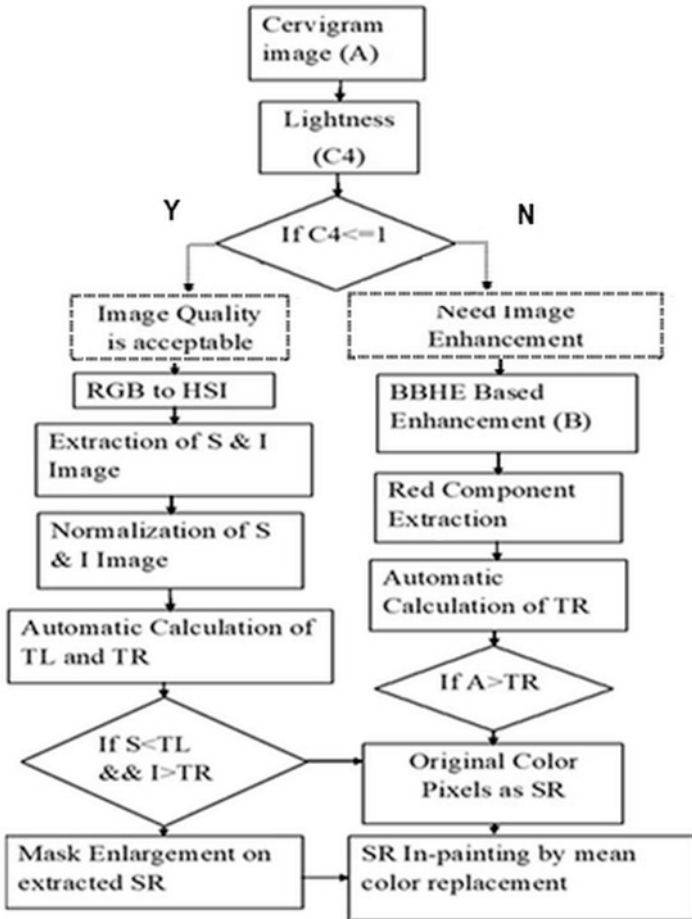


Fig. 14.3 ASRDC workflow

14.3.4 SR Inpainting

Further SR inpainting is carried out to generate the SR free image. An iterative non-zero averaging filter creates an SR free image [10]. The complete flow of the ASRDC method arises in Fig. 14.3 with its algorithm.

ASRDC Algorithm

1. Take the input cervix image and calculate the lightness.
2. If lightness < 1 ,
 - (i) RGB to HSI conversion to separate saturation (S) and intensity (I) images
 - (ii) Compute left (TL) and right threshold (TR) using the ASRDC method
 - (iii) Collect pixels lying between intensities of S less than TL and intensities of I greater than TR, as SR pixels
 - (iv) Perform mask enlargement on the output of step 2 (iii)
3. If lightness > 1 , Apply BBHE on the input image and extract red component
 - (i) Calculate TR from BBHE image
 - (ii) Collect pixels of the input image which are greater than TR, as SR pixels
4. Inpaint detected SR pixels by mean color replacement.

14.4 Results and Discussions**14.4.1 The Dataset**

The present exploration involves digitized uterine cervix pictures collected by the National Cancer Institute (NCI) from four epidemiological studies made in the USA, e.g., “Costa Rican Natural History Study of HPV and Cervical Neoplasia (NHS),” “ASCUS LSIL Triage Study (ALTS),” “Biopsy Study,” and “Costa Rica Vaccine Trial (CVT)” on HPV and CC screening [25]. The trials comprise a total of 612 images from all 4 datasets distributed as NHS (200), ALTS (200), Biopsy (50), and CVT (162). This research work selects images randomly from the available databases with resolutions for pictures in the ALTS and NHS equal to 2891×1973 and for the Biopsy and CVT, 4256×2832 .

The acceptance of the image enhancement output entails the evaluation of the quality of the input image. As talked over in Sect. 14.3.3, the p -value is calculated to obtain the correlation between image attributes. Table 14.3 displays the p -values for various arrangements of images from the datasets.

Table 14.3 p -values between C4 and C1, C2, and C3

Dataset	p -value		
	C4-C1	C4-C2	C4-C3
ALTS + Biopsy (21 images)	0.1577	0.0487	1.29×10^{-6}
ALTS + Biopsy + CVT (61 images)	0.1195	0.1401	7.73×10^{-9}
All 4 datasets (113 images)	0.006	0.309	1.64×10^{-11}

C1, C2, C3, and C4 represent the colorfulness, sharpness, contrast, and lightness attributes, respectively. The p-values of C3 are very low (i.e., <0.05 for all combinations of the dataset). However, C1 and C2 show significant p-values concerning the significance level. This implies a correlation between lightness and contrast. Thus, the lightness can be combined with contrast to test the image quality. The present analysis selected 80 images (20 from each dataset) to determine the dominant feature between lightness and contrast. This experiment aims to confirm the necessity of image enhancement through no-reference image attribute. The contrast of all 80 images ranges between 0.45 and 0.5, which did not give a noteworthy threshold as a decision parameter. However, a significant change in the value of lightness is observed for all 80 images, as below and above value 1. Thus, lightness is chosen as a dominant feature of the cervix color image to decide the input quality. Experimentation concluded the adaptability condition as if the lightness is less than 1, input image quality is satisfactory, and the ASRDC algorithm should get applied without image enhancement. For an image with lightness greater than 1, it should be enhanced before applying the ASRDC algorithm.

14.4.2 Experiments

The S and I images are normalized to the original grayscale range of 0 to 255. TL is calculated for the S image, and TR is calculated for I the image, as explained in Sect. 14.3.2. The original Kittler method and the MKM are applied to normalized S and I images. The final SR pixels are detected using Eq. 14.2. Table 14.4 compares the average threshold for S and I images using both methods. The thresholds given by the original Kittler method show nonuniformity over different sets of cervix images and detect a very less number of SR pixels. This affects the accuracy of SR pixel detection. However, the approximate range of difference between TL and TR by the suggested modification ($TR - TL =$ dynamic range of intensities of non-SR pixels) is constant for all four datasets under experimentation. This, in turn, increases the accuracy of SR as well as non-SR pixel detection.

The SR is detected using the recommended modification explained in Sect. 14.3.2 (Fig. 14.4) that contemplates the fact that the SR pixels are heterogeneous regarding other image pixels and that they can be easily observed by the human eye. The performance of enhancement relying on SR detection for low-quality images

Table 14.4 Average left-side and right-side threshold

Database	Threshold for S image (TL)		Threshold for I image (TR)	
	Original image	Proposed method	Original image	Proposed method
ALTS	16.4	63.38	253	165.4
Biopsy	68	69.78	88.85	157.7
CVT	73.05	45.11	107.8	163
NHS	24.4	28.5	227.9	179.1

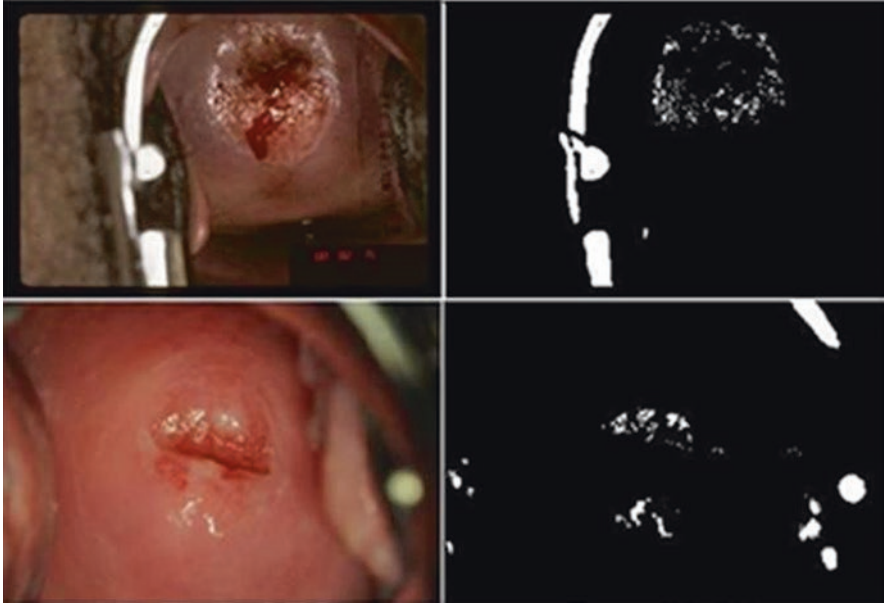


Fig. 14.4 SR pixel detection



Fig. 14.5 Performance of enhancement-based SR detection for low-quality image

corroborates the prerequisite of adaptability from Sect. 14.3.4. Figure 14.5b shows the detected SR pixels from the original low-quality image, whereas accurate SR detection from the enhanced high-quality image after the ASRDC application appears in Fig. 14.5c showing that the SR detection is effective to the adaptive enhancement of the low-quality image.

14.4.3 SR Inpainting

The iterative mean color replacement from Sect. 14.3.2 takes away the detected SR pixels (refer to Fig. 14.6). The ASRDC method adaptively selects the SR detection tactic to be applied with or without input image enhancement based on the lightness

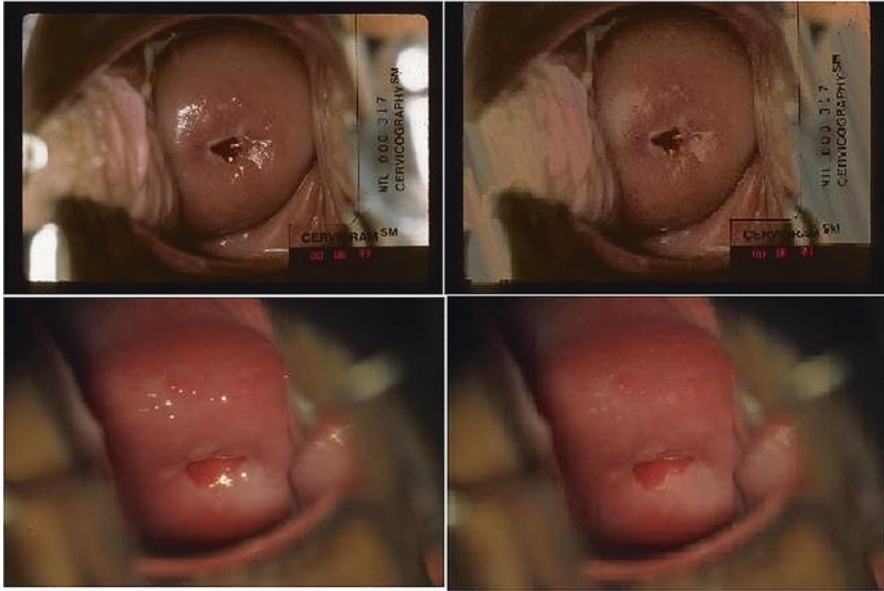


Fig. 14.6 SR Inpainting using mean color replacement

measure of an image. The enhancement initiates automatically for low-quality images before applying the ASRDC technique.

14.4.4 *Quantitative Evaluation of Proposed Method*

Most of the reported literature spoke about visual comparisons of various SR detection and removal methods [3–5, 13, 14, 17]. Due to the unavailability of ground reality images captured with proper illumination, the quantitative evaluation is complicated.

However, the ASRDC system compares results utilizing NR image quality attributes of the original and inpainted image on the dataset under experimentation. Table 14.5 provides the average calculations of mean and standard deviation, respectively. It proves that an inpainted image has a low mean as compared to the original image that is to say SR (bright intensity pixels) are removed. The SR free image is homogeneous due to uniformity in image intensities and has less deviation from the mean, i.e., a decrease in the standard deviation. Table 14.6 illustrates the attributes of color image, viz., colorfulness, sharpness, and standard deviation. The SR removal decreases the colorfulness due to mean color replacement, makes the input image sharper, and decreases the proportion of distortion present in the input image, i.e., decrease in lightness. These observations depict a close agreement with the theoretical concepts of NR color image quality metrics.

Table 14.5 Comparison of statistical characteristics of original and inpainted image

Database	Mean		Standard deviation	
	Original image	Inpainted image	Original image	Inpainted image
ALTS	66.7	55.31	57.49	39.99
Biopsy	73.52	72.56	42.06	40.58
CVT	81.82	71.35	42.59	40.58
NHS	75.38	64.13	60.8	48.8

Table 14.6 Comparison of color image attributes of original and inpainted image

Quality measure/ database	Colorfulness		Sharpness		Lightness	
	Original image	Inpainted image	Original image	Inpainted image	Original image	Inpainted image
ALTS	1.378	1.276	0.415	0.662	1.28	1.08
Biopsy	1.564	1.512	0.475	0.748	1.002	0.97
CVT	1.373	1.272	0.392	0.689	1.002	0.94
NHS	1.588	1.496	0.489	0.619	1.22	1.09

14.4.5 Qualitative Analysis for State-of-the-Art Methods

Figure 14.7 illustrates the comparative visual difference between the ASRDC method and other state-of-the-art implementations aiming at SR detection and mitigation suggested in [9, 12, 14]. It follows that the novel ASRDC technique outsmarts the reported practices in terms of SR detection for images collected from different databases. Kudva et al. suggested the use of the Jaccard Index (JI) to measure the quantitative performance of SR detection techniques with manually marked SR pixels for images having practically visible SR pixels [9]. The JI value must be higher for the selected image to have accurate detection.

Table 14.7 parallels outcomes for the maximum JC for the ASRDC scheme and other state-of-the-art techniques to validate the new approach. The present analysis considered only four images for the JC evaluation. However, the method can be extended for the entire database assessment. Recently, efforts relying on artificial intelligence (AI), data mining, and fuzzy-based methodologies addressed the SR detection issue [26, 27]. Health 4.0 protocols have also provided new insights regarding the usage of medical resources to handle various medical emergencies [28–31]. These lines of attack may lead to a revolution in CC detection and treatment.

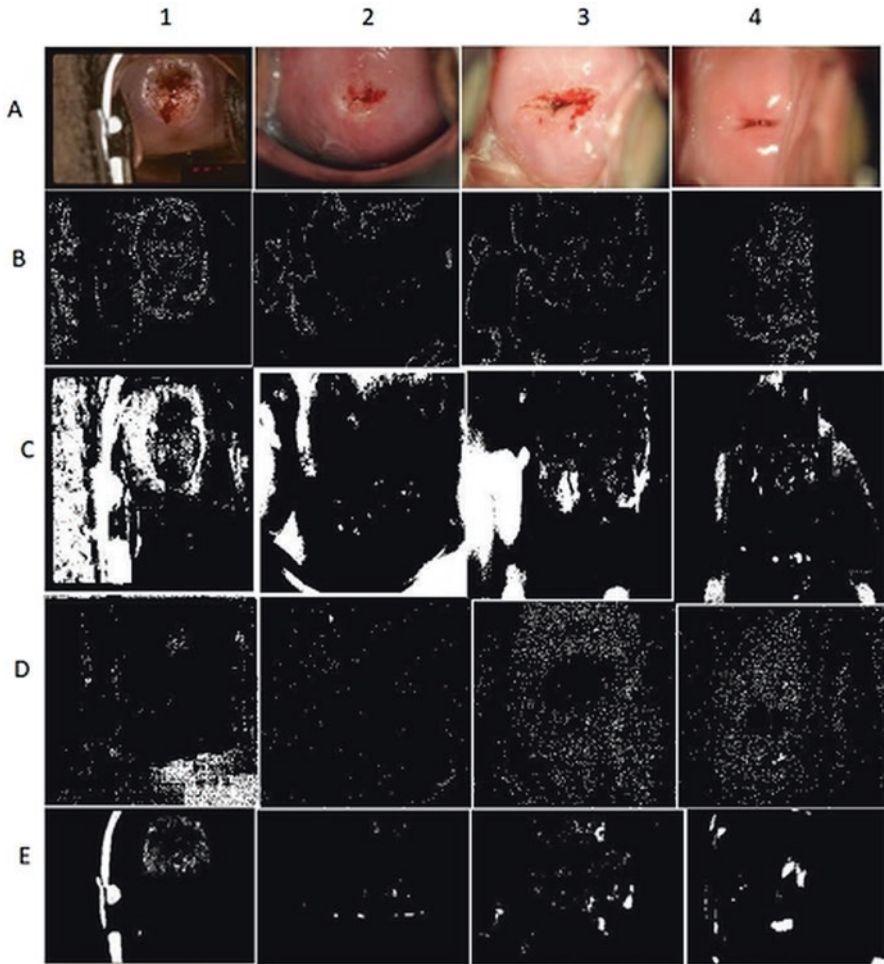


Fig. 14.7 Comparative analysis of state-of-the-art methods for SR detection. (a) Original image; (b) SR detection with [12]; (c) SR detection using [14]; (d) SR detection via [9]; (e) SR detection using the ASRDC method

Table 14.7 Qualitative analysis with state-of-the-art methods of SR detection

Image	JC using [12]	JC using [14]	JC using [9]	JC for the ASRDC method
1	0.0033	0.0413	0.0099	0.1005
2	0.0041	0.1737	0.0852	0.4923
3	0.0012	0.1334	0.0282	0.3571
4	0.0029	0.2208	0.0421	0.4695

14.5 Conclusions

This research puts forward the ASRDC as an adaptive method for detection and removal of SR from input cervix image, i.e., cervigrams. Experimentation was carried out on 612 images collected from NCI. The ASRDC method overcomes significant limitations of current SR detection techniques, i.e., dependency on shape and size of the kernel, selection of arbitrary constant, and every time training of the system. The ASRDC methodology uses the lightness as an NR quality measure to check the necessity of image enhancement, automatic enhancement of low-quality images before SR detection technique, and automatic selection of threshold by the MKM. Subjective and objective quality evaluation over different datasets highlights the ASRDC significance. Noise and resolution of the biomedical image largely depend on the quality of the equipment used for the capture and the skills of the expert (human intervention). In general, noise content and resolution of any biomedical images can be improved by using equipment that is more sophisticated. In addition to this, the ASRDC methodology will be an additional tool to enhance the grade of the biomedical images under study.

The inpainted images generated by the ASRDC adaptive system can be passed to further stages of early CC detection for additional feature extraction, segmentation, and classification techniques.

The authors are aware that when it comes to analyses of 3D images and 2D or 3D video, other shortcomings may affect SR detection as well as correction. For the cases when the dimensionality is high and several imaging modalities become necessary, soft computing strategies may lessen the processing time, help with more challenging settings, and work with other objective metrics [32–42]. It should be pointed out that SR detection and removal can benefit from the knowledge obtained in other similar image-processing tasks that share some characteristics and caveats with this problem.

Acknowledgments The authors gratefully acknowledge support from Dr. M. Schiffman and the team of the National Cancer Institute for providing the data from NCI Guanacaste and ALTS projects.

Ethical Approval This article does not contain any studies with human participants or animals, performed by any of the authors.

Funding The work reported in this manuscript does not receive any funding from any source/agency.

References

1. WHO cervix cancer report. Available at: <http://www.who.int/cancer/prevention/diagnosis-screening/cervical-cancer/en>
2. H. Shen et al., Simple and efficient method for specularly removal in an image. *Appl. Opt.* **48**(14), 2711–2719 (2009)

3. A. Das et al., Elimination of specular reflection and identification of ROI: The first step in automated detection of cervical cancer using digital colposcopy. In: IEEE International Conference on Imaging Systems and Techniques, 237–241 (2011)
4. K. Yoon et al., Fast separation of reflection components using a specularly invariant image representation. In: Proceedings of IEEE International Conference on Image Processing, 973–976 (2006)
5. M. Tao et al., Depth estimation and specular removal for glossy surfaces using point and line consistency with light-field cameras. IEEE Trans. Pattern Anal. Mach. Intell. **38**(6), 1155–1169 (2016)
6. J. Suo, D. An, X. Ji, H. Wang, Q. Dai, Fast and High Quality Highlight Removal from a Single Image. IEEE Trans. Image Process. **25**(11), 5441–5454 (2016)
7. N. Lamprinou et al., Fast detection and removal of glare in gray scale laparoscopic images. In: Proceedings of the 13th international joint conference on computer vision, imaging and computer graphics theory and applications 4, 206–212 (2018)
8. K. Panetta, G. Chen, A. Sos, No reference color image contrast and quality measures. IEEE Trans. Consum. Electron. **59**(3), 643–651 (2017)
9. V. Kudva, K. Prasad, S. Guruvare, Detection of specular reflection and segmentation of cervix region in uterine cervix images for cervical cancer screening. IRBM **38**(5), 281–291 (2017)
10. X. Zhiyun et al., Comparative performance analysis of cervix ROI extraction and specular reflection removal algorithms for uterine cervix image analysis. In: Proceedings of SPIE Medical Imaging, 6512 (2007)
11. G. Yefei et al., Dynamic searching and classification for highlight removal on endoscopic image. In: International Congress of Information and Communication Technology, 762–776 (2017)
12. Z. Gali, G. Hayit, Automatic Detection of Specular Reflections in Uterine Cervix Images. In: Proceedings of SPIE Medical Imaging, 6144, 2037–2045 (2006)
13. H. Akbar, N. Herman, Removal of highlights in dichromatic reflection objects using segmentation and inpainting. In: International Conference on Robotics, Automation and Sciences (ICORAS), 1–4 (2016)
14. S. Alsaleh et al., Automatic and robust single-camera specular highlight removal in cardiac images: 37th Annual International Conference of the IEEE Engineering in Medicine and Biology Society (EMBC), 675–678 (2015)
15. S. Mehmet, S. Bulent, Survey over image thresholding techniques and quantitative performance evaluation. J. Electron. Imag **13**(1), 146–165 (2004)
16. T. Ridler, S. Calvard, Picture thresholding using an iterative selection method. IEEE Trans. Syst. Man Cybern. **8**(8), 630–632 (1978)
17. R. Gonzales, C. Woods, Digital Image Processing. 2nd Edition Wesley, an imprint of Pearson Education, 598–608 (2000)
18. J. Kapur, P. Sahoo, A. Wong, A new method for grey level picture thresholding using entropy of the histogram. IEEE Trans Comp. Vis. Graph. & Image Process. **29**(3), 273–285 (1985)
19. J. Kittler, J. Illingworth, Minimum error thresholding. IEEE J Pattern Recog **19**(1), 41–47 (1986)
20. D. Bailey, *Histogram operations*, 1st edn. (John Wiley and Sons (Asia) Pte. Ltd., 2011)
21. S. Patra, R. Gautam, A. Singla, A novel context sensitive multilevel thresholding for image Segmentation. Appl. Soft Comput. **23**, 122–127 (2014)
22. M. Osadebey, M. Pedersen, D. Arnold, W. Katrina, No-reference quality measure in brain MRI images using binary operations, texture and set analysis. IET Image Process. **11**(9), 672–684 (2017)
23. D. Lee, Alternatives to p value: Confidence interval and effect size. Korean J. Anesthesiol. **69**(6), 555–562 (2017)
24. K. Yeong, Contrast enhancement using brightness preserving Bi histogram equalization. IEEE Trans Consum Electron **43**(1), 1–8 (1997)
25. R. Herrero, M. Schiffman, Design and methods of population based natural history study of cervical neoplasia in rural Costa Rica: The Guanacaste Project. Pan Am. J. Public Health **1**(5), 362–375 (1997)

26. P. Oak, B. Iyer, Specular reflection detection for early prediction of cervix cancer. Lecture Note. Electr. Eng. **569**, 683–691 (2020)
27. P. Oak, B. Iyer, Specular reflection detection and substitution: A key for accurate medical image analysis. Lecture Note. Electr. Eng. **570**, 223–241 (2020)
28. A. Khelassi, *Artificial reasoning systems: Theory and medical applications* (Lambert Academic Publishing (LAP), Saarbrücken, 2013)
29. A. Khelassi, RAMHeR: Reuse and mining Health 2.0 resources. Electron. Physician **7**(1), 969–970 (2015)
30. A. Khelassi, C. Amine, Cognitive amalgam with a distributed fuzzy case-based reasoning system for an accurate cardiac arrhythmias diagnosis. Int. J. Inf. Commun. Technol. **7**(4/5), 348–365 (2015)
31. V.V. Estrela, A.C.B. Monteiro, R.P. França, I. Yuzo, A. Khelassi, N. Razmjoooy, Health 4.0: Applications, management, technologies and review. Med Technol J **2**(4), 262–276 (2019)
32. P. Musa, F.A. Rafi, M. Lamsani, A review: Contrast-Limited Adaptive Histogram Equalization (CLAHE) methods to help the application of face recognition. 2018 Third International Conference on Informatics and Computing (ICIC), 1–6 (2018)
33. S. Yelmanov, O. Hranovska, Y. Romanyshyn, A new approach to the implementation of histogram equalization in image processing. 2019 3rd International Conference on Advanced Information and Communications Technologies (AICT), 288–293 (2019)
34. A.C.B. Monteiro, R.P. Franca, V.V. Estrela, S.R. Fernandes, A. Khelassi, R.J. Aroma, K. Raimond, Y. Iano, A. Arshaghi, UAV-CPSs as a test bed for new technologies and a primer to Industry 5.0, in *Imaging and sensing for unmanned aircraft systems*, ed. by V. V. Estrela, J. Hemanth, O. Saotome, G. Nikolakopoulos, R. Sabatini, vol. 2, 1, (IET, London, 2020), pp. 1–22
35. A. Deshpande, P. Patavardhan, V.V. Estrela, N. Razmjoooy, Deep learning as an alternative to super-resolution imaging in UAV systems, in *Imaging and sensing for unmanned aircraft systems*, ed. by V. V. Estrela, J. Hemanth, O. Saotome, G. Nikolakopoulos, R. Sabatini, vol. 2, 9, (IET, London, 2020), pp. 177–212
36. N. Razmjoooy, V.V. Estrela, H.J. Loschi, A study on metaheuristic-based neural networks for image segmentation purposes, in *Memon QA*, ed. by S. A. Khoja, (Data Science – Theory, Analysis and Applications, 2019). <https://doi.org/10.1201/9780429263798-2>
37. R. Laptik, D. Navakauskas, Application of ant colony optimization for image segmentation. Elektronika Ir Elektrotechnika **80**, 13–18 (2015)
38. S. Sengupta, N. Mittal, M. Modi, Improved skin lesion edge detection method using ant colony optimization. Skin research and technology: Official journal of International Society for Bioengineering and the Skin (ISBS) [and] International Society for Digital Imaging of Skin (ISDIS) [and] International Society for Skin Imaging (2019)
39. N. Razmjoooy, M. Ashourian, M. Karimifard, V.V. Estrela, H.J. Loschi, D. do Nascimento, R.P. França, M. Vishnevski, *Computer-aided diagnosis of skin cancer: A review* (Current Medical Imaging, Bentham Science Publishers, Sharjah, 2020). <https://doi.org/10.2174/1573405616666200129095242>
40. S. Bosse, D. Maniry, K. Müller, T. Wiegand, W. Samek, Deep Neural Networks for no-reference and full-reference image quality assessment. IEEE Trans. Image Process. **27**, 206–219 (2018)
41. S. Chakraborty, S. Chatterjee, A. Chatterjee, K. Mali, S. Goswami, S. Sen, Automated breast cancer identification by analyzing histology slides using metaheuristic supported supervised classification coupled with bag-of-features. 2018 Fourth International Conference on Research in Computational Intelligence and Communication Networks (ICRCICN), 81–86 (2018)
42. L. Duan, F. Xu, Y. Qiao, D. Zhao, T. Xu, C. Wu, An automated method with attention network for cervical cancer scanning. In: Proceedings of the Second Chinese Conference on Pattern Recognition and Computer Vision, Part II, PRCV 2019, Springer. (2019)

Chapter 15

Implementation of Image Encryption by Steganography Using Discrete Wavelet Transform in Verilog



K. B. Sowmya , Prakash S. Bhat , and Sudheendra Hegde 

15.1 Introduction

Most image encryption algorithms often transfer the message image into a noise-like image, which indicates the presence of an encrypted hidden image. Hence, in this method of image steganography, the message image is embedded into an image by changing the values of some pixels, which are chosen by the encryption algorithm. The recipient of the image must be aware of the same algorithm to know which pixels must be selected to extract the hidden message from the encrypted image.

Medical image data is the most important part of diagnostics in the present healthcare information systems. With the emergence of various methods of high-speed communication systems, the sharing of information in every domain has increased manifold. This process of sharing information plays a very important role in medical applications as it can allow experts to share diagnosis data of a patient with a certain disease and work on its treatment effectively. However, as the patient medical data is the most sensitive information, it must be protected from any modification or tampering. The cryptographic techniques of medical image data must be completely reversible with no loss of any data due to the sensitivity of the information it holds. In the present processing technology, reconfigurable hardware implementation provides better speed and performance than software implementations regarding real-time security applications. Henceforward, FPGA employments of encryption techniques are widely preferred over software implementations.

Images are the most important file formats used in medical applications, and hence a large number of techniques for image steganography have been proposed in recent years. The most common image steganographic approaches can be classified

K. B. Sowmya (✉) · P. S. Bhat · S. Hegde
Department of Electronics and Communication Engineering, R V College of Engineering,
Bengaluru, India
e-mail: prakashsbhat.ec17@rvce.edu.in; sudheendrah.ec17@rvce.edu.in

as (1) spatial domain, (2) transform domain, (3) spread spectrum, (4) statistical, and (5) distortion-based [5].

Out of all the methods, the spatial domain LSB replacement technique (also known as LSB substitution method) and transform domain method involving wavelet transform are widely used in image steganographic applications. Both of these methods have fewer computations and give good capacity and robustness and hence have attracted a lot of research works in recent years [17]. Substitution methods involve replacing the redundant parts of the cover image with a secret message in the spatial domain. Transform domain techniques embed secret information in the frequency domain information (transform space) of the cover image.

In this paper, we present a method of image steganography by modifying the conventional LSB replacement method and applying transform domain techniques to it. In the proposed method, we take Haar DWT of the cover image and fuse the message image pixel values into the A, H, V, and D components [2–4]. For the proposed fusing technique, the message image dimensions must be less than or equal to half of the dimensions of the cover image. Then inverse DWT is taken to get a visually appealing encrypted cover image on the encryption side. On the receiving side, the DWT of the encrypted image is computed, and the message image is retrieved with the use of a key.

Section 15.2 lists the few works done in this domain. Section 15.3 explains methods to implement the proposed image steganography in which two approaches are explained along with retrieving methods. Sections 15.4 discusses the results obtained. Sections 15.5 and 15.6 present the conclusions and future scope, respectively.

15.2 Literary Review

The various image steganography algorithms carried out both in time and the frequency domain are reviewed. Among a large number of techniques, few techniques are reviewed in the literature: Ref. [1] proposed an approach of image steganography which uses DWT to convert spatial domain information to frequency domain information. The algorithm proposed uses only the LL band for further image steganographic process. The technique uses a pre-shared key for both encryption and decryption to provide increased security. Ref. [5] has proposed an image steganography technique using DWT and LSB methods. This paper analyzes the performance of the steganographic algorithm with different values in the n-bit LSB method. Ref. [6] presented the method to perform steganography using the LSB method and verified its performance by FPGA implementation. In this paper, various LSB methods are implemented, and its performance comparison is presented. Ref. [7] provided an overview of image steganography. In this research, secret data is embedded in the grey image, and image compression is done with DWT on hardware. The total processing time taken by the software and hardware method is compared. Ref. [8] proposed a method of image steganography using DWT and hybrid

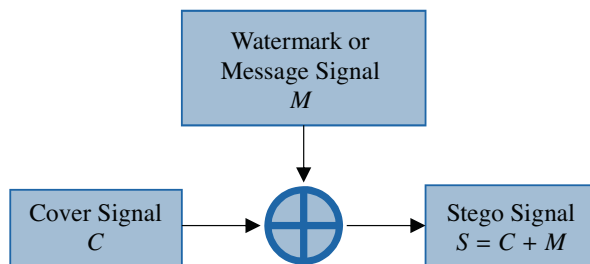
wavelet transform. In this method, the images are normalized and transformed to generate four sub-bands, which are fused to obtain the stego image.

15.3 Methodology

As discussed previously, the LSB substitution technique is the most widely used spatial domain steganographic technique as it is simple and easy to implement and has a high capacity. But as spatial domain techniques are easily detectable by various steganalysis methods, transform domain techniques are preferred to increase the security of data [6]. The cover image can be transformed to the frequency domain by various transforms such as the discrete Fourier transform (DFT), discrete cosine transform (DCT), and discrete wavelet transform (DWT), Fourier-Mellin transform (FMT), fractal transform, etc. [1]. Wavelet transform partitions the image pixel data into different wavelet components based on the frequency. The discrete wavelet transform (DWT) method is favored over other transform methods, owing to the resolution that the DWT provides to the image at various levels [18]. The Haar transform is the simplest of the wavelet transforms and is found effective in applications involving image compression as it provides a simple and computationally efficient approach for analyzing the frequency domain features of a signal [10–13, 17] (Fig. 15.1).

The LSB replacement technique involves replacing least significant n -bits out of 8-bit pixel or 24-bit pixel image with that many bits of message image data. It is found that a 2- or 3-bit LSB technique provides better results in terms of BER, MSE, and PSNR [5]. Hence in the proposed method, we modify the standard LSB replacement technique where instead of replacing LSB bits of the cover image with secret data, we add the secret data to a specified number of LSB bits in the cover image. With this addition technique, there will be less distortion of data in the cover image as compared to the standard method. Also, as we are using frequency domain data of both message and cover image, the robustness and security of the stego image are increased. As the secret data is added to the existing cover image data, the cover image is required and acts as a key during decryption of the message at the receiver side.

Fig. 15.1 Stegoing process [9]



The proposed method explains both encryption and decryption. The encryption side involves taking Haar DWT of the cover image, fusing the message image, and taking inverse DWT to get the encrypted image. The decryption side involves taking DWT of encrypted image and cover image, decoding, and retrieving the message image. As each pixel data of an image is very important in medical applications, a lossless approach for steganography is presented here, as all bits of message image data are embedded into the cover image. The process is explained stepwise in the following subsections.

15.3.1 Encryption

Encryption of message image is done in the following order, as shown in Fig. 15.2.

Haar DWT The image is taken as input to the Verilog module using the \$readmemh() method. To implement Haar DWT, the pixel values are taken four at a time at positions (i, j) , $(i, j + 1)$, $(i + 1, j)$, and $(i + 1, j + 1)$ where i and j are the row and column indices and corresponding transformed pixel values are evaluated. Considering the cover image as an $m \times n$ image, the A, V, H, and D components (LL, LH, HL, HH sub-bands) after Haar DWT will be of $(m/2) \times (n/2)$ dimension. The fusing technique involves distributing the message image data to all four components

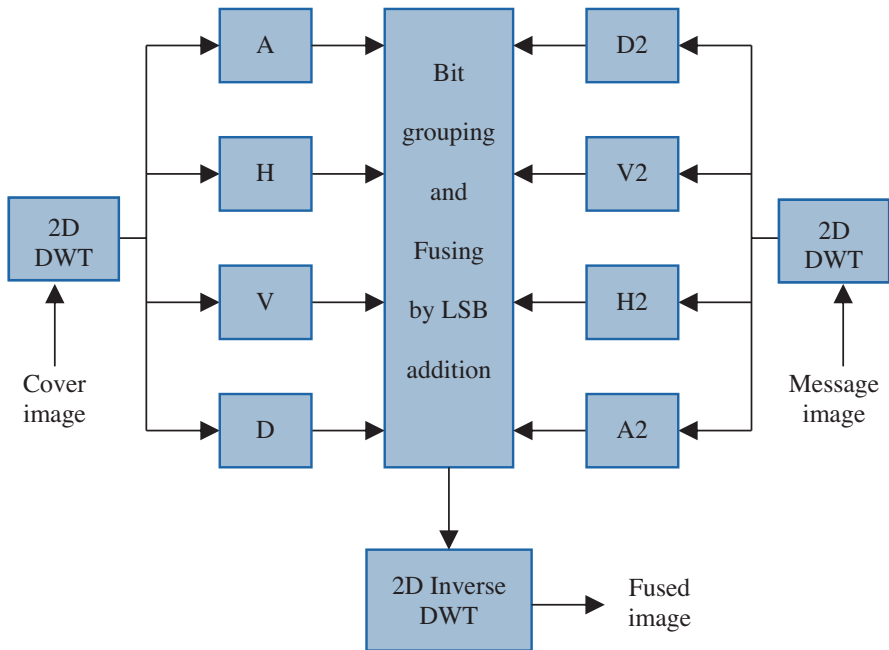


Fig. 15.2 Encryption block diagram

of the cover image. Hence, for proper fusing, the message image must be less than or equal to $(m/2) \times (n/2)$ dimension. These A, V, H, and D components of the image are obtained by evaluating the pixel values of the image using Eqs. 15.1a, 15.1b, 15.1c, and 15.1d, where $C_{i,j}$ represents cover image pixel values at position (i, j) . Haar DWT is operated on the message image to get transformed domain sub-bands A2, V2, H2, and D2.

$$A_{i,j} = \left(+C_{i,j} + C_{i,j+1} + C_{i+1,j} + C_{i+1,j+1} \right) / 4 \quad (15.1a)$$

$$H_{i,j} = \left(-C_{i,j} - C_{i,j+1} + C_{i+1,j} + C_{i+1,j+1} \right) / 4 \quad (15.1b)$$

$$V_{i,j} = \left(-C_{i,j} + C_{i,j+1} - C_{i+1,j} + C_{i+1,j+1} \right) / 4 \quad (15.1c)$$

$$D_{i,j} = \left(+C_{i,j} - C_{i,j+1} - C_{i+1,j} + C_{i+1,j+1} \right) / 4 \quad (15.1d)$$

Fusing As mentioned earlier, the message image can be a maximum of size $(m/2) \times (n/2)$ if the cover image has an $m \times n$ dimension. The message image has $(m/2) \times (n/2)$ 8-bit pixel values, and hereafter each of the sub-band will have $(m/4) \times (n/4)$ 8-bit pixel data. For example, if the cover image has (512×512) pixels, then the maximum size of the message image can be (256×256) . And the corresponding transform domain sub-bands of the cover image (A, H, V, and D) and message image (A2, H2, V2, and D2) will have a size of (256×256) and (128×128) , respectively. Now to embed (128×128) message image sub-band data into (256×256) cover image sub-band, we use LSB addition technique where each 8-bit cover image pixel is added with 2 bits of a message image pixel. And hence each of the cover image pixels will contain a 2-bit secret data hidden in it. The approximation component (LL or A) contains the lowest frequency image data, which is highly sensed by the human eye. And hence to reduce distortion in the approximation component of the cover image (A), it is added with a high-frequency component of message image (HH or D2). And correspondingly vertical (V2), horizontal (H2), and approximation (A2) components of message image are embedded into horizontal (H), vertical (V), and diagonal (D) components, respectively. The method of fusion can be seen using the set of Eqs. 15.2, given below.

$$A_{i,j} = A_{i,j} + D2_{i,j} [8 : 7] \quad (15.2a)$$

$$A_{i,j+1} = A_{i,j+1} + D2_{i,j} [6 : 5] \quad (15.2b)$$

$$A_{i+1,j} = A_{i+1,j} + D2_{i,j} [4 : 3] \quad (15.2c)$$

$$A_{i+1,j+1} = A_{i+1,j+1} + D2_{i,j} [2 : 1] \quad (15.2d)$$

$$H_{i,j} = H_{i,j} + V2_{i,j} [8 : 7] \quad (15.2e)$$

$$H_{i,j+1} = H_{i,j+1} + V2_{i,j} [6 : 5] \quad (15.2f)$$

$$H_{i+1,j} = H_{i+1,j} + V2_{i,j} [4 : 3] \quad (15.2g)$$

$$H_{i+1,j+1} = H_{i+1,j+1} + V2_{i,j} [2 : 1] \quad (15.2h)$$

$$V_{i,j} = V_{i,j} + H2_{i,j} [8 : 7] \quad (15.2i)$$

$$V_{i,j+1} = V_{i,j+1} + H2_{i,j} [6 : 5] \quad (15.2j)$$

$$V_{i+1,j} = V_{i+1,j} + H2_{i,j} [4 : 3] \quad (15.2k)$$

$$V_{i+1,j+1} = V_{i+1,j+1} + H2_{i,j} [2 : 1] \quad (15.2l)$$

$$D_{i,j} = D_{i,j} + A2_{i,j} [8 : 7] \quad (15.2m)$$

$$D_{i,j+1} = D_{i,j+1} + A2_{i,j} [6 : 5] \quad (15.2n)$$

$$D_{i+1,j} = D_{i+1,j} + A2_{i,j} [4 : 3] \quad (15.2o)$$

$$D_{i+1,j+1} = D_{i+1,j+1} + A2_{i,j} [2 : 1] \quad (15.2p)$$

Inverse DWT After fusing hidden data, inverse DWT has to be taken to obtain back the encrypted image. The modified A, H, V, and D values at each position are evaluated using the set of Eqs. 15.3, to get back the group of 4-pixel values, which were used to transform the image.

$$EI_{i,j} = A_{i,j} - H_{i,j} - V_{i,j} + D_{i,j} \quad (15.3a)$$

$$EI_{i,j+1} = A_{i,j} - H_{i,j} + V_{i,j} - D_{i,j} \quad (15.3b)$$

$$EI_{i+1,j} = A_{i,j} + H_{i,j} - V_{i,j} - D_{i,j} \quad (15.3c)$$

$$EI_{i+1,j+1} = A_{i,j} + H_{i,j} + V_{i,j} + D_{i,j} \quad (15.3d)$$

Inverse DWT and DWT operations cancel each other when performed on a 2D array. However, it results in a small error if the array is transposed or mirrored before DWT operation.

15.3.2 Decryption

The decryption method of the encrypted image depends on the fusing technique used. The block diagram of decryption is shown in Fig. 15.3.

Haar DWT of Encrypted and Cover Image Using the same set of Eqs. (15.1) as mentioned in the encryption part, Haar DWT is operated on an encrypted image and the cover image. The original cover image must be transformed using Haar DWT, which acts as a key for decryption. Let the DWT components of the encrypted image be A3, H3, V3, and D3 and that of the original cover image be A, H, V, and D.

Retrieving the Message Image For the addition method, the difference between pixel values of transformed, encrypted image and the cover image is taken to get 2 bits each from each component [22, 23]. The four pairs of 2-bit values from each of A, H, V, and D components are combined to get the transform domain sub-bands

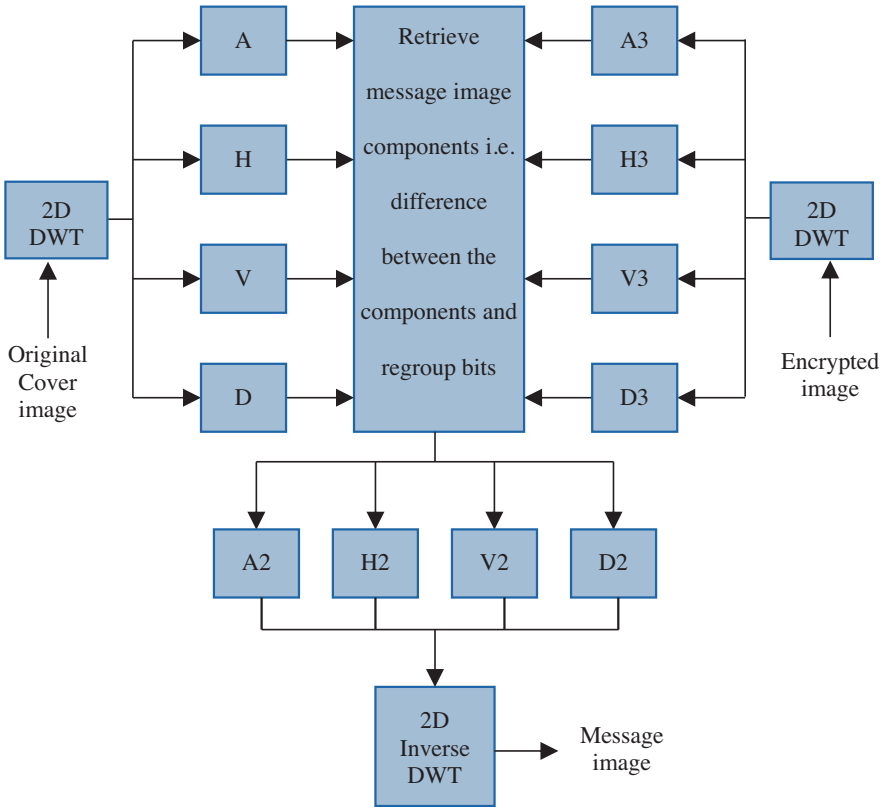


Fig. 15.3 Decryption block diagram

(A2, H2, V2, D2) of the message image. The set of Eqs. 15.4, given below, is used for the decryption process, from which sub-band components of message image are obtained.

$$A2_{i,j} [8 : 7] = D3_{i,j} - D_{i,j} \quad (15.4a)$$

$$A2_{i,j} [6 : 5] = D3_{i,j+1} - D_{i,j+1} \quad (15.4b)$$

$$A2_{i,j} [4 : 3] = D3_{i+1,j} - D_{i+1,j} \quad (15.4c)$$

$$A2_{i,j} [2 : 1] = D3_{i+1,j+1} - D_{i+1,j+1} \quad (15.4d)$$

$$H2_{i,j} [8 : 7] = V3_{i,j} - V_{i,j} \quad (15.4e)$$

$$H2_{i,j} [6 : 5] = V3_{i,j+1} - V_{i,j+1} \quad (15.4f)$$

$$H2_{i,j} [4 : 3] = V3_{i+1,j} - V_{i+1,j} \quad (15.4g)$$

$$H2_{i,j} [2 : 1] = V3_{i+1,j+1} - V_{i+1,j+1} \quad (15.4h)$$

$$V2_{i,j} [8 : 7] = H3_{i,j} - H_{i,j} \quad (15.4i)$$

$$V2_{i,j} [6 : 5] = H3_{i,j+1} - H_{i,j+1} \quad (15.4j)$$

$$V2_{i,j} [4 : 3] = H3_{i+1,j} - H_{i+1,j} \quad (15.4k)$$

$$V2_{i,j} [2 : 1] = H3_{i+1,j+1} - H_{i+1,j+1} \quad (15.4l)$$

$$D2_{i,j} [8 : 7] = A3_{i,j} - A_{i,j} \quad (15.4m)$$

$$D2_{i,j} [6 : 5] = A3_{i,j+1} - A_{i,j+1} \quad (15.4n)$$

$$D2_{i,j} [4 : 3] = A3_{i+1,j} - A_{i+1,j} \quad (15.4o)$$

$$D2_{i,j} [2 : 1] = A3_{i+1,j+1} - A_{i+1,j+1} \quad (15.4p)$$

The inverse DWT operation is applied by using the set of Eqs. 15.3 to retrieve the message image from the obtained frequency domain components (A2, H2, V2, D2).

15.4 Results Obtained

These results were obtained by simulating the image steganography code written in Verilog. Inputs to the Verilog module were hex files having pixel values of different images generated using MATLAB. Output pixel values were used in a MATLAB code to generate pictures from the pixel values. A gray color map [gray (256)] was used while producing images.

Figure 15.4a shows the cover image of size 512 pixels by 512 pixels. Figure 15.4b, c shows the message images each of size 256 pixels by 256 pixels. Figure 15.5 shows the A, H, V, and D components of the cover image after taking Haar DWT. Figure 15.6a, b is obtained after fusing the message images 1 and 2, respectively. Figure 15.7a, b is obtained after decryption from Fig. 15.6a, b, correspondingly.

There are various evaluation techniques for different steganography types, but the main evaluation methods are the PSNR and MSE. Peak signal-to-noise ratio (PSNR) is a measure of the difference between the original cover image and the Stego image [17]. It can be computed as

$$PSNR = 10 \times \log_{10} (n^2 / MSE), \tag{15.5}$$

where n is the maximum possible pixel value (here, for 8 bits it is $2^8 - 1 = 255$). The mean square error (MSE) can be defined as the average square error between the cover image and the Stefano image [17]. It can be expressed as

$$MSE = \frac{1}{m \times n} \times \sum_m \sum_n^{i=1, j=1} [Im(i,j) - Im'(i,j)]^2. \tag{15.6}$$

The PSNR and MSE of the images are given in Table 15.1. Along with the test images shown above, other test images such as Barbara (512 × 512) [19], Lena (512 × 512) [20], Lena (256 × 256) [20], and House (256 × 256) [21] are evaluated

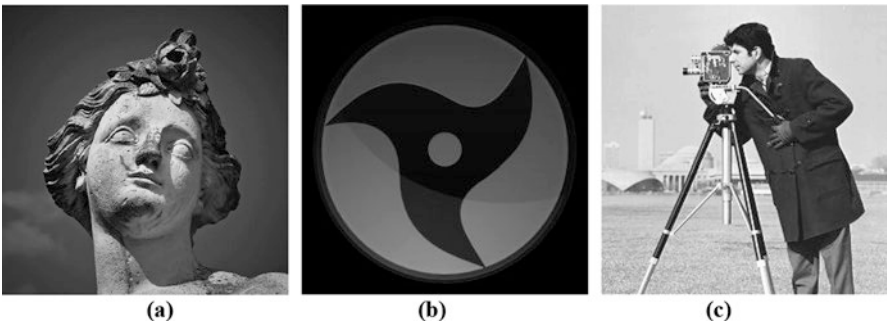


Fig. 15.4 (a) Original cover image, statue (512 × 512) [14]; (b) original message image 1, circular symbol (256 × 256) [15]; and (c) original message image 2, cameraman (256 × 256) [16]

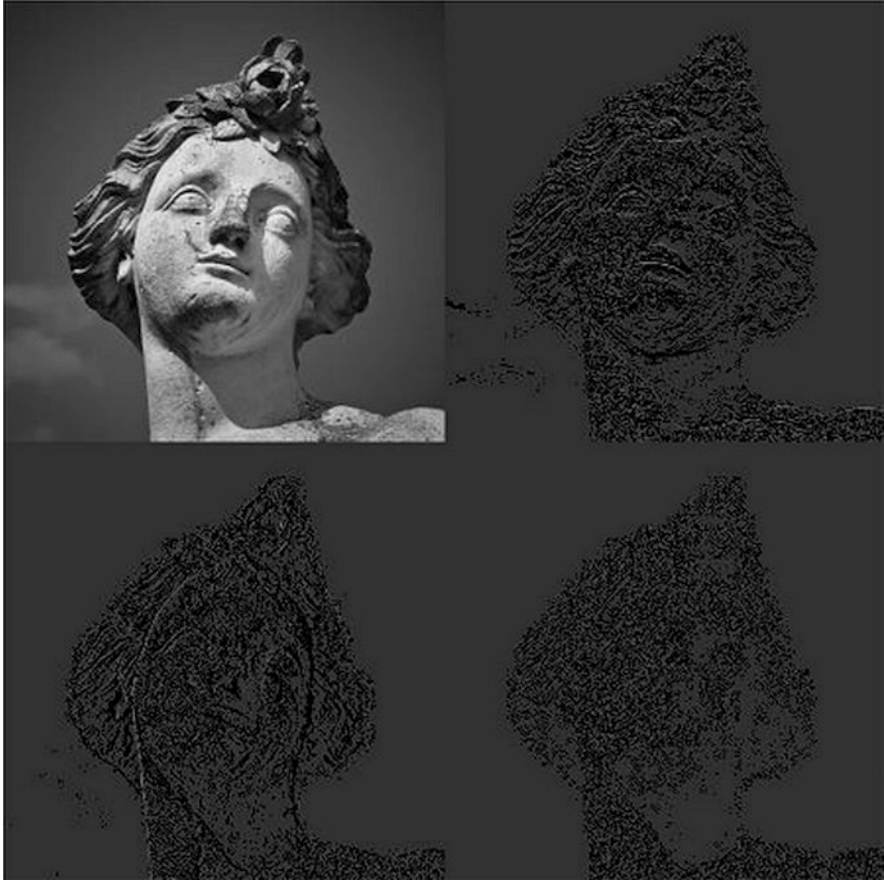


Fig. 15.5 (From top – left to right) A, H, V, and D components of the cover image (enhanced for visibility)

with this encryption algorithm, and their performance is tabulated in the table. The performance of the conventional LSB replacement technique (message image pixel values replace least significant 2 bits in the A, H, V, and D components of the Haar wavelet transformed cover image) for the same test images is also tabulated for comparison. It is observed that the modified LSB technique applied to the transformed message image shows about 5 dB increment in the PSNR value as compared to the LSB replacement technique having the same capacity.

In the analysis of the proposed steganographic method, the effect of the channel noise is not considered. This is because the transmission of the stego image is assumed to be done through a reliable digital link. The effect of noise (if any) will be there on the message image. The various noises affecting the image can be modeled mathematically, and on the receiving side, steganalysis methods must be able to differentiate the message and naturally occurring noise. Therefore, the analysis of

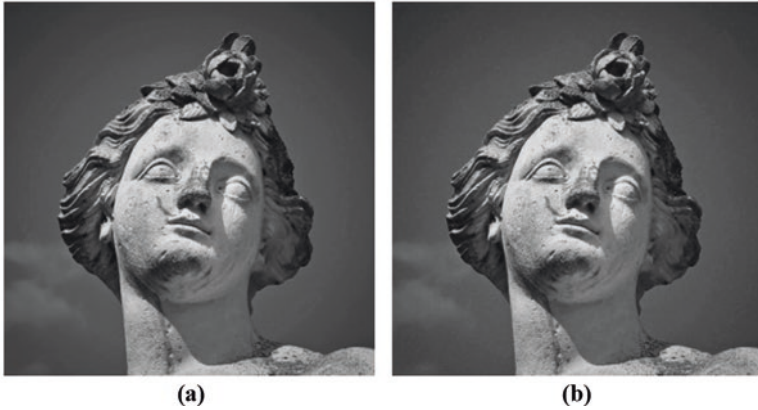


Fig. 15.6 (a) Encrypted image using message image 1 and (b) encrypted image using message image 2

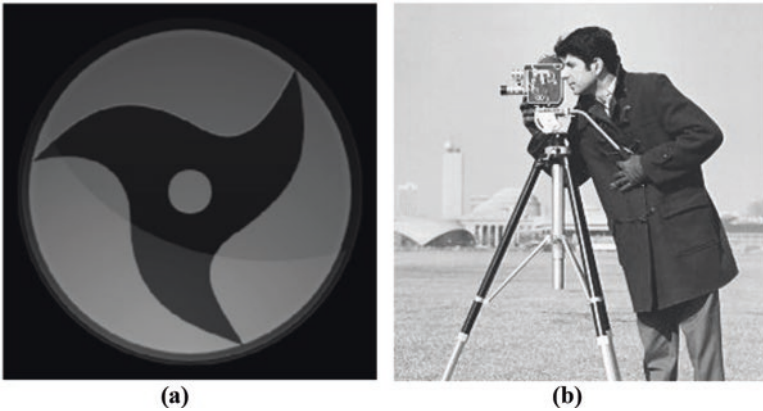


Fig. 15.7 (a) Retrieved message image 1 and (b) retrieved message image 2

different sources of noise and filtering methods must be applied such that the message signal inside the stego signal is not affected.

15.5 Future Scope

Future work in this domain can be focused on extending this algorithm to three-band RGB images and video data. A single-colored image can contain three hidden message images (grayscale) of the resolution mentioned in the proposed algorithm where each channel (R, G, and B) contains a message image. The whole encryption process can be improved by adding a key or using other standard encryption

Table 15.1 PSNR and MSE of the images (without channel effects)

Message → Cover ↓	Circular symbol		Cameraman		Lena (256 × 256)		House		
	Proposed method	LSB replacement method	Proposed method	LSB replacement method	Proposed method	LSB replacement method	Proposed method	LSB replacement method	
Statue	MSE	3.266	14.091	11.666	37.101	9.7384	98.803	11.223	34.204
	PSNR(dB)	43.024	36.675	37.495	32.471	38.279	31.280	37.664	32.824
Lena (512 × 512)	MSE	3.569	13.026	11.559	28.278	9.844	39.401	10.907	25.917
	PSNR(dB)	42.640	37.017	37.534	33.651	38.233	32.209	37.788	34.029
Barbara	MSE	3.605	13.630	11.588	27.529	9.856	37.571	10.933	25.083
	PSNR(dB)	42.587	36.820	37.525	33.767	38.228	32.416	37.777	34.171

methods before fusing the message image with the transformed cover image. The key can be used to encrypt the message image before fusing or to determine the order in which the message image data is fused, for example, a key can determine the position in which the message image pixel should get fused. An automated script can be used to select either the cover image of which the source is restricted to the public or a reasonably old message image (not relevant anymore) to be used as a cover image. Along with images, the transfer of data in terms of the video also plays a very important role in the process of medical research. Therefore, there is a requirement of faster and secure hardware solution which can process and encrypt videographic data. Medical image data is very sensitive, and each pixel data holds highly valuable information. Hence, future research works in this domain must focus on lossless encryption techniques that can be used in medical applications.

The main challenge in constructing a steganographic system is to uphold a fair tradeoff among robustness, safety, and imperceptibility in addition to higher bit embedding rate [24, 25]. Multiple image modalities and video analysis pose problems in healthcare applications that need research [26–31]. The policy to pick different cover media aimed at different purposes and situations with a few contemporary steganalysis systems relying on metaheuristics and the Cloud [32–35].

15.6 Conclusion

In this text, a lossless image steganography algorithm based on the Haar wavelet transform has been presented. A modified version of a 2-bit LSB technique is used in the encryption algorithm. From the obtained results, it is clear that the encrypted image (fused cover image) is visually similar to the original cover image while maintaining a relatively high PSNR of about 37 dB. The stego image formed after encryption has the same size as that of the cover image, with 25% of its content representing the message image embedded in it. The algorithm requires the original cover image as a key during decryption. Henceforth, this approach, along with the traditional image encryption techniques, proves to be useful in increasing the security of data.

Acknowledgments We wish to acknowledge with deep gratitude the valuable guidance received from Mrs. Sowmya K B. We wish to thank our institute, RV College of Engineering, for allowing us to carry out this work. We would also like to thank all the people who supported us directly or indirectly.

References











1. H.N.N. Simha, P.M. Prakash, S.S. Kashyap, S. Sarkar, FPGA implementation of image steganography using Haar DWT and modified LSB techniques. in 2016 IEEE International Conference on Advances in Computer Applications (ICACA) (2016), pp. 26–31
2. P.J.V. Fleet, The Discrete Haar wavelet transformation. in Joint Mathematical Meetings (2007)
3. L. Bao, Y. Zhou, C.L.P. Chen, Image encryption in the wavelet domain. *Proc. SPIE* **8755**, 875502 (2013)
4. S.C. Ou, H.Y. Chung, W.T. Sung, Improving the compression and encryption of images using FPGA-based cryptosystems. *Multimedia Tools Appl.* **28**(1), 5–22 (2006)
5. K.S. Shete, M. Patil, J. Chitode, Least significant bit and discrete wavelet transform algorithm realization for image steganography employing FPGA. *Int. J. Image Graphics Signal Process.* **8**, 48–56 (2016)
6. B.J. Mohd, S. Abed, T. Al-Hayajneh, S. Alounch, FPGA Hardware of the LSB steganography method. in *IEEE Transaction on Consumer Electronics*, 978-1-4673-1550-0/12, IEEE (2014)
7. C.S. Maya, G. Sabarinath, An optimized FPGA implementation of LSB replacement steganography using DWT. *Int. J. Adv. Res. Electr. Electron. Instrum. Eng.* **2**(special issue 1), 586–593 (2013)
8. A. Danti, G.R. Manjula, Secured data hiding of invariant sized secrete image based on discrete and hybrid wavelet transform. in *IEEE International Conference on Computational Intelligence & Computing Research*, pp. 1–6, India (2012)
9. I. Avcibas, N. Memon, B. Sankur, Steganalysis using image quality metrics. *IEEE Trans. Image Process.* **12**(2), 221–229 (2003)
10. A.A.J. Altaay, S.B. Sahib, M. Zamani, An introduction to image steganography techniques. in 2012 International Conference on Advanced Computer Science Applications and Technologies (ACSAT), pp. 122–126, Kuala Lumpur (2012)
11. K.B. Sowmya, J.A. Mathew, Discrete wavelet transform based on coextensive distributive computation on FPGA. *Mater. Today Proc.* **5**(4, Part 3), 10860–10866 (2018) ISSN 2214-7853
12. Image processing on FPGA using Verilog HDL (2020), <https://www.fpga4student.com/2016/11/image-processing-on-fpga-verilog.html>. Last accessed 20 May 2020
13. Discrete wavelet transform – Wikipedia, https://en.wikipedia.org/wiki/Discrete_wavelet_transform. Last accessed 20 May 2020
14. Sculpture head in front of the Benrath Castle in Dusseldorf, <https://pixabay.com/photos/statue-sculpture-figure-1275469/>. Last accessed 20 May 2020
15. Sharingan icon 1.5, <http://www.softicons.com/culture-icons/sharingan-icons-1.5-by-hare-nome-razanajato/itachi-alt-icon>. Last accessed 20 May 2020
16. Cameraman.bmp, <https://www.hlevkin.com/06testimages.htm>. Last accessed 20 May 2020
17. H.A. Al-Korbi, A. Al-Ataby, M.A. Al-Tae, W. Al-Nuaimy, Highly efficient image steganography using Haar DWT for hiding miscellaneous data. *Jordanian J. Comput. Inf. Technol.* **2**(1), 17–36 (2016). <https://doi.org/10.5455/jjcit.71-1450117397>
18. H. Reddy, K.B. Raja, High capacity and security steganography using Discrete Wavelet Transform. *Int. J. Comput. Sci. Secur.* **3**(6), 462–472 (2009)
19. Barbara, <https://www.hlevkin.com/TestImages/barbara.bmp>. Last accessed 20 May 2020
20. Lenna, <https://www.hlevkin.com/TestImages/lenna.bmp>. Last accessed 20 May 2020
21. House, https://www.io.csic.es/PagsPers/JPortilla/content/BLS-GSM/test_images/house.png. Last accessed 20 May 2020
22. N. Razmjooy, B. Somayeh Mousavi, F. Soleymani, A hybrid neural network Imperialist Competitive Algorithm for skin color segmentation. *Math. Comput. Model.* **57**(3–4), 848–856 (2013)
23. N. Razmjooy et al., Image thresholding based on evolutionary algorithms. *Int. J. Phys. Sci.* **6**(31), 7203–7211 (2011)

24. I.J. Kadhim, P. Premaratne, P.J. Vial, B. Halloran, Comprehensive survey of image steganography: techniques, evaluations, and trends in future research. *Neurocomputing* **335**, 299–326 (2019)
25. H.J. Loschi, V.V. Estrela, D.J. Hemanth, S.R. Fernandes, Y. Iano, A.A. Laghari, A. Khan, H. He, R. Sroufe, Communications requirements, video streaming, communications links and networked UAVs, in *Imaging and Sensing for Unmanned Aircraft Systems*, ed. by V. V. Estrela, J. Hemanth, O. Saotome, G. Nikolakopoulos, R. Sabatini, vol. 2, (IET, London, 2020), pp. 113–132
26. Q. Zhang, L. Ren, W. Shi, HONEY: A multimodality fall detection and telecare system. *cTelemed. J. e-health Off. J. Am. Telemed. Assoc.* **19**(5), 415–429 (2013)
27. S. Parikh, H.A. Sanjay, K.A. Shastry, K.K. Amith, Multimodal data security framework using steganography approaches. in 2019 International Conference on Communication and Electronics Systems (ICCES), 1997–2002 (2019)
28. V.V. Estrela, A.M. Coelho, State-of-the-art motion estimation in the context of 3D TV, in *Multimedia Networking and Coding*, ed. by R. A. Farrugia, C. J. Debono, (IGI Global, Hershey, 2013), pp. 148–173. <https://doi.org/10.4018/978-1-4666-2660-7.ch006>
29. A.M. Coelho, V.V. Estrela, EM-based mixture models applied to video event detection, in *Principal Component Analysis – Engineering Applications*, ed. by P. Sanguansat, (IntechOpen, London, 2012), pp. 101–124. <https://doi.org/10.5772/38129>
30. A.A. Abdulla, H. Sellahewa, S.A. Jassim, Improving embedding efficiency for digital steganography by exploiting similarities between secret and cover images. *Multimed. Tools Appl.* **1–25** (2019)
31. F.Y. Moraes, M. Giuliani, N.K. Quartey, J.A. Cardozo, N. Icliates, Z. Tittenbrun, J.K. Papadacos, J. Brierley, Closing the gap on the availability of cancer staging information for healthcare providers in the global cancer community: Development of a multilingual cancer staging video series. *J. Global Oncol.* **4** (2018)
32. D.K. Sarmah, A.J. Kulkarni, A. Abraham, *Optimization models in steganography using metaheuristics*, Intelligent Systems Reference Library (Springer, Cham, 2020)
33. N. Razmjoo, V.V. Estrela, *Applications of Image Processing and Soft Computing Systems in Agriculture* (IGI Global, Hershey, 2019), pp. 1–300. <https://doi.org/10.4018/978-1-5225-8027-0>
34. H.R. Boveiri, R. Khayami, On the performance of metaheuristics: A different perspective. *ArXiv, abs/2001.08928*, (2020)
35. S.I. Bejinariu, H. Costin, A comparison of some nature-inspired optimization metaheuristics applied in biomedical image registration. *Methods Inf. Med.* **57**(5–06), 280–286 (2018)

Chapter 16

Nondestructive Diagnosis and Analysis of Computed Microtomography Images via Texture Descriptors



Sandro R. Fernandes , Joaquim T. de Assis , Vania Vieira Estrela ,
Navid Razmjoooy , Anand Deshpande , P. Patavardhan , R. J. Aroma ,
K. Raimond , Hermes J. Loschi , and Douglas A. Nascimento 

16.1 Introduction

The low spatial resolution of a typical medical computed tomography (CT), which is of the order of 100 μm , does not allow accurate analysis of reservoir rocks and other types of structural investigations for other knowledge areas. X-ray computed

S. R. Fernandes (✉)

IF Sudeste de Minas Gerais – Campus Juiz de Fora, Juiz de Fora, MG, Brazil
e-mail: sandro.fernandes@ifsudestemg.edu.br

J. T. de Assis

Universidade do Estado do Rio de Janeiro, Instituto Politécnico, Nova Friburgo, RJ, Brazil
e-mail: joaquim@iprj.uerj.br

V. V. Estrela

Department of Telecommunications, Federal Fluminense University (UFF),
Niterói, RJ, Brazil
e-mail: vania.estrela.phd@ieee.org

N. Razmjoooy

Department of Electrical Engineering, Tafresh University, Tafresh, Iran

A. Deshpande

Angadi Institute of Technology & Management, Belgaum, India

P. Patavardhan

Dayananda Sagar University, Bengaluru, India

R. J. Aroma · K. Raimond

Department of Computer Science and Engineering, Karunya University, Coimbatore, India
e-mail: kraimond@karunya.edu

H. J. Loschi · D. A. Nascimento

Universidade Estadual de Campinas, Campinas, SP, Brazil

Uniwersytet Zielonogórski, Zielona Góra, Poland

e-mail: eng.hermes.loschi@ieee.org; eng.douglas.a@ieee.org

© Springer Nature Switzerland AG 2021

A. Khelassi, V. V. Estrela (eds.), *Advances in Multidisciplinary Medical Technologies – Engineering, Modeling and Findings*,
https://doi.org/10.1007/978-3-030-57552-6_16

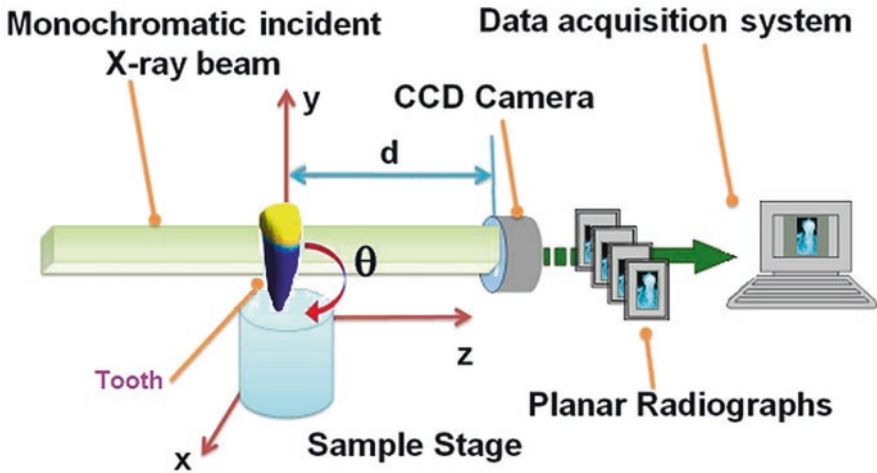


Fig. 16.1 Microtomography of a tooth

microtomography (μ CT), which was initially implemented to study sedimentary rocks, can solve this caveat [1–3].

X-ray μ CT is a nondestructive technique, used to inspect cross sections of a particular material, through a set of projections of the plane, possessing the same physical principle of CT [2]. The difference is the length of the focus of the X-ray tube, which has the order (magnitude) of micrometers. The operating principle of a μ CT consists of a system containing both the detector and the radiation source fixed. The object is rotated between them, as can be seen in Fig. 16.1.

The μ CT non-destructible nature assists archaeological and paleontological analyses of objects [4–6]. Noninvasive inspection is essential for the preservation of the physical integrity of ancient samples from museums. Archaeological findings require detailed characterization of species, along with the generation of 3D images. Digitalized versions of museum collection items require a suitable image representation that allows investigating an object from different viewpoints with details unavailable to the bare eye.

In μ CT applications in the biological area, as in the study of fractures, quantitative analyses were essential for the comparative study of the two groups studied, besides providing a visualization of bone microstructure, which allowed a visual comparison between the groups [7–9].

Results obtained in the study of dental crowns demonstrate that the μ CT is beneficial in dental investigations, e.g., in the calculation of spacing, both with the use of 2D views and in a 3D image [10, 11]. Such a state of things happens because μ CT has a focus size in the order of micrometers, which delivers a higher resolution power, besides giving other quantitative analysis tools that allow us to have a more overview. Besides, 3D imaging helped visualize spacings/gaps between structures and allowed a visual comparison of the groups.

The μ CT usage as a non-destructible testing technique:

1. Does not entail prior preparation of the specimen
2. Provides high-resolution visualizations of microstructures from 2D and 3D images
3. Outputs a colossal variety of quantitative parameters useful in the study and characterization of structures and materials
4. Enables comparative studies

In the process of image acquisition and reconstruction using μ CT, loss of quality is possible. Computed microtomography (μ CT) devices offer the user a choice of configurations, such as voltage (measured in kV) and current (expressed in μ A). The two images from Fig. 16.3 resulted from varying the microtomography configurations for the same acrylic object. The equipment was the SkyScan 1174 Compact Micro-CT from Fig. 16.2 [12–15].

When analyzing μ CT images, it appears that their quality is related to the accuracy of the reproduction of these images and the configuration of the equipment. The Kilovoltage (kV), milliamperage (mA), and exposure time (expressed in seconds) are the so-called exposure factors. These factors control, respectively, the contrast, density, and sharpness of an image. These variations affect image quality and may produce different results than expected (Fig. 16.3).

In this study, a methodology for analyzing μ CT images was developed. This methodology allows an assessment of the images in a way that advises which configuration of the exposure factors used in the μ CT equipment produced the best outcomes.

Section 16.2 describes the methodology. Results appear in Sect. 16.3. Finally, Sects. 16.4 and 16.5 allude, respectively, to discussions and conclusions.

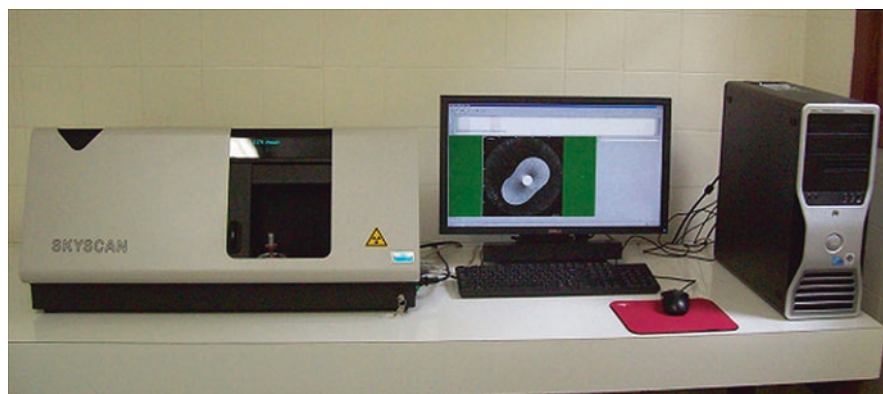


Fig. 16.2 Microtomograph SkyScan 1174 from the Instituto Politecnico do Rio de Janeiro (IPRJ/UERJ)

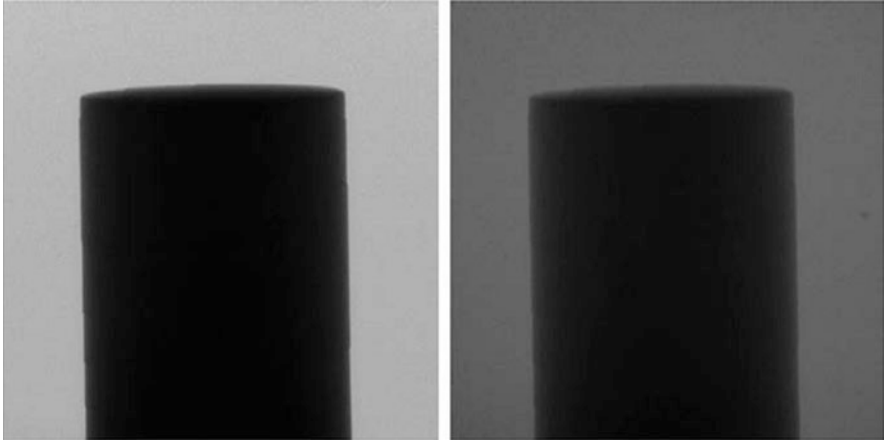


Fig. 16.3 Images obtained with variations of (a) 40 kV and 800 μ A and (b) 50 kV and 800 μ A

16.2 Methodology

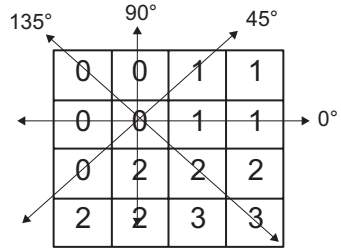
Even though there is no formal definition of texture [14–18], this descriptor provides measurements of image properties such as smoothness, roughness, and regularity. One of the most straightforward approaches to describing textures is through the moments of the gray level histogram of an image or a region. These texture measures have the limitation of not carrying information about the relative position of the pixels concerning each other. One way to bring this information to the texture analysis process is to consider not only the intensity distribution but also the pixel positions with equal or similar intensity values.

To address this limitation, novel ways of approaching the extraction of characteristics are being proposed. Predominantly, three image classification approaches describe textures: statistical strategies, structural methodologies, and spectral schemes [14–18]. As the statistical approach leads to the characterization of textures like smooth, rough, granular, and so on, it became the initial choice for this investigation. Textures not displaying reasonable regularity can also benefit from this approach.

One of the most used statistical methods for the analysis of textures is the matrix of co-occurrence of the gray levels (C) of an image [19]. Each entry of C represents the frequency with which a gray level pixel X and another gray level Y occur in the image, separated by a distance of dx rows and dy columns, or, equivalently, $d = (dx, dy)$. Given that, the distribution of the gray pixel levels can be described by second-order statistics as the probability that two pixels will have a specific gray level happening with a particular spatial relationship.

This statistical approach builds on the assumption that information about the image texture occurs in the average or global spatial distribution ratio of the gray levels in the image [10]. Textural information can be specified using spatial

Fig. 16.4 Co-occurrence matrix angles



dependency matrices of the gray levels computed at various angles (0°, 45°, 90°, and 135°) and distances between pixels (Fig. 16.4). In this study, we used the 135° angle and the 1-pixel distance. Then, the matrix is normalized, where normalization constants are defined for each angle covered. In this way, this matrix (baptized the co-occurrence matrix) can help various second-order statistical calculations, as in the case of feature extraction [8]. Five characteristics, from a set of 14 statistical measures [6], were chosen for this study as follows:

Maximum Probability (P_{\max}): The maximum value found in the co-occurrence matrix C whose entries are c_{ij} given by

$$P_{\max} = \max(c_{ij}) \tag{16.1}$$

Difference Moment (D): It has a relatively low value when the values of the co-occurrence matrix (C) are close to the main diagonal, due to the differences (ij) being smaller in this region.

$$D = \sum_i \sum_j (i - j)^2 c_{ij}. \tag{16.2}$$

Inverse Difference Moment (ID): It has the opposite effect of a different moment. For $i \neq j$, it amounts to

$$ID = \sum_i \sum_j \frac{c_{ij}}{(i - j)^2}. \tag{16.3}$$

Entropy (H): The entropy or degree of dispersion of gray levels expresses the disorder contained in the image texture.

$$H = - \sum_i \sum_j c_{ij} \log c_{ij}. \tag{16.4}$$

Uniformity or Energy (E): It expresses the uniformity of the texture of an image according to

$$E = \sum_i \sum_j c_{ij}^2. \tag{16.5}$$

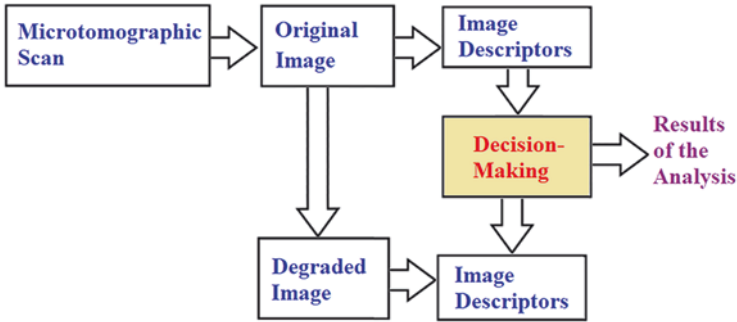


Fig. 16.5 Flowchart of the methodology used

The analyses made with different materials served to address the different configurations needed on the tomograph and their respective effects on the results in the images. Figure 16.5 illustrates the flowchart of the methodology used in this work.

First, texture descriptors are extracted from each of the original test images: maximum probability, the difference moment, inverse difference moment, entropy, and uniformity. Then, degradations were applied to the ground truth images. For this test, the degradation applied was a Poisson noise. After using the degradation, the texture descriptors are extracted again for quantitative comparison with the original texture descriptors.

To validate the methodology, an experiment was carried out with 186 images obtained by the microtomography of the different materials mentioned and varied configurations. Figure 16.6 shows an example of each group of samples with and without noise.

16.3 Experimental Results

The following groups of materials were scanned: bone structure (corresponding to an amphibian in the family Leptodactylidae), concrete, and polymers (acrylic and polypropylene) [14, 15, 18].

The graphs shown below show the results of the texture descriptors found for the original images and the degraded images. In all figures, the images comply with the following arrangement:

- (a) Images 1 to 65 are concrete samples.
- (b) Images 66 to 146 are samples of polymers.
- (c) Images 147 through 166 are samples of bone structure.
- (d) Images 167 through 186 are samples of polymers.

The graph showing the values found for the maximum probability descriptor appears in Fig. 16.7.

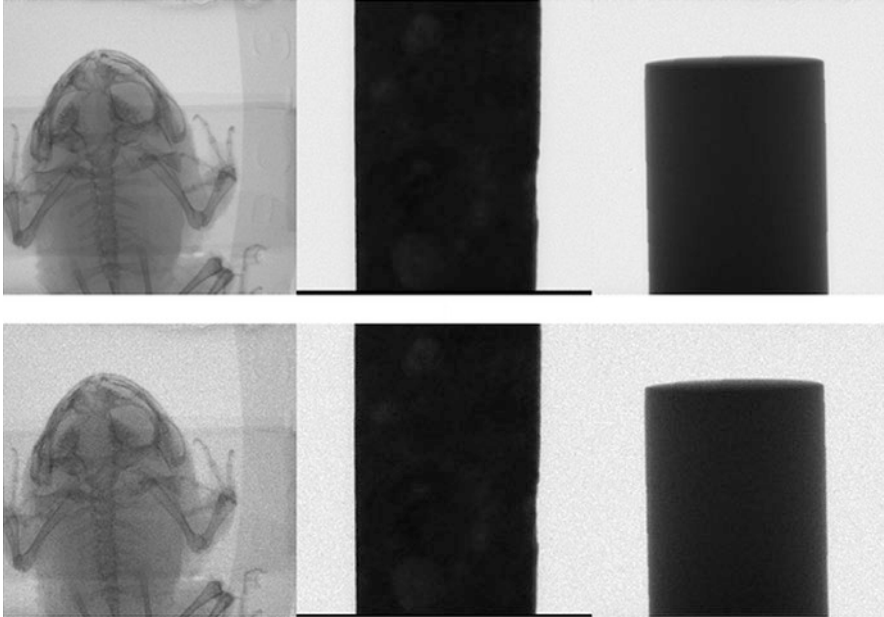


Fig. 16.6 The original sample images (above) and the images degraded with Poisson noise (below) with SNR = 30 dB

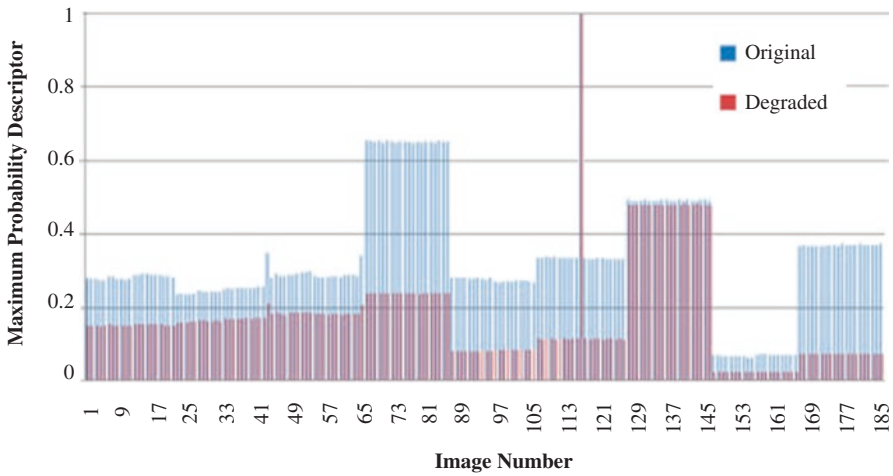


Fig. 16.7 The maximum probability of occurrence descriptor, before and after degradation

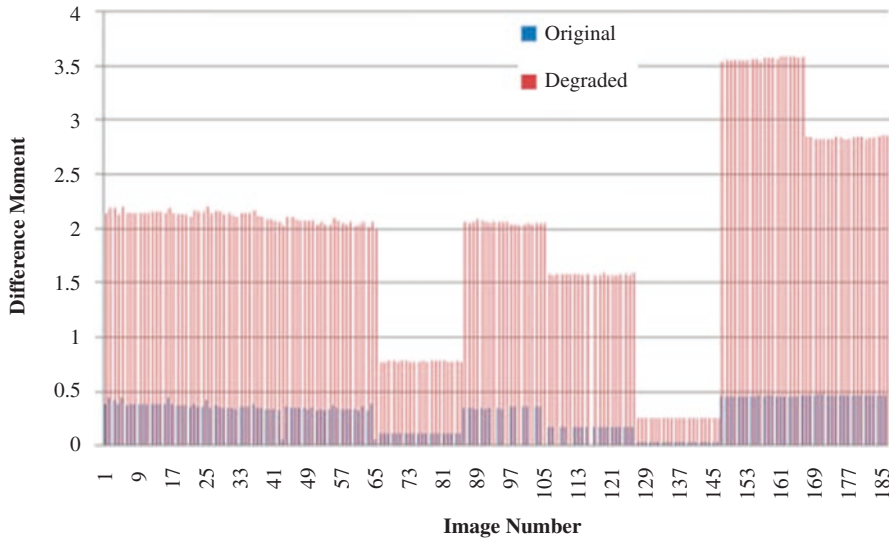


Fig. 16.8 Difference moment texture descriptor, before and after degradation

The graph, which shows the probability values found for the descriptor of the difference moment, can be seen in Fig. 16.8.

The graph, which shows the values found for the descriptor of the inverse difference, can be seen in Fig. 16.9.

The graph, which shows the values found for the entropy descriptor, can be seen in Fig. 16.10.

The graph, which shows the values found for the uniformity descriptor, can be seen in Fig. 16.11.

The texture descriptors used, shown in the graphs above, had a similar behavior for the test images, even though they were different materials. The values found for the descriptors appear in the graphs above. These handpicked features show the following behavior:

1. The maximum probability descriptor was higher for the non-degraded images.
2. The difference moment descriptor was lower for non-degraded images.
3. The descriptor of the inverse difference moment has lower values for the non-degraded images.
4. The entropy descriptor has lower values for non-degraded images.
5. The uniformity descriptor had higher values for non-degraded images.

The purpose of using different characteristics of materials in the same analysis as the texture descriptors is to portray different contents/properties within the same object. Therefore, the results for the different subjects are presented together.

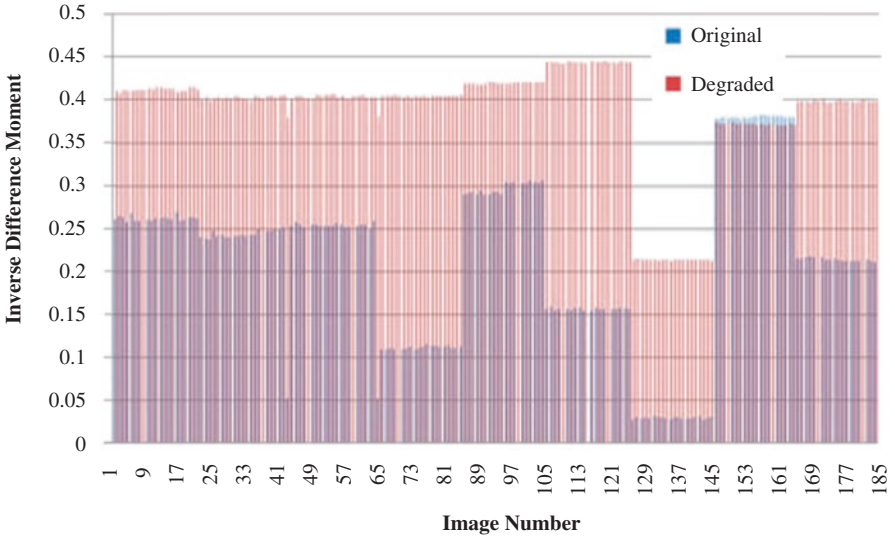


Fig. 16.9 Inverse difference moment texture descriptor, before and after degradation

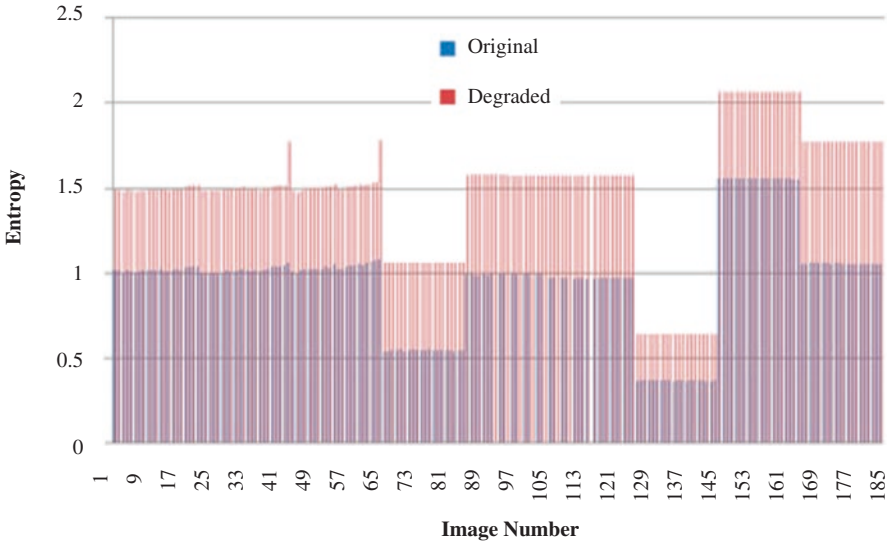


Fig. 16.10 Entropy texture descriptor, before and after degradation

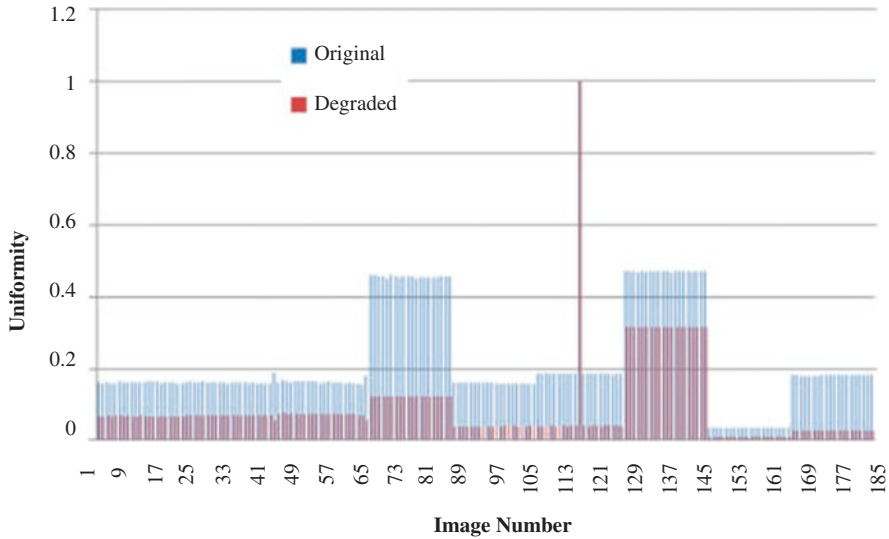


Fig. 16.11 Uniformity texture descriptor, before and after degradation

16.4 Discussion and Future Work

X-ray microtomography enables new discernments about high-resolution imaging for several kinds of porous media investigations, geometric features, and elements present in samples. Pore space studies concerning functional properties customarily necessitate the segmentation of image areas into different classes utilizing the brightness information. Image segmentation is a nontrivial task with an intense impact on all the next image-processing stages. This work focuses on the calculation of handcrafted texture descriptors with noiseless images and pictures containing moderate Poisson noise ($SNR = 30$ dB). Frequently, the major origin for poor segmentation outcomes is image blur. Other raw data caveats are noise, ring artifacts, and image brightness variations, in which image enhancement methods can mitigate.

An aspect that calls for investigating the effect of increasing the number of features (Haralick et al.) had 14 types of moments [16]. The authors intend to run experiments analyzing different types of quality metrics, e.g., misclassification error, precision, recall, F-measure, volume fraction, area under the curve (AUC), specific interfacial area, and connectivity measures, to name a few. Image pre-processing segmentation before classification can contribute to more precise results that can be assessed with the performance metrics from the previous sentence.

The performance of different segmentation methods relying on different feature vectors can point toward the best strategy to recover the morphological properties of the object in real-life conditions.

The authors would also like to investigate how to integrate deep and handcrafted features in a way that improves the classification results without a heavy computational load [20].

It is important to point out that X-ray motion analysis helps to track the displacement of objects via X-rays. This type of study requires placing the subject to be scrutinized in the center of the X-ray beam to record its motion with a high-speed camera together with an image intensifier. Such an arrangement allows for high-quality videos with a high amount of frames per second. Depending on the μ CT settings, it is possible to envisage specific specimen structures, e.g., bones or cartilage. X-ray motion analysis can examine gait, probe joint movements, or document the movement of bones concealed by soft tissue. These experiments can offer cues on the capability to quantify skeletal motions, which is crucial to understand vertebrate biomechanics, energetics, and motor control. These videos can capture 3D images directly or infer the 3D geometry from 2D frames [21–28].

Finally, metaheuristics can help to speed up the optimization processes since hard computing can be computationally cumbersome [29, 30].

16.5 Conclusion

The main objective of this study was to present a methodology for analyzing microtomography images using texture descriptors. Texture descriptors can be arranged in a feature vector whose entries have properties that serve to recognize patterns in different imaging modalities. Standards can be considered quality characteristics in images. Therefore, the use of texture descriptors to analyze images, in this case, μ CT imageries, is feasible.

It is not presented in this study, but this methodology was used to analyze image enhancement techniques, demonstrating positive results in the three-dimensional reconstruction of μ CT images. Images in which the enhancement techniques were applied (brightness, saturation, histogram equalization, and the median filter) had an increase in the value of the maximum probability and uniformity descriptors and a decrease in the value of the descriptors of the difference moment, inverse difference moment, and entropy.

The texture descriptors allow the characterization of microtomographic images aiming at their quality. Texture descriptors have already been used for the characterization of mammograms showing calcifications. The application of the methodology used in this study can achieve more accurate outcomes since the enhancement techniques applied to the images resulted in better visualizations.

References

1. V. Cnudde, M.N. Boone, High-resolution X-ray computed tomography in geosciences: A review of the current technology and applications. *Earth-Sci.Rev.* **123**, 1–17 (2013)
2. J. Hsieh, *Computed Tomography: Principles, Design, Artifacts and Recent Advances*, 2nd edn. (SPIE, Bellingham, 2009)
3. P.D. Jacques, A.R. Nummer, R.J. Heck, R. Machado, The use of microtomography in structural geology: a new methodology to analyse fault faces. *J. Struct. Geol.* **66**, 347–355 (2014)
4. W.-A. Kahl, B. Ramminger, Non-destructive fabric analysis of prehistoric pottery using high-resolution X-ray microtomography: a pilot study on the late Mesolithic to Neolithic site Hamburg-Boberg. *J. Archaeol. Sci.* **39**, 2206–2219 (2012)
5. P.F. Wilson, M.P. Smith, J. Hay, J.M. Warnett, A. Attridge, M.A. Williams, X-ray computed tomography (XCT) and chemical analysis (EDX and XRF) used in conjunction for cultural conservation: the case of the earliest scientifically described dinosaur *Megalosaurus bucklandii*. *Heritage Sci.* **6** (2018)
6. F. Bernardini, E. Leghissa, D. Prokop, A. Velušček, A.D. Min, D. Dreossi, S. Donato, C. Tuniz, F. Princivalle, M.M. Kokelj, X-ray computed microtomography of Late Copper Age decorated bowls with cross-shaped foots from central Slovenia and the Trieste Karst (North-Eastern Italy): technology and paste characterisation. *Archaeol. Anthropol. Sci.* **11**, 4711–4728 (2019)
7. R. Mizutania, Y. Suzukib, X-ray microtomography in biology. *Micron* **43**, 104–115 (2012)
8. C. Murphy, D.Q. Fuller, C.J. Stevens, T. Gregory, F. Silva, R.D. Martello, J. Song, A.J. Bodey, C. Rau, Looking beyond the surface: Use of high resolution X-ray computed tomography on archaeobotanical remains. *Interdiscip. Archaeol. – Nat. Sci. Archaeol.* **10**, 7–18 (2019)
9. F.S. Ahmann, I. Evseev, M.G.F. Paz, R. Lingnau, I. Ievsieieva, J.T. de Assis, H.D.L. Alves, X-ray computed microtomography as a tool for the comparative morphological characterization of *Proceratophrys bigibbosa* species from southern Brazil, in Proc. 2011 International Nuclear Atlantic Conference – INAC, Belo Horizonte, MG, Brazil, 2011 (2011)
10. C. Zanolli, C. Dean, L. Rook, L. Bondioli, A. Mazurier, R. Macchiarelli, Enamel thickness and enamel growth in *Oreopithecus*: combining microtomographic and histological evidence. *Comptes rendus – Palevol* **15**, 209–226 (2016)
11. B. Oglakci, M. Kazak, N. Donmez, E.E. Dalkilic, S.S. Koymen, The use of a liner under different bulk-fill resin composites: 3D GAP formation analysis by x-ray microcomputed tomography. *J. Appl. Oral Sci.* **28**, e20190042 (2019)
12. SKYSCAN, 2011 – Nrecon User Manual. <http://bruker-microct.com/>
13. SKYSCAN, 2013 – Morphometric parameters measured by Skyscan™ CT – Analyser software. <http://bruker-microct.com/>
14. E.F. Teixeira, S.R. Fernandes, Development of a computational tool for classification of image patterns (in Portuguese). *Seminários de Trabalhos de Conclusão de Curso do Bacharelado em Sistemas de Informação*, Vol. 1, 1, Juiz de Fora, MG, Brazil. ISSN: 2525-3131 (2016)
15. S.R. Fernandes, Image Characterization of X-Ray Microtomography Using Texture Descriptors (in Portuguese). D.Sc. Dissertation, UERJ-IPRJ, Nova Friburgo, RJ, Brazil, 2012
16. R.M. Haralick, K. Shanmugan, I. Dinstein, Textural features of images classification. *IEEE Trans. Syst. Man Cybernetics* **SMC-3**, 610–621 (1973)
17. A.E. Herrmann, V.V. Estrela, Content-based image retrieval (CBIR) in remote clinical diagnosis and healthcare, in *Encyclopedia of E-Health and Telemedicine*, ed. by M. M. Cruz-Cunha, I. M. Miranda, R. Martinho, R. Rijo, (IGI Global, Hershey, 2016). <https://doi.org/10.4018/978-1-4666-9978-6.ch039>
18. W.R. Schwartz, F.R. de Siqueira, H. Pedrini, Evaluation of feature descriptors for texture classification. *J. Electron. Imaging* **21**(2), 023016.1–023016.17 (2012)
19. F.R. Siqueira, W.R. Schwartz, H. Pedrini, Multi-scale gray level co-occurrence matrices for texture description. *Neurocomputing* **120**, 336–345 (2013)
20. A. Bizzego, N. Bussola, D. Salvalai, M. Chierici, V. Maggio, G. Jurman, C. Furlanello (2019) bioRxiv 568170; <https://doi.org/10.1101/568170>

21. S.M. Gatesy, D.B. Baier, F.A. Jenkins, K.P. Dial, Scientific roscoping: A morphology-based method of 3-D motion analysis and visualization. *J. Exp. Zool.Part A.* **313**(5), 244–261 (2010)
22. V.V. Estrela, A.M. Coelho, State-of-the-art motion estimation in the context of 3D TV, in *Multimedia Networking and Coding*, ed. by R. A. Farrugia, C. J. Debono, (IGI Global, Hershey, 2013), pp. 148–173. <https://doi.org/10.4018/978-1-4666-2660-7.ch006>
23. H.R. Marins, V.V. Estrela, On the use of motion vectors for 2D and 3D error concealment in H.264 AVC video, in *Feature Detectors and Motion Detection in Video Processing*, ed. by N. Dey, A. S. Ashour, P. K. Patra, 1st edn., (IGI Global, Hershey, 2017). <https://doi.org/10.4018/978-1-5225-1025-3.ch008>
24. S. Guan, H.A. Gray, F. Keynejad, M.G. Pandy, Mobile biplane X-ray imaging system for measuring 3D dynamic joint motion during overground gait. *IEEE Trans. Med. Imaging* **35**(1), 326–336 (2016)
25. G.B. Sharma, G. Kuntze, D. Kukulski, J.L. Ronsky, Validating dual fluoroscopy system capabilities for determining in-vivo knee joint soft tissue deformation: A strategy for registration error management. *J. Biomech.* **48**(10), 2181–2185 (2015)
26. A. Deshpande, P. Patavardhan, V.V. Estrela, N. Razmjoooy, Deep learning as an alternative to super-resolution imaging in UAV systems, in *Imaging and Sensing for Unmanned Aircraft Systems*, ed. by V. V. Estrela, J. Hemanth, O. Saotome, G. Nikolakopoulos, R. Sabatini, vol. 2, (IET, London, 2020)
27. D. Panetta, L. Labate, L. Billeci, N.D. Lascio, G. Esposito, F. Faita, G. Mettivier, D. Palla, L. Pandola, P. Pisciotta, G. Russo, A. Sarno, P. Tomassini, P.A. Salvadori, L.A. Gizzi, P.M. Russo, Numerical simulation of novel concept 4D cardiac microtomography for small rodents based on all-optical Thomson scattering X-ray sources. *Sci. Rep.* **9**, 1–12 (2019)
28. M. Voltolini, J.B. Ajo-Franklin, The effect of CO₂-induced dissolution on flow properties in Indiana Limestone: an in situ synchrotron X-ray micro-tomography study. *Int. J. Greenhouse Gas Control* **82**, 38–47 (2019)
29. A. Veith, A.B. Baker, A non-destructive method for quantifying tissue vascularity using quantitative deep learning image processing. *bioRxiv* (2020)
30. T.V. Spina, G.J. Vasconcelos, H.M. Gonçalves, G.C. Libel, H. Pedrini, T. Carvalho, N.L. Archilha, Towards real time segmentation of large-scale 4D micro/nanotomography images in the Sirius synchrotron light source. *Microsc. Microanal.* **24**, 92–93 (2018)

Correction to: Acoustic Contrast Between Neutral and Angry Speech: Variation of Prosodic Features in Algerian Dialect Speech and German Speech



F. Ykhlef and D. Bouchaffra

Correction to:
Chapter 4 in: A. Khelassi, V. V. Estrela (eds.),
Advances in Multidisciplinary Medical
Technologies — Engineering, Modeling and Findings,
https://doi.org/10.1007/978-3-030-57552-6_4

Reference [18] is now corrected as follows:

F. Ykhlef, A. Derbal, W. Benzaba, R. Boutaleb, D. Bouchaffra, H. Meraoubi, Far. Ykhlef, in *The IEEE International Conference on Advanced Electrical Engineering. Towards building an emotional speech corpus of Algerian dialect: criteria and preliminary assessment results.* (Algiers, 2019).

The updated online version of this chapter can be found at
https://doi.org/10.1007/978-3-030-57552-6_4

Index

A

- Abnormal blood cells, 116
- Acoustic contrast (AC), 43, 46
- Adaptive Specular Reflection Detection in Cervigrams (ASRDC)
 - as adaptive method, 229
 - automatic SR detection, 219, 220
 - block diagram, 219
 - experiments, 224, 225
 - image enhancement, 224
 - input image QA, 221
 - p*-values, 223, 224
 - quantitative evaluation, 226, 227
 - SR detection, 225
 - state-of-the-art methods, 227, 228
 - trials, 223
 - workflow, 222
- Aid in diagnosis, 117, 124
- Algerian dialect (AD), 42, 43
- Anderson-Darling test, 46
- Angry speech
 - acoustic contrast, 50
 - AD speech, 43
 - and calm emotional states, 46
 - EMODB corpus, 44, 45
 - energy and pitch, 42
 - English speech, 43
 - P*-value, 43
 - speech files, 47
 - statistical proof, 48
 - utterances, 42
- Anthropometric assessment, 20
- Application Unit (AU), 163
- Artificial intelligence, 3
 - advantages, 132–133
 - applications, 131, 133, 134
 - BC algorithms, 62, 63
 - BCs (*see* Bolus calculators (BCs))
 - computed tomography, 133
 - DeepMind technology, 131
 - dental science, 134
 - diagnostic system, 131
 - digital health program, 134
 - in future, 135
 - IoMT (*see* Internet of medical things (IoMT))
 - limitations, 133–134
 - magnetic resonance imaging, 133
 - non-small cell lung cancer, 135
 - personalized medicines, 131–132
 - research and clinical applications, 133
 - treatment and diagnosis, 131
 - ultrasound examinations, 133
 - X-ray, 133
- Artificial intelligence techniques, 11
- Artificial neural networks (ANNs), 62
- Assistive learning, 31
- Assistive learning engine (ALE), 32
- ASTM Elecsys, 91, 93–95, 99
- Automated insulin dosage advisor (AIDA), 65
- Automatic speech analysis, 42

B

- BaliBASE benchmark, 104, 110, 111
- Basal-bolus insulin therapy, 69
- Basal insulin, 57
- BG meters (BGM), 57
- Biomedical image processing, 210
- Biomedical technology, 90

- Biophotonics, 90
 - Biopsy, 90
 - Biosensors
 - bioreceptors, 90
 - DNA biosensors, 90
 - integrated circuit (IC) microchips, 90
 - living structures, 90
 - Bit error rate (BER), 196
 - Blockchain
 - advantages, 137
 - applications, 137, 138
 - clinical trials, 140
 - data encryption and cryptography technologies, 136
 - data exchange, 136, 138
 - data lakes, 136
 - description, 135
 - global health security, 139
 - in hospital activities, 137
 - intelligent cooperation, 136
 - interoperability, 135, 136
 - limitations, 138–139
 - OmniPHR system, 139
 - for personalized medical application, 136–137
 - properties, 136
 - security risk, 139
 - smart contract, 135
 - Blood glucose concentration (BGC), 57
 - Bolus calculators (BCs)
 - AI methodologies, 56
 - ANNs, 62
 - assessment, 66
 - BC algorithms based on AI techniques, 62, 63
 - carbohydrate-to-insulin ratio, 59
 - CBR algorithms, 61
 - challenges, 69, 70
 - closed-loop system, 61
 - control algorithms, 66
 - decision support systems, 56
 - development, 60, 71
 - fuzzy logic, 61
 - glucose meters, 59
 - glycemic control, 60
 - HBGI, 67
 - implementation, 67
 - in vivo evaluation, 67–68
 - insulin bolus dose, 58
 - insulin pumps, 59
 - insulin therapy, 60
 - metal content, estimation, 63
 - open-loop system, 61
 - phone application, 60
 - R2R algorithms, 61
 - smartphones, 59
 - statistical measure
 - AUC, 66
 - BG level range, 66
 - CVGA, 67
 - LBGI, 67
 - mean of the blood glucose data, 66
 - SD, 66
 - T1D in silico simulation, 64, 65
 - Bolus insulin, 57
- C**
- Carbohydrate-to-insulin ratio, 59
 - Carry look ahead (CLA) adder, 186, 188, 190, 192
 - Case-based reasoning (CBR) algorithms, 61
 - Cervical cancer (CC)
 - CAD systems, 215
 - mortality rate, 215
 - Pap smear, 215
 - Cervigrams
 - ASRDC (*see* Adaptive Specular Reflection Detection in Cervigrams (ASRDC))
 - Chronic diseases, 70
 - Closed-loop artificial pancreas (AP), 69
 - Closed-loop system, 61
 - Cloud computing (CC), 36
 - Cloud of Things (CoTs), 36
 - Cognitive Internet of Things (CIoT), 36
 - Computer science, 3
 - Consumer-centric care, 129
 - Contemporary medicine, 7
 - Continuous glucose monitoring (CGM), 57, 61–64, 66, 67, 70
 - Control-variability grid analysis (CVGA), 67
 - Co-occurrence matrix, 120
 - Cover image, 234–237, 239, 241
 - Cyber-physical system, 32
- D**
- Decision support systems, 56
 - Deep learning (DL), 112, 132
 - Deep Variant, 131
 - DeepMind technology, 131
 - Denosing application, 196
 - Desired stability, 6
 - Detail coefficients, 78, 80, 85
 - Diabetes
 - diabetic ketoacidosis, 57

DSM for T1D patients, 58
 glucose homeostasis, 56
 IDGU, 56
 IIGU, 56
 insulin, 56
 ketone bodies, 57
 T1D treatment, 57, 68
 Diabetes Control and Complications Trial (DCCT), 59
 Diabetes mellitus, 55
 Diabetes self-management (DSM), 58
 Diabetic ketoacidosis, 57
 Digital natives (DNs), 37
 Digital signal processing (DSP) tool, 200
 Discrete wavelet transform (DWT), 77–80, 85, 235
 encrypted image, 234
 and LSB methods, 234
 Haar DWT, 236, 239
 inverse DWT, 238, 240
 Distance education (DE)
 IoT and cloud-enabled solutions, 31
 long-distance learning, 29
 paced (PDE), 31
 self-paced (SPDE), 31
 Distributed ledger technology (DLT), 135, 145
 DNA analysis, 91
 DNA biochips
 advantage, 91
 biological analysis, 91
 DNA analysis, 91
 integrated optics, 91
 integration techniques, 92
 measurement methods, 93
 medical diagnosis, 91
 micro-and nanoscale miniaturization, 91
 microphonics medical chips, 90
 modern miniaturized high-tech tool, 91
 (*see also* Network Time Protocol (NTP))
 new biological analysis systems, 91
 NTP protocol, 92
 optical circuits, 91
 DNA biosensors, 90
 Dynamic System for Assemblage and Execution of Interactive Classes (SISDI), 31, 32, 36, 37
 Dyscalculia, 29

E
 ECG signal denoising, 191
 E-health services, 127

Electrocardiography (ECG) signals, 77–80, 85
 VD-CLA, 187
 VD-CLA FIR filter, 191
 WGN, 186
 Emerging diseases, 127
 Emotion recognition (ER), 41–43
 Emotional health tracking, 41
 Emotional Speech Corpus of the AD (ESCAD), 43, 44
 Emotions, 30
 Empathy, 4, 6, 7
 Empirical mode decomposition (EMD), 77
 Enlightenment, 6
 Entropy texture descriptor, 257
 Europe
 rapid industrialization, 6
 Europeinterpreters, 6

F
 Field-programmable gate arrays (FPGAs)
 analytic power, 201
 brightness, 203
 DSP applications, 201
 enhancement techniques, 200
 fast-developing hardware technologies, 207
 hardware architectures, 199
 hardware design, 200
 image manipulation, 205
 image processing and computer vision, 206
 image processing techniques, 201
 improvement, 211
 MATLAB and Verilog outputs, 205
 NoCs, 207
 optimization algorithms, 210
 SEM alveoli, 204
 short computational times, 206
 Finite impulse response (FIR)
 architectures, 186
 channel, 187
 filter implementations, 185
 N-tap FIR filter, 188
 VD-CLA FIR filter, 187, 196
 FIR filter (FIRF)
 benefits, 185
 decimator FIRF, 185
 GA-based, 185
 MAC unit, 187
 normal FIRF, 185
 parallel-based, 185
 paybacks, 185

FIR filter (FIRF) (*cont.*)
 VD-CLA adder FIRF, 187
 VD-CLA FIRF architecture, 188
 VD-CLA FIRF method, 186, 191
 FPGA technology, 124
 Fuzzy logic, 61

G

Genetics-driven medicine, 3
 German Corpus of Emotional Speech (EMODB), 43–48
 German language (GL)
 acoustic contrast, 50
 and AD, 43
 EMOB, 43, 44
 ESCAD, 47
 neutral and angry states, 51
 Glucose, 56
 Glucose area under the curve (AUC), 66
 Glucose homeostasis, 56
 Glycemic control, 56–58, 60, 68, 69
 God's ethics, 6
 Gonzalez technique, 45
 Governance, 6
 Gray-level co-occurrence matrix (GLCM), 117–120, 124
 Gtarget, 58

H

Haar DWT, 234, 236, 237, 239, 241
 Haar transform, 235
 Haralick's coefficients, 118
 contrast, 118
 correlation, 119
 energy, 118
 entropy, 118
 homogeneity, 119
 Haralick's features (HFs), 116–118, 120
 Health informatics, 3
 Healthcare
 AI (*see* Artificial Intelligence (AI))
 and tax-paying stratum, 8
 and tax-paying work force, 7
 blockchain (*see* Blockchain)
 empathy for patient's experience, 7
 European sector, 8
 financial inflow and outflow, 8
 Health 1.0, 128
 Health 2.0, 128
 Health 3.0, 128
 Health 4.0, 128
 IoMT (*see* Internet of medical things (IoMT))

medicine, 9
 personalized, 3, 4
 revolutions, 128
 stages, 128
 Healthcare provision, 7
 Heart image
 FPGAs (*see* Field-programmable gate arrays (FPGAs))
 Hidden image, 233, 243
 Hierarchical governing system, 5
 High blood glucose index (HBGI), 67
 Homeostasis, 56
 Human intelligence, 131
 Human-machine interface (HMI), 67
 Human papillomavirus (HPV), 215
 Hybrid algorithm, 112
 Hybrid multi-objective ABC (HMOABC), 104
 Hyperledger Fabric, 145

I

Image enhancement, 199, 205
 Image processing, 199
 Image sharpening techniques, 202, 203
 Image steganography
 approaches, 233
 challenge, 245
 conventional LSB replacement method, 234
 message image, 233
 using DWT, 234
 in Verilog, 241
 In silico, 64
 Independent component analysis (ICA), 85
 Information technology, 11
 Infrastructure-reliant network, 155
 Inpatient medication, 130
 Input image quality assessment (QA), 221
 Inspection
 combined real-time inspection system, 24
 CRN4 inspection team, 13
 descriptive statistics, 12
 formal inspection data mining, 24
 inspectors, 12
 professional, 24
 professional practice, 13
 quantitative, 13
 RVT, 13
 Insulin
 AIDA, 65
 basal-bolus insulin therapy, 69
 basal insulin, 57, 58
 bolus insulin, 57, 58
 CBR, 62
 ICR, 58

- IDGU, 56
- IIGU, 56
- insulin pumps, 59
- IOB, 58
- ISF, 58
- rapid-acting insulin, 57
- short-acting insulin, 57
- T1D treatment, 57
- Insulin-dependent glucose uptake (IDGU), 57
- Insulin-independent glucose uptake (IIGU), 56
- Insulin on board (IOB), 58
- Insulin sensitivity factor (ISF), 58
- Insulin therapy, 55, 57, 60
- Insulin-to-carbohydrate ratio (ICR), 58
- Intensive insulin therapy (IIT), 57
- Internet of medical things (IoMT)
 - actuators, 140
 - advantages, 142
 - applications, 144
 - challenges, 144–145
 - communication protocols, 143
 - comprehensive patient care, 140
 - EHR systems, 143
 - empowered devices, 141
 - essential role, 141
 - for personalized medical application, 141
 - healthcare activities, 143
 - integration of healthcare, 140
 - limitations, 143
 - ontology-inspired models, 145
 - processors, 140
 - protection approaches, 146
 - quality of care, 147
 - security and privacy attributes, 146
 - sensing and wearable devices, 141
 - sensors, 140
 - stakeholder centric approach, 146
 - wearable devices, 142
 - wearable sensors, 144
- Internet of Things (IoT), 31, 33, 36
- Internet-integrated technology, 3

- K**
- Kernel application process, 202
- Ketone bodies, 57

- L**
- Linear discriminant analysis (LDA), 78, 80, 82, 84, 85
- Long-Term Institution for the Elderly (LTIE)
 - clinical nutrition, 21, 22
 - qualitative indicators, 21–22
 - quantitative indicators, 22
 - quantitative indicators outcome, 23
 - RVT Clinical Nutrition, 15
- Low blood glucose index (LBGI), 67
- LSB replacement technique, 234, 235, 242
- Lung image
 - FPGAs (*see* Field-programmable gate arrays (FPGAs))

- M**
- Machine learning, 132
- Macronutrients, 68
- Math anxiety, 30
- Math skills, 30
- Mathematical tools, 11
- Mean squared error (MSE), 196
- Medical machinery, 3
- Medical personnel, 3
- Medical service, 4
- Medicine, 9
- MedRec Blockchain technology, 139
- Micrometers, 250
- Microphonics medical chips, 90
- Microtomograph SkyScan 1174, 251
- Microtomography (μ CT/micro-CT)
 - applications, 250
 - beneficial in dental investigations, 250
 - compact, 251
 - devices, 251
 - enhancement techniques, 259
 - image classification, 252
 - image quality, 251
 - non-destructible nature, 250
 - operating principle, 250
 - settings, 259
 - texture descriptors, 259
 - tooth, 250
 - X-ray, 249, 258
- Mining techniques, 11
- Mobile ad hoc networks (MANETs)
 - AHN, 155
 - handheld devices, 156
 - heterogeneous, 156
 - innovative, 155
 - mobile node network, 155
 - nodes, 156
 - objectives, 156
 - vs.* VANETs, 165
 - energy restrictions, 164
 - frequent interruption, 164
 - production cost, 164
 - quickly variable topology, 164
 - reliability, 164
 - wireless networks, 155
- Modified Kittler method (MKM), 220

Multi-objective GA (MSAGMOGA), 104

Multiple sequence alignment (MSA)

ad hoc mutation operators, 104

bottlenecks, 112

CRO algorithm, 104

HMOABC, 104

MSAGMOGA, 104

PSO variants, 112

PSO-TS algorithm, 103

TS components, 108

TS updates, 108

Multipliers, 186

N

Nanorobotics, 3

National Health Service (NHS), 131

Natural language processing, 132

Network Time Protocol (NTP)

access control, 94

authentication, 94

computer time synchronization, 94

DNA database, 98

implementation, 98

in Linux, 94

real-time synchronization, 92

servers and security rules, 94

service overcomes, 98

SNTP, 97

synchronization, 93, 96, 97

Network-on-Chip (NoC), 207

Neutral speech, 43, 46, 47

Nobility obligates, 7

Noise reduction, 200

Nondestructive analysis, 250

Noninvasive inspection, 250

Nutrition

Collective Feeding FNU, 16

CRN4, 12

FNU, 15, 17, 18

hospital and similar institutions, 20

inspection actions, 12

O

Object-oriented (OO) system, 32

On-Board Unit (OBU), 157, 162, 163

Ontologies, 145

Optimal outpatient clinical decision support system, 130

Organized stroke unit care, 130

Outpatient care, 130

Outpatient clinical decision support system, 130

P

Particle swarm optimization (PSO)

benefits, 112

and Clustal X aligner, 104

description, 105

drawback, 106

PSO-TS

algorithm, 103

algorithm flowchart, 106

cooperation, 106

procedure, 109

using JCreator version 3.5, 109

variants, 112

Patients

contemporary medicine, 7

hospitals, 8

medicine, 9

personalized care, 3

personalized medicine, 3

privacy concerns, 4

survival outcomes, 9

telemedicine, 9

Peak signal-to-noise ratio (PSNR), 196

Personalized care, 3

Personalized healthcare, 3, 4

Personalized medicine, 3, 4

AI approaches, 132

AI system, 132

Deep Variant, 131

description, 128

diagnostic tests, 129

enzymes, 130

function, 132

genetic information, 132

HER2, 129

in pharmaceutical and medical

industries, 128

medications, 129

prevention and treatment, diseases, 131

preventive healthcare strategies, 128

Siri iOS application, 132

tailoring treatments, 132

Preventive medicine, 5

Principal component analysis (PCA), 78, 80, 82–85

Professional practice

CFN/CRN system, 14

data mining techniques, 24

feedback text mining, 11

specialization, 20
 technical visits, 13
 Public health, 11, 24

R

Rapid-acting insulin, 57
 Real-time hardware systems, 200
 Roadside unit (RSU), 157, 163
 Run-to-run (R2R) algorithms, 61
 RVT Clinical Nutrition, 15

S

Sequencing technology, 3
 Short-acting insulin, 57
 Signal processing, 185, 196
 Signal-to-noise ratio (SNR), 196
 Simple Network Time Protocol (SNTP), 97
 Siri iOS application, 132
 Social anxiety, 30
 Social ethics, 7
 Social extortion, 8
 Softcore processor, 199
 Specular reflection (SR), 215, 216
 Speech corpora
 ESCAD, 44
 Speech corpus
 Anderson-Darling test, 46
 EMODB, 44, 45
 P-value, 46
 statistical hypothesis testing, 46
 Standard deviation (SD), 66
 State-of-the-art technology
 automatic recognition and
 removal, SR, 216
 features, 219
 limitations, 219
 morphological kernels, 216
 specularity-invariant pixels, 216
 SR detection categories, 217, 218
 SR discovery approaches, 217
 thresholding techniques, 218
 threshold-picking strategies, 218
 Statistical measures, 78–80, 85
 Steganography
 LSB method, 234
 medical image data, 233
 See also Image steganography
 Stego image, 235, 241, 242
 Stegoing process, 235
 Stress classification, 84, 85
 Supervised professionals, 12

Support vector machine (SVM), 78, 80,
 82, 84, 85
 Surface Plasmon Resonance (SPR)
 imaging, 92
 SymBiosis, 146

T

Tabu list length (TLL), 108
 Tabu search (TS), 103, 104, 112
 Technical Visit Routes (RVT), 13–16,
 22, 23, 25
 Technical visits, 13
 Technologies
 AI (*see* Artificial intelligence (AI))
 blockchain (*see* Blockchain)
 consumer-centric care, 129
 drug discovery and delivery, 127
 in healthcare system, 127, 128
 Texture descriptors, 254, 256, 259
 Texture features, Haralick's, 116, 117
 Time management, 30
 Type 1 diabetes (T1D)
 automatic BC with automatic speech
 recognition, 63
 DSM, 58
 IIT, 57
 in silico simulation environment, 64, 65
 insulin therapy, 55, 57
 optimal glycemic control, 58
 rapid-acting insulin, 57
 short-acting insulin, 57
 UVA/PADOVA T1D simulator, 62
 Type 1 Diabetes Metabolic Simulator
 (T1DMS), 65
 Type 2 diabetes (T2D), 55, 57
 Type 2 human epidermal growth factor
 receptor (HER2), 129

U

UNIX Server platform, 93, 98

V

Vedic design (VD), 186, 187
 Vedic design-carry look-ahead (VD-CLA),
 186, 187, 190, 192
 Vedic math, 196
 Vedic multiplier, 188–190, 193
 Vehicle-to-Infrastructure (V2I), 157, 158
 Vehicle-to-Vehicle (V2V), 157, 158

- Vehicle-to-Vehicle-to-Infrastructure (V2V2I), 157, 159
 - Vehicular ad hoc networks (VANETs)
 - architecture
 - OBU, 162, 163
 - RSU, 163
 - AUs, 163
 - bandwidth utilization, 171
 - cluster-based routing protocol, 167
 - geo-cast routing protocol, 167
 - MAC protocols, 165
 - mobile wireless devices and networks, 157
 - network latency per user, 172
 - normal simulation mode, 802.11p protocol, 170, 173, 174
 - percentage of the network, 170
 - position-based routing, 167
 - proactive routing, 166
 - reactive routing, 166
 - routing protocol
 - basic AODV, 168, 169, 171
 - route discovery initialization process, 168
 - topologies, 168
 - routing protocols, 165
 - SNR *vs.* PER graph, 170
 - V2I, 157
 - V2V, 157
 - V2V2I, 157
 - Vehicular network challenges
 - bandwidth restrictions, 162
 - connectivity, 162
 - fading of signals, 162
 - mobility, 160
 - responsibility, 161
 - scalability, 161
 - trifling operative diameter, 161
 - volatility, 160, 161
 - volatility protocol, 161
 - Verilog Hardware Description Language (HDL), 199, 211
 - Verilog module, 236, 241
- W**
- Weighted k-nearest neighbors (WKNN), 78, 80, 83–85
 - Weighted total variation (WTV) denoising technique, 77
 - White Gaussian noise (WGN), 186
 - Wireless Area Network (WAN), 157
- X**
- X-ray motion analysis, 259
 - X-ray source focal spot, 200
 - X-ray μ CT, 250
- Z**
- Zone of relevance (ZOR), 167